ESPOO 2005 VTT PUBLICATIONS 567

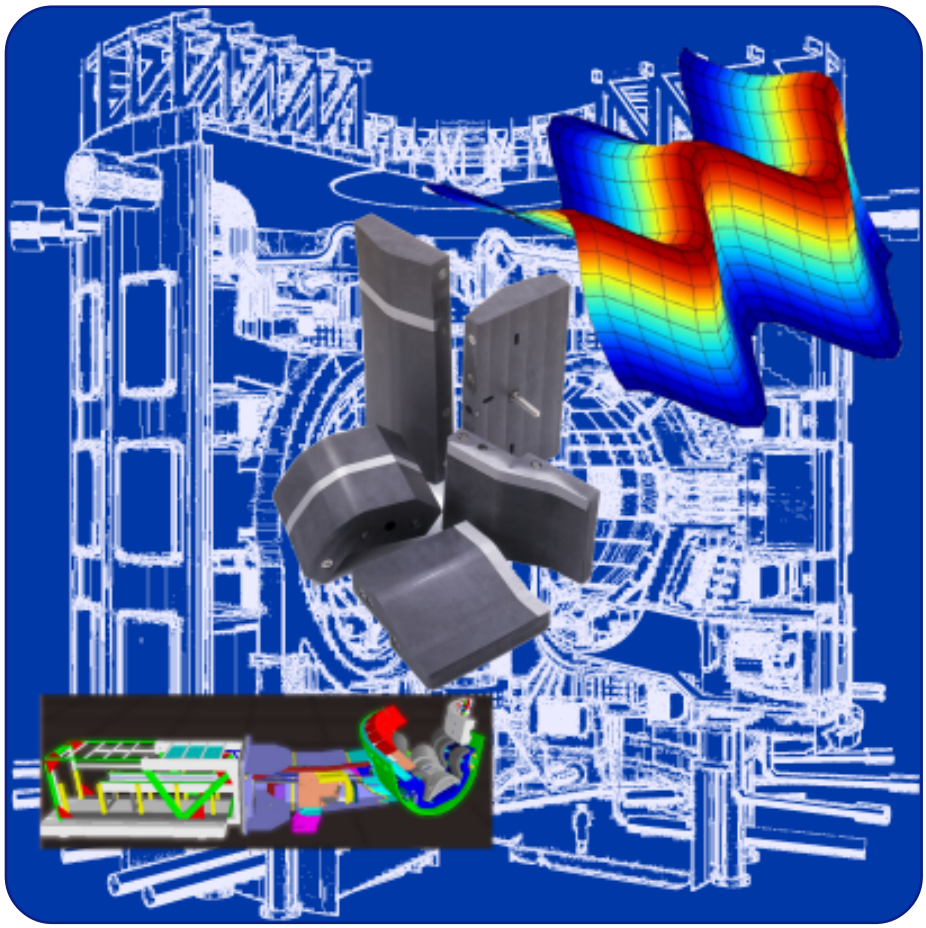

FUSION YEARBOOK

Association Euratom-Tekes
Annual Report 2004

VTT PUBLICATIONS 567

FUSION YEARBOOK

Association Euratom-Tekes Annual Report 2004

Seppo Karttunen & Karin Rantamäki (eds.)

VTT Processes

ISBN 951–38–6642–4 (soft back ed.)
ISSN 1235–0621 (soft back ed.)

ISBN 951–38–6643–2 (URL: http://www.vtt.fi/inf/pdf/)
ISSN 1455–0849 (URL: http://www.vtt.fi/inf/pdf/)

JULKAISIJA – UTGIVARE – PUBLISHER

VTT, Vuorimiehentie 5, PL 2000, 02044 VTT
puh. vaihde 020 722 111, faksi 020 722 4374

VTT, Bergsmansvägen 5, PB 2000, 02044 VTT
tel. växel 020 722 111, fax 020 722 4374

VTT Technical Research Centre of Finland, Vuorimiehentie 5, P.O.Box 2000, FI–02044 VTT, Finland
phone internat. +358 20 722 111, fax +358 20 722 4374

VTT Prosessit, Otakaari 3 A, PL 1608, 02044 VTT
puh. vaihde 020 722 111, faksi 020 722 6390

VTT Processer, Otakaari 3 A, PB 1608, 02044 VTT
tel. växel 020 722 111, fax 020 722 6390

VTT Processes, Otakaari 3 A, P.O.Box 1608, FI–02044 VTT, Finland
phone internat. +358 20 722 111, fax +358 20 722 6390

Keywords fusion, fusion reactors, reactor materials, fusion physics, remote handling, testing, Joint European Torus, modelling, control

Cover: Background ITER, EFDA-JET and DIARC Technology Oy, TUT IHA, UH

Valopaino Oy, Helsinki 2005

FOREWORD

The FUSION technology programme by Tekes provides the national frame for fusion research activities of the Association Euratom-Tekes. It is fully integrated into the European Fusion Research Area in the 6th Framework Programme. The emphasis of the Finnish fusion activities is in EFDA technology research and development work, which is carried out in close collaboration with Finnish industry. Our plasma physics and plasma-wall research is very much concentrated on the EFDA JET work.

The international commitment to ITER is very strong among ITER parties, which came clear when the United States rejoined and the People's Republic of China and the Republic of Korea joined to the ITER negotiations in 2003. In addition, Brazil and India have expressed their interest in participating in ITER. The European position in is based on three principles: i) the ITER Project should realise in the widest possible international framework, ii) ITER should be a part of the broader approach to the realisation of fusion energy and iii) ITER should be sited at the EU site of Cadarache in view of its technical, scientific and environmental advantages. Negotiations on the ITER site did not move significantly during 2004, but some movement took place in the latest high level negotiation with Japanese as both parties expressed their strong commitment to solve the site issue and find a six party agreement by July 2005.

Research activities by the Association Euratom-Tekes are focused on the two areas: 1) EFDA JET work and 2) vessel/in-vessel field of the EFDA technology programme. Tekes contributions to JET in 2004 covered radio-frequency heating experiments, modelling of the real time control of transport barriers, predictive integrated modelling of tokamak plasmas, diagnostics and studies on material transport in the edge plasmas supported by surface analysis of the JET divertor and limiter tiles.

Technology work in the vessel/in-vessel field included e.g. mechanical testing of reactor materials under neutron irradiation, characterisation of irradiated Ti-alloys, simulations of carbon and tungsten sputtering, beam welding, upgrade welding robot and development of water hydraulic manipulator for the ITER divertor maintenance. Some effort was also devoted to neutronics, socio-economic and power plant studies.

The absolute highlight of the year 2004 was the EFDA decision to select the Association Euratom-Tekes to host the divertor test platform (DTP2) for ITER. The facility is sited in Tampere and managed by VTT with the Tampere University of Technology. Remote handling development has been very successful in the Finnish programme, which was certainly a key reason for the EFDA decision to offer the DTP2 to the Tekes Association.

Finally, I would like to express my sincere thanks to the whole fusion team of the Finnish Research Unit and to the companies involved for the dedicated and successful contributions to the European Fusion Programme.

Seppo Karttunen
Head of the Research Unit
Association Euratom-Tekes

CONTENTS

1 INTRODUCTION

The "FUSION" technology programme for 2003–2006 is the national frame for the fusion research activities of the Association Euratom-Tekes. The FUSION programme is fully integrated into the European Fusion Programme in the 6th Framework Programme or the European Fusion Research Area. Financing is provided by Euratom and nationally by Tekes (National Technology Agency of Finland), Finnish Academy, participating institutes and industry. The Association Euratom-Tekes was established in 1995 and the present Contract of Association between Euratom and Tekes extends to the end of 2006. The total budget of the Fusion Research Unit is about 3.5 M€ corresponding to the manpower over 35 ppy. Other agreements of the EU Fusion Programme include the multilateral European Fusion Development Agreement (EFDA), JET Implementing Agreement (JIA) and the Staff Mobility Agreement. The Research Unit of the Association Euratom-Tekes covers research groups from

- Technical Research Centre of Finland (VTT),
- Helsinki University of Technology (TKK),
- Tampere University of Technology (TUT),
- Lappeenranta University of Technology (LUT) and
- University of Helsinki (UH).

This Annual Report summarises the fusion research activities of the Finnish Research Unit of the Association Euratom-Tekes in 2004. The activities of the Research Unit are divided in the Fusion *Physics Programme* and the Fusion *Technology Programme*.

The Physics Programme is carried out at the Technical Research Centre of Finland (VTT) Helsinki University of Technology (TKK) and University of Helsinki (UH). The research areas of the Physics Programme are:

- Heat and particle transport, MHD physics and plasma edge phenomena
- Radio-frequency applications – heating, current drive and diagnostics
- Plasma-wall interactions and material transport in SOL region.

Association Euratom-Tekes participates actively in the EFDA JET Workprogramme 2003–2004 and JET operations. Three persons were seconded to the UKAEA operating team and one person acted as a Deputy Task Force Leader in TF H (heating) and other person started as a Deputy Task Force Leader in TF T (transport) in later 2004. S/T Order/Notification activities continued the work that started in 2000. Practically all physics activities of the Research Unit are carried out in collaboration with other Associations with the focus on EFDA JET work. In addition to EFDA JET activities, the Tekes Association participated in the 2004 experimental programme of ASDEX Upgrade (AUG).

The Technology Programme is carried out at the Technical Research Centre of Finland (VTT), Helsinki University of Technology (TKK), Tampere University of Technology (TUT) and Lappeenranta University of Technology (LUT) in close collaboration with Finnish industry. The main companies involved in 2004 activities are: Fortum (Finnish EFET partner), Outokumpu Poricopper, Metso Powdermet, Hollming Works, Diarc Technology, Plustech, Hytar, Adwatec and Prizztech Oy.

The technology research and development in 2004 is focused on the fusion reactor vessel/in-vessel area:

- Multimetal in-vessel components, joining technology and materials testing and characterisation
- Plasma facing materials including erosion studies, material transport and tritium issues
- Remote handling of divertor maintenance, and welding/cutting robotics
- Preparation of the ITER Divertor Test Platform (DTP2).

A number of EFDA Technology Tasks are underway in 2004 and activities in Underlying and Long Term Technology, Power Plant Studies as well as Socio-Economic studies will continue. Two persons were seconded to the EFDA CSU – Garching in 2004.

Technology collaboration was active with Euratom Associations FZK Karlsruhe (IFMIF, ITER neutronics and gyrotrons), Risø Roskilde and SCK-CEN Mol (In-reactor materials testing), UKAEA Culham (JET Technology), CEA Cadarache and ENEA Brasimone (divertor maintenance tools and manipulators),

The following Staff Mobility actions have been taken place in 2004:

1. Frej Wasastjerna from VTT to Forschungszentrum Karlsruhe, 89 days, 6 January – 3 April 2004
2. Jari Likonen from VTT to UKAEA Culham, mission 7 days, 29 February – 6 March 2004.
3. Johnny Lönnroth from HUT (JOC Secondee) to JAERI Naka, mission 5 days, 27 March – 10 April 2004.
4. Olgierd Dumrajs from HUT to NTUA Greece, 35 days, 28 March – 1 May 2004
5. Karin Rantamäki from VTT to IPP Garching, mission 4 days, 18 April – 21 April 2004
6. Mervi Mantsinen from HUT to IPP Garching, mission 4 days, 18 April – 21 April 2004
7. Marko Santala from HUT (JOC Secondee) to IPP Garching, mission 3 days, 19 April – 21 April 2004
8. Antti Salmi from HUT to IPP Garching, mission 3 days, 19 April – 21 April 2004
9. Markus Airila from HUT to Forschungszentrum Jülich, 31 days, 31 May – 30 June 2004
10. Jari Likonen from VTT to UKAEA Culham, 23 days, 19 June – 11 July 2004.
11. Taina Kurki-Suonio from HUT to IPP Garching, 28 days, 8 July – 4 August 2004.
12. Johnny Lönnroth from HUT (JOC Secondee) to JAERI Naka, 28 days, 28 August – 25 September 2004.
13. Taina Kurki-Suonio from HUT to IPP Garching, 17 days, 7–23 October 2004 (second part of the visit in January 2005)
14. Olgierd Dumbrajs from HUT to IPP Garching, 30 days, 1–30 November 2004
15. Markus Nora, Karin Rantamäki and Tuomas Tala to UKAEA Culham, 6 days, 28 November – 3 December 2004.

The total volume of the mobility actions in 2004 was 336 days (11.6 man-months). More detailed descriptions on the Staff Mobility visits are given in Section 10.4. In addition, there were several shorter visits outside the Staff Mobility arrangements. These are listed in Section 10.

2 OBJECTIVES OF THE PROGRAMME

The Finnish Fusion Programme, under the Association Euratom-Tekes, is fully integrated into the European Programme, which has set the long-term aim of *the joint creation of prototype reactors for power stations to meet the needs of society: operational safety, environmental compatibility and economic viability.* The objectives of the Finnish programme (FUSION) is to carry out high-level scientific and technological research and to make a valuable and visible contribution to the European Fusion Programme and to the international ITER Project in our focus areas. This can be achieved by close collaboration between the Research Unit and Finnish industry, and by strong focusing the R&D effort on a few competitive areas. Active participation in the EU Fusion Programme and ITER provides challenging opportunities for the technology R&D and Finnish high-tech industry increasing know-how and beneficial technology transfer.

3 FUSION PROGRAMME ORGANISATION

3.1 Association Euratom-Tekes

The National Technology Agency of Finland (Tekes) is funding and co-ordinating technological research and development activities in Finland. The Association Euratom-Tekes was established on 13 March 1995 when the Contract of Association between Euratom and Tekes was signed. Other agreements of the Association Euratom-Tekes include multilateral European Fusion Development Agreement (EFDA), JET Implementing Agreement (JIA) and Staff Mobility Agreement. Tekes was a member of the JET Joint Undertaking from 7 May 1996 until its end December 1999. The fusion research co-ordinator in Tekes is Juha Lindén.

3.2 Fusion Research Unit

The Research Unit of the Association Euratom-Tekes consists of several research groups from VTT and universities. The Head of the Research Unit is Seppo Karttunen from VTT Processes.

The following institutes and universities participated in the fusion research during 2004.

1. VTT – Technical Research Centre of Finland:
VTT Processes (co-ordination, physics, materials, socio-economics)
VTT Industrial Systems (materials, remote handling, welding, DTP2)

2. Helsinki University of Technology (TKK):
Department of Engineering Physics and Mathematics (physics, system studies)

3. University of Helsinki (UH):
Accelerator Laboratory (physics, materials)

4. Tampere University of Technology (TUT):
Institute of Hydraulics and Automation (remote handling, DTP2)
Laboratory of Electromagnetics (superconductors)

5. Lappeenranta University of Technology (LUT):
Institute of Mechatronics and Virtual Engineering (remote handling).

The following industrial companies collaborated with the Fusion Research Unit: Fortum Nuclear Services (Fortum is the Finnish EFET partner), Outokumpu Poricopper, Hollming Works, Mekarita, Patria Finavitec, PI-Rauma, Mäntyluoto Works, Platom Metso Powdermet, Metso Engineering, Diarc Technology, Creanex, Hytar, Advatec, Delfoi, Solving and Rocla. The industrial activities were co-ordinated by Prizztech.

The contact persons and addresses of the participating research institutes and companies can be found in Appendix B.

3.3 Association Steering Committee

The research activities of the Finnish Association Euratom-Tekes are directed by the Steering Committee, which comprises the following members in 2004:

Chairman 2004:	Prof. Hardo Bruhns, EU Commission, Research DG
Members:	Prof. Jouko Suokas, VTT Industrial Systems
	Mr. Reijo Munther, Tekes,
	Dr. David Campbell, EFDA CSU Garching
	Dr. Eduard Rille, EU Commission, Research DG
	Dr. Harri Tuomisto, Fortum Nuclear Services Oy
Head of Research Unit:	Dr. Seppo Karttunen, VTT Processes
Secretary:	Dr. Jukka Heikkinen, VTT Processes

The Steering Committee had one meeting in 2004, this time at VTT, Espoo, on 21 October.

3.4 National Steering Committee

The FUSION programme national steering committee advises on the strategy and planning of the national research effort and promotes collaboration with Finnish industry. It sets also priorities for the Finnish activities in the EU Fusion Programme. The national steering committee had the following members in 2004:

Chairman:	Dr. Harri Tuomisto, Fortum Nuclear Services Oy
Members:	Mr. Iiro Andersson, Prizztech Oy
	Mr. Juha Lindén, Tekes
	Mr. Reijo Munther, Tekes
	Mr. Ben Karlemo, Outokumpu Poricopper Oy
	Prof. Rainer Salomaa, Helsinki University of Technology
	Dr. Pentti Pulkkinen, Finnish Academy
	Dr. Jouko Pullianen, Metso Powdermet Oy
	Prof. Rauno Rintamaa, VTT Industrial Systems
	Dr. Arto Timperi, Creanex Oy
Programme Manager:	Dr. Seppo Karttunen, VTT Processes
Secretary:	Dr. Tuomas Tala, VTT Processes

The FUSION national steering committee had four meetings in 2004.

3.5 The Finnish Members in the EU Fusion Committees

Consultative Committee for the Euratom Specific Research and Training Programme in the Field of Nuclear Energy – Fusion (CCE-FU)
Seppo Karttunen, VTT
Reijo Munther, Tekes

Fusion Industry Committee (CFI)
Juho Mäkinen, Outokumpu Oyj

EFDA Steering Committee
Reijo Munther, Tekes
Seppo Karttunen, VTT

Euratom Science and Technology Committee (STC)
Rainer Salomaa, TKK

Administration and Financing Advisory Committee (AFAC)
Juha Lindén, Tekes
Rainer Salomaa, TKK

Science and Technology Advisory Committee (STAC)
Seppo Karttunen, VTT
Rauno Rintamaa, VTT
Rainer Salomaa, TKK

EFDA Public Information Committee (CPI)
Seppo Karttunen, VTT (CPI Chairman)

Finnish representatives in the following fusion committees and expert groups:

Reijo Munther is a member of the IEA Fusion Power Co-ordinating Committee (FPCC).

Rainer Salomaa ia a member of the Programme Committee of the ASDEX-Upgrade, Max Planck Gesellschaft.

Jukka Heikkinen is a member of the Co-ordinating Committee for Fast Waves (CCFW).

Seppo Karttunen is a member of the Co-ordinating Committee for Lower Hybrid Waves (CCLH).

Olgierd Dumbrajs is a member of the international expert commission on Electron Cyclotron Wave Systems.

Rainer Salomaa was a member of the ad-hoc-group monitoring the heating and current drive systems for JET enhancements and ITER

Rainer Salomaa is the Tekes administrative contact person in EFDA JET matters

Seppo Tähtinen is a Materials Liaison Officer in the European Blanket Project (EBP).

Harri Tuomisto is a member of the International Organising Committee, of the Symposium on Fusion Technology (SOFT).

Jukka Heikkinen is a member of the Scientific Committee of the European Fusion Theory Conference.

3.6 Public Information and Media

3.6.1 Mass Media – Newspapers and television

Fusion and ITER received a lot of interest in Finnish mass media, mostly treated in a positively manner. The ITER negotiations have bee followed closely and many short articles (some positive and some sceptical) have been published in newspapers. National public TV channel YLE TV 1 prepared a half hour programme on fusion energy research in their science series "Tutkittu Juttu (Research Case)". The programme consists of interviews of Finnish fusion experts, an interview of Sir Chis Llewellyn Smith and video clips from "Starmakers". The programme will be send out in spring 2005. In addition, there were some radio and TV interviews on fusion in general and on the Divertor Test Platform, which will be hosted by VTT and Tampere University of Technology.

3.6.2 Conferences and seminars

The Finnish Energy Congress was held in Tampere in October. The Association Euratom-Tekes had a stand with posters on ITER, Finnish Fusion Research and industrial activities. Material included Finnish and EU Fusion brochures. A large number of participants visited then stand.

The Annual Fusion Seminar of the Association Euratom-Tekes was held at Tampere University of Technology on 1–2 June 2004. The Seminar provided a summary of the research activities of the Finnish Fusion Research Unit and industrial R&D projects. The invited speaker was the EFDA Leader M.Q. Tran, who gave an excellent overview on EFDA activities related to ITER.

The summary of the work carried out by the Finnish Research Unit is collected to the FUSION Yearbook 2003 – Annual Report of the Association Euratom-Tekes which was published prior the Annual Seminar.

Three invited talks in Studia Generalia and Rotary Meetings were given.

3.6.3 Newsletters

Finnish FUSION Newsletter appeared three times in 2004 telling the main news and stories on national, EU and ITER research activities as well as the important political news related fusion research and ITER negotiations. EFDA Newsletter and JET Bulletin are distributed electronically to main target groups

3.6.4 Fusion courses

A course on fusion technology at the Helsinki and Lappeenranta University of Technology was given during the spring term 2004. The lecture courses on fusion technology take place every two years alternating with a plasma and fusion physics course.

3.6.5 Brochures and www-pages

A six-page brochure on the Finnish fusion programme in Finnish was completed in early 2004. Additional technology pages on materials and remote handling are under preparation. The target group for those is the Finnish industry. An English version will

follow in early 2005. The EFDA and Commission brochures have been very welcome and widely distributed.

Tekes fusion pages:
http://akseli.tekes.fi/Resource.phx/enyr/fusion/index.htx
Finnish Fusion homepages:
http://www.vtt.fi/pro/research/fusion2003_06/indexe.htm

3.7 Funding and Research Volume 2004

In 2004, the estimated expenditure of the Association Euratom-Tekes was about 3.694 Mio Euro including Staff Mobility actions. The estimated Euratom support is k€ 1 145. The major part of the national funding comes from Tekes. The rest of the funding comes from other national institutions, such as the Finnish Academy, research institutes participating in the fusion research (VTT, TKK, TUT, UH, LUT) and industry. The funding was allocated as following: fusion plasma physics 35% including EFDA JET activities, Underlying Technology 9%, EFDA Technology Tasks (Art. 5.1a) 44%, EFDA Art. 5.1b Contracts 7% and EFDA CSU Secondments 5%. The hot cell work, capital investments and co-operation with other Associations under the Preferential Support exceeded k€ 891 and the expenditure on the Staff Mobility actions were k€ 57. The total volume of the 2004 activities was about 37 professional man-years.

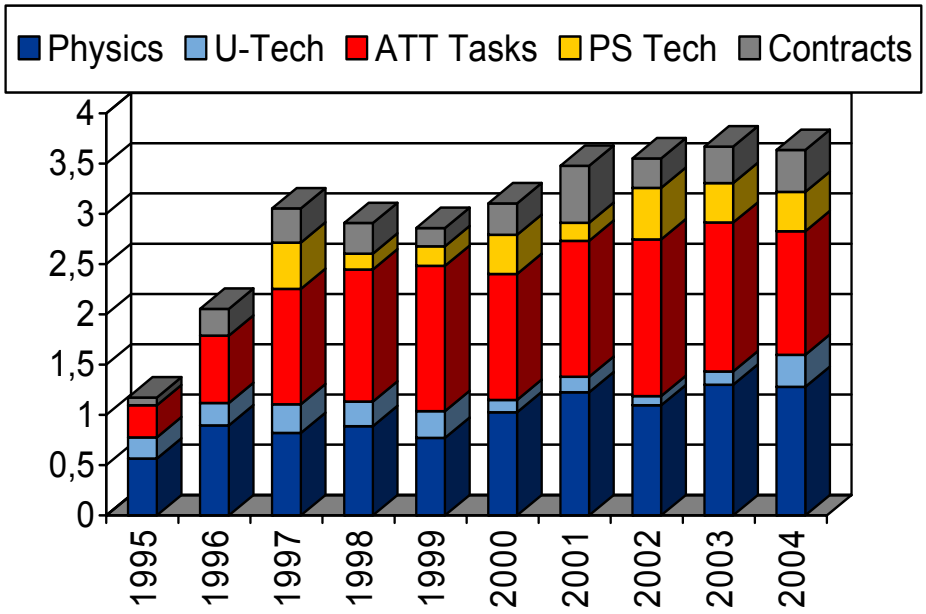

Figure 3.1: Breakdown of the expenditures of the Association Euratom-Tekes in 1995–2004. Numbers are based on Annual Accounts (1995–2003) and estimated expenditures in 2004. Categories are from bottom: Physics Programme, Underlying Technology, EFDA Technology Tasks, EFDA Contracts, and Orders together with work and items under Preferential Support.

4 PHYSICS PROGRAMME – FUSION PHYSICS

Institute:	**VTT Processes**
Research scientists:	Dr. S.J. Karttunen (Head), Dr. J.A. Heikkinen, MSc. J. Lönnroth (seconded to JOC), Dr. K.M. Rantamäki, Dr. T.J.J Tala (Deputy Task Force Leader)
Institute:	**Helsinki University of Technology** Department of Engineering Physics and Mathematics Laboratory of Advanced Energy Systems
Research scientists:	Prof. R. Salomaa (Head); Dr. P. Aarnio, Dr. M. Airila, Prof. O. Dumbrajs, Dr. T. Kiviniemi, Dr. T. Kurki-Suonio, Dr. M. Mantsinen (Deputy Task Force Leader, seconded to JOC), LicSc. S. Saarelma, MSc. A. Salmi, Dr. M. Santala (seconded to JOC), Dr. S. Sipilä, MSc G. Zemulis, MSc V. Hynönen, MSc. S. Janhunen; Students: Mr. M. Nora, Ms. P. Kåll, Mr. D. Siponen, Mr. S. Henriksson, Mr. T. Ekholm, Ms. L. Aho-Mantila. Mr. M. Kortelainen, Mr. T. Ikonen, Mr. E. Ahtinen
Collaboration:	EFDA JET, IPP Garching, CEA Cadarache, IPP Prague, ENEA Frascati, FZK Karlsruhe, FZJ Jülich, UKAEA Culham and Ioffe Institute St. Petersburg

4.1 EFDA JET Workprogramme 2003–2004

4.1.1 Overview

TF-H: Tekes provided Deputy Task Force Leader of TF-H, session leader for H-4.1; H-7.2 and H-9.5 and scientific co-ordinators for the experiments H-7.1; H-9.1; H-9.2; H-9.3-2; H-9.5 and H-10.5. Other Tekes activities included modelling of ICRF and LHCD experiments and code development.

TF-T: Tekes Association was strongly involved in the preparation and execution of Task Force T providing Deputy Task Force Leader of TF-T and two research scientists. The work included predictive transport modelling and real-time control of internal transport barriers (ITBs) using JETTO transport code, and transport modelling of power modulation experiments with JETTO. Involvement in the work programme of the TF-T as a co-ordinator of the working group of modelling of real-time control of ITBs, and performing predictive and interpretative transport modelling.

Tekes was also involved in the execution of the TF-T work programme as Predictive Transport Modelling Expert and ELMy H-mode and Edge Pedestal Specialist and simulations of NBI ion losses as Neoclassical Transport Modelling Expert.

TF-S2: Tekes provided a scientific co-ordinator for S2-7.2 ICRF mode conversion in ITB plasmas. Tekes Association was involved in the preparation and execution of Task Force

S2 experimental programme during C8-C14 campaigns under the EFDA-JET Workprogramme. The work included the preparation of experiments with Real-Time Control (RTC) of q and ρ_T^*.

TF-E: Tekes was strongly involved in the preparation and execution of the Task Force E experimental programme during C9–C14 campaigns under the EFDA-JET Workprogramme. The work included erosion/redeposition studies and transport of impurities in the SOL region using surface analysis methods.

TF-D: Diagnostics work included involvement in the preparation, execution and analysis of the TF D experiments relating to neutral particle analysers. Support for NPA operations in any experiments where NPA was requested.

4.1.2 Low tritium fraction ICRH physics experiments: Investigation of pT fusion with hydrogen minority heating (H-9.2-1)

Proton-Tritium (pT) fusion is a neutron-producing reaction between tritons and energetic protons with a large cross-section above 1 MeV. In prior work, it has been observed in JET through excess neutron production in purely rf-heated high-tritium fraction (>90%) plasmas during the DTE1 campaign. We have performed a systematic study of pT fusion in purely ICRF-heated plasmas in the TTE campaign. pT fusion is important for interpreting neutron diagnostics data properly in purely rf-heated plasmas containing tritium, as it causes discrepancy between broad-energy total neutron yield measurement and narrow energy-band DD and DT neutron measurements. It is also interesting, because the pT fusion yield depends strongly on the effective proton tail temperature above 1 MeV. However, measuring pT fusion yield is challenging in JET because a broad, predominantly low-energy neutron spectrum is produced. It can only be carried out through measuring the neutron excess, i.e., total yield minus the contribution from DD and DT fusions.

In the experiment, we measured the neutron excess while varying tritium input and rf power deposition in plasma (monochromatic vs. polychromatic heating). In otherwise identical pulses, the excess was found to increase monotonically with tritium input, which is strong evidence of inducing pT fusion in plasma. Less excess was observed with polychromatic heating than with monochromatic heating which is consistent with broader power deposition profile leading to less energetic proton tail. However, some neutron excess was also observed with no tritium input, suggesting that other, not tritium-related processes may also be causing excess neutron production.

4.1.3 Low tritium fraction ICRH physics experiments: fundamental and second harmonic heating of tritium (H-9.2-2/3)

The JET Trace Tritium experimental (TTE) campaign provided a rare opportunity to study ion cyclotron resonance frequency heating of tritium (T) at low concentrations in deuterium plasmas. Accelerating the T minority at its fundamental cyclotron frequency ($\omega=\omega_{cT}$) is an attractive though technically challenging heating scenario, which is currently outside the ITER rf-system frequency range but would have particular advantages during its commissioning. It requires on JET the highest equilibrium magnetic fields (3.9 to 4T) and the lowest available generator frequency (23 MHz), at which only modest levels of ICRF power are available. In TTE, tritium was introduced either by gas puffs of ~5 mg per discharge, or by beam injection (~0.2 mg in 300 ms). Although tritium increments per shot were small, after a sequence of discharges tritium concentration could be built up to levels

~ 1%. ICRF powers of 1 to 1.5 MW were coupled, producing energetic tails in the triton distribution with effective temperatures between 80 and 120 keV, as derived from the neutron emission spectroscopy data. Such energies are close to the maximum of the D-T fusion reaction rate. Increases in the suprathermal neutron emission by about three orders of magnitude were accordingly observed during the rf pulses (up to 2.9×10^{16}/s with gas puff, and 5×10^{16}/s with beam injection). The neutron emission profiles show an emission peak a few centimetres on the low field side of the T cyclotron layer, consistent with fast trapped or non-standard triton orbits grazing the latter. Comparison was made between non-directive and directive phasing (i.e. dipole, +90 and –90 phasing) of the antenna arrays, which exhibited differences in neutron emission and evidence of opposite fast ion toroidal rotation.

Discharges were also devoted to accelerating tritium at its second cyclotron harmonic ($\omega=2\omega_{cT}$), yielding fast tritons above 700 keV (deduced from gamma ray spectra).

4.1.4 Study of fast particles generated via parasitic absorption of LH power at the grill mouth (H-9.3-2)

Tekes provided a scientific co-ordinator for the parasitic experiment on observing the fast particle generation via parasitic absorption of LH power.

Parasitic absorption and the resulting fast electron generation at the grill mouth may limit the lower hybrid (LH) power at high power densities, since the fast particle beam may cause impurity influx from hot spots on the wall structures. During lower hybrid current drive (CD) experiments, series of hot spots were detected on the inner and outer divertor apron, which are magnetically connected to the LH grill region.

A CCD camera was used to observe hot spots on the divertor aprons with good spatial resolution. Since the line of sight of the CCD camera is fixed, the hot spots can only be seen at specific q_{95}-values. The Infra Red Movie Analyser, IRMA software was used to analyse the CCD videos of the pulses that showed hot spots on the divertor apron. The analysis shows clear increases in the brightness of the measuring points in the second phase of the shots.

The spots were also analysed as a function of various parameters. The brightness clearly decreases with the distance between the limiter and the LCFS. The distance seems to be the most important parameter affecting the brightness of the spots. This is beneficial for ITER, which is designed to work at a large LCFS to limiter distance. The brightness also increases with the LH power as has been seen on Tore Supra and on TdeV as well as in theoretical analysis.

4.1.5 ICRF phasing in H-mode control and phasing effects on core/edge ICRH interaction (H-10.5)

Using variable numbers of antenna straps and phasing, ICRF power absorption in plasma core was found to scale with the width of the launched $k_{||}$-spectrum and with the single-pass absorption fraction suggesting that a good heating efficiency may be possible for monopole phased heating in ITER plasma.

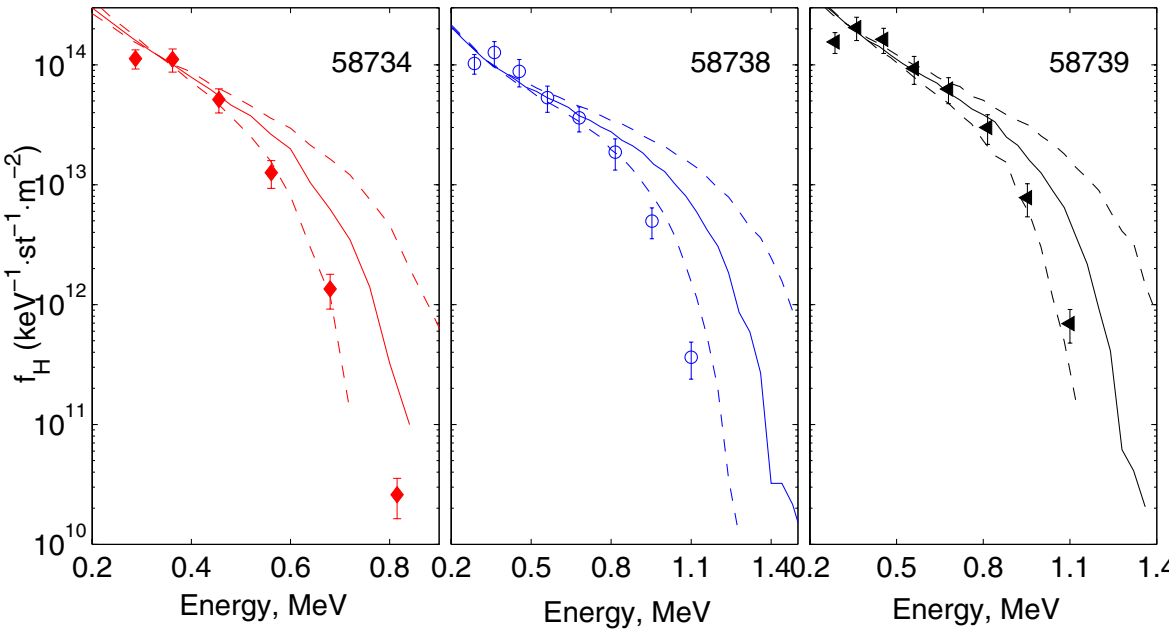

Figure 4.1: High-energy parts of the resonant hydrogen distributions. Points with error bars are the NPA measurements, full lines from the FIDO simulations and dashed lines are the estimated errors for the simulations (due to uncertainty in plasma parameters).

4.1.6 Study of finite-Larmor-radius effects with second harmonic ICRF heating of hydrogen (H-9.5-1)

The new experiments done on the JET tokamak with second harmonic ICRF heating of hydrogen in deuterium plasma have given valuable experimental data on the detailed nature of wave-particle interaction in high-energy, MeV, range. By measuring the high-energy ion energy distribution with the neutral particle analyser it is seen that above certain energy E* (here ~1 MeV) almost no ions were detected. By selecting a set of appropriate plasma and heating parameters (electron density and ICRF power most importantly) for a number of discharges this observation could be verified to be due to finite Larmor radius effects. Resonant ion distributions were also simulated with a good match with the experimental measurements. Figure 4.1 shows the final results including error estimates for the simulated distributions.

4.1.7 Predictive transport modelling of ITBs in the multi-tokamak database

The main aim in this study has been to test semi-empirical and physics-based transport models in plasmas with Internal Transport Barriers (ITBs). So far, only empirical models have been able to reproduce the time dynamics of ITBs satisfactorily. In order to obtain a consistent picture over a large plasma parameter and geometry regimes, a multi-machine experimental tokamak ITB database, called the International Tokamak Physics Activities (ITPA) ITB database, has been employed. The emphasis has been on the ITB formation and dynamics, in particular investigating the timing of the onset and the radial location of the ITB. As a consequence, the time-dependent transport simulations carried out in this work are very different from those where only the steady-state phase of the discharges are simulated.

The question of the ITB formation and dynamics is assessed with fully predictive transport modelling. By fully predictive transport modelling we mean that five transport equations (electron and ion heat, q, density and toroidal rotation) are solved. In order to obtain the most realistic and consistent understanding of the ITB behaviour, it is very important to predict also the density and toroidal rotation which are often taken from the experiments. Three pairs of high performance discharges from JET, JT-60U and DIII-D are simulated with the Bohm/GyroBohm and Weiland transport models using the JETTO transport code. One of the discharges in each pair has a low positive or zero magnetic shear whereas the other one has a negative magnetic shear. Although the ITB formation mechanisms are not known precisely, it is clear that the role of magnetic shear is significant.

The ITB formation in the original semi-empirical Bohm/GyroBohm transport model is based on turbulence suppression by the combined effects of the magnetic shear and $\omega_{E\times B}$ flow shear. In this study, the effect of Shafranov shift, so-called (α-stabilisation), has been added in the ITB formation threshold condition. The Weiland transport model includes, in addition to those mechanisms mentioned above, also turbulence suppression by the dilution effects, i.e. plasma impurities or Z_{eff}, density peaking and the effects of plasma geometry, such as elongation.

In general with the Bohm/GyroBohm model, the agreement in all transport channels with respect to the onset and radial location of the ITB between the experiments and transport simulations was good in JET and JT-60U, but not as good in DIII-D. This suggests that the mechanisms that govern the physics of the ITB may be different in DIII-D from those in JET and JT-60U, where the combined effect of the magnetic shear and $\omega_{E\times B}$ flow shear seemed to be enough to explain the behaviour of ITBs. On the other hand in DIII-D, the role of α-stabilisation turned out to be significant. This is shown in Figure 4.2 where the experimental and simulated ion and electron temperatures, electron density, toroidal rotation and the q-profile for the two of the six simulated discharges (DIII-D discharges) are illustrated. The green dashed-dotted curves represent the simulations with α-stabilisation included whereas the red dashed curves are predictions without the α-stabilisation. It can be clearly seen that the radial location of the ITBs moves closer to the experimental ones (black solid curves) when the α-stabilisation was taken into account in DIII-D plasmas. In JET and JT-60U, only minor changes were observed when including the α-stabilisation in the ITB threshold condition. Therefore, in order to reproduce ITBs within the same good accuracy also in DIII-D, the α-stabilisation had to be included into the model. In conclusion, having modelled tokamaks with different sizes demonstrated the significant role played by the α-stabilisation in governing the physics of the ITBs.

The Weiland model did not predict a clear ITB in any of the six simulated discharges. Because of this, in most of the simulations it tended to underestimate the central values of the predicted quantities, in particular the ion temperature. The effect of the magnetic shear on transport in the Weiland model is much weaker than experimentally observed or that in the Bohm/GyroBohm model. However, there is a new version of the Weiland model to be released soon, which has varying correlation lengths and a much stronger dependence of magnetic shear and q. The preliminary results with the modified model are encouraging.

The key question to be raised is how reliably we can predict the behaviour of the ITB plasmas in future devices, for example in ITER. The semi-empirical Bohm/GyroBohm model with its ITB formation threshold condition was derived empirically from JET ITB plasmas. Although it works very well in JET and in a similar size tokamak JT-60U, and

also in a smaller size tokamak DIII-D when including the α-stabilisation, it does not prove that the same modelling capability and accuracy can be extrapolated to much larger size tokamaks. On the other hand, the predictions with the physics-based transport models, like the Weiland model, are not in a satisfactory agreement even with the experimental results from the present tokamaks.

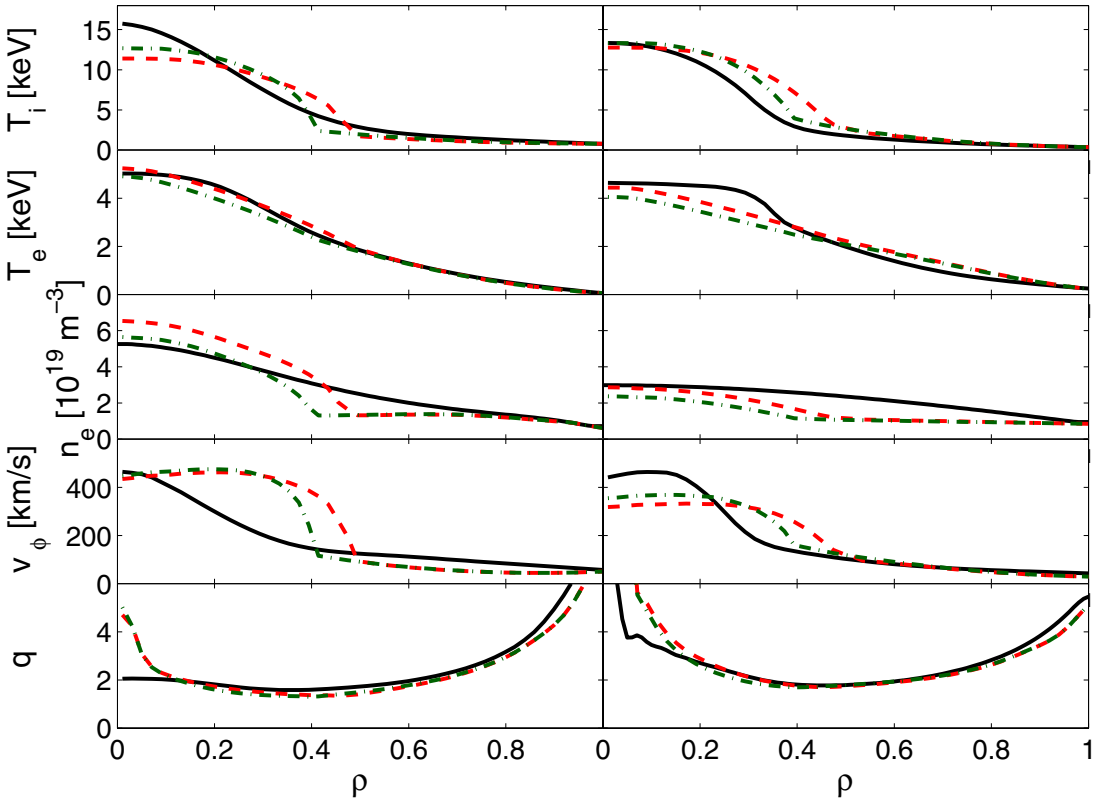

Figure 4.2: Effect of including the α-stabilisation in the Bohm/GyroBohm model for DIII-D discharges no. 34487 at t=1.85s (left) and 39056 at t=0.95s (right). The solid curves correspond to the experimental data and the dashed and dash-dotted curves to the simulation predictions with taking into account the α-stabilisation and without it, respectively.

4.1.8 Optimising the linear response matrix by means of predictive transport modelling (S2-7.1)

JETTO transport simulations have been used in the preparation for experiments with Real-Time Control (RTC) of the *q*-profile and the strength and location of the ITB, characterised by ρ_{Te}^{*}. Although plasma transport, in particular that of the ITB, cannot be described perfectly with present transport codes and models, there are several reasons why the real-time control techniques have been implemented in transport codes in parallel with the experiments. One reason is that high power RTC experiments on JET are limited to about 10s due to restrictions on the NBI power system. This is shorter or at most of the order of the resistive current diffusion time on JET and therefore, extending the simulations to pulse lengths well beyond this time is useful to further assess the validity of the control scheme for steady state operation. Another reason is that the identification of linear state-space models is difficult from the experimental data due to unsatisfactory data quality from the measurements and data pollution by the MHD events, such as ELMs and NTMs whereas the transport simulation data is free from them. As a consequence, transport simulations can be used for developing the required skills for an optimum identification scheme.

Thirdly, the transport simulations can be used in the determination of the control matrix, in view of using it also in the RTC experiments. And lastly, the transport simulations with RTC can be used to test and validate different versions of the control algorithms, with increasing degrees of completeness, before implementing them in the experimental control systems.

In this work, the linear response matrix has been found with fully predictive transport simulations where the LH, ICRH and NBI powers have been modulated. The optimum linear response matrix has been determined in steady-state conditions (steady-state of current) and as a consequence, the transport simulations have been extended beyond the experimental length of JET ITB discharges (up to t=30s). This is required because the steady-state current profile cannot be reached in the JET ITB experiments. This work is strongly linked to the fully predictive closed-loop simulations of the current and temperature profiles presented in Section 4.1.9.

4.1.9 Fully predictive simulations of current and temperature profile control in JET advanced tokamak plasmas

An important experimental programme is in progress on JET (see Sec. 4.1.8) to investigate plasma control schemes which could eventually enable ITER to sustain steady-state burning plasmas in an "advanced tokamak" operation scenario. The triggering and subsequent controllability of ITBs are major issues for fulfilling this goal. Uncontrolled ITBs are generally not stationary, as often observed on JET, and the coupled evolution of the plasma parameter profiles in high performance non-inductive discharges often leads to the premature loss of the good confinement ITB regime, or alternatively to too large pressure profiles, with major MHD events, sudden barrier collapse and/or abnormal plasma termination. Recently, a multi-variable model-based technique was developed for the simultaneous control of the current, temperature and/or pressure profiles in JET ITB discharges, using lower hybrid current drive (LHCD) together with NBI and ICRH. This Real-Time Control (RTC) scheme relies on the experimental identification, and on a truncated singular value decomposition of a linearised integral model operator.

The related algorithms have been implemented in the JET control system, allowing the use of three actuators that are the power levels of NBI, ICRH and LHCD systems. The identical algorithms to those used in the experiments have been also implemented in the JETTO transport code. This work covers primarily the progress achieved in fully predictive transport modelling of ITB plasmas when applying the real-time control algorithms in the closed-loop transport simulations to control the q-profile and the strength and location of the ITB (electron temperature and electron temperature gradient profile).

This is the first time when predictive transport simulations with a non-linear plasma model (Bohm/GyroBohm transport model) have been used in closed-loop simulations to control the q-profile and the strength and location of the ITB characterised by ρ_{Te}^{*}. All five transport equations (T_e, T_i, q, n_e, v_Φ) are solved and the power levels of LHCD, NBI and ICRH are controlled by the feedback controller matrix and the difference between the set-point (target) and simulated values of q and ρ_{Te}^{*}.

The modelling results obtained in the closed-loop simulations when applying the real-time control to the q-profile and ρ_{Te}^{*} are illustrated in Figure 4.3. In each frame, one open-loop and one closed-loop (i.e. with RTC) simulations are compared. In left frame, the set-point q-profile is monotonic and the set-point ρ_{Te}^{*}-profile is small, indicative of no ITB, and

shown by the dashed green lines. The corresponding closed-loop simulations are denoted by the red and blue solid curves, respectively. For a comparison, a reference open-loop simulation with constant power levels is illustrated by the solid black curves in each frame.

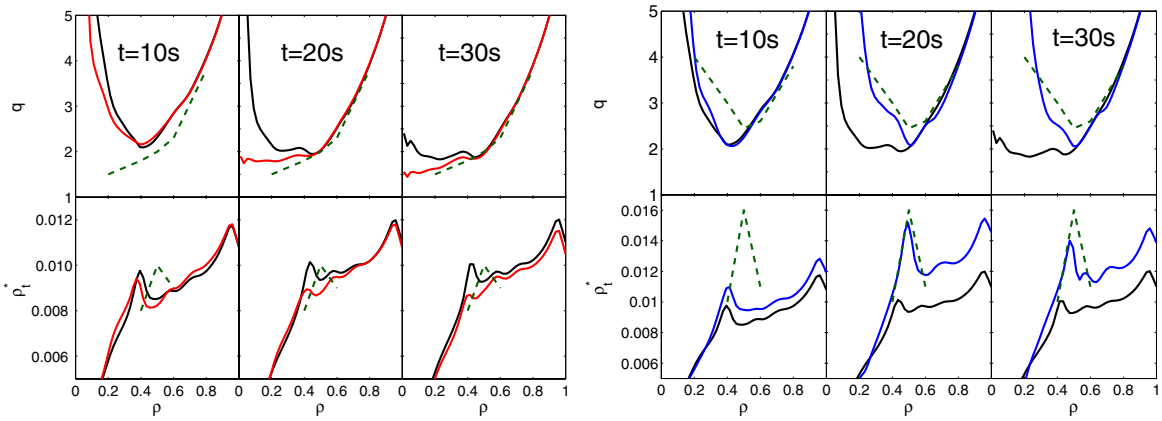

Figure 4.3: Left frame: q and ρ_t^* for the closed-loop simulation (red) together with its set-point profiles (dashed green) at three instants. Right frame: q and ρ_t^* for the closed-loop simulation (blue) together with its set-point profiles (dashed green.) The same open-loop reference simulation is shown by the black curves at three instants in both frames.

By having two extreme cases (difference between the left and right frames) as the set-point profiles, the closed-loop simulations have demonstrated that varieties of set-point q-profiles and ρ_{Te}^*-profiles are possible to achieve and control simultaneously. The time when the set-point values are reached may be of the order of the current diffusion time (~10–20s), i.e. longer than what can be experimentally achieved at high power on JET. Again, the reason for the long time to reach the set-point profiles in the simulations was that the initial q- and ρ_{Te}^*-profile were chosen quite far from the set-point profiles (extreme examples are shown here). As a consequence, smaller overall gains multiplying the controller have been used in the simulations, in order to guarantee the stability of the controller.

The fully predictive closed-loop simulations have demonstrated that the real-time control of q can be carried out successfully within the resistive current diffusion time which is beyond the experimental capabilities of JET tokamak. Within the limits of the present transport model, the simulation with the reversed q-profile and strong ITB as the set-point ρ_{Te}^*-profile (solid blue curves in Figure 4.3) also showed the way to achieve strong ion ITBs, desirable for high fusion performance. The three different simulations presented here also demonstrated the fact that the variations due to the ITB appearance/disappearance in the ρ_{Ti}^*-profiles are much larger than those in the ρ_{Te}^*-profiles. This can be regarded as an indication that the real-time control of ρ_{Ti}^* could make sense and should be feasible, at least from the physics point of view.

4.1.10 Modelling of transient transport experiments in JET

Transient transport studies are a valuable complement to steady-state transport analyses for the understanding of many transport mechanisms and also for the validation and tests of transport models. Both in the experiments and in the modelling work, transient transport has been approached with two different methods, one using modulated heating power and Fourier transform, and the other one using cold pulses generated by e.g. laser ablation or shallow pellet injection.

In this study, the JETTO transport code has been used to simulate an H-mode discharge where ICRH power modulation with mode conversion scheme (electron heating) has been employed. Both the Weiland and the Bohm/GyroBohm transport models have been tested in order to see whether they can reproduce the experimental results, in particular the amplitude and phase of the electron heat wave, i.e., the perturbative electron heat diffusion coefficient χ_e^{pert}. Both transport models tended to overestimate the steady-state electron and ion temperatures. Therefore, even though the steady state values did not directly dictate the transient transport, it was not surprising that the Fourier transforms differed from the experimental ones. Both the steady state profiles and the slightly too steep slopes of the amplitude and phase curves, given by the Fourier analysis, indicate that the models underestimated transport under the H-mode plasma conditions. There was no significant difference in the performances of the models in this case.

The JETTO transport code and the aforementioned transport models have also been used to simulate the cold pulse induced heat wave scheme. The goodness of the simulation results has been decided on the basis of the following four factors: maximum amplitude (temperature drop) profile, time-to-peak profile, time delay of propagating cold pulse and the overall agreement between the simulated and experimental temperature time traces. The results indicated that in the case of the cold pulse induced by laser ablation, the Bohm/gyroBohm transport model is able to reproduce the experimental behaviour (amplitude, time-to-peak and time delay) with a fair accuracy, whereas the Weiland model is unable to predict the cold pulse propagation observed in the experiments. The characteristic profiles for the cold pulse induced by laser ablation of JET discharge no. 55809 are presented in Figure 4.4.

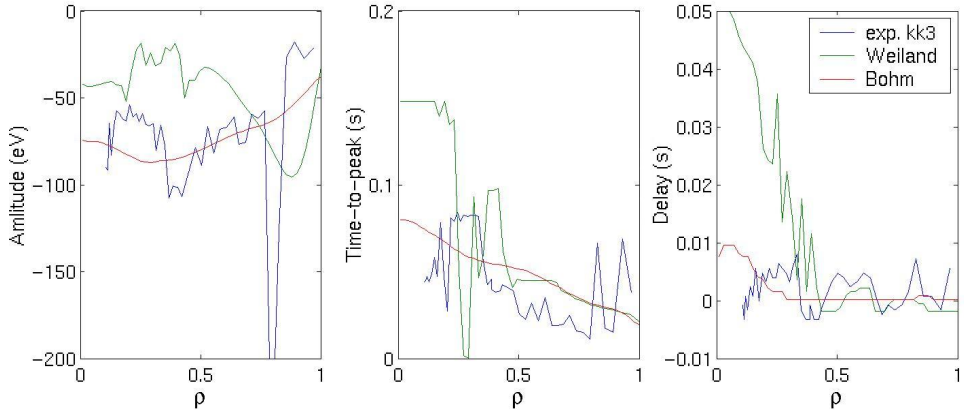

Figure 4.4: Amplitude, time-to-peak and time delay profiles for the cold pulse induced by laser ablation for JET discharge no. 55809. The blue curve corresponds to the experimental data and the red and green correspond to the simulations performed with Bohm/gyroBohm and Weiland models, respectively.

The results of the Weiland model in the central region of r/a = 0–0.5 have demonstrated the difficulties that the physics-based transport models often have in reproducing specific transport phenomena. Due to the small, almost vanishing magnitude of the amplitude, also the time-to-peak and time delay profiles become meaningless even if the time delay profile is just the profile that tells most about the transport properties of the plasma and we are thus most interested in. The same problem of not being able to reproduce the experimental amplitude of the cold wave has been met when the simulations of the cold pulses induced by the shallow pellets have been performed. The dependence of the validity on the amplitude has been taken to be a subject of forthcoming studies.

4.1.11 Integrated predictive modelling of ELM physics

An ELM occurring at the outer midplane of a tokamak results in first an electron heat pulse and later an ion heat pulse arriving first at the outer target and then at the inner target. In experiments at the JET tokamak, the propagation times of the ion heat pulse to the outer and inner targets have been measured to be about 100 μs and 300 μs, respectively.

The propagation of a heat pulse induced by an ELM localized at the outer midplane has been studied with the integrated core-edge transport code COCONUT, which is a self-consistent coupling of the 1.5D core transport code JETTO and the 2D edge transport code EDGE2D / NIMBUS. A heat pulse has been induced by increasing the perpendicular transport coefficients in the edge transport barrier on the 1D core grid radially uniformly and in the 2D scrape-off layer (SOL) radially and poloidally non-uniformly for the duration of the ELM. Poloidally, the perpendicular transport enhancement is distributed as a narrow Gaussian function peaking at the outer midplane. Parallel transport is given by the 21-moment approximation, but will in the future be calculated kinetically.

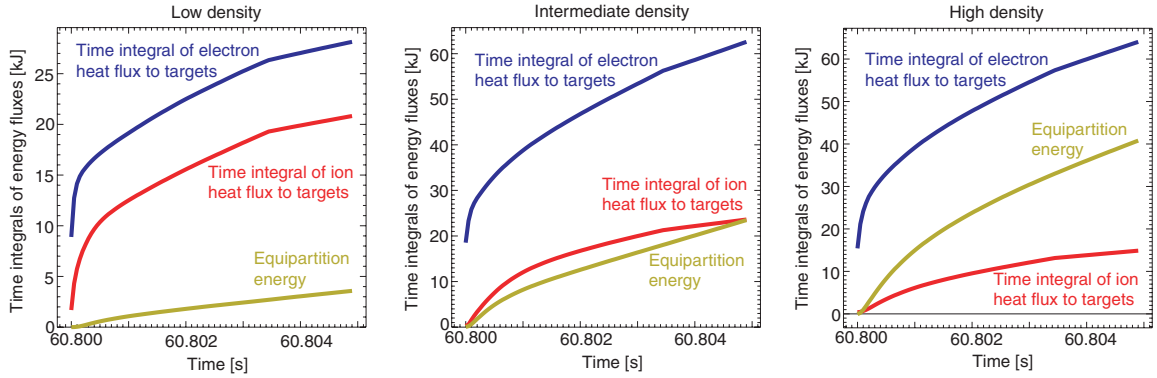

Figure 4.5: Time-integrals of electron heat flux to both targets, ion heat flux to both targets and volume-integrated ion-electron equipartition energy in three transient scenarios: low density (left-hand figure), intermediate density (centre figure) and high density (right-hand figure). An ELM of 100 μs duration is induced at the start of the 5 ms period under inspection.

It has been studied what assumptions about perpendicular and parallel transport in the SOL have to be made in order to reproduce the experimentally observed propagation times of the electron and ion heat pulses to the outer and inner targets as well the magnitude and distribution of the heat fluxes. Initial results indicate that reasonable propagation times can be obtained in simulations with relatively simple assumptions of the transport model. It has been shown that the relative amounts of ion heat going to the wall and the targets depend sensitively on the radial enhancement profiles of perpendicular transport, the parallel flux limiting factors and the density. It has also been demonstrated that ion-electron equipartition increases strongly with collisionality. It has been concluded that because of the strong sensitivity of the heat fluxes on the heat transmission coefficients, the fluid approach assuming temporally and spatially constant transmission factors is insufficient during the transient and has to be complemented by a kinetic approach. For this reason, the parallel heat flux limiting factors and sheath heat transmission coefficients are being determined in PIC simulations for relevant transient scenarios. Preliminary results indicate that these parameters vary strongly as a function of time during the transient. The kinetic results are being parameterized and included in the fluid simulations, so that more accurate results and predictions are obtained.

4.1.12 Predictive transport modelling of type I ELMy H-mode with a theory-motivated ballooning model

A theory-motivated ELM model based on linear ballooning stability theory has been developed. The model can be written as a linear differential equation for the mode amplitude of an unstable ballooning mode. The growth rate of the mode is determined by a term that becomes finite once a critical pressure gradient is exceeded. The damping of the mode is controlled by a second term that drives the mode amplitude towards the level of background fluctuations. When coupled to a transport simulation, the model can qualitatively reproduce the experimental dynamics of type I ELMy H-mode, including an ELM frequency that increases with the external heating power. It has been shown that whether or not discrete oscillations are obtained is related to how transport is perturbed radially during the ELMs and to how the pressure gradient evolves as a result of this.

4.1.13 Predictive transport modelling of type I ELMy H-mode with a theory-motivated combined ballooning-peeling model

A theory-motivated combined ballooning-peeling model for type I ELMy H-mode analogous to the pure ballooning model has been developed. In the ballooning-peeling model, two independent linear differential equations, one for ballooning modes and one for peeling modes, are solved separately and the calculated mode amplitudes are added up to give a total mode amplitude. When coupled to a transport simulation, the model can qualitatively reproduce the experimental dynamics of type I ELMy H-mode. The dynamics of individual ELM cycles has been studied. Each ELM is usually triggered by a ballooning mode instability. The ballooning phase of the ELM reduces the pressure gradient enough to make the plasma peeling unstable, whereby the ELM continues driven by the peeling mode instability, until the edge current density has been depleted to a stable level. Simulations with current ramp-up and ramp-down have been studied as examples of situations in which pure peeling and pure ballooning mode ELMs, respectively, can be obtained.

4.1.14 Interpretative modelling and MHD stability analysis of JET / JT-60U similarity experiments

During 2003 and 2004 a series of dimensionless pedestal identity experiments have been carried out at JET and JT-60U. Despite an enforced match in dimensionless pedestal parameters and the very similar dimensional parameters of the two machines, identity discharges from JET and JT-60U have very different plasma performance. In particular, the JT-60U plasmas are characterized by a higher ELM frequency and by a lower pedestal pressure and hence lower confinement than their JET matches.

MHD stability analysis of JET and JT-60U dimensionless pedestal identity plasmas with the codes MISHKA and HELENA revealed that there is no significant difference in MHD stability between discharges from the two machines. Comparable JET and JT-60U discharges often both have access to second stability. It was concluded that a difference in MHD stability is not the reason for why JT-60U plasmas generally have lower pedestal performance than JET identity plasmas.

The effect on MHD stability of varying the aspect ratio was studied separately, because the major radius is about 10% larger in JT-60U than in JET. As expected, it was found that the effect of the aspect ratio is small and thus insufficient to explain the experimentally observed differences between JET and JT-60U.

Plasma rotation was identified as another possible mechanism that could explain the different plasma characteristics of JET and JT-60U. The rotation profiles are generally quite different in the two devices. The JT-60U plasmas counter-rotate, whereas the JET identity plasmas co-rotate, among other things. Using a version of the MISHKA MHD stability code with first-order effects of plasma rotation taken into account, it was found that rotation does not significantly affect the overall MHD stability of the discharges, which goes in line with other studies. Similarly, transport analysis indicated that the effect of toroidal rotation on plasma performance is minor. It was therefore concluded that even though experiments show that plasma rotation clearly influences the performance of JT-60U plasmas, the differences in rotation between JET and JT-60U dimensionless pedestal identity plasmas cannot explain the significant differences in confinement and ELM frequency between the two machines.

With no major differences in plasma characteristics attributable to differences in MHD stability or plasma rotation, ripple losses were identified as the most likely cause. The discreteness of the toroidal magnetic field coil configuration in tokamaks shows up as ripple in the toroidal magnetic field, which results in ripple losses of both thermal and fast ions. In the H-mode, which is characterized by the formation of an edge transport barrier with a reduction of transport to a low neo-classical level, the influence of additional ion thermal transport due to ripple losses at the edge can be very discernible. JT-60U, which has only 18 toroidal field coils, is characterized by much stronger ripple (up to 3% at the outer midplane separatrix) than JET with 32 coils (about 0.1% ripple at the outer midplane separatrix). Indeed, predictive modelling with the JETTO transport code yielded results indicating that the large ripple losses in JT-60U, which result in additional ion thermal transport in the edge plasma, might explain the differences in pedestal performance between JET and JT-60U.

If the ripple-induced additional ion thermal transport is very edge-localized, the increased edge losses due to the additional transport lead to a flattening of the pressure gradient in a narrow region just inside the separatrix. This effective narrowing of the pedestal results in a lower pressure at the top of the pedestal, which due to profile stiffness translates into lower core pressure and thus reduced confinement. Thanks to increased transport inside the pedestal due to the temperature dependence of Bohm transport, the ELM frequency increases, whereby the energy and particle losses per ELM decrease. Assuming that the widths of the eigenfunctions of the unstable modes controlling the ELMs scale with the pedestal width, a further increase in ELM frequency might result from the effective narrowing of the pedestal. These mechanisms might explain the significant differences between JET and JT-60U observed in pedestal identity experiments and could potentially be used as a tool for ELM mitigation in future tokamaks.

Interestingly, further simulations indicate that ripple losses need not necessarily have a detrimental influence on confinement. A wider ripple-induced transport perturbation leads to a reduction of the ELM frequency, because the longer ELM recovery time resulting from increased edge losses becomes the dominating effect. As a result of the lower ELM frequency, the average temperature at the top of the pedestal increases, whereby the core pressure and thus overall confinement also increase thanks to profile stiffness. Indeed, an initial phase with a slight improvement of confinement was observed in previous ripple experiments at JET in 1995. Another example of an experimental result potentially attributable to a similar mechanism is the high level of confinement measured with an edge transport enhancement due to the introduction of a stochastic magnetic boundary in recent DIII-D experiments.

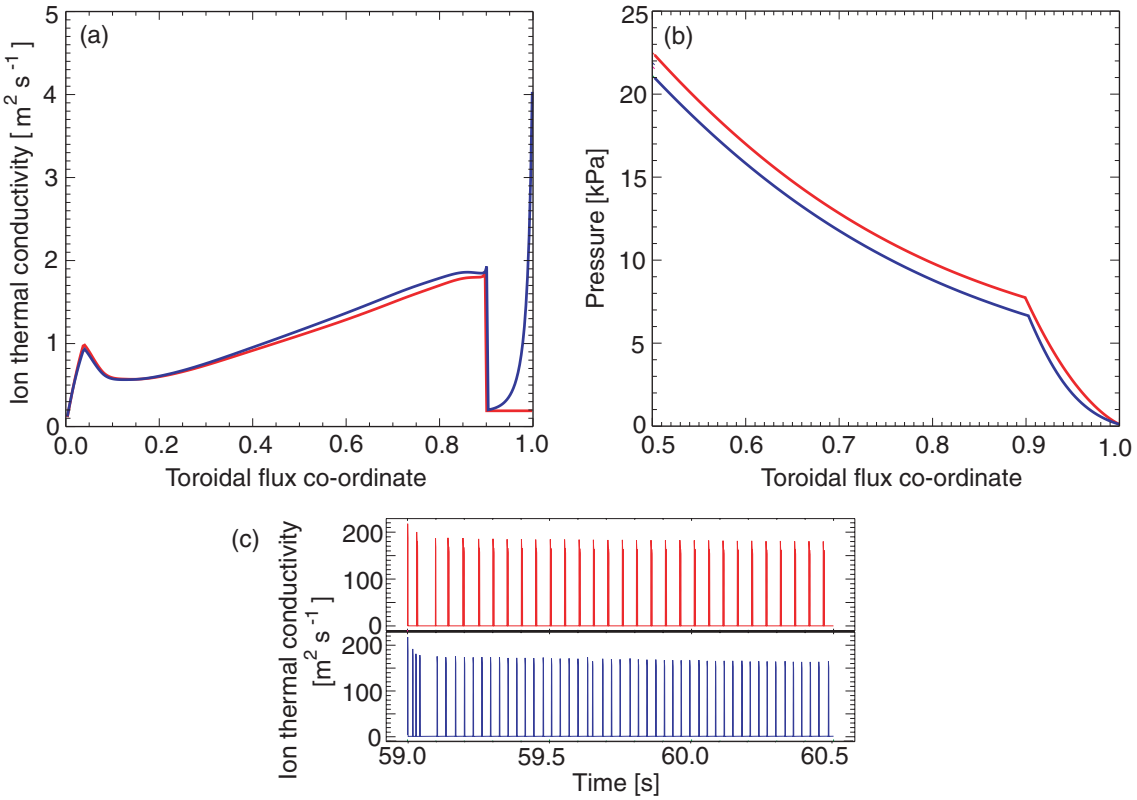

Figure 4.6: A sequence of figures illustrating the effects of toroidal magnetic field ripple localized to a narrow region just inside the separatrix. This mechanism might explain the differences in pedestal performance and ELM frequency between JET and JT-60U dimensionless pedestal identity plasmas. (a) Radial profiles of ion thermal conductivity in two predictive transport simulations with (blue curve) and without (red curve) ripple-induced ion thermal transport at the edge. (b) Radial profiles of the total pressure in the same simulations. (c) Ion thermal conductivity at a radial location just outside the top of the pedestal as a function of time in the same simulations. This gives a comparison of the ELM frequencies.

4.1.15 Predictive transport modelling of plasmas with type II ELMs

A model for mixed type I-II ELMy H-mode derived from MHD stability analysis of JET plasmas with type I, type II and type III ELMs has been used in predictive transport simulations with the 1.5D core transport code JETTO. The modelling reproduces the experimental dynamics of mixed type I–II ELMy H-mode including the right levels of confinement and energy loss per ELM and a time evolution featuring quasi-continuous tiny type II ELMs interrupted by occasional large type I ELMs. Adapted versions of the model have also been used successfully for modelling of type I and type III ELMy H-modes, reproducing the experimental dynamics of these modes of operation and explaining the experimentally observed transition from type I to type III ELMy H-mode triggered by an increase in the level of external neutral gas puffing as a transition from second to first ballooning stability. In various tokamaks, type II ELMs have been observed in discharges with strong external neutral gas puffing, with quasi double null magnetic configurations, with high poloidal beta (beta being the ratio of the total pressure to the kinetic pressure) and with combinations of high edge safety factor and high triangularity. MHD stability analysis with the codes HELENA and MISHKA performed on interpretative and predictive JETTO simulations shows that each of these situations are favourable for the occurrence of type II ELMs according to the model.

4.1.16 Simulation of NBI-ions in JET using ASCOT code and preliminary septum height studies

Simulation of slowing down distributions of NBI ions and losses of these ions in JET using the ASCOT code was started. Similar work has already been going on for ASDEX Upgrade. This work should continue and show the level and localisation of the fast beam ion losses as a function of ripple amplitude, NBI power, plasma parameters and magnetic configuration. Also, the X-point height effect was tested moving the X-point below the septum as in recent JET experiments but the scan was found to be sensitive to the boundary conditions and needs further testing.

4.1.17 ICRF mode conversion in ITB plasmas (S2-7.2)

With ICRF mode conversion using ^{3}He in D plasma, stronger barriers and higher D-D fusion yield were obtained than in equivalent discharges with H and ^{3}He minority heating, despite the relatively high ^{3}He concentration in the range of 10–20%.

4.1.18 Edge stability analysis of DOC discharges (M-1.1)

Edge plasma stability analysis of Diagnostic Optimised Configuration (DOC) discharges with the emphasis on finding the triggering mechanism for the ELMs was studied.

The edge temperature and density profiles of well-diagnosed discharges were used to create self-consistent equilibria including the bootstrap current. The stability of the equilibria was analysed to find the triggering mechanism of the ELMs in JET. It was found out that Type I ELMs are triggered when the plasma reaches the intermediate-n peeling-ballooning mode stability boundary. The edge pressure gradient is then above the first stability limit for high-n ballooning modes. Increasing gas puffing or decreasing heating power in the experiment has been found to cause a transition to Type III ELMs. In the stability analysis, it was found that in discharges with increased gas puffing or decreased heating power, the edge plasma pressure gradient becomes limited by the high-n ballooning mode stability boundary at a considerably lower pressure gradient value than that given by the intermediate-n stability boundary in Type I plasmas. This change in the edge stability properties can explain the transition between the ELM types, different ELM behaviour between Type I and Type III ELMs. The reason for the different stability properties is due to the higher collisionality in Type III ELMy discharges. The high collisionality reduces the edge current (both bootstrap and ohmic) and closes the second stability access for high-n ballooning modes.

4.1.19 Neutral particle analysers

In JET two neutral particle analysers (NPA) are installed. The high energy NPA (GEMMA-2M, diagnostic ID: KF1, Figure 4.7) is installed on top of the JET machine and has a vertical line-of-sight. It can be configured to measure one ion species on eight energy channels with energy of 250–1600 keV for hydrogen isotopes and up to 3500 keV for He. The low energy NPA (ISEP, diagnostic ID: KR2, Figure 4.8) has a horizontal, radial line-of-sight through plasma centre. It measures simultaneously all three hydrogen isotopes on a total of 32 channels. The energy range can be configured from 5 keV to 750 keV (for H) by varying the electric and magnetic fields within the diagnostic. The diagnostic hardware as well as all data collection electronics has been supplied to JET by Ioffe Institute, St. Petersburg.

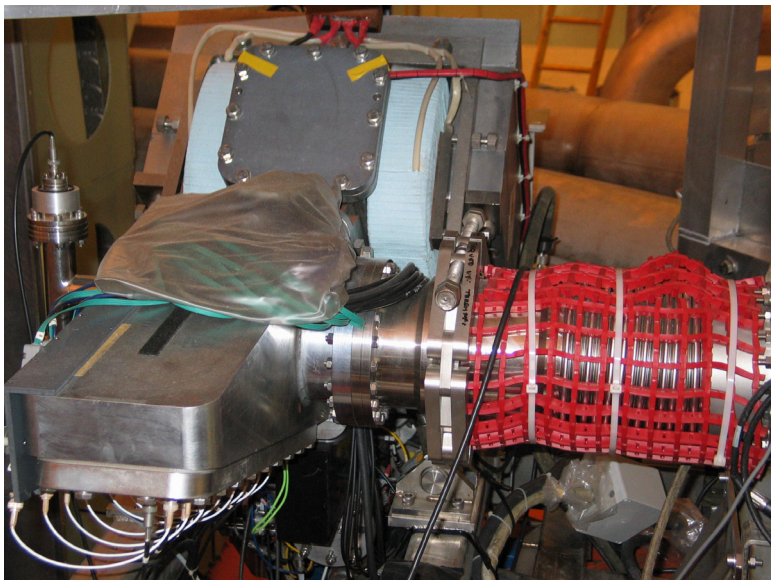

Figure 4.7: High-energy NPA. Detector assembly in front, 90 degree bending magnet at back, vacuum pumps on right. Atoms enter the diagnostic from below the magnet, are ionised by a thin carbon foil, are mass- and energy-separated by the magnet and an electric field, and finally detected by scintillator detectors within detector assembly.

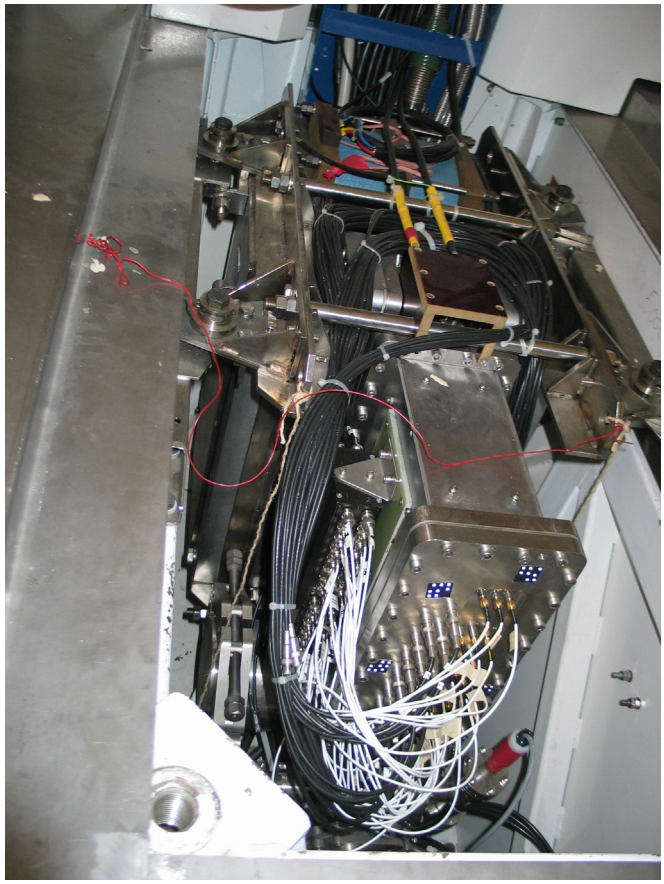

Figure 4.8: Low-energy NPA (KR2) within its radiation shielding box. Atoms enter diagnostic near bottom of the image, and are bent by the magnet through 180 degrees. Detector assembly near camera with preamplifiers attached to side.

Tekes has provided technical support for operating and maintaining the JET NPAs. The NPAs had suffered from manning problems earlier and were underutilised in JET experiments. During the campaigns in 2004 requests for NPA operation were frequent. In particular, Taskforce H has requested NPA operation in most of its experiments. During the long shutdown period started in 2004, broken components have been replaced and recalibration is planned for the restart in 2005. Substantial amount of administrative work has been caused by this as the work has involved breaching vacuum boundary which is connected to the main torus vacuum.

Software development for processing NPA data has continued. New tools have been developed for easy viewing of the data in Matlab environment, to replace command-line oriented Fortran codes. Codes are also being developed for post-processing the atom flux data and for long-term monitoring of the diagnostic performance.

4.1.20 Validation of plasma isotopic composition (D.11.1.3)

The purpose of the experiment was to study the plasma isotopic composition by all available diagnostics while performing a gradual changeover from 100% deuterium (D) plasma to 100% hydrogen (H) plasma. Furthermore, pulsed H puffing into D plasma and D puffing into H plasma was carried out to evaluate the capability of the KR2 NPA to measure ion transport in plasma. The experiment was carried out by starting from pure deuterium plasma and by pulsing the hydrogen gas valve several times during the plasma discharges to increase the hydrogen concentration while maintaining constant neutral beam heating power. This allowed the collection of NPA data from plasmas of varying hydrogen concentration, and this can be compared with spectroscopic measurements. Due to the prior failure of the active Alfvén Eigenmode Diagnostic (AEAD) it was not possible to carry out the planned cross-correlation between AEAD and NPA. The well-defined hydrogen and deuterium pulsing permitted, in principle, the study of pulse diffusion into plasma, however, the quality of this data was below expectations because the limited available heating power prevented reaching high enough plasma temperature.

The main heating mechanism employed was neutral beam heating. After the long NBI phase a shorter pulse of ICRF heating (2nd harmonic H) was applied. On some pulses, LH power was applied as well. This allowed a study of the effects of different auxiliary heating methods to neutral particle signals.

4.1.21 Erosion/deposition and transport of impurities (E-3.1; E-12.4)

Tekes participated in Task force E with the competence of plasma wall expert (PWE). The main aim of the work has been to study erosion/redeposition of divertor materials, impurity transport in SOL and long term tritium retention.

Prior to the 2004 shutdown, an experiment was devised to provide specific information on material transport and SOL flows observed at JET. $^{13}CH_4$ and $B(CH_3)_3$ were injected into the plasma boundary from the outer divertor in the last day of discharges using one type of discharge only. The purpose of the experiment was to determine how the ^{13}C and boron are transported around the SOL, and where they are eventually deposited. The amount of puffed ^{13}C was about 3 times bigger than during the previous ^{13}C puffing experiment in 2001. The amount of boron was comparable to the amount of puffed Si in 2001. Boron was detected spectroscopically at the outer divertor. Preliminary post-mortem surface analysis has shown that there is ^{13}C deposited on the collector probe.

4.1.22 Material transport and erosion/deposition in JET torus

Institute:	**VTT Processes (VTT PRO)** **Helsinki University**, Accelerator Laboratory (UH AL) **Helsinki University**, Department of Chemistry (UH CHE) **JET/UKAEA**
Company:	DIARC Technology Oy
Research Scientists:	Dr. J. Likonen (VTT PRO, Project Manager), Dr. E. Vainonen-Ahlgren (VTT PRO), MSc. T. Renvall (VTT PRO), MSc R. Zilliacus (VTT PRO), Prof. J. Keinonen (UH AL), Dr. K. Arstila (UH AL), Dr. Leonid Khriachtchev (UH CHE), Dr. P. Coad (JET/UKAEA), MSc. J. Kolehmainen (Diarc), MSc. S. Tervakangas (Diarc)
EFDA Task:	JW4-FT-3.15

Background

Experiments with the Mk I divertor in JET in 1994–1995 demonstrated that much of the carbon responsible for co-deposition in the divertor is sputtered from the walls of the main chamber, even though the primary plasma contact areas are in the divertor. However, the main areas and the amounts of erosion around the chamber walls have not yet been ascertained. Results obtained under previous JET TF-FT tasks show that inner wall guard (IWGL) and outer poloidal (OPL) limiters are not the main erosion source. Some areas on IWGL tiles have very thick deposits (> 10 μm) whereas the amount of erosion is less than 10 μm. Also, it is not known how much erosion takes place in the outer divertor where erosion is expected, and to where such eroded material is transported. To try and answer these queries, a set of tiles with a C+10% B layer on a Re interlayer were installed in the Mk IIGB divertor, together with inner guard limiter and outer poloidal limiter tiles during the 1999 shutdown. A small amount of erosion results in thinning of these layers, and for regions of deposition, the Re layer acts as a marker to determine the original surface when profiling through the deposits. These tiles were removed in the 2001 shutdown, and analysed to determine the erosion/deposition profile over the entire divertor cross-section and at a selection of points around the walls of the main chamber. Surface analyses have, however, shown that C+B layer have been eroded completely at outer divertor indicating that thicker coatings are required.

Surface analysis of JET tiles and sample handling

The batch of MkIIA tiles delivered to VTT contained two divertor inner wall and two floor tiles. Hardware design of the secondary ion mass spectrometry (SIMS) instrument and the tandem accelerator used in the characterisation work require the sample size be below 20 mm in diameter. So, the CFC tiles were sampled in a glove box using a drill saw to cut cylinders of 17 mm diameter at the marker stripe. Pieces of about 10 mm high were cut from the core samples.

SIMS analysis was made with a double focussing magnetic sector instrument (VG Ionex IX-70S). A 5 keV O_2^+ primary ion beam was used. Some selected SIMS samples were measured with time-of-flight elastic recoil detection analysis (TOF-ERDA) technique to obtain elementary concentrations at the near surface region. In the measurements, the 5 MV tandem accelerator EGP-10-II with a 43 MeV beam of $^{79}Br^{8+}$ ions was used. Tiles

have also been analysed by nuclear reaction analysis (NRA) and Rutherford backscattering spectrometry (RBS) methods with 2.5 MeV H^+ ions at the University of Sussex.

Erosion and deposition

The analysed MkIIA tiles did not have any marker coatings and therefore it was not possible to investigate possible erosion. The analysed tiles have areas of net deposition. Thicknesses of the deposits were obtained to be below 10 μm at the inner divertor wall. Analysed floor tiles had somewhat thicker deposits the maximum thickness being about 30 μm.

Figure 4.9 shows SIMS depth profiles from centre of inner divertor wall tile 3. There is a deposit with thickness of about 7 μm. Deposit contains quite high amounts of H, D, Be (Be/C ~ 1) and O. No double layer structure found on MkIIGB divertor tiles was observed on MkIIA tiles.

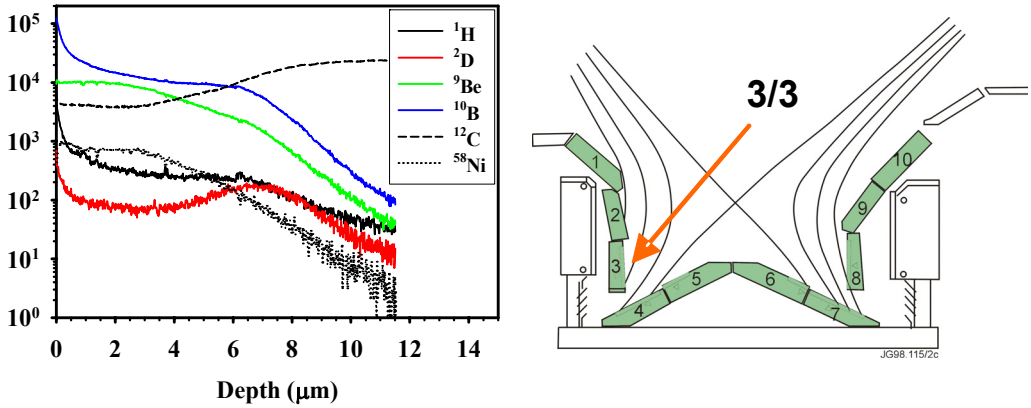

Figure 4.9: SIMS depth profiles from centre of inner MkIIA divertor wall tile 3 and MkIIA divertor.

Unexpectedly, the combination of analysis techniques has demonstrated that the nature of the deposition at the inner divertor changed from that previously seen at JET at some point towards the end of 1999–2001 experimental campaign. SIMS analyses have shown a double layer structure in the deposits on the inner MkIIGB divertor wall tiles; C-rich layer on the surface and a Be-rich layer underneath. The reason for the change in the composition is not yet known and one possibility could be the temperature decrease of JET main wall in December 2000 which may have decreased chemical erosion of carbon. Moreover, IBA and SIMS analyses have shown that Be/C ratio in the deposits on IWGL tiles is clearly lower than on the inner divertor wall tiles and no double layer structure in the deposits was observed. The double layer structure and high Be content in the deposits on the inner divertor wall tiles are thus specific for the divertor. If the temperature is responsible for the outer layer, then there should only be a single Be-rich layer on earlier divertors such as the Mk IIA. The results obtained under this task support this view.

W coated marker tiles installed in 2001 were removed from JET at the end of 2004. Visual inspection shows that the outer baffle tile is almost intact with no damage (see Figure 4.10). The W coating has survived on the outer strike point tile and visual inspection indicates that in some areas it appears buried under a layer of carbon. Thorough characterisation of the W coated tiles will be done on 2005.

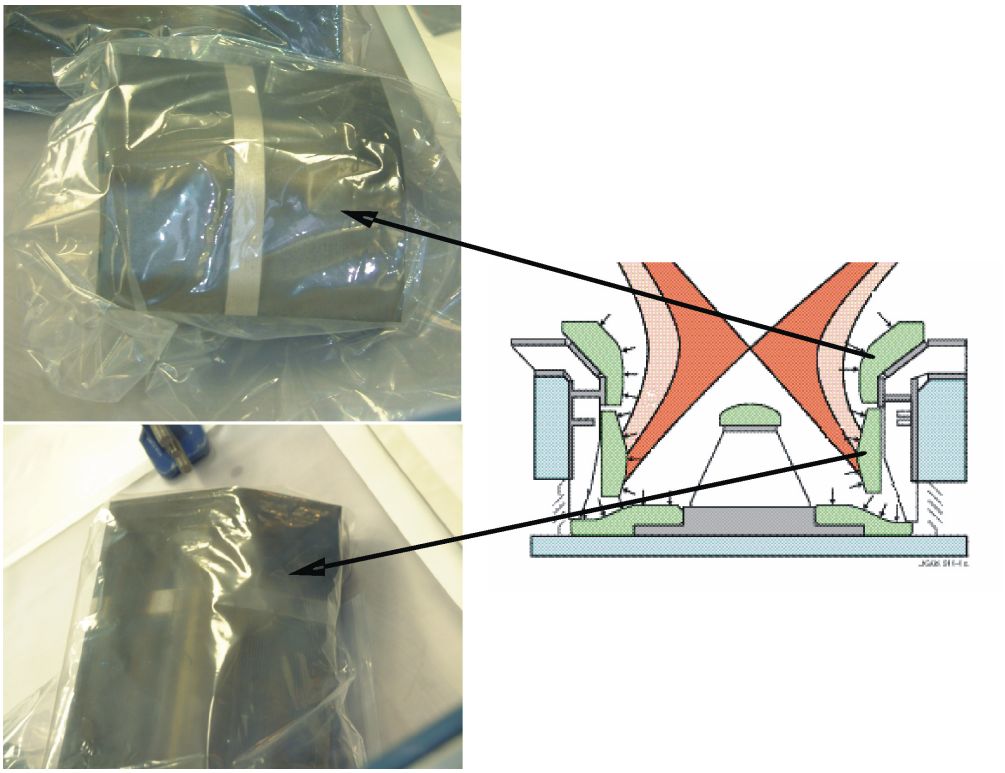

Figure 4.10: W coated marker tiles after exposure in 2001–2004 at JET.

New marker tiles

Surface analyses of the coated tiles with C+B and Re marker layers exposed in 1999–2001 showed that in the erosion dominated areas the C+B marker layer had been eroded completely and that the erosion front was in the Re marker layer. Re has much lower erosion rate than C which indicates that erosion of C from uncoated areas may be larger than 2–3 µm. In order to attempt a better quantitative balance between sources and sinks in JET, several divertor and wall tiles have been coated with 10 µm thick C layer and 3 µm thick W layer, each of which can give a definitive value for the local carbon and tungsten erosion.

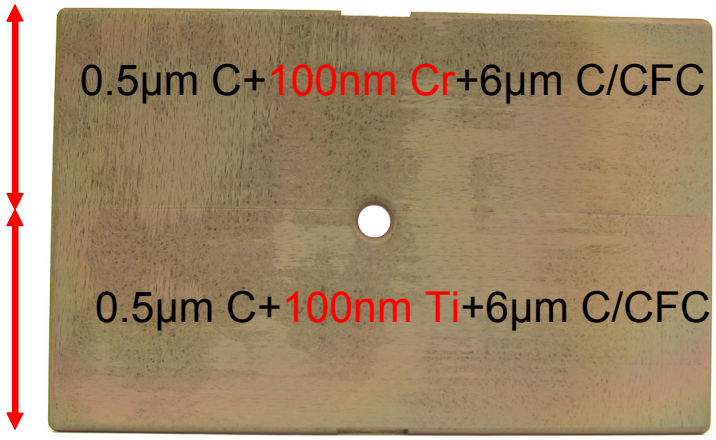

Figure 4.11: Coated inner wall marker tile for in-situ erosion studies.

For in-situ erosion studies one inner wall cladding tile (see Figure 4.11) has been coated with C, Cr and Ti marker layers. One KS3 spectrometer fibre with horisontal line-of-sight looks at this tile and when the topmost C layer has been eroded, aim is to measure emitted light from the Cr and Ti marker layers.

In addition to marker coatings for erosion and deposition studies, several tiles for ITER-like wall project have been coated with Re and W with various thicknesses. Aim is to investigate how well Re and W coatings can withstand high heat loads at the neutral beam injection (NBI) shine-through, re-ionisation and load bearing septum replacement areas.

4.1.23 Other JET related activities

Development of the JAMS integrated modelling suite

In 2004, a major code integration project was launched at JET with the aim of providing graphical user interfaces and common standards for input and output for a number of mainly transport and MHD stability codes used on site. This integrated suite of codes is known as JAMS (JET Application Management System). Currently, JAMS features graphical user interfaces for the core transport codes JETTO, CRONOS and ASTRA, the edge transport code EDGE2D, the MHD stability codes HELENA and MISHKA and the gyrokinetic microturbulence code KINEZERO as well as a number of tools for data preparation, manipulation and storage. Association Euratom-Tekes has been heavily involved in developing the graphical user interfaces for the HELENA and MISHKA MHD stability codes and in developing advanced features such as ELM, transport and rf heating models and applications for the JETTO transport code, which is being improved with sophisticated features on a continuous basis.

JETTO/FRTC development

A model to take into account the wave scattering from the density fluctuations has been developed for the FRTC ray-tracing code. This is expected to help in smoothing the peculiarities of the LH power deposition profiles. Currently, the radial deposition profiles often have two peaks, which is believed not to be the case in reality. The model is a rotation of the wave vector in the plane perpendicular to the magnetic field and makes use of Monte Carlo technique. The tokamak geometry makes the calculation slightly complicated. The analytic work has been performed. The model will be included in the FRTC ray-tracing code used in JETTO transport code, which is used for modelling lower hybrid power deposition. The FRTC package is quite large and poorly documented. Therefore, a lot of effort has to be put in understanding the code before it can be modified.

Modelling of LH power and current

Modelling of JET discharges has been started. A set of three pulses with different scenarios to obtain negative shear has been chosen for this work. The effect of the LH driven current on the current profile and the q-profile has been studied. The work will continue with comparing the results to other scenarios to obtain negative shear. The first pulse, which is a pulse with LHCD in the preheat phase has been modelled. The two other shots, one with ohmic heating and a fast current ramp in the preheat phase, and another with strong NBI heating, will be studied later and compared to the first pulse. The effect of edge density profile was studied in a few simulations. The lower edge density had a small effect on the current profile. A reduction in the edge electron temperature seemed to slightly fill in the hole between the two peaks in the radial LH current profile.

In another study, which was done in collaboration with CRPP, the effect of the density profile, the temperature profile and the q-profile on the deposition and current profiles was studied. The density profile was varied from a very flat one to a highly peaked one. In this case too, the effect of the density on the power deposition profile was much smaller than expected.

In a third study, the fast wave current drive experiments H-7.2 were supported by modelling the effect of the driven FWCD on the *q*-profile evolution with JETTO transport code. In addition, LHCD has been modelled for various experiments in order to see its effect on the *q*-profile evolution.

4.2 Participation in AUG Programme 2004

4.2.1 ELM stabilization with impurities

Impurities in the plasma edge increase the effective charge (Z_{eff}). This in turn lowers the bootstrap current driven by the steep pressure gradient at the edge transport barrier. In the stability analysis it was found that since the ELM-triggering instability is caused by a combination of pressure driven ballooning modes and the bootstrap current driven peeling modes, the decrease of the bootstrap current tends to stabilise the plasma against ELMs. This can be one of the factors in explaining why quiescent H-mode with its usually higher Z_{eff} than a normal ELMy H-mode does not display ELMs.

4.2.2 The effect of the core pressure on the edge stability

In the advanced tokamak (reversed or low central shear) operation, the core pressure of the plasma increases significantly from a normal H-mode level due to the formation of a internal transport barrier. In the stability analysis, it was found that if the core pressure does not increase too much (and trigger an internal mode), the increasing core pressure can have an indirect stabilising effect on the ELM-triggering edge instabilities in highly triangular plasmas. The Shafranov-shift caused by the high core pressure squeezes the flux surfaces closer together on the low-field side of the tokamak. On the high-field side, the flux surfaces move further away from each other. The net effect on the edge is that the bootstrap current is reduced. This, combined with the increase of the "favourable" average curvature due to the shift, stabilises the ELM-triggering low- to intermediate-n peeling-ballooning modes.

The amount of bootstrap current required for the destabilisation of the mode was found to increase as the global β_p is raised. The improved stability against the ELM-triggering instabilities can explain the higher edge pressure pedestal that has been observed during high β_p operation for instance in JT-60U.

4.2.3 Characterisation of AUG wall tiles and plasma facing components with surface analytical techniques

Institute:	**VTT Processes** (VTT PRO) **IPP Garching** /ASDEX Upgrade Team (AUG)
Company:	**DIARC Technology Inc.**
Research Scientists:	Dr. E. Vainonen-Ahlgren (VTT PRO, Project Manager), Dr. J. Likonen (VTT PRO), MSc. T. Renvall (VTT PRO), Dr. V. Rohde (AUG), Dr. M. Mayer (AUG), MSc. J. Kolehmainen (Diarc), MSc. S. Tervakangas (Diarc).

Introduction

Erosion and re-deposition are issues of major importance for ITER in that the rate of erosion of the divertor targets and building up of deposited films (and the T retained therein) may ultimately limit the choice of divertor materials and the operational space for ITER. Moreover, carbon deposition in nowadays tokamaks has been observed to be much higher at the inner than outer divertor. The reason for this asymmetry is unclear. A possible explanation might be a drift in the scrape-off layer (SOL) from outboard to inboard side. This work is a close collaboration with IPP under the Task Force IV (Divertor Physics and First Wall Materials), and focuses on experimental investigation of material transport in SOL and the study of in/out asymmetries in divertor deposition.

For the operational campaign in 2003 a set of AUG divertor tiles were coated with poloidal carbon stripes on the top of marker rhenium layer. This set of tiles was installed in the AUG divertor during the shutdown in end of 2002. The stripes were deposited by the company DIARC Technology Inc. using the DIARC plasma method. A carbon and rhenium beams were created by plasma generators and masked tiles were exposed to it while being rotated in a rack. The deposition was carried out in vacuum at room temperature.

Results and Discussion

The poloidal carbon stripes on rhenium interlayer were deposited on 11 AUG tiles by DIARC Technology Inc. using the Diarc® method and sent to IPP Garching for ion beam analysis. The thickness of the coating (3μm) has been determined using profilometry. The major impurities (Fe, Cr, Ni) have been analysed using various ion beam techniques.

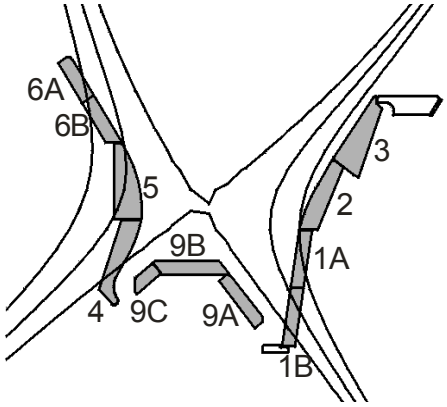

Figure 4.12: Sketch of divertor IIB together with the magnetic surfaces. Numbers correspond to the divertor tile numbers.

Sketch of divertor IIB together with the magnetic surfaces in presented in Figure 4.12. Numbers correspond to the divertor tile numbers. In the end of the campaign $^{13}CH_4$ was puffed into the torus from the outer mid-plane during 13 identical bottom single null H-mode (ELM type I) discharges.

For ^{13}C ex-situ profiling secondary ion mass spectrometry (SIMS) was utilised. Detailed distribution of ^{13}C together with strike point position from magnetic reconstruction during last 13 shots of the campaign as a function of s-coordinate is presented in Figure 4.13. S-coordinate represents the distance from the top of the inner divertor along the surface of the tiles and describes poloidal positions (s = 0 corresponds to the top edge of tile 6A). ^{13}C peaks are observed on tiles 6A (s = 0.05 m), 4 (s = 0.48 m) and 1B (s = 1.07, 1.09 and 1.15 m). The

peaks on the tiles 4 and 1B are shifted toward the roof baffle with respect to the inner and outer strike points, respectively.

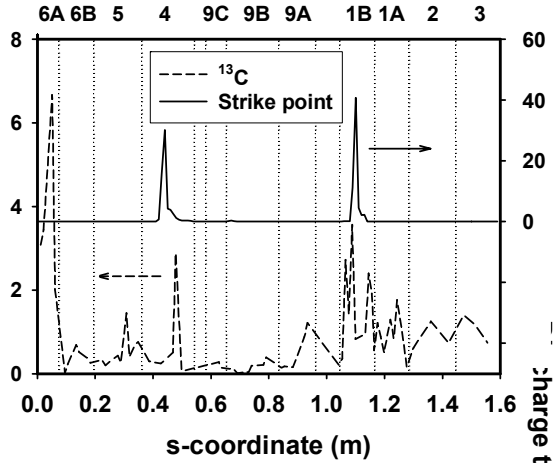

Figure 4.13: ^{13}C distribution at the divertor (dashed line) together with strike point position from magnetic reconstruction during last 13 shots (solid line).

A peak at s = 1.15 m might be associated with area shadowed by the neighbouring tile 1A. A small bump detected on the roof baffle at s = 0.93 m (tile 9A) could be caused by ^{13}C particles escaped from tile 1B after being deposited there.

A very high peak of ^{13}C was observed at the top of the tile 6A (Figure 4.13). The amount of ^{13}C transported to this place corresponds to 59% of total ^{13}C detected on the inner divertor. However, no similar accumulation of ^{13}C at the top part of the outer divertor was detected. It might be explained by the higher drift of the SOL particles from the outer mid-plane to inboard than to outboard.

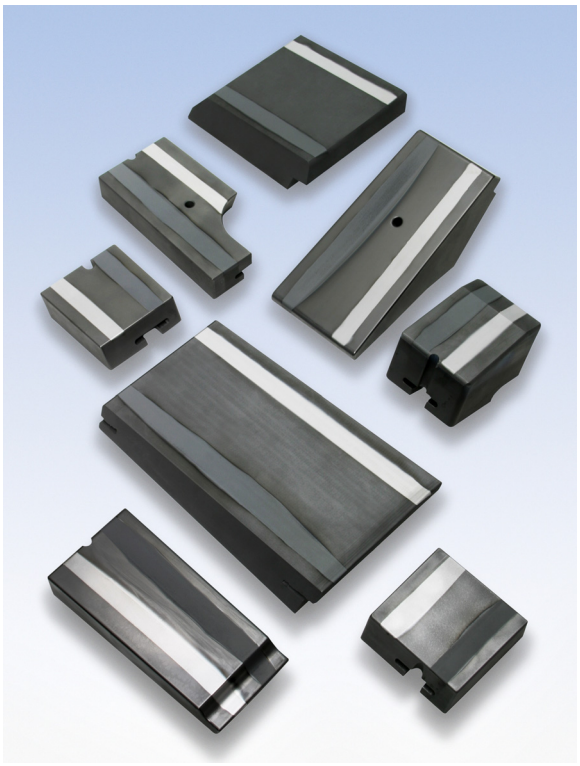

Figure 4.14: C- and W-coated AUG upper divertor tiles.

Our data demonstrate the total amount of ^{13}C transported to inner divertor is a factor of 1.5 smaller than the one found at the outer divertor. In this experiment ^{13}C is primarily transported by the plasma along field lines. However, subsequently it migrates (erodes and redeposits) in small steps to positions where there is no further erosion. The time scale of the experiment was very short that ^{13}C (attributed with the main chamber) would be re-eroded and redeposited many times. So the re-eroded/redeposited ^{13}C does not travel around the torus.

The poloidal carbon stripes (of 3 μm thick) on rhenium interlayer (about 300 nm thick) and tungsten stripes (of 1 μm thick) were deposited on upper divertor tiles by DIARC Technology Inc. using the Diarc® method (see Figure 4.14). This set of tiles was installed in the AUG divertor during the shutdown in end of 2004.

4.2.4 Comparative study of ELM dynamics at TCV, AUG, and JET

The dynamics of ELMs was studied by analyzing ELM interval time series in order to find out whether ELMs are dominantly chaotic or random. In a chaotic operating regime chaos control algorithms could in principle be used to control ELMs by small perturbations of appropriate control parameters. In the non-chaotic case no control is possible, but random ELMs can still be described by their statistical properties.

Three types of methods were used:

1) methods that search for the so-called unstable periodic orbits (UPOs),
2) linear and nonlinear predictors,
3) methods that calculate various characteristic numbers of the time series, such as Hurst exponent, block entropy and Lyapunov exponents.

Common to all methods is that results obtained for experimental time series are compared to results for so-called surrogate series. The surrogates are created by randomly reordering the original time series which preserves the statistical properties of the time series but erases any structure stemming from the dynamics of the system. A significant difference in the results for experimental and surrogate data would therefore tell apart chaos and randomness.

The ELM dynamics studies began as search for UPOs on JT-60U tokamak in 1999 and continued on TCV tokamak in 2001. Especially in the latter study a significant number of UPOs indicating chaos was found. Motivated by this result a similar study was initiated on ASDEX Upgrade. ELM time series were searched for UPOs using two methods also used in the TCV study, namely the recurrence method and the fixed point transform. Mostly the results were negative: only five time series out of almost 300 analyzed contained significant numbers of UPOs.

Further research on the ELM time series of ASDEX Upgrade was done by applying various linear and nonlinear predictors, including the state-space prediction and state-space averaging methods. Hurst exponents of the time series were calculated using rescaled range analysis, and the largest Lyapunov exponents of the series were evaluated. Block entropies of the series were calculated using a reading procedure called lumping, which is optimal for detecting chaos. The results obtained were generally negative for chaos. The block entropy method revealed vague hints of chaos in only two of the 25 series analyzed, and the other methods showed no significant indication of its existence at all.

Another approach to the problem, the autoregressive moving average (ARMA) model, was studied in collaboration with University of Latvia. We had a visit from Dr. Guntars Zvejnieks from Institute of Solid State Physics, University of Latvia. Dr. Zvejnieks has extended the study also to ELM time series from JET. In the ARMA model ELM dynamics is assumed noise-dominated, i.e. random, and ELMs are described only by their statistical properties. It is not possible to control noise-dominated systems, but ARMA could be used for simulation and possibly for short term predictions.

4.2.5 Fast ions in the AUG edge pedestal region

In standard H-mode, the edge MHD behaviour, notably individual ELM events, can lead to unacceptable loads to plasma-facing component. In the so-called Quiescent H-mode (QHM) more continuous, benign MHD behaviour called Edge Harmonic Oscillations (EHO) is observed. This MHD activity has all the desired properties: it facilitates density control and impurity exhaust while leaving the good core confinement intact. It is not clear what is the trigger for EHO, neither is it understood what suppresses the ELMs. However, since QHM has been obtained so far only with counter-injection of neutral beams fast ions probably play a role.

Until summer 2004 the interpolation algorithms used to obtain magnetic backgrounds for ASCOT calculations were too inaccurate to reliably evaluate NBI slowing down distributions. A sufficiently accurate interpolation algorithm is now in use, and the fast ion distributions are being evaluated for different discharges in ASDEX Upgrade.

To find if the fast ions have a significant role in the edge MHD behaviour, their distributions are modelled for standard H-modes (with co-injection of the neutral beams) as well as for QH-modes. A pair of simulations, carried out for a QHM-shot and a 'virtual' shot obtained by switching the sign of both the toroidal field and plasma current in the code, Figure 4.15, shows the principal difference between co- and counter-injection: with counter-injection there exists a significant fast ion population in the edge pedestal region, while no such population is formed with co-injection. This population could have a significant impact on the edge MHD stability properties.

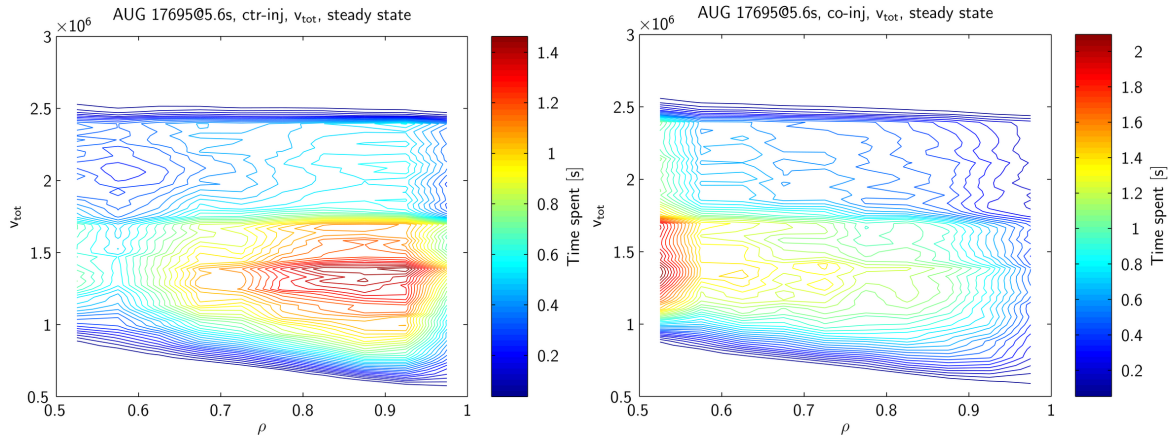

Figure 4.15: The velocity distributions given by ASCOT simulations for (a) co-injected and (b) counter-injected ions in ASDEX Upgrade edge region. The counter-injection is found to provide a much larger fast ion population in the pedestal region.

According to the current understanding of ELMs, they are a result of a peeling-ballooning type of an instability. The peeling mode is a current-driven mode and, thus, if the fast ions affect the edge current distribution, they can also affect the onset of an ELM. In

Figure 4.16 the parallel current due to the finite orbits of NBI ions are shown for co- and counter-injected beams. For counter-injected beams the NBI contribution to the edge current is neglibible in the pedestal region ($\rho > 0.9$), where also the ELMs disappear for this injection direction.

To quantitatively show that the fast ions affect the edge MHD behaviour, the distributions obtained are used as input to MHD stability codes. To this end, ASCOT now provides the fast ion distributions in four dimensions (2 spatial and 2 velocity coordinates) and in general enough form to be used by the stability codes.

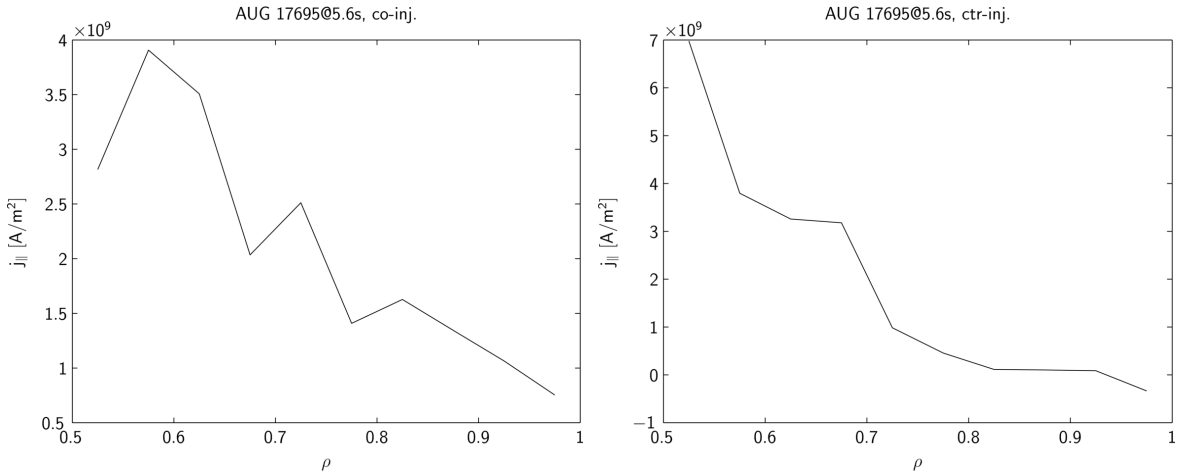

Figure 4.16: The parallel current given by ASCOT simulations for co-injected (a) and counter-injected (b) ions in ASDEX Upgrade edge region. The amount of parallel current driven by counter-injection is found negligible in the pedestal region.

4.2.6 Erosion of the poloidal limiter by fast ions

Measurements of tungsten erosion at one of the outboard limiters of ASDEX Upgrade suggest that fast particles play an important role. The fast particle loads (fluxes and energy distribution) on the limiter were simulated using ASCOT. The results were in qualitative agreement with the measurements, but it was concluded that the model used for the toroidal ripple in ASCOT is too simplistic. Thus a project to create a numerical, divergence-free ripple model was initiated.

4.2.7 Simulation of material transport in SOL

Plasma-induced erosion of first-wall components and divertor tiles as well as tritium co-deposition with carbon are critical issues concerning ITER. Extensive experimental and modelling campaigns are being carried out in order to gain understanding of these related issues.

ERO is a 3D Monte Carlo simulation code originally developed at IPP, presently at Forschungszentrum Jülich (FZJ), Germany, for modelling erosion, migration and redeposition of impurities in the vicinity of solid surfaces in magnetic fusion devices. The code follows the motion of test particles sputtered from the surface due to the impinging background plasma ions. Several atomic and molecular processes like dissociation, ionization and compound formation are taken into account. As a result, the code returns the erosion and redeposition rates of different elements over the surface as well as detailed spectroscopic data for comparison to experiments. While the ERO code has a long history

in the simulation of limiter-type experiments like TEXTOR, a version suitable for divertor machines was developed only recently and has so far been limited to two spatial dimensions.

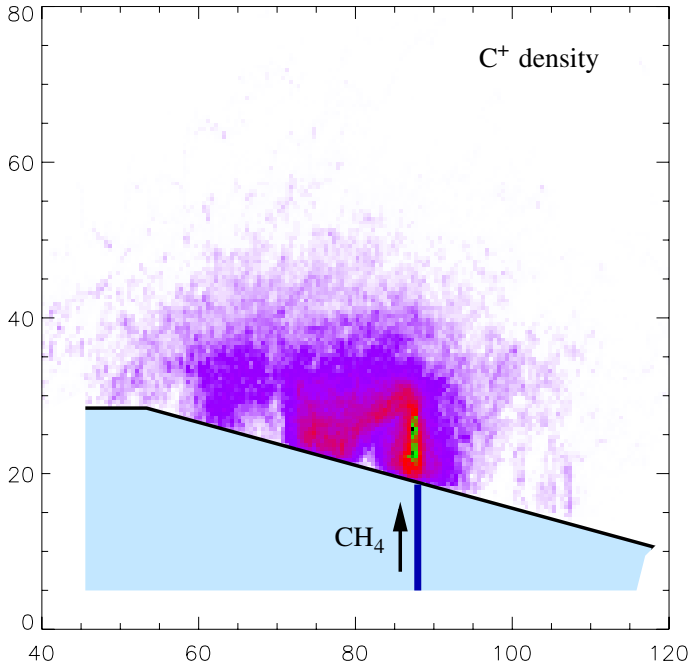

Figure 4.17: Density of C^+ ions in the vicinity of a gas valve during a CH_4 puffing experiment as simulated with ERO.

In 2004, TKK started collaboration with FZJ in order to contribute to further development of ERO. During 2004 we set up the local simulation environment with necessary helper applications and performed benchmarking simulations. Figure 4.17 shows the simulated distribution of C^+ ions in the vicinity of a puffing valve during methane puffing. We also participated actively in the development of ERO by implementing some enhancements to the code and working on a version for 3D simulation of divertor-type experiments. In the near future, CH_4 puffing experiments and related surface analyses carried out by VTT will be modelled. Our long-term goal is to apply the code to a variety experiments on ASDEX Upgrade and JET.

4.2.8 NBI-aided measurement of the magnetic field direction

In experiments at the W7-AS stellarator a rather peculiar instability was found in the LH frequency range. This instability seems to be initiated by fast ions and it has three features that could be used for determination of the magnetic field direction, namely

1) the unstable waves propagate transverse to magnetic field with very high accuracy
2) the instability region is highly localized in space due to its double-resonance characteristic
3) with Collective Thomson Scattering (CTS) diagnostics one can measure the wave vector of the wave activity generated inside the plasma.

Thus the direction of the local magnetic field could, at least in principle, be obtained by scanning the scattering volume (i.e. probing and receiving beams) in space (toroidally and poloidally) and looking for the conditions, where the received signal from LH turbulence is maximal (i.e. received k-vector in perpendicular to B).

The CTS equipment is now moved to ASDEX Upgrade, and it is ready to do the measurements to try to find the LH instability. However, the conditions for the LH instability in ASDEX Upgrade tokamak may be quite different from those in a stellarator where the strong convective losses of toroidally trapped particles provide strong gradients in the velocity space. Preliminary, simple Fokker-Planck calculations showed that, at ASDEX Upgrade:

1) an unstable distribution may exist only during transient switching-on (of a neutral beam) phase (about 10 ms), and
2) a stationary beam distribution provides a very effective stabilization mechanism, i.e. if one beam is already switched-on and has reached a steady-state, then switching-on of a second beam would not result in the instability.

More refined calculations require calculation of the slowing-down distribution for the ASDEX Upgrade neutral beams. ASCOT simulations providing such distributions were initiated.

4.3 Collaboration with Other European Experiments

4.3.1 Modelling of lower hybrid current drive

The near-field of the FTU LH grill has been simulated with the 2d3v PIC code XOOPIC. The difference in the FTU compared to previous work is that the driven frequency is clearly higher, i.e. f_{FTU}=8 GHZ versus f=3.7 GHZ at JET and Tore Supra. The wave propagation inside the waveguides to the grill mouth is followed as well as the coupling to the plasma. The coupling is studied from the reflection coefficient. In the simulations, the reflection coefficient can be obtained for each waveguide. Since the reflection coefficients at FTU can be measured in each waveguide, this gives a good opportunity to compare the code with and benchmark against the experimental results.

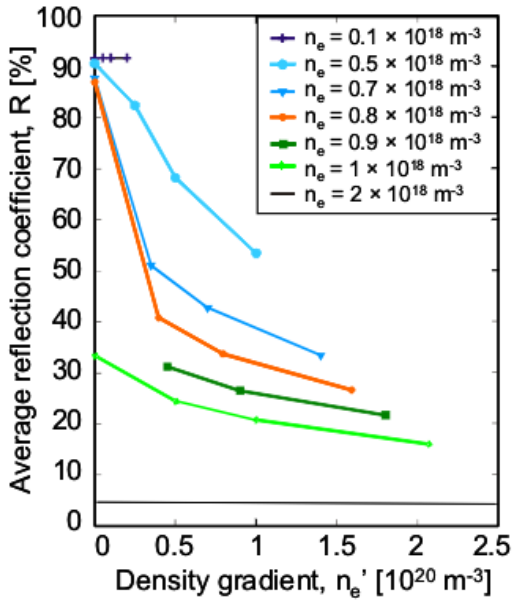

Figure 4.18: Average reflection coefficients as a function of density gradient for various edge densities. The edge densities ranging from n_e=0.1 to 2×10^{18} m^{-3} are denoted in the legend. The calculations have been made for a full LH grill of 12 waveguides.

The effect of the edge density on the coupling is investigated as well as the dependence on a linear density gradient in front of the launcher. First, the simulations were performed with just 4 waveguides in order to find the relevant parameter range. Later, the full 12-waveguide grill was used. In both cases, the density dependence was first studied with a homogeneous density ranging from n_e=0 to 4×10^{18} m^{-3}. With the homogeneous density profile the reflection starts to decrease above the cut-off density $n_{cut\text{-}off}$=0.794×10^{18} m^{-3}. An optimum density was found at about 3-4×10^{18} m^{-3}. This is about 4 to 5 times the cut-off density and twice the analytically found optimum density. However, previous simulations for Tore Supra and JET showed similar behaviour. When a linear density gradient was added a remarkable improvement in the coupling at edge densities around the cut-off density was observed, as can be seen in Figure 4.18. As in earlier studies, well above the cut-off density the effect of the density gradient was very small.

4.3.2 Interferometry

The sightline optimization task for the multichannel laser interferometer of W7-X was completed. We found a matrix formulation for the inverse problem of reconstructing local electron densities from line integrated density measurements. This approach allowed us to find a transparent and computationally simple optimization method for the sightline positioning problem.

We investigated separately four- and eight-sightline arrangements and optimized their orientations for the standard conditions of magnetic configuration and density profile, see Figure 4.19. The robustness of the solution was demonstrated by a variation of the relative positions of the plasma and the interferometer. Also the effect of measurement noise on the quality of reconstructions was investigated.

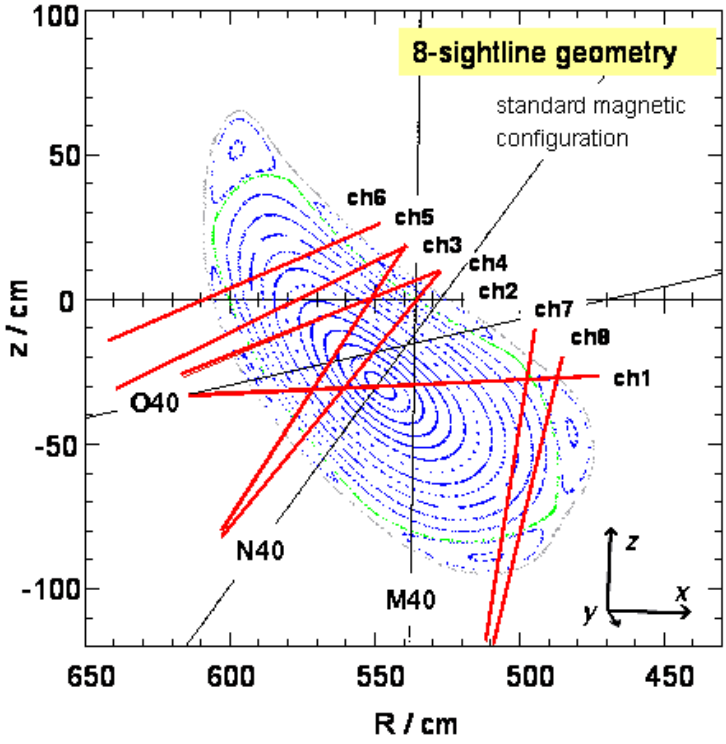

Figure 4.19: The optimized set of eight sightlines traversing the plasma cross section in Wendelstein 7-X.

4.3.3 Role of energetic ions on the divertor load asymmetries

The effect of ion orbit loss on divertor load asymmetries has been simulated using the guiding centre Monte-Carlo code ASCOT in realistic JET magnetic geometry. Self-consistent simulations with normal and reversed magnetic field direction have been made to see if ion orbit loss alone can explain the experimentally observed divertor load profiles.

The effect of field reversal on target power profiles was quite dramatic, with the outer profiles drastically broadened and peak values reduced, in contrast to experiment where little change in profile width was observed, see Figure 4.20. It was thus concluded that orbit loss is *not* directly responsible for the observed target profiles. More likely, ion orbit loss carries power down the pedestal gradient and into the SOL, where (neo-)classical collisional transport takes over. The effect of SOL and divertor collisionality on the target loads will be studied more closely in 2005.

Non-self-consistent trace simulations have also been made to assess the effect of, e.g., magnetic field ripple and anomalous radial diffusion on the divertor target loads on JET. It was found that the weak ripple of JET does not affect the target load profiles significantly. Anomalous radial diffusion, however, was found to have a strong equalizing effect on the loads of the inner and the outer target.

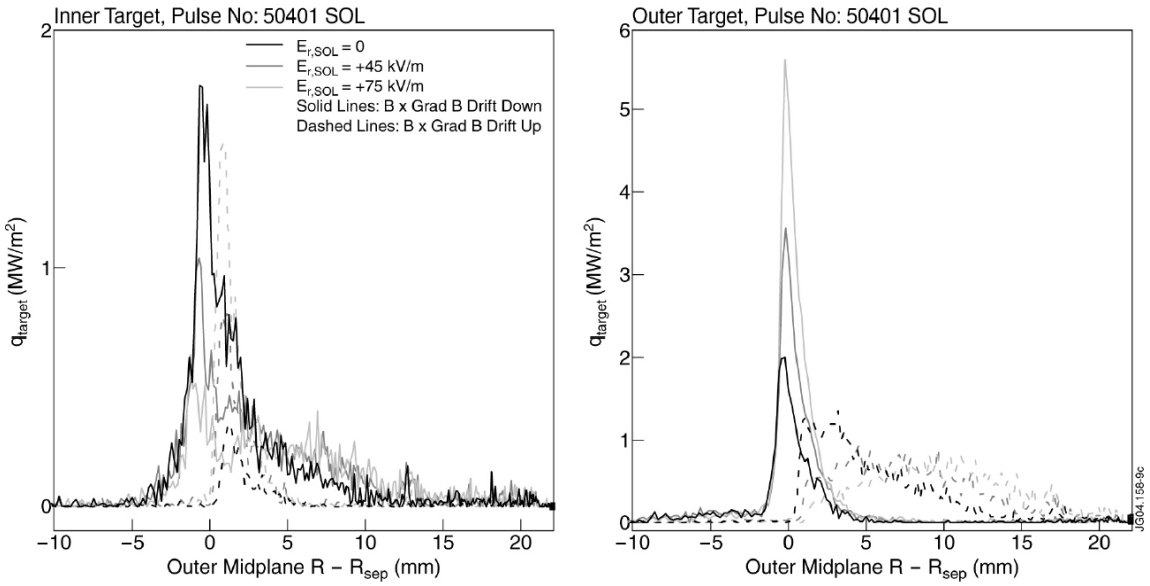

Figure 4.20: ASCOT simulated ion orbit loss target power profiles, forward B vs. reversed B.

4.3.4 The role of supersonic poloidal rotation in ITB formation

ASCOT simulations of low current tokamak discharges have indicated an enhanced radial electric field over the standard neoclassical predictions. This enhancement is presently considered to arise from a neoclassical rotation runaway mechanism known to exist when the $\boldsymbol{E}\times\boldsymbol{B}$ poloidal rotation velocity exceeds the poloidal projection of the parallel thermal velocity. Gyrokinetic ELMFIRE simulations of the neoclassical and turbulent behaviour of the LH-heated FT-2 discharges (Ioffe Institute) support this result. A transition to an internal transport barrier is found in agreement with the experimental results when the plasma current is low enough and the ion pressure gradient large enough.

4.3.5 Deuterium surface activation parameters in tungsten

Institutes: **University of Helsinki**, Accelerator Laboratory
VTT Processes,
Royal Institute of Technology, Sweden

Reseachers: T. Ahlgren, K. Heinola, J. Keinonen, E. Vainonen-Ahlgren, J. Likonen, A. Hallen

Introduction

Low sputtering yields of high Z materials, such as tungsten, make them good candidates for the first wall material at critical locations in next step fusion reactors. In addition to the sputtering due to the hydrogen bombardment, the tritium inventory is of crucial importance when selecting the first wall material. Retention, re-emission and diffusion of hydrogen isotopes in tungsten are of importance in the study of deuterium and tritium recycling and inventory in the first walls and divertor area.

Experimental

To study how D molecules desorb from tungsten surface, high purity (99.99%) polycrystalline W samples were implanted with 30-keV D^+ ions. Two sets of samples with D ion doses of 5.7×10^{15} and 5.7×10^{16} at./cm^2 were prepared in order to produce maximum concentrations of 0.5 and 5 at.%, respectively. The purpose was to check the effect of the implantation induced damage to deuterium diffusion. The quite low implantation fluences and high energies were chosen to make the concentration profile measurements by secondary ion mass spectrometry (SIMS) more accurate and to avoid blister formation.

Samples were then annealed during which thermodesorption spectra for the D_2 molecules were recorded with a quadrupole mass-spectrometer (QMS). For the 5 at.% samples the annealing temperatures were 200 and 250°C with annealing times of 40 and 30 min, respectively. For the 0.5 at.% samples the annealing temperature was 300°C for 60 min.

Results

The as implanted and annealed D concentration profiles in W measured with SIMS are presented in Figure 4.21. Diffusion of hydrogen in W is very fast, so all D seen in the profiles are trapped in either intrinsic or implantation induced defects.

The figure shows that annealing at maximum temperature of 470 K for 30 minutes and 520 K for 15 minutes reduces the amount of implanted D in the bulk with approximately 40%. The peculiar fact that the 470 and 520 K annealed concentration profiles are so similar even though their maximum annealing temperature is very different, could be explained by assuming that the profiles actually show the concentration of D in deeper traps that require higher temperatures than 520 K for D to be de-trapped. To check this assumption, the 520 K, 15 min annealed sample was re-annealed at the same temperature and time. During this annealing, no quadropole mass spectrometry, QMS-signal from desorbed D_2 molecules was observed, and no change of the concentration profile compared with the one prior the additional annealing was detected in post mortem SIMS measurements either. Thus, the 470 and 520 K annealed profiles can be identified with D trapped in deep traps that need higher than 520 K temperature to be de-trapped. The distribution of shallow and deep traps are plotted in Figure 4.22.

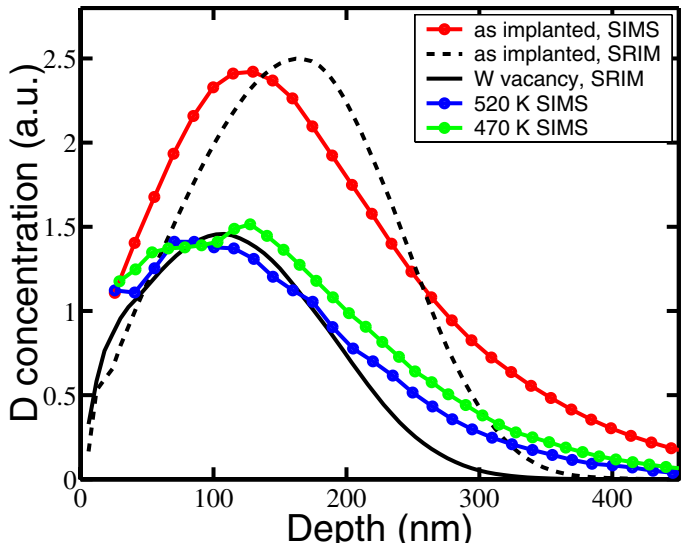

Figure 4.21: As implanted and 470 and 520 K annealed D concentration profiles in tungsten measured with SIMS. Shown are also as implanted D and implantation induced vacancy distributions simulated by SRIM.

Figure 4.23 a) and b) show the experimental and numerical desorption of D_2 molecules from the sample surface and sample temperature as a function of time, respectively. Due to the low annealing temperature, the deeper traps plotted in Figure 4.22 are entirely occupied by D during annealing. Thus, the D seen in the desorption curves in Figure 4.23 are D de-trapped from trap distribution 1, where temperature of about 440 K is enough to detrap D.

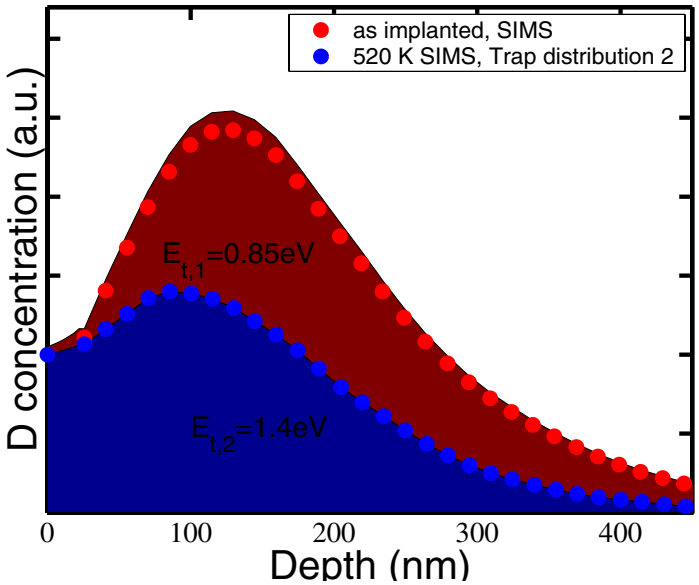

Figure 4.22: Distributions of shallow and deep traps. Red and blue distributions show the shallow and deep traps, respectively.

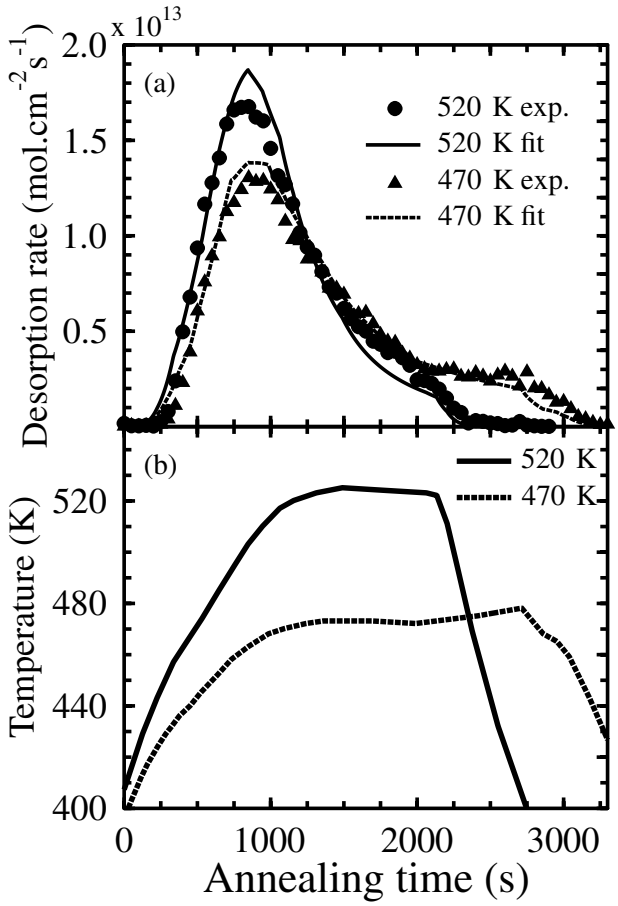

Figure 4.23: a) Deuterium thermodesorption spectra for the annealings. b) The temperature as a function of time during annealing.

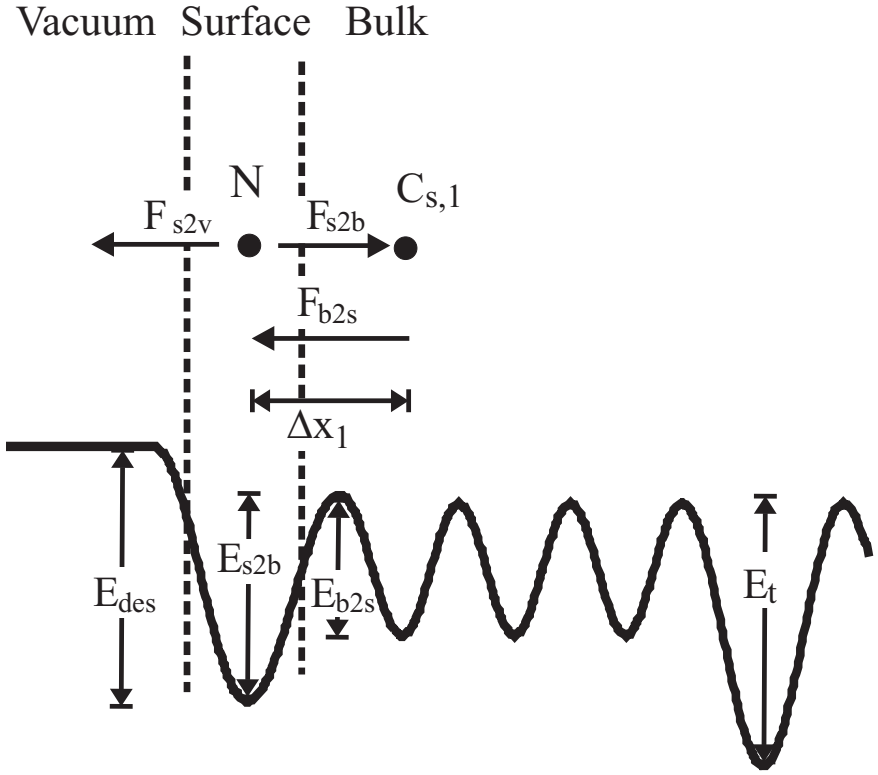

Figure 4.24: Atomic deuterium potential energy diagram in tungsten.

To obtain values for the surface parameters in tungsten, we fitted to the experimental desorption profiles in Figure 4.23, numerically calculated ones using least squares fitting. The four fitted parameters, illustrated in Figure 4.24, are: 1) energy barrier, E_{s2b}, for a D atom to jump from surface to bulk, 2) energy barrier, E_{b2s}, for a D atom to jump from bulk to surface, 3) and 4) pre-exponential factor and surface energy barrier for different surface processes, including possible detrapping from surface impurities, surface diffusion and desorption energy for D atoms to move from strongly bound chemisorption state to form D molecules which desorb to vacuum. All the other parameters to the numerical calculations were taken from the literature. The results from fitting are summarized in Table 4-1 and drawn in Figure 4.24.

Table 4-1: Fitted deuterium surface activation parameter values in tungsten.

E_{s2b}	Surface to bulk activation energy	1.82 eV
E_{b2s}	Bulk to surface activation energy	0.62 eV
E_{surf}	Surface activation energies	3.1 eV

4.4 Code Development

ASCOT and ELMFIRE codes represent plasma particle simulation tools which are under most active development within the Association. Presently, the ASCOT code is used publicly for several European tokamaks while the ELMFIRE code is almost completely at the development stage. These codes are run at the IBM eServer Cluster 1600 supercomputer (2.2 Teraflops in 512 processors), which is provided by the Center for Scientific Computing owned by the Finnish Ministry of Education. The ASCOT code is a multipurpose and versatile guiding-centre code for evaluation of plasma particle distributions and related variables in tokamaks and stellarators. The ELMFIRE code is a global full-*f* particle gyrokinetic plasma turbulence code that can simulate large and rapid dynamic plasma changes in tokamak discharges.

4.4.1 ASCOT code development

AUG magnetic background

During the fall 2003, peculiar results were obtained when simulating AUG discharges. The reason of the anomalies was traced back to the magnetic background files which were found not to satisfy div **B** = 0 accurately enough. An example of this is shown in Figure 4.25. The non-vanishing divergence introduced non-physical drifts that dominated the physical ones. For other machines the non-physical drifts have been negligible.

In the retrieval of the magnetic background the primary data is the poloidal flux which has to be interpolated and differentiated in order to get the R and z-components of the magnetic field on the dense 600x600 grid used by ASCOT. The toroidal component of the magnetic field doesn't affect the divergence because toroidal symmetry is assumed. In the old version of BASDEX, the pre-processor used to retrieve the magnetic background, the order of the interpolation was too low. Additionally, the AUG-maintained kk-routines that were previously used for interpolation worked only in single precision.

To remedy the situation, BASDEX was written anew replacing the kk-routine interpolations with equivalent NAG library functions. Currently there are two options: E02DAF and E02DCF. If the former is used, the user needs to specify the distance

between knots used in the interpolation. The latter function only needs an overall smoothness parameter as an input, the knots are then placed automatically. Both are working equally well, although the most used combination is E02DAF with 10 cm knot distance. Figure 4.26 shows an example of the divergence of the improved magnetic background. The observed non-physical drifts have been reduced to acceptable levels, and are now comparable to those observed for other machines.

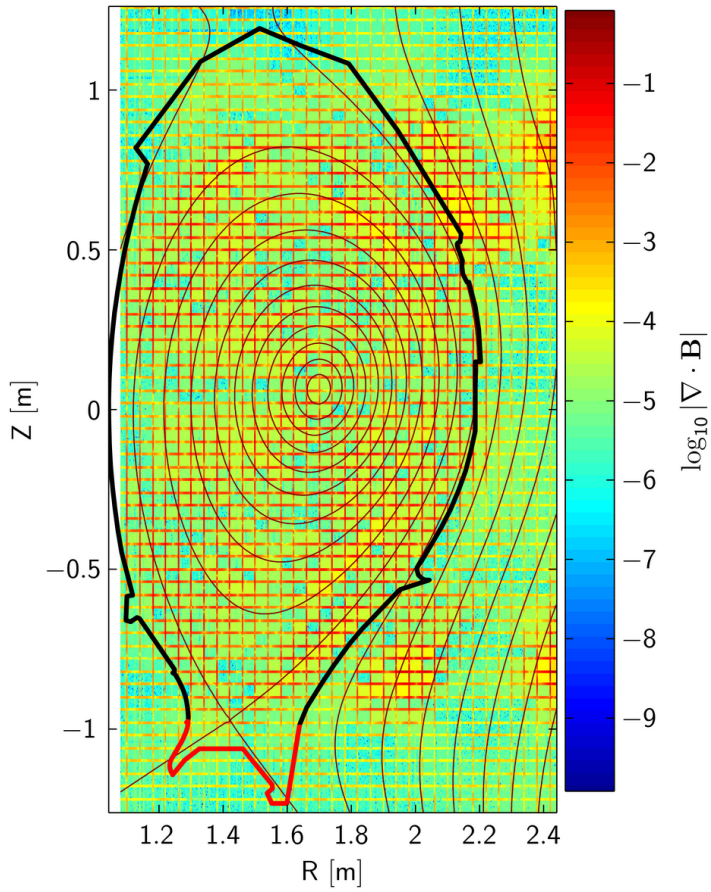

Figure 4.25: The divergence of the magnetic field in logarithmic scale. The grid-like structure originates from discontinuities in the derivatives of the magnetic field components caused by low-order interpolation.

The original pre-processor has been replaced by a new one that utilizes the pedestal profile database under MDSplus, hence the name MDS2ASCOT. Using MDSplus is in accordance with the proposals made by the ITPA Pedestal and Edge Group. The functional part of MDS2ASCOT was taken from BASDEX and it includes the new interpolation of the poloidal flux. Using of MDSplus database to store the simulation results of ASCOT is also investigated.

3D Ripple

In high performance plasmas the fast ion losses are considered as one of the major contributors to the loads on material surfaces. The ripple-induced losses may significantly enhance these loads. This has been analyzed on JET using ASCOT but, since the level of ripple in normal operation is low in JET ($\delta B/B < 0.002$), the effect was found to be insignificant. However, JET has the unique possibility of controlling the strength of the toroidal ripple. Experiments with varying ripple strength would certainly shed more light on the confinement of ions trapped in local magnetic mirrors. Also, ripple-induced

transport as a tool for ELM mitigation is currently under investigation, and ASCOT simulations could be used to reliably evaluate the transport coefficients for the transport code JETTO. For these reasons, it is of interest to upgrade the simple 2D ripple model used in ASCOT to include more detailed physics.

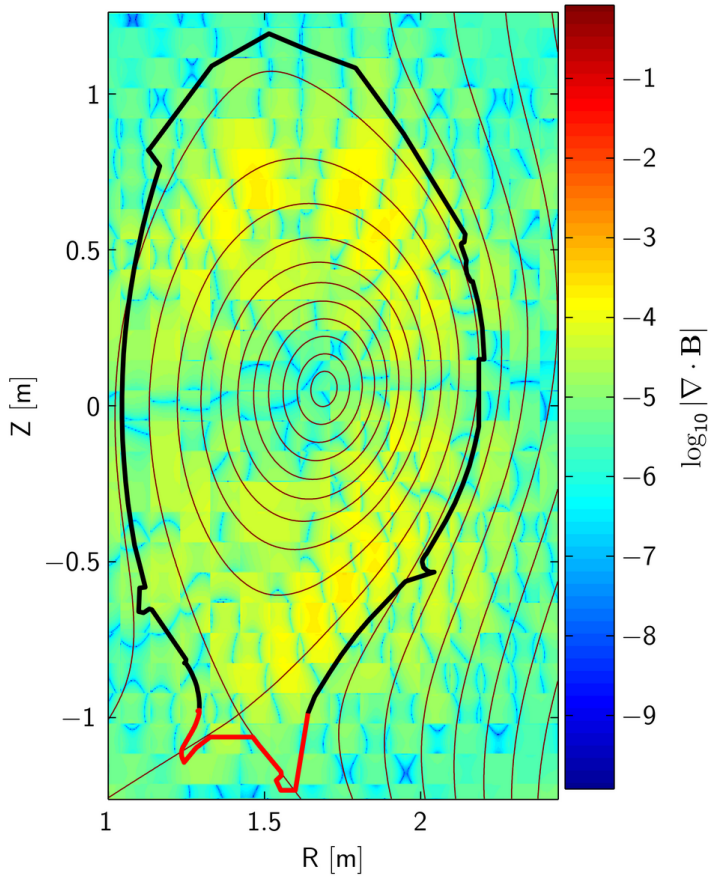

Figure 4.26: The divergence of the improved magnetic background. The higher order of interpolation has removed the grid although the figure still gets divided into panes showing the positions of the knots.

A JET-based code which calculates the toroidal magnetic field configuration in JET (in R, Z and φ coordinates) for different current levels in the two sets of 16 toroidal coils (with the two sets shifted by π/16 in toroidal direction) is used to obtain the ripple field. An interface to this data has been programmed into ASCOT to upgrade the model to 3D. With the new model, a much more realistic estimate for the ion losses is computed by ASCOT to show the level and localization of the losses as a function of the ripple amplitude, plasma parameters and the magnetic configuration. An example of a guiding centre orbit in the presence of collisions with fixed background in the new 3D ripple field is shown in Figure 4.27.

Output and post-processing

In addition to the new AUG background and the 3D ripple, a new four-dimensional (ρ, θ, v_{par}, v_{perp}) distribution has been added to ASCOT. The 4D-distribution can be used as input for MHD stability codes such as HAGIS, but for this to succeed, the distribution has to be in physical units. So far most of the ASCOT output distributions have been in arbitrary units, but this has now been changed. Considerable effort has also been put into writing routines for Matlab and Scilab to ease up the processing and visualization of the various distributions.

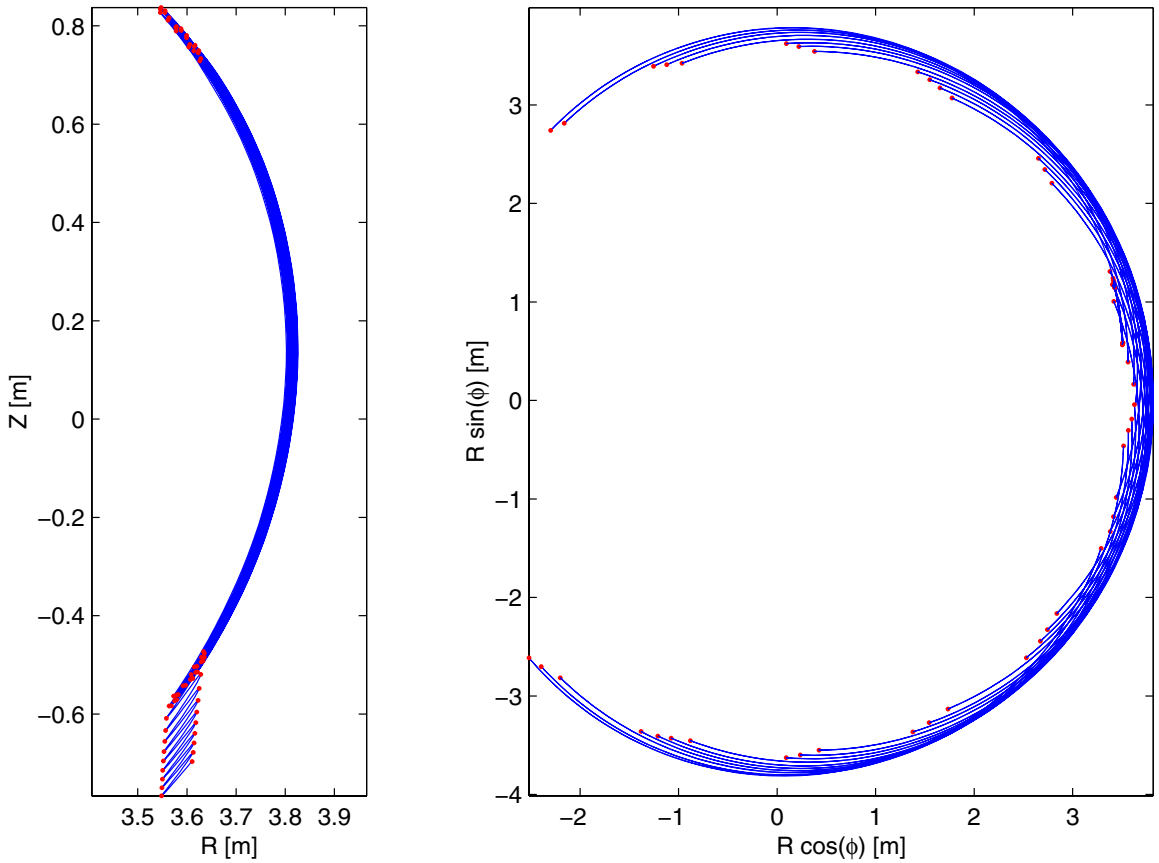

Figure 4.27: A banana orbit changes to ripple-trapped orbit due to collisions.

Stellarator Version

Further benchmark testing of the ASCOT code for stellarator configurations (W7-X) has continued. Together with the Ukrainian scientists (Kiev), the neutral beam slowing-down ion distributions in velocity and configuration space have been studied. Both the collision and orbit loss effects on the distributions have been investigated. Special attention has been devoted to the orbit integration accuracy with appropriate interpolation methods for the background magnetic field grid data.

4.4.2 ELMFIRE code development

The ELMFIRE code, which is so far run only electrostatically in a quasi-toroidal configuration (circular poloidal cross-section of magnetic surfaces with no Shafranov shift) has now several advanced gyrokinetic simulation features:

- Implicit treatment of the electron parallel acceleration and direct implicit sampling of the (polarization) coefficients in the gyrokinetic Poisson equation. This makes the code compatible with strong variations of the bulk plasma distributions.
- Quasiballooning coordinates and radial boundary conditions allowing transport through the outer edge.
- Neutral ionization model as a particle source and recycling of lost particles on the limiters.
- Binary collision model (among ion and electron species) and loop voltage to sustain the plasma current.

- Impurity ion species included.
- Quiescent start along orbit invariants and various (rf + Ohmic) heating sources for the particles.
- Diagnostics of Reynolds stress and plasma flows, and a complete Fourier analysis package for the mode evolution including correlation survey and movie presentation of a variety of transport quantities.

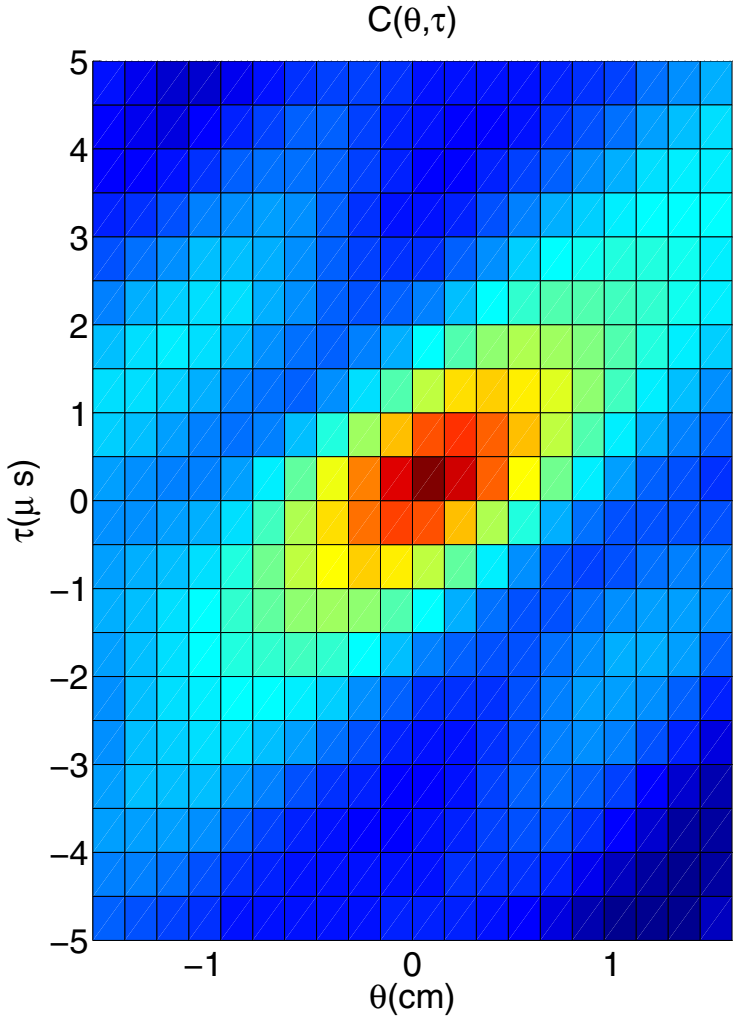

Figure 4.28: Two-dimensional correlation function from ELMFIRE simulation.

The ELMFIRE code has been benchmarked against the Cyclone base case both in adiabatic and kinetic electron limits in regard to the ITG/TEM mode growth rates, frequencies, and nonlinear saturation of the resulting turbulence. Also, geodesic acoustic mode (GAM) frequencies, damping and residual levels have been checked in appropriate configuration limits to the analytical estimates. Most importantly, the neoclassical radial electric field in the presence of turbulence has been verified from the code in good agreement with the neoclassical theory (both in subsonic and supersonic poloidal rotation regimes). The turbulent eddies and the related transport have been studied with correlation and PDF analysis. An example of a two-dimensional correlation function used for determining the lifetime and poloidal size of turbulent eddies is shown in Figure 4.28. The code can predict the spontaneous formation of an internal transport barrier under conditions close to those under which it is found in low current LH ion heated FT-2 experiments at the Ioffe Institute. In Figure 4.29 the radial electric field before and after transition is shown.

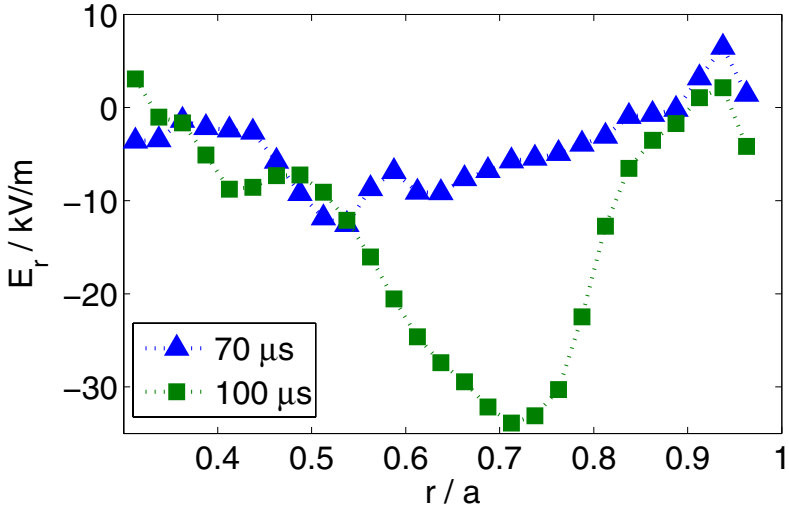

Figure 4.29: Radial electric field before and after transition.

5 EFDA TECHNOLOGY – PHYSICS INTEGRATION

5.1 Coaxial Cavity Gyrotron Development

Institute: **Helsinki University of Technology**
Department of Engineering Physics and Mathematics
Laboratory of Advanced Energy Systems

Research scientists: Prof. O. Dumbrajs

EFDA Task: TW3-THHE-CCGDS1

The gyrotron work in 2004 was mainly devoted to accomplish the ITER task TW3-THHE-CCGDS1. In accordance with the goal of this task theoretical investigations on the cavity of a 2 MW, CW 170 GHz coaxial gyrotron have been performed. The $TE_{34,19}$ mode has been chosen as a working mode and the corresponding cavity has been designed.

This has been accomplished by means of a code written at the Helsinki University of Technology. This code can be regarded as a significant improvement over the code which exists at the Forschungszentrum Karlsruhe. In particular the new code apart from the features already incorporated in the FZK code makes it possible:

1. to calculate the second harmonic interaction,
2. to calculate competition among opposite rotations of one and the same mode,
3. to calculate mode competition in the presence of reflections,
4. to calculate ohmic losses in the coaxial insert on the basis of a newly developed theory based on the method of singular integral equation which goes beyond the standard but less accurate surface impedance method,
5. to treat longitudinal corrugations with variable depth along the longitudinal direction,
6. to take into account the final width of the electron beam,
7. to investigate hysteresis effects in gyrotrons.

Thorough calculations with this code have been performed and operational domains in the desired $TE_{34,19}$ mode in the parameter space (current, voltage and magnetic field) of the gyrotron have been identified.

First experimental results with the 165 GHz coaxial cavity gyrotron at FZK modified for operation at 170 GHz in the $TE_{34,19}$ mode have confirmed the excitation of this mode and two neighbouring modes in the designed cavity.

Other gyrotron work activities were devoted to studies of the influence of reflections on operation of gyrotrons with both the axial and radial output and to mode selection for a terahertz gyrotron based on a pulse magnet system.

A comprehensive review has been written on the history and the present status of coaxial gyrotrons.

5.2 Molecular Dynamics Simulations of Carbon and Tungsten Sputtering

Institute: **University of Helsinki**
Department of Physical Sciences, Accelerator Laboratory

Research scientists: Prof. K. Nordlund, Dr. A. Krasheninnikov, Dr. A. Kuronen, P. Träskelin, K.O.E. Henriksson, N. Juslin

EFDA Task: TW4-TPP-CARWMOD

5.2.1 Erosion of C during H and noble gas bombardment

Carbon is widely used in contemporary tokamaks and will be used in the high heat flux components of the divertor in ITER. However, its high erosion yield and tritium retention are detrimental with respect to its application as a first wall material. In this context, a major issue to be dealt with in the design of ITER is the erosion of carbon surfaces by impurity ions, i.e. ions which are not the main plasma constituents, H, D or T. These ions, the most important ones being Ar, Ne and He, will not only erode the carbon surface but also penetrate it. The mixed layers which are formed with different carbon/ion ratios could be re-eroded by incoming hydrogen ions. Since the erosion with Ar, Ne and He ions may differ from the erosion with only hydrogen, the erosion behaviour of these layers needs to be studied, not only during the deposition of hydrogen but also only with these ions.

We estimated this issue systematically with molecular dynamics computer simulations. We generated amorphous hydrogenated carbon cells with properties typical to those found in tokamaks, and bombarded them either with H only or with a mixture of H and 10% noble gas impurities, and examined the erosion behaviour. As expected from previous work, a H supersaturation built up at the surface, reducing the erosion yield. The surprising fact was the effect of the ion energy on the surface structure. 5 eV ions lead to a dense surface structure and low erosion rates, while 10 eV ions produced a very loosely bound surface which caused enhanced erosion of C due to sputtering of large hydrocarbons, see Figure 5.1.

Comparison of the cases with and without impurity atoms did, however, show that the C erosion rate is essentially the same regardless of whether there is or is not impurities in the plasma. This is a good result in that it indicates the small amount of noble gas impurities which will be present in the ITER divertor region plasma need not be taken into account in the erosion coefficients.

5.2.2 Tungsten co-bombardment

We also examined the interaction with a fusion plasma and a W-based reactor first wall. The blistering of W due to low-energy H and He implantation in a tokamak divertor have been investigated by molecular dynamics simulations. We first examined near-surface blistering due to He or H during very-high-flux conditions. The calculations were carried out on a block of (001) W at 0 and 300 K, for 50 and 100 eV He ions impinging on it. This energy is far below the threshold energy needed to create lattice displacements by He projectiles in W, which is about 0.50 keV. We directly observed the surface rupture due to the gas bubbles, and have found that the mechanism is akin to microcracking, i.e. the bubble pressure produces a small crack to the surface which allows the gas to escape, see Figure 5.2.

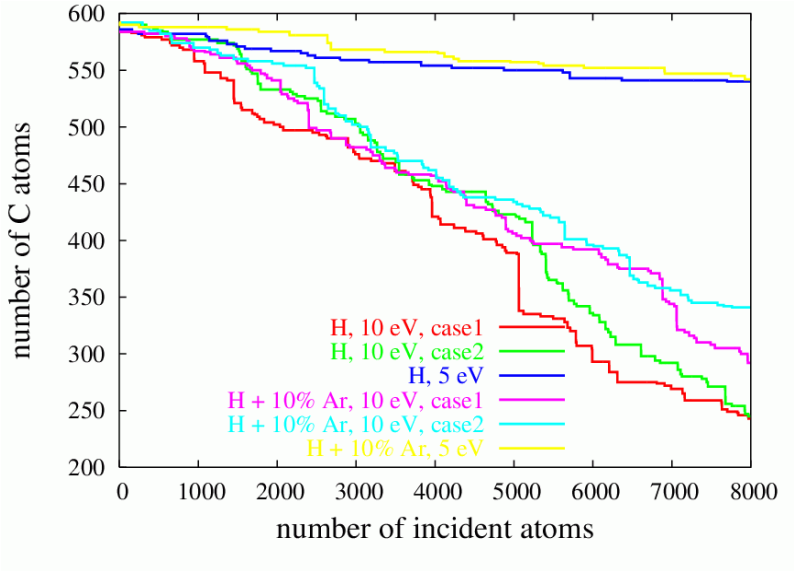

Figure 5.1: Carbon erosion as a function of the number of bombarding ions from an a-C:H surface by incoming H and noble gas ions from the fusion plasma. The initial number of carbon atoms in the cell was about 590. Hence the decrease observed is due to the carbon erosion. Note the major difference between the 5 and 10 eV cases, but also that inclusion of 10% Ar among the bombarding species does not affect the outcome.

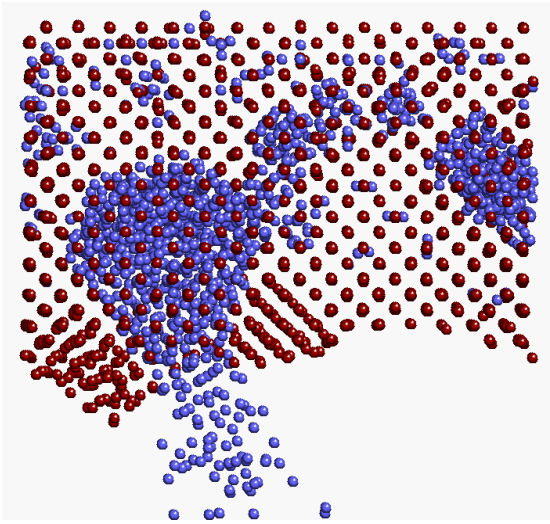

Figure 5.2: Release of He from a near-surface bubble. The blue atoms are He and red atoms the W matrix to which the He has been implanted.

We have also examined why the H blistering during ordinary fluxes occurs very deep in the sample using kinetic Monte Carlo and MD methods. With KMC methods we have been able to rule out that a thermal gradient could explain the effect, and found that if H traps with other mobile H atoms the blistering would occur too near the surface for reasonable H migration rates. We are currently using MD methods to examine whether there is a barrier to H self-recombination which could explain the very deep blistering depths observed.

6 FUSION TECHNOLOGY – VESSEL/IN-VESSEL

6.1 In Reactor Fatigue Testing of Copper Alloys

Institutes: **VTT Industrial Systems**
Risø National Laboratory
SCK.CEN

Research Scientists: P. Moilanen, S. Tähtinen, S. Saarela

EFDA Task: TW3-TVM-COFAT2

6.1.1 Introduction

It has been known for a considerable period of time that the deformation behaviour of metals and alloys is substantially altered by irradiation with energetic particles such as fission or fusion neutrons, particularly at temperatures below the recovery stage V. This effect of irradiation on mechanical properties has been a subject of extensive investigations for more than 40 years. The post-irradiation deformation experiments (i.e. tensile tests) have demonstrated consistently that (a) the yield strength of metals and alloys increases with increasing dose level, (b) materials irradiated to a displacement dose beyond a certain level exhibit the phenomenon of yield drop and (c) the irradiation causes almost a complete loss of work hardening ability and a drastic reduction in the uniform elongation (i.e. ductility). Under these conditions, in many cases the specimens show a clear sign of plastic instability immediately beyond the yield drop. It is interesting to note that these features are common to all three crystal structures, fcc, bcc and hcp.

It is this prospect of irradiation induced drastic decrease in ductility and the possibility of initiation of plastic instability that has given rise to a serious concern regarding the mechanical performance and lifetime of materials used in structural components of a fission or a fusion reactor. In view of the seriousness of this technological concern, it is only prudent to consider the relevance of these adverse effects of neutron irradiation observed in the post-irradiation experiments to the performance of materials exposed simultaneously to an intense flux of neutrons and stresses in a real reactor environment. The reason for considering this issue of relevance is the recognition of the fact that the materials tested in the post-irradiated state respond to conditions that are fundamentally different from those that are likely to be experienced by the materials exposed to a dynamic irradiation environment in a fission or a fusion reactor.

In the case of post-irradiation experiments, for example, the samples are first irradiated in unstressed condition to a certain displacement dose level to accumulate a certain amount of displacement damage in the form of defect clusters (which are responsible for hardening and reduction in ductility). This means that the damage accumulation takes place in the absence of deformation-induced mobile dislocations. The irradiated samples are then tensile tested outside of the reactor, i.e. in the absence of continuous production of defect clusters. The materials employed in the structural components of a fission or a fusion reactor, on the other hand, will be exposed simultaneously to internal and external stresses and irradiation-induced defects and their clusters continuously produced during irradiation. Under these conditions, both the magnitude and the spatial distribution of defect accumulation and hence the deformation behaviour may be significantly different from that in the case of post-irradiation experiments. It is, therefore, relevant to consider as to

whether or not the results and the conclusions of the post-irradiation deformation experiments can be taken to represent the behaviour of materials employed in the structural components of a fission or a fusion reactor. In our view, this question can be answered properly and reliably only by determining experimentally the deformation behaviour of materials in the neutron environment of a nuclear reactor.

6.1.2 Test module and irradiation rig

In order to carry out fatigue experiments, a special test facility consisting of a pneumatic fatigue test module and a servo controlled pressure adjusting loop was designed and constructed.

The basic principle of the fatigue test module is based on the use of two pneumatic bellows to introduce tensile and compressive stresses and a linear variable differential transformer (LVDT) sensor to measure the resulting displacement produced in the tensile specimen. The outside diameter of the module is 55 mm and the total length of the module together with the LVDT is about 200 mm.

The pneumatic servo controlled pressure adjusting loop is based on closed helium gas flow through the electrically controlled servo valve. The movement of the bellows is controlled by LVDT sensor which also gives the feedback signal for the servo controller. The fatigue tests will be performed under strain controlled with continuous cycle and with compressive and tensile hold times.

To accommodate the test module and the necessary instrumentation to perform the fatigue test in the reactor, special irradiation rigs were designed and constructed at Mol. The tensile test module together with instrumented irradiation rig is shown in Figure 6.1. During irradiation the whole test assembly including the module and the specimens will remain submerged in flowing reactor pool water. The temperature profile in each module will be measured by three thermocouples placed at different levels in the rig and also dosimeters will be placed at the specimen level to measure the neutron flux.

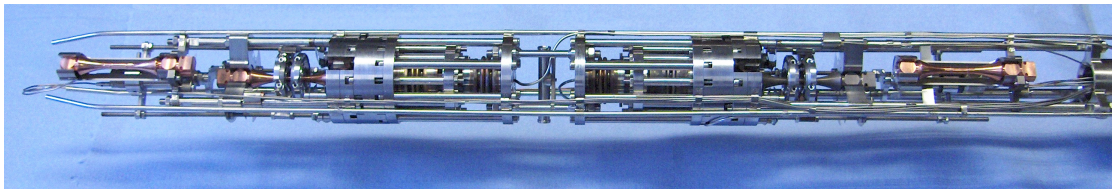

Figure 6.1: The in-reactor fatigue test module together with instrumented irradiation rig.

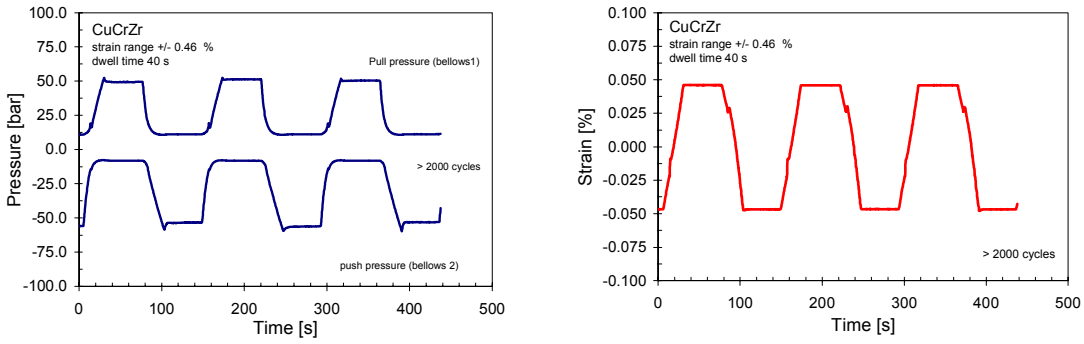

Figure 6.2: Typical pressure (stress) and strain variations during fatigue cycle.

6.2 Characterisation of the CuCrZr/SS Joint Strength for Different Blanket Manufacturing Conditions

Institutes: **VTT Industrial Systems**
CEA Grenoble

Research Scientists: S. Tähtinen, P. Moilanen

EFDA Task: TW3-TVM-JOINT

6.2.1 Objective

The copper alloys in ITER are used due to their good heat conduction properties in the first wall and divertor components. Copper alloys are bonded in between stainless steel structure material and Beryllium or CfC armour materials. The joint interfaces are subject to thermal and mechanical loads under neutron irradiation. In the present manufacturing rules there is no clear quality or strength criteria for the Cu/SS or SS/SS joint interfaces. Particularly the strength of CuCrZr alloy is very sensitive to heat treatments during manufacturing cycle and consequently also the strength of Cu/SS joints.

6.2.2 Fracture toughness of Cu/SS joints

Different blanket manufacturing conditions with separate solution annealing and aging treatments after HIP were considered and manufacturing of test blocks were carried out by CEA Grenoble. The HIP treatment at 1040^{o}C simulate single step manufacturing were both stainless steel to stainless steel and copper alloy to stainless steel joints will be produced simultaneously. In the case of two step manufacturing second HIP treatment after joining of stainless steel parts is followed at 980^{o}C to produce copper alloy to stainless steel joints. The main advantage of the latter manufacturing route is smaller grain size of CuCrZr alloy compared to high temperature HIP method. The optimal strength of the CuCrZr alloy is achieved by subsequent separate solution annealing treatment at 980^{o}C for 30 minutes followed by quenching at medium cooling rate of 70–80 ^{o}Cmin^{-1}. The joining process of the beryllium armour is simulated by aging treatment at 560^{o}C for 2 hours. A summary of different manufacturing routes for blanket module is shown in Table 6-1 and corresponding tensile properties of CuCrZr base alloys and CuCrZr / 316L stainless steel joints are shown in Tables 6-1 and 6-2. Normalized load displacement curves and corresponding fracture resistance curves are shown in Figure 6.3.

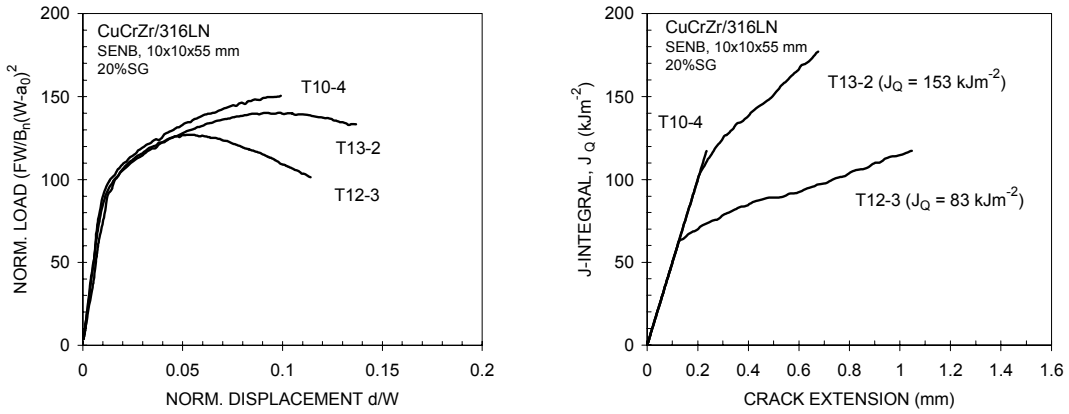

Figure 6.3: a) Normalised load-displacement curves and corresponding b) fracture resistance curves of CuCrZr/316LN joint specimens.

Table 6-1: Summary different manufacturing routes for blanket modules.

Code	HIP	Annealing	Aging
T10-4	1040°C / 2hrs / 140MPa	980°C / 0.5hrs / MCR	560°C / 2hrs
T12-3	980°C / 2hrs / 140MPa	980°C / 0.5hrs / MCR	480°C / 2hrs
T13-2	980°C / 2hrs / 140MPa	980°C / 0.5hrs / MCR	560°C / 2hrs

Table 6-2: Tensile properties of CuCrZr base alloys and CuCrZr / 316L stainless steel joints after different manufacturing routes.

Code	Material	YS (MPa)	UTS (MPa)	UE (%)	TE (%)
T10-4	base (CuCrZr)	199	318	13.0	26.5
	joint (CuCrZr/316L)	209	327	8.2	16.1
T12-3	base (CuCrZr)	271	393	15.8	26.0
	joint (CuCrZr/316L)	253	384	11.9	18.1
T13-2	base (CuCrZr)	205	327	13.5	25.1
	joint (CuCrZr/316L)	205	327	9.7	18.3

The difference between T10-4 and T13-2 was the applied HIP temperature during manufacturing cycle which is expected to affect both grain growth and dissolution and subsequent precipitation of Cr and Zr during the HIP thermal treatment and aging. It is noted Cu/SS joint specimens T13-2 and T10-4 showed similar tensile properties and fracture toughness J_Q values. The manufacturing cycle for T12-3 and the aging heat treatment at 480°C is expected to result an optimum strength and precipitate structure for base CuCrZr alloy compared to overage heat treatment at 560°C. The tensile strength of T12-3 was clearly higher and fracture toughness J_Q value was clearly lower compared to other two Cu/SS joint specimens.

6.3 Effect of Low Dose Neutron Irradiation on Ti Alloy Mechanical Properties

Institute: **VTT Industrial Systems**

Research Scientists: S. Tähtinen, P. Moilanen

EFDA Task: TW3-TVM-TICRFA

6.3.1 Objective

Recent experiments have shown that the irradiation of (α+β) alloy at 350°C to 0.3 dpa leads to a very significant increase in the yield strength and a corresponding decrease in the uniform elongation. This effect seems to be related to the appearance of a very high density of irradiation-induced precipitates in this alloy. Surprisingly, these changes do not appear to have any noticeable effect on the low cycle fatigue behaviour of this alloy irradiated at 350°C to 0.3 dpa. The main objective of the present task is to investigate the effect of irradiation on the microstructure and mechanical properties of these alloys (i.e. both α and (α+β)) at about 200°C which is closer to the expected service temperature in ITER.

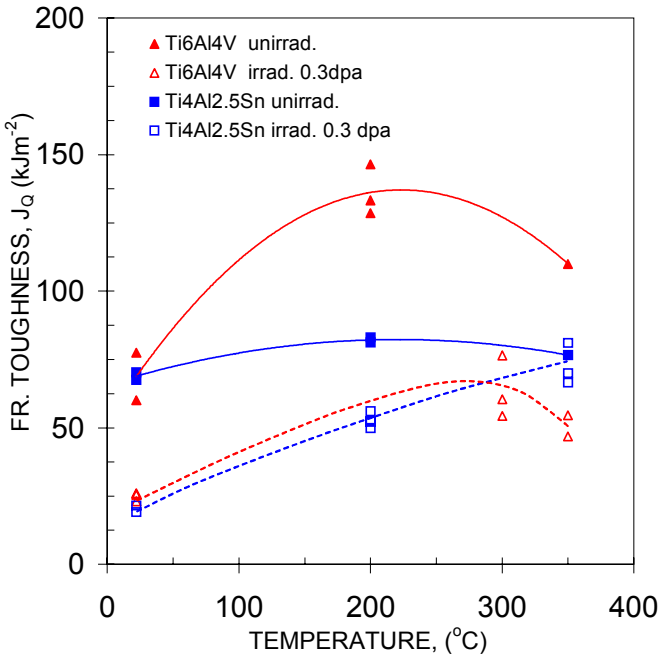

Figure 6.4: Fracture toughness of α and (α+β) titanium alloys in unirradiated and neutron irradiated conditions.

6.3.2 Fracture toughness

Both α and (α+β) titanium alloys were irradiated to a dose level of 0.3 dpa at about 150°C. Fracture toughness of post irradiated specimens were determined at 200 and 300 Fracture toughness of post-irradiated specimens of Ti6Al4V alloy were determined at 300°C and of Ti5Al2.5Sn alloy at 200°C. Fracture toughness behaviour is illustrated in Figure 6.4. It seems that fracture toughness behaviour of irradiated α and (α+β) titanium alloys is quite similar at ambient temperatures. At elevated temperatures fracture toughness of (α+β) titanium alloy decreases whereas that of α alloy increases continuously. In earlier studies it has been shown that (α+β) titanium alloy is unstable after irradiation at elevated temperatures.

6.4 Qualification Testing of New CuCrZr/SS Tube Joint

Institute: **VTT Industrial Systems**

Research Scientists: S. Saarela, S. Tähtinen

EFDA Task: TW3-TVD-CUSS

6.4.1 Objectives

The extremely high surface heat loads expected in the divertor of the ITER require that the cooling tube of divertor and port limiter is made of CuCrZr alloy. This leads to the need of a CuCrZr/SS tube joint to enable the connection to the main cooling circuit of the high heat flux components.

6.4.2 Slow strain rate tests

The test specimens were prepared by electric discharge machining from the tubes delivered to VTT by Ansaldo, Genova. The tube samples were produced by electrodepositing Ni

layer on CuCrZr alloy followed by TIG welding between electrodeposited Ni layer and 316L stainless steel.

Two SSRT runs with four specimens were conducted in an autoclave testing system with recirculating high temperature water that contained controlled amounts of hydrogen peroxide, sulphates and chlorides. Nominal concentrations of sulphate, chloride and hydrogen peroxide were 10 mgl^{-1}, 4 mgl^{-1} and 5–10 mgl^{-1}, respectively. The applied strain rate during the tests was 10^{-7} s^{-1}. The nominal temperature and pressure were 150ºC and 60 bar respectively. Redox potential, conductivity, temperature, pressure, inlet and outlet oxygen contents, stresses and electrochemical corrosion potential of each test specimen were continuously measured during the tests. The contents of sulphate and chloride were analyzed from water samples taken directly from the autoclave and hydrogen peroxide content was estimated indirectly from outlet oxygen content during the SSRT runs.

The stress-strain curves of the SSRT run no. 2 is presented in Figure 6.5 and summarised in Table 6-3. All specimens fractured in the gauge section along the interface between Ni-insert and stainless steel TIG weld. The interface between CuCrZr alloy and Ni-insert was deformed but no cracking was observed along the interface. Fracture mode was mostly ductile and partly interface type of fracture close to or along interface between Ni-insert and stainless steel TIG weld. The facture path is close to TIG weld due to both heavy corrosion and large grain size in heat affected zone of Ni-insert.

Table 6-3: A summary of the data from the specimens of both SSRT runs.

	Specimen							
	SSRT no.1				SSRT no.2			
	1A	3A	4B	5A	4A	5B	6A	6B
Failure time [hrs]	257	162	210	250	185	157	203	289
Max stress [MPa]	166	145	175	189	180	147	170	179
Strain at max stress [%]	5.0	3.7	4.8	3.7	4.6	4.1	4.6	6.0
Max strain [%]	7.7	5.3	6.1	7.4	6.7	5.6	7.3	10.4
Average corrosion potential [mV(SHE)]	7	71	8	-62	-5	92	-30	12

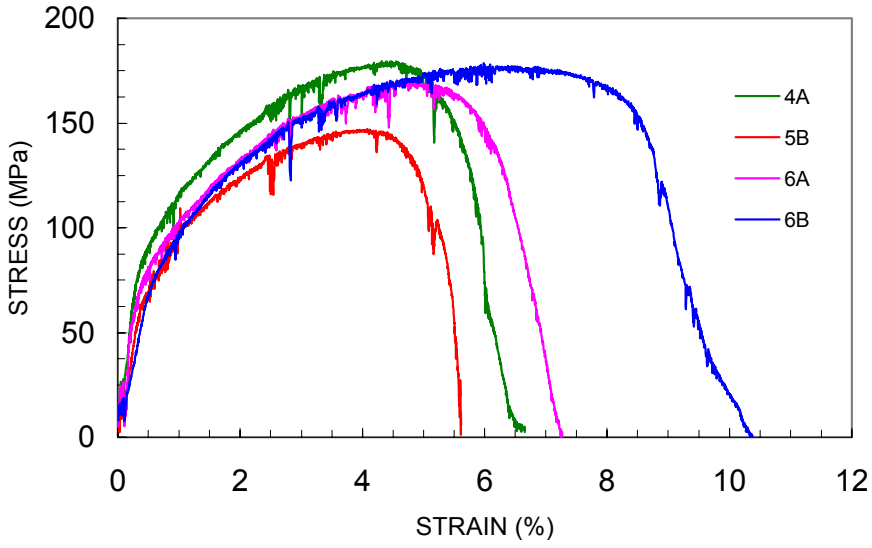

Figure 6.5: Stress-strain curves of CuCrZr/316L joint specimens in SSRT run no. 2.

6.5 Ultrasonic Testing of Primary First Wall Mock-Ups and Panels

Institute: **VTT Industrial Systems**

Research Scientists: S. Tähtinen, H. Jeskanen, P. Kauppinen

EFDA Contract: EFDA 01-602

6.5.1 Objective

A Research and Development programme for the Blanket-shield of ITER has been implemented to provide input for the design and manufacture of the full-scale production components. It involves in particular the manufacturing and testing of Primary First Wall Mock-ups and Panels. These mock-ups and panels consist of plane layers of 316L Stainless Steel (SS) plate joined to Copper (Cu) alloy plates with the addition of a Beryllium (Be) layer.

Non Destructive Examination has to be performed during manufacturing by the manufacturers. In particular, all the Be/Cu alloy and Cu alloy/SS joints have to be examined by ultrasonic technique after each joining operation to check the quality of the joints. The aim of this contract is to ask a Third Party to perform independent NDE and inspect the mock-ups and panels before and after thermal fatigue testing.

Several Primary First Wall Mock-ups and Panels have been examined during year 2004 by using ultrasonic techniques. Figure 6.6 show an example of ultrasonic examination of a medium scale (615 mm x 165 mm x 87 mm) copper stainless steel first wall panel manufactured by CEA. Ultrasonic images illustrate cooling water manifold and tube arrangement. No defect indications were observed on interfaces but some indications were found connected to stainless steel tubes in copper layer.

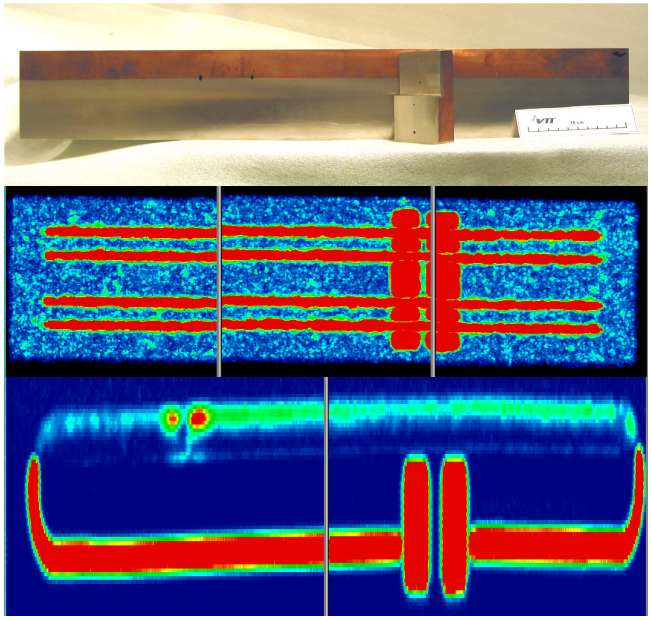

Figure 6.6: The medium scale copper stainless steel a) first wall mock-up and corresponding ultrasonic images illustrating b) copper to copper and copper to stainless steel interfaces examined on copper surface and c) cooling tube arrangement examined on side surface.

6.6 CMM and SCEE Design Update

Institute:	**Tampere University of Technology**, Institute of hydraulics and automation (TUT/IHA)
Research Scientists:	M. Siuko, M. Pitkäaho, M. Toivo, J. Mattila, J. Poutanen, M.Vilenius, H. Saarinen, A. Raneda, H. Mäkinen, S. Verho, A. Mäkelä, H. Koivisto, A. Muhammad, T. Nykänen
EFDA Tasks:	TW3-TVR-MOVER and TW4-TVR-DTP2.1

6.6.1 Introduction

ITER divertor replacement and component refurbishment is expected to be required 4 times during the lifetime of ITER. The main reasons are the erosion of the plasma facing components and the experimental nature of the reactor, when alternative designs of the divertor are possibly tested. The divertor consists of 54 cassettes. There is three RH ports which provide access to replace them. Each cassette weights more than ten tons and they should be placed within few millimetres accuracy. The equipment for the divertor cassettes replacing consists of the cassette multifunctional mover (CMM) with a set of end effectors, and the cassette toroidal mover (CTM).

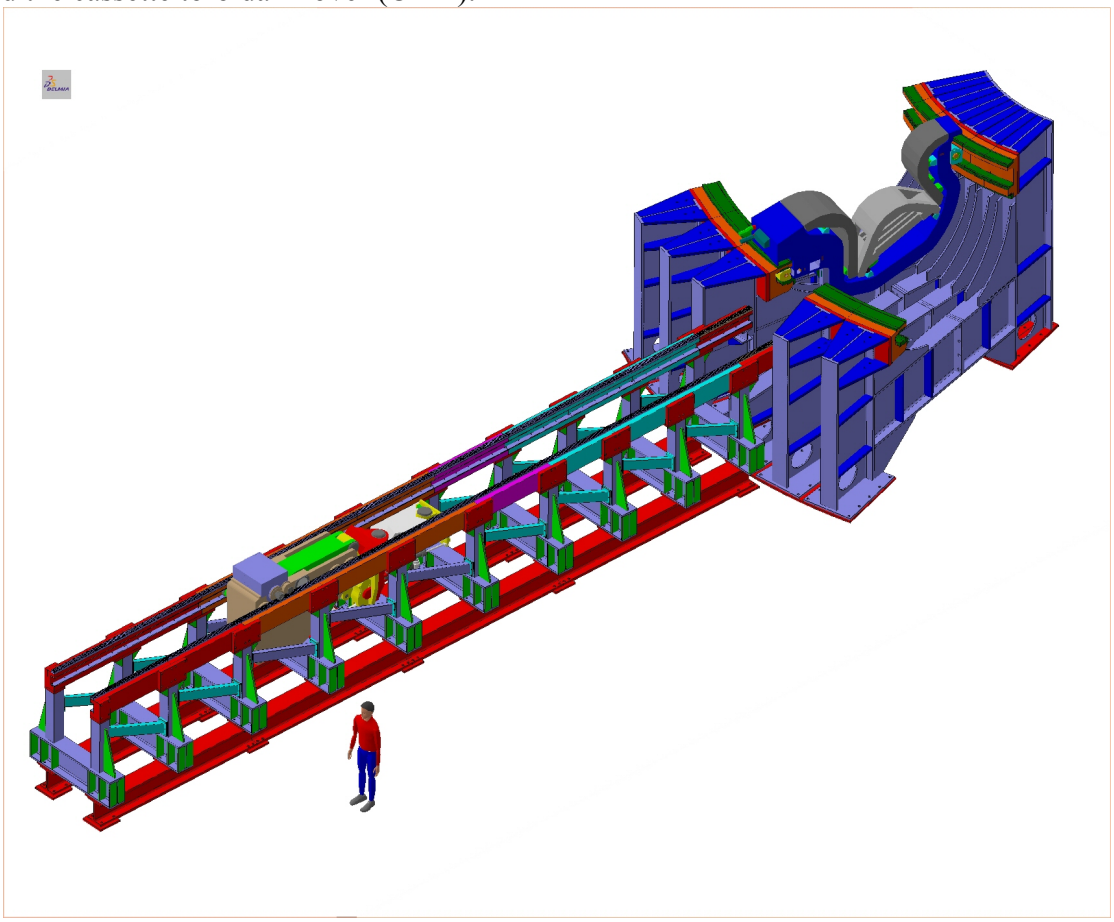

Figure 6.7: DTP2 test facility.

6.6.2 Divertor test platform – DTP2

The divertor replacements and the related maintenance preparing and closing actions are complicated and very critical at the point of view of the ITER long term availability.

Therefore the divertor replacement operations are necessary to be demonstrated and carefully studied. For this, a new remote handling test facility, Divertor Test Platform, DTP2, will be constructed in VTT Industrial Systems laboratory hall, Tampere. The operation of DTP2 is carried out in co-operation by TUT/IHA and VTT Industrial Systems.

The DTP2 facility comprises mock-up of the bottom part sector of the reactor with toroidal and radial rails, and the divertor cassette mock-up, Figure 6.7. The facility will also include prototypes of the maintenance equipment, CMM and SCEE (Second Cassette End-Effector).
Due to its special nature, the second cassette (cassette next to the access port) replacing is the first operations to be demonstrated on DTP2. Later the DTP2 platform can be updated to provide test environment also for the maintenance preparations and closing operations, the cassette toroidal mover and possibly also for other maintenance equipment development and testing.

Under the project TW3-TVR-MOVER during 2004 IHA was finishing the reference design of the CMM and SCEE and assisting EFDA in writing technical specifications for the mover call-for-tender documentation.

Under the project TW4-TVR-DTP2.1 IHA started evaluation of the effects of recent ITER-reactor element design modifications to the cassette replacement equipment.

6.7 Testing of Revised PFC Multilink Attachments

Institute:	**Tampere University of Technology**, Institute of hydraulics and automation (TUT/IHA)
Research Scientists:	M. Siuko, M. Pitkäaho, M. Toivo, J. Mattila, J. Poutanen, M. Vilenius, H. Saarinen, A. Raneda, H. Mäkinen, S. Verho, A. Mäkelä, H. Koivisto, A. Muhammad, T. Nykänen
EFDA Contract:	TW4-TVD-PFCATT, EFDA 03-1133

6.7.1 Background

A method for connecting the divertor cassette components to the body element is called multi-link joint. The multi-link joint incorporates several adjacent links which connect the cassette body and the element to be connected. The links are inserted into slots of the elements and a hollow pin is inserted into the hole formed by the hole of the links and holes of the element. Once the pin is inserted, a mandrel is pulled through it, when the pin is expanding forming a locked joint.

Previously IHA has studied the properties of joint locked by a 35 mm pin. The work was carried out in co-operation with EFDA and company NNC Ltd. During the year 2004 the characteristics of revised multi-link attachment were studied. The pin diameter was increased up to 45 mm. The work was done as previously, under EFDA supervisory, IHA was performing testing and the results were analysed by NNC Ltd. The study examines the physical properties of an attachment sample, so called single-link joint. The single-link joint incorporates one link which is connected to a fork-kind housing by a 45 mm AlBr pin which is inserted into the link holes and then expanded by pulling a mandrel through it. The pin to link connection should be tight (no clearance), but allow rotation of the joint without too much resistance. The joint should also be strong enough to sustain short term

max 180 kN tensile load force, and long term cyclic loads without loosing its mechanical properties.

6.7.2 Test equipment

The test equipments used were the pin swaging bench and the pin articulation and tensile loading test bench. Also simple test bench for plate-pin tests was used. The equipment design was as follows:

The sample joints for further tests were made with the pin swaging test bench, Figure 6.8. Hydraulic cylinder is used to pull the mandrel through the pin. The maximum pulling force (swaging force) is 150 kN. Swaging speed is 12 mm/min. Servo control is used to keep the swaging speed constant. During the swaging, the mandrel position and swaging force are measured and recorded.

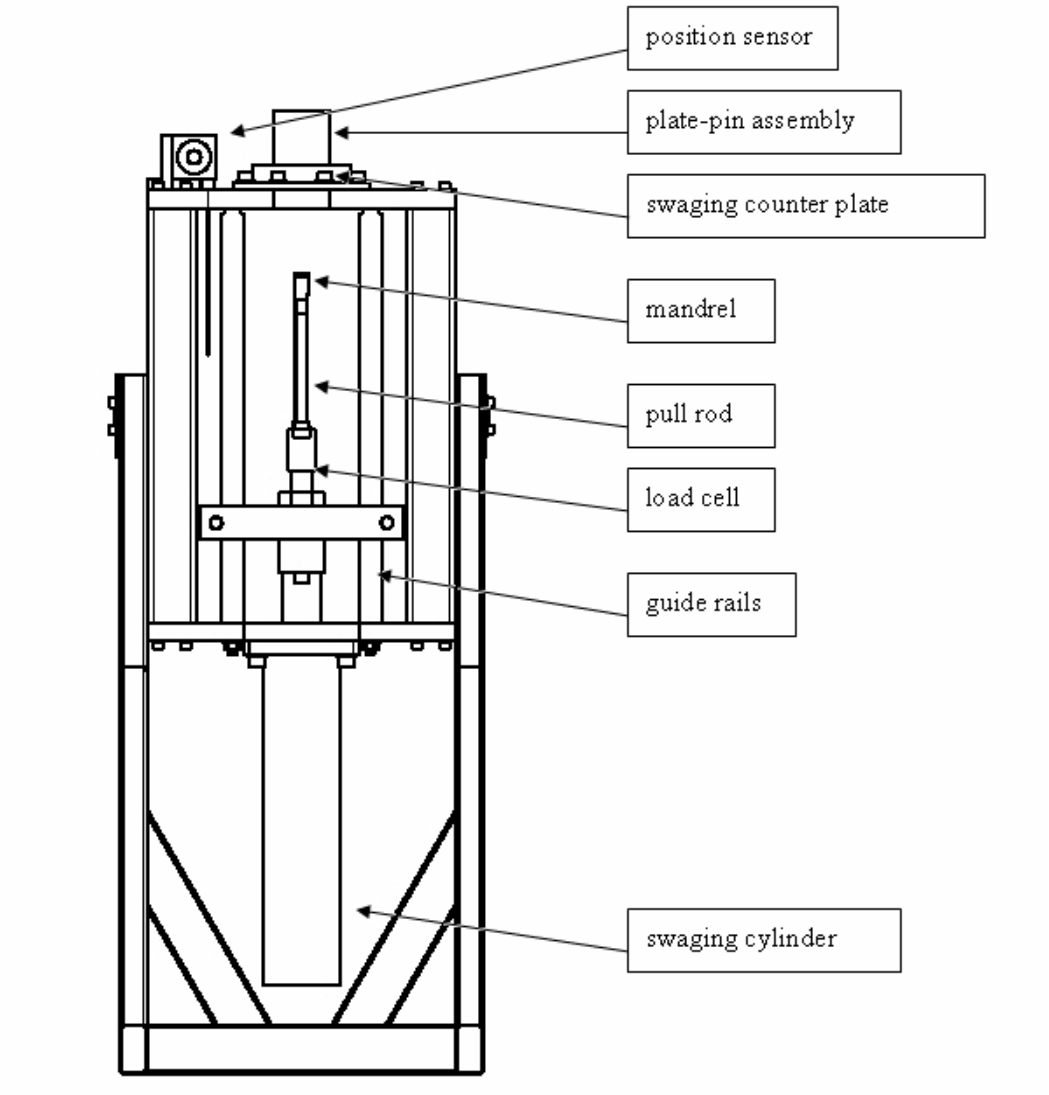

Figure 6.8: The bench for swaging pin samples.

The first joint samples were made by swaging a pin inside simple round plates. The torque required for articulating the plates was measured with the plate-pin torque measurement bench. The pin was locked to the test bench and a hydraulic cylinder is used for the plate rotation. The plate rotation torque and rotation angle were measured and recorded.

The loading and articulation tests were made for the single-link test samples. The tests were made with the tensile test bench, Figure 6.9. The test bench incorporates a 160/90 mm hydraulic cylinder designed for producing 204 kN tensile load, frame where the sample joint is attached and articulation mechanism for articulating the sample joint ± 1 degree with max torque 2500 Nm. The tensile load, sample torque, sample deflection and rotation were measured and recorded.

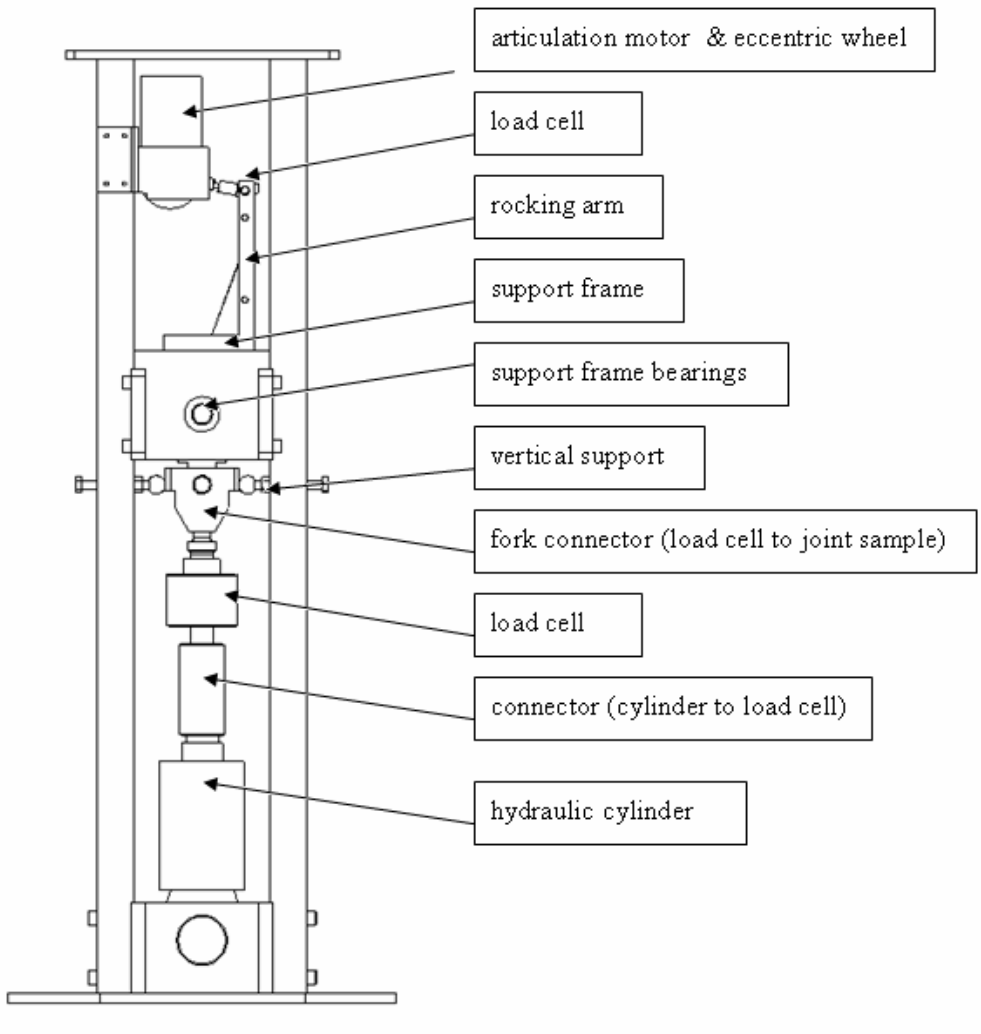

Figure 6.9: A joint sample tensile loading and articulation test bench.

6.7.3 Test procedure

Tests:

Material tests:

To verify that the pin material strength and elongation properties are as expected 8 material tensile tests were made.

Free pin tests:

The free pin tests were made to examine pin expansion and other geometrical effects during swaging to define the joint initial clearances and swaging mandrel for further tests. Free pin tests were made by swaging just a free pin without anything around it. Total of 12 free pin swaging tests were made with 22.45, 22.50 and 22.59 mm diameter mandrels. As a results 22.59 mm mandrel size was recommended for plate pin tests.

Plate-pin tests:
In Plate-pin tests a pin was swaged in a set of round plates of which rotating torque was then measured. Total 6 pins with 8 plates on each pin were swaged with 22.59 and 22.70 mm diameter mandrels. The aim was to find out the suitable plate to pin initial clearance and mandrel size combination that would produce the desired post swaging contact between pin and plates. As a result, 22.59 mm mandrel and 0.40 mm initial plate to pin clearance were recommended for swaging of tensile tests samples.

The first type of the tensile tests was made for single link joint sample. Test was made with the tensile test bench. The sample was attached in the bench and the tensile load was increased by 10 kN steps up to 180 kN. Between each load level, the load was decreased to 0. Total 5 tests with 2 samples were made. 4 were tested up to 180 kN and one up to 200 kN load. The aim was to examine the joint deflection and possible yielding during tensile loading.

Tensile test type 1 results (see Figure 6.10):

- Joint deflection at load, which represents the joint stress-strain properties.
- Residual deflection measured after every 10 kN load step, which shows joint yielding.

The result of the tests shows that the joint deflection behaviour was as expected according to Ansys analysis, although yield limit is slightly lower that assumed.

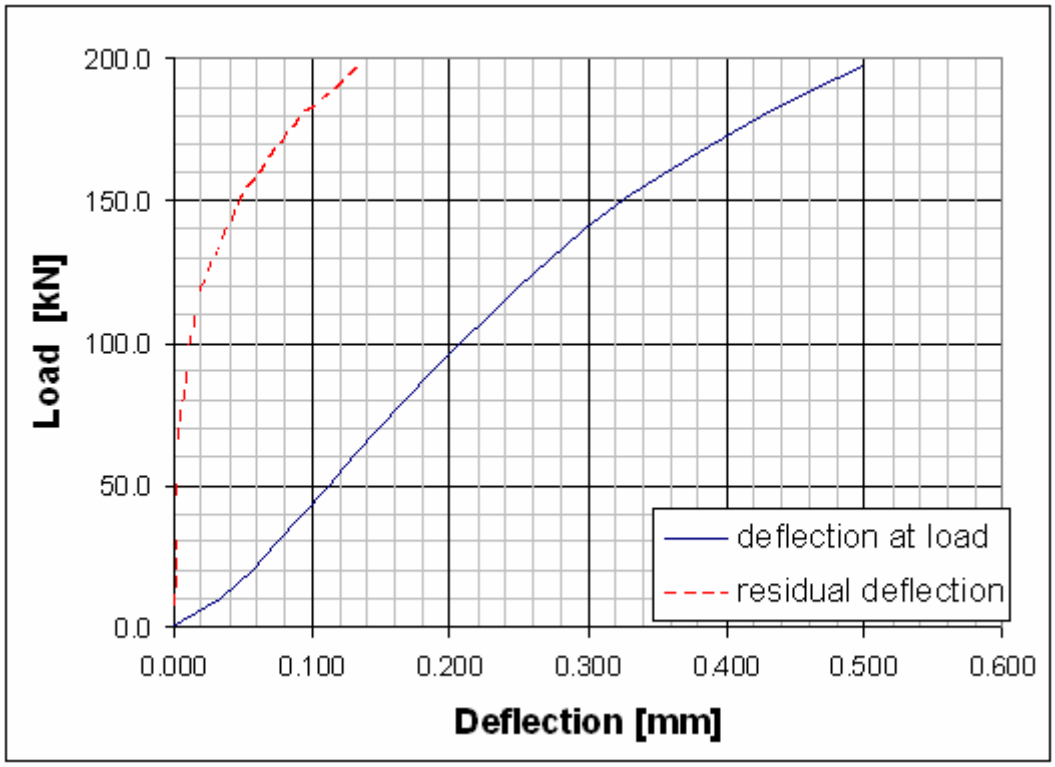

Figure 6.10: The force-deflection curve of tensile loading test of the single link sample.

6.7.4 Next actions

Next test will be made for single link joint samples with tensile test bench using tensile loading and also articulation. Long lasting articulation (1000 cycles) is done before and after the tensile test, in order to examine joint endurance properties. The aim of the test is

to examine joint properties (deflection, yielding, pin to plate connection torque, etc.) during cyclic tensile loading.

6.8 Development of a Water Hydraulic Manipulator

Institute: **Tampere University of Technology**,
Institute of hydraulics and automation (TUT/IHA)

Research Scientists: M. Siuko, M. Pitkäaho, M. Toivo, J. Mattila, J. Poutanen, M. Vilenius, H. Saarinen, A. Raneda, H. Mäkinen, S. Verho, A. Mäkelä, H. Koivisto, A. Muhammad, T. Nykänen

EFDA Task: TW4-TVR-WHMAN

6.8.1 Three-joint manipulator studies

Manipulator design specifications

A prototype of three Degrees of Freedom (DOF) manipulator developed in this work was designed for testing teleoperation applications by using water hydraulic components. The first two joints were actuated by cylinders and the third joint by a vane actuator. The load carrying capacity was defined to be 200 kilos where 100 kilos were reserved for future robot 3 DOF wrist weight and other 100 kilos for payload.

In mechanical design the structural stiffness of all components and the kinematics of the manipulator were optimized for force control purposes. Due to the weight saving potential compared to stainless steel or carbon steel aluminium was selected to be the link material. During the design process the strength and the stiffness of the links were analyzed by using FEM software. The optimal length of the links was determined by minimizing the criterion that the condition number increases most slowly in the vicinity of the isotropic configurations. The isotropic configurations of the manipulator can be obtained from the graph like Figure 6.11 which shows the condition number as a function of the joint angles.

Manipulator workspace

Manipulator structure is defined by the following DH-parameter table (Table 6-4).

Table 6-4: Denavit-Hartenberg parameters of three-link planar manipulator.

Link	a_i	α_i	d_i	θ_i
1	l_1	0	0	θ_1
2	l_2	0	0	θ_2
3	l_3	0	0	θ_3

Table 6-5 shows the motion ranges of the manipulator joints.

Table 6-5: Motion ranges of the manipulator joints.

	θ_{min}	θ_{max}
θ_1	-10°	110°
θ_2	-120.5°	-0.5°
θ_3	-145°	55°

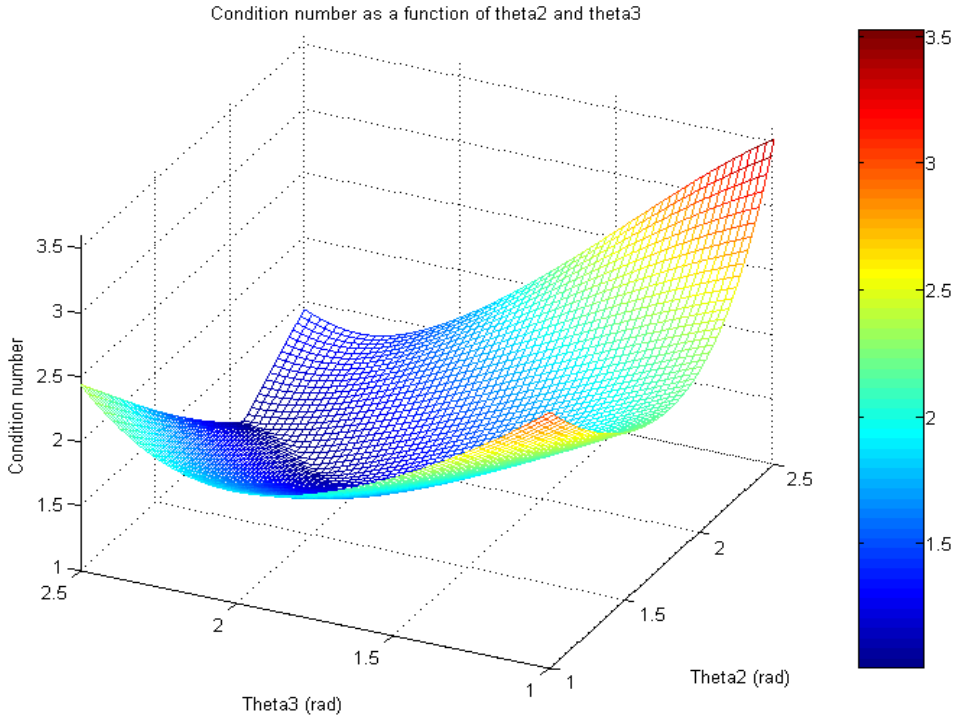

Figure 6.11: Condition number as a function of the joint angles.

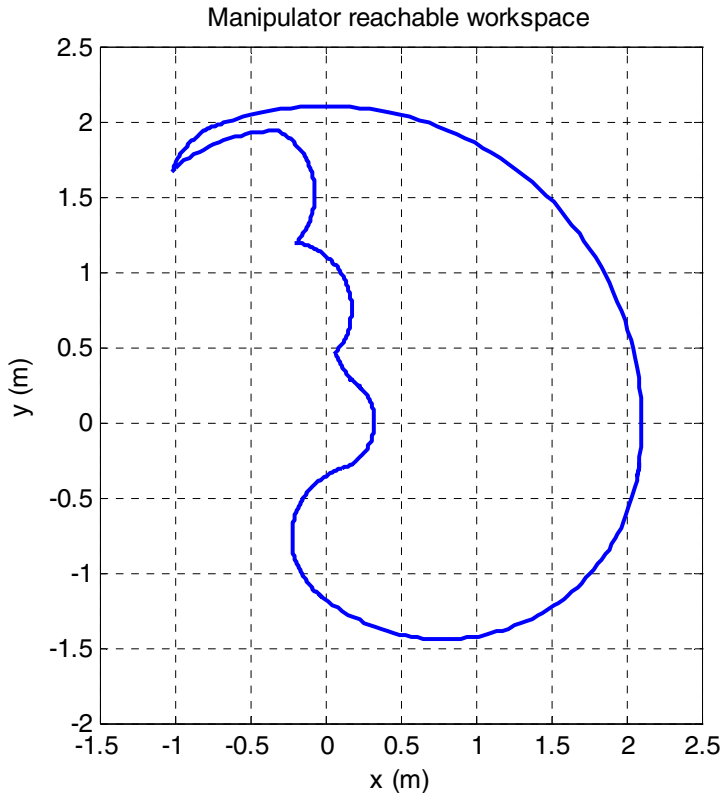

Figure 6.12: Reachable workspace of the manipulator.

Based on the manipulator motion ranges the reachable workspace of the manipulator was created into Figure 6.12.

Structural dynamic characteristics

With well designed manipulators, the stiffness of the hydraulics actuators has dominant affect to the stiffness of the manipulator. In the next the lowest natural frequency of the designed manipulator is shown. In Figure 6.13 manipulator links are assumed to infinitely rigid structures.

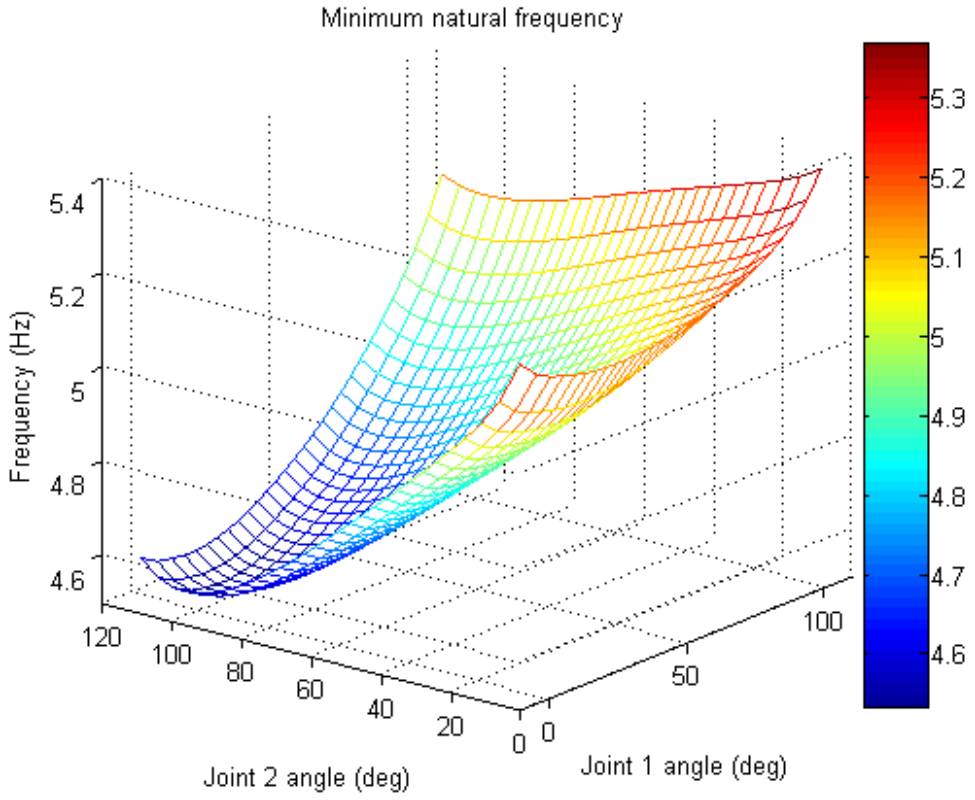

Figure 6.13: Minimum natural frequency of the manipulator.

Manipulator measurements

Combined position and force/torque controller was designed to control the manipulator. Measurements were carried out for preliminary tests to provide experience on the designed force controlled water hydraulic manipulator. Measurements were performed with two different controller parameter settings. In the first case, the controller gains were adjusted for good position accuracy and in the second case the emphasis was at the force tracking accuracy. From the back-driveability point of view the first case acts as a stiff spring and the second case acts as a loose spring.

In both cases the desired Cartesian position of the manipulator tip was the input to the cascade force-based position controller. Trajectory generator is used to create smooth joint motions between the reference Cartesian positions. The gravitation compensation proved to be quite sensitive to small changes in the weights and centres of gravities of the links. A kinematic calibration and identification of gravity related parameters have to be carried out later to enable the accurate gravitation compensation over the whole motion range of the manipulator.

The positions of the joints (blue) and their references (green) are shown in Figure 6.14. Figures 6.14–6.15 indicate that the position of the manipulator is controlled relatively

accurately and smoothly along the reference trajectories when the position tracking accuracy of the designed cascade motion controller is weighted.

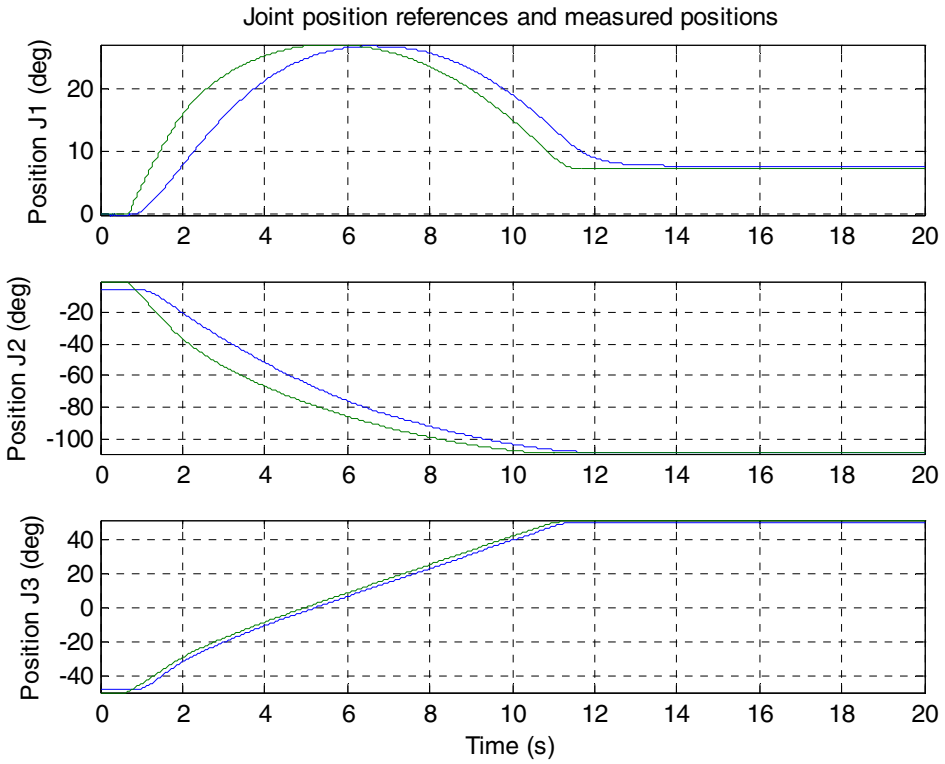

Figure 6.14: Joint positions and position references, measurement 1.

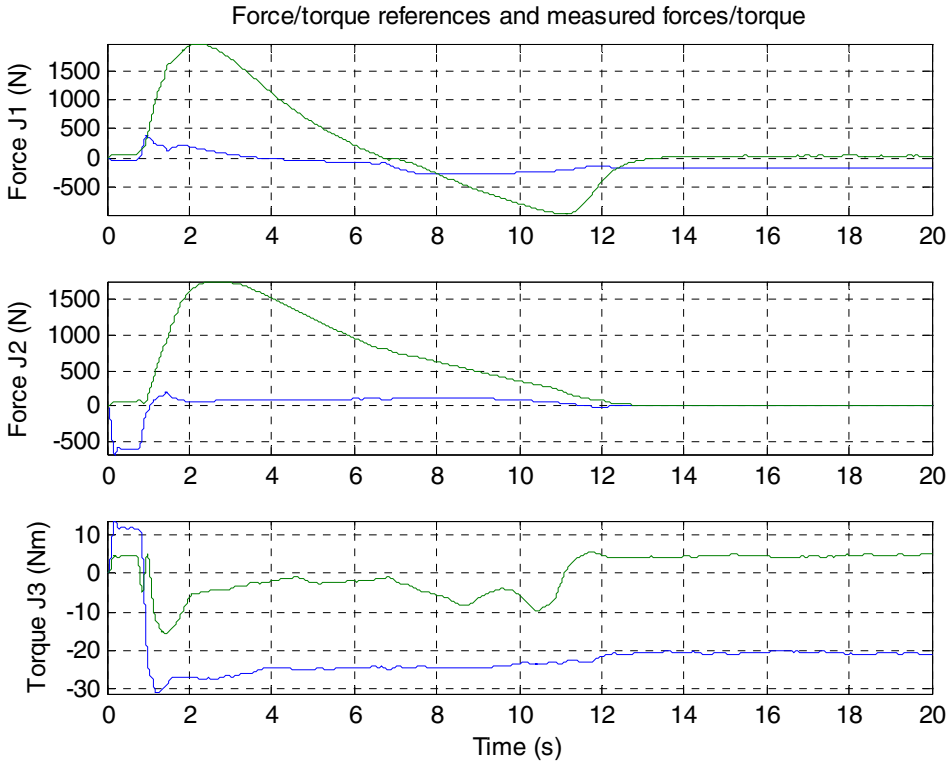

Figure 6.15: Joint force/torque and force/torque references, measurement 1.

6.8.2 Single joint test bench

Force/pressure controller

In the teleoperation the controlled slave manipulator has to be optimized to enable accurate force and position control with the haptic device. There are some shortcomings in both load cell based and pressure sensor based force control of hydraulic actuators.

Measurements were done to compare force, pressure and combined force/pressure controllers. It was studied, if the combined force/pressure controller would have the good qualities of single feedback controllers. The force feedback controller is the outer loop controller and the pressure feedback controller the inner loop controller on the combined controller. Outer loop controller is of PI-type because it has to be sensitive to external forces and have high static accuracy. Inner loop controller is of P-type in order to react fast to changes of the valve input. The combined force/pressure controller is shown in Figure 6.16.

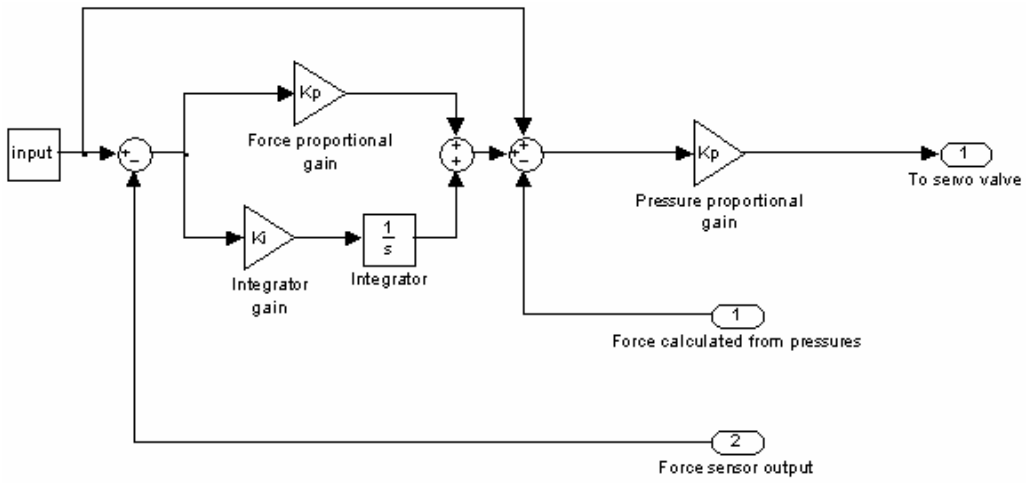

Figure 6.16: Block diagram of combined force/pressure signal controller.

1 DOF test bench measurements

The measurements were done with proportional (P) force feedback controller, proportional (P) pressure feedback controller and combined proportional-integral (PI) force signal and proportional (P) pressure signal controller.

The properties of each controller were measured by frequency response, step response and by the droop test. Frequency response measurement was used to define the maximum achievable bandwidth for each control system. The open-loop frequency response measurement of the test bench was first performed. The result from valve input to velocity without contact revealed bandwidth (-90°) of 11.3 Hz. The rest of the measurements were done with the boom in contact with stiff environment with the constant reference force to the cylinder was 2500 N.

Input signal was band-limited white noise (BLWN) with amplitude of approximately 500 N. Frequency responses were identified based on BLWN input and force output with ETFE (Empirical Transfer Function Estimate)-function of Matlab's Identification toolbox. The bandwidth of pure pressure signal feedback was (-90°) was 64,2 Hz and the bandwidth

(-90°) of the pure force signal feedback was 21,5 Hz. Figure 6.17 shows that the bandwidth (-90°) f the combined force/pressure signal feedback is 47,0 Hz.

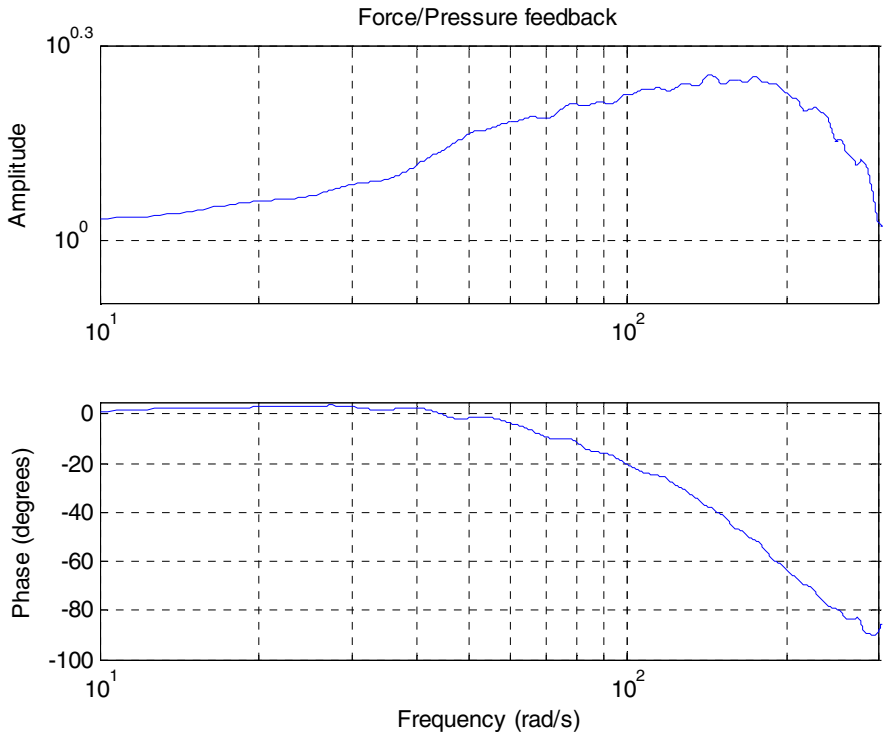

Figure 6.17: Frequency response of combined force/pressure signal feedback.

These results support the assumptions that the pressure feedback is faster than the force feedback. As expected, the bandwidth of the combined force/pressure signal is narrower than the bandwidth of the pure pressure signal. However, the bandwidth of the combined force/pressure signal is wider than the bandwidth of the force signal feedback

Step responses were used to verify the results obtained from frequency response measurements. They were also measured when the boom was in contact with the stiff environment and the step initial value was -500 N and the final value -4500 N. The signals were filtered afterwards with the same fifth order Butterworth filter with cutoff frequency defined as 10 Hz. Figure 6.18 shows the step responses of the force and pressure signal feedbacks. These graphs indicate that the pressure feedback signal reacts faster to the change in valve input than force feedback. Figure 6.19 on the other hand shows that the combined feedback reacts to change in valve signal input similarly to force signal feedback, but the pressure signal feedback improves the response by making it faster. Also the highly improved static accuracy with combined controller can be observed from Figure 6.19.

Droop measurements were made to compare sensitivities between force and pressure signal feedbacks. The measurements were done by moving the boom by hand up and down few times with different velocities. By comparing Figure 6.20 and Figure 6.21, the influence of friction can clearly be seen on pressure signal feedback. The static friction is different depending on the direction of motion. Also the Coulomb and viscous friction effect is noticeable from these Figures. Ideally the increased cylinder velocity would not increase the impedance. This would require that the force is compensated immediately when velocity is increased and that the servo valve would not saturate at the speeds required.

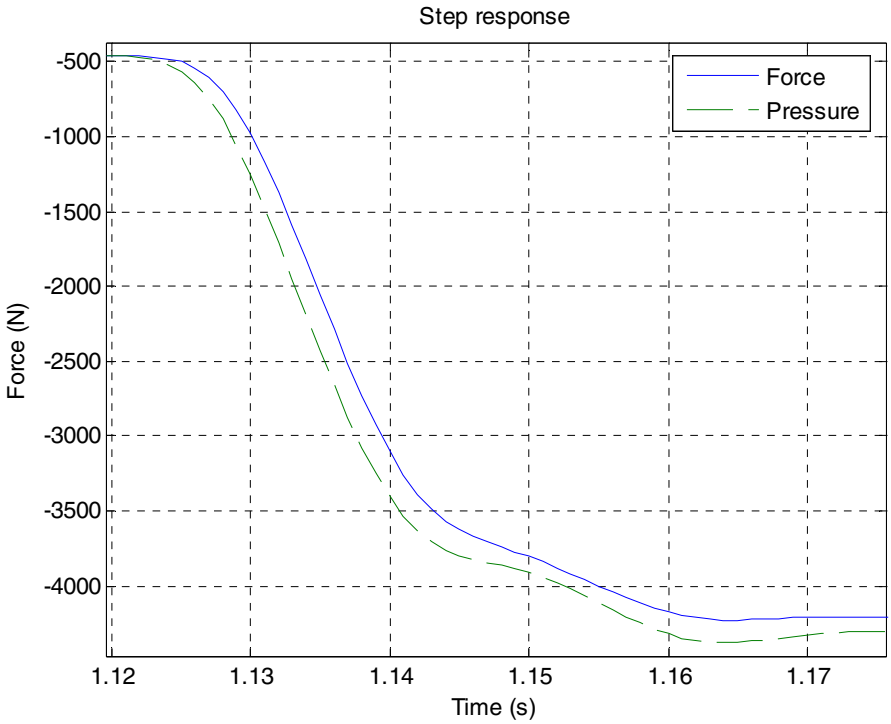

Figure 6.18: Step responses of force and pressure signal feedbacks.

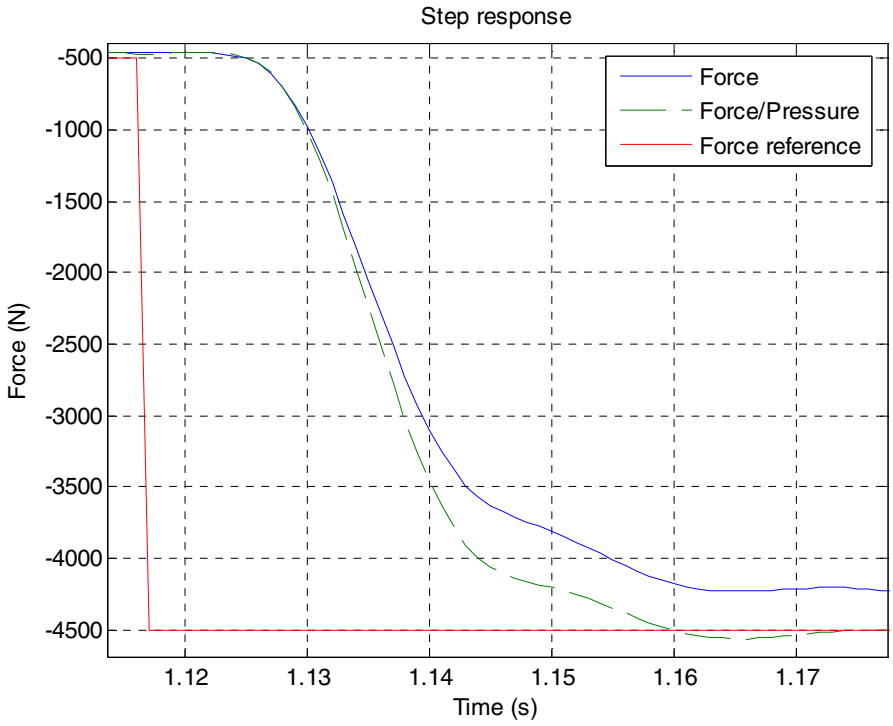

Figure 6.19: Step responses of force and force/pressure signal feedbacks.

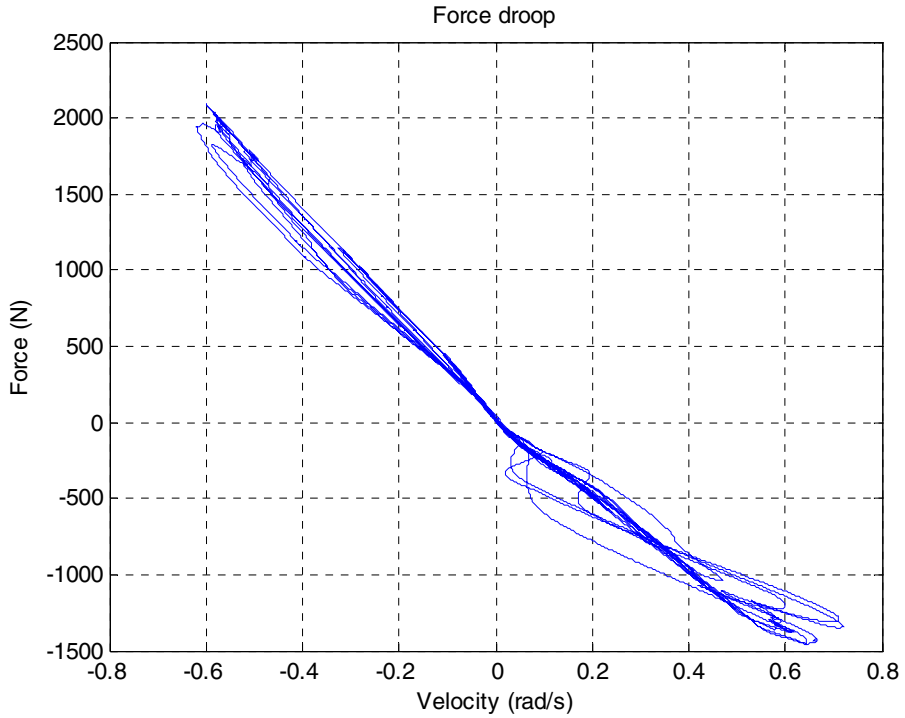

Figure 6.20: Force signal feedback droop.

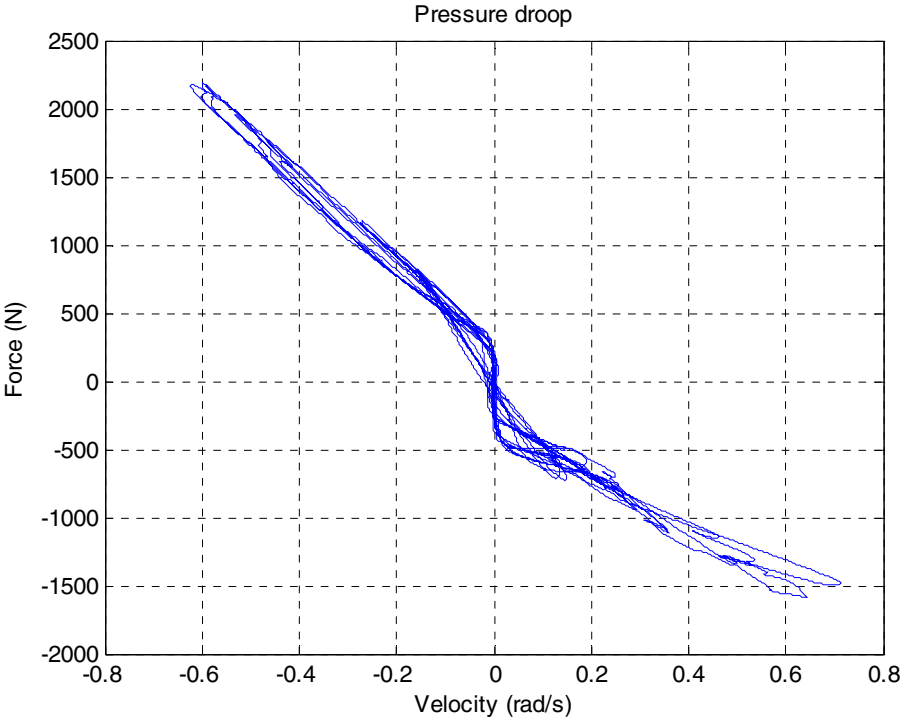

Figure 6.21: Pressure signal feedback droop.

6.9 Design and Development towards a Parallel Water Hydraulic Weld/Cut Robot for Machining Processes in ITER Vacuum Vessel

Institute: **Lappeenranta University of Technology**
Institute of Mechatronics and Virtual Engineering (IMVE)

Research Scientists: H. Handroos, H. Wu, P. Pessi, Y. Liu, E. Tenkanen, H. Yousefi

EFDA Task: TW3-TVV-ROBASS

6.9.1 Introduction

In task Task TW3-TVV-ROBASS; Upgrade Robot to Include Water Hydraulics and a Linear Track the 5DOF oil hydraulic parallel-robot Penta-WH developed in TW2-TVV-ROBOT will be converted into water hydraulic. A short linear track, carriage and clamping system is designed according to concepts proposed in EFDA 00-524. The mechanical parts of the robot are currently manufactured. Final design and selection of the water hydraulic components is currently carried out. In task TW4-TVV-Robot; Further Development of Safety, Stability and Accuracy of IWR a monitoring program is being developed for the robot controller. In addition to these novel methods for measuring the position of water hydraulic cylinders by using laser transducer and suppressing machining vibration with a piezo actuator are developed. In addition to development of the water hydraulic IWR the oil hydraulic prototype is equipped by a seam tracker provided by CEA. The interface between commercial seam tracker PC and the robot controller is built.

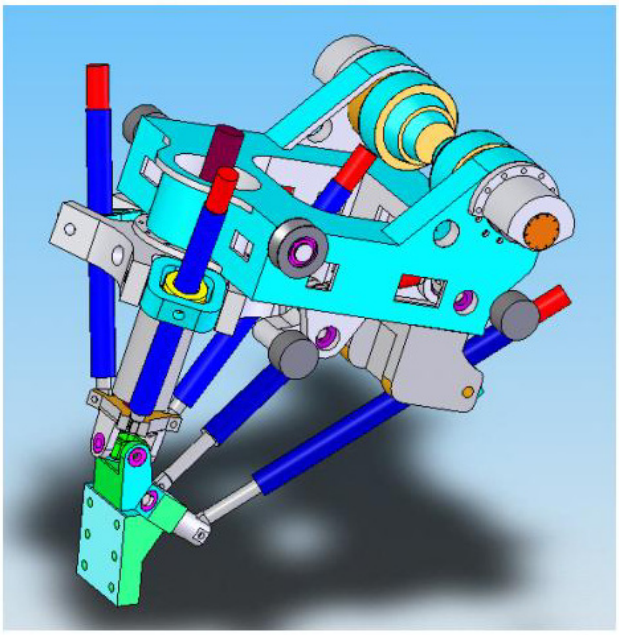

Figure 6.22: Water hydraulic IWR with carriage.

6.9.2 Mechanics and hydraulics of water hydraulic IWR

Figure 6.22 shows the assembly of the next version of IWR. The water hydraulic 5DOF robot is mounted on a steel carriage which is driven by two separate servo motors including cyclo gears. The carriage moves along the track by employing rack and pinion drive. A water hydraulic pressure controlled mechanism is maintaining constant contact

force between bearing wheels and rails. Since the radius of the track is varying the distance between the upper and lower wheel must vary in order to prevent damage. The mechanical parts of the robot are currently manufactured by Imatran Kone Oy. The component selection for the water hydraulic system of the robot is completed. The water hydraulic servo cylinders are currently designed.

6.9.3 Monitoring program for IWR

Methods for monitoring the transducer damages and return the robot into safety position are being developed. Since the robot is a hydraulic robot the actuator forces can easily be measured by means of pressure transducers. By using the Jacobean matrix for the robot the actuator space forces can be converted into Cartesian forces. The machining and contact forces can continuously be monitored by using the proposed method. In addition to force sensing the loss of position encoder signal can be detected by indirect calculation of speed by using hydraulic continuity equations. Thus, by measuring the pressures and servovalve inputs the resulting cylinder speeds can be approximated. When these are compared with those approximated by deriving the position encoder signals the encoder condition can be detected. By following this procedure the monitoring program is being constructed in the state flow form.

6.9.4 Novel methods for improving the static and dynamic accuracy of IWR

In the project two novel methods for improving the static and dynamic accuracy of the robot were proposed. Firstly, a method based on laser interferometer measurement was developed for precision measurement of water hydraulic cylinders. According to theoretical study the method is applicable but expensive and it requires precise temperature measurement because the measurement principle is extremely sensitive to temperature variations. Also variations in water pressure must be taken into account.

In addition to the laser measurement the applicability of piezo actuators for suppressing the machining induced vibrations in the robot was studied. A suitable actuator was purchased and a simple test system built. Experimental studies are currently carried out. In principle it is possible to integrate hydraulic cylinder and a piezo acutuator to form a hybrid actuator.

6.10 Further Development of E-Beam Welding Process with Filler Wire and Through Beam Control

Institute: **VTT Industrial systems**

Research Scientists: T. Jokinen, M. Karhu, V. Kujanpää

EFDA Task: TW3-TVV-EBEAMS

6.10.1 Introduction

During year 2002, work was carried out under TW2-TVV-EBFILL (UKAEA) and TW2-TVV-EBROOT (TEKES) to construct the necessary equipment and begin the development of a novel combination of e-beam welding process which offers significant benefits for VV sector welding in terms of distortion minimisation and speed of production. These first experiments need to be extended and the processes refined in order to optimise the processes. Development work has to be carried out to optimise the root welding using

through current control and also to increase the fill depth of the wire fill welding process at ITER welding positions.

6.10.2 Objectives

In this task electron beam welding, with using of filler wire and through current system developed in previous task TW2-TVV-EBROOT, will be studied in order to use the system in welding of vacuum vessel sectors of ITER. The task consists of building up the filler wire feeding system to be mounted inside the vacuum chamber of EB-welding machine of VTT. Together with through current control system, suitability of EB welding with filler wire will be studied in root weld of vacuum vessel sectors of ITER. Because of enormous sized of the vessel sectors, it is difficult to adjust sectors to be welded together within the tolerances needed in autogenous EB-welding. In order to fill the root of the weld, filler metal will be needed. Although filler wire is used in EB-welding process, still the heat input is in very low level comparing to the traditional welding methods. The welding will be happened in the mode of keyhole welding, so the distortions will be in direction of the plates and not closing the upper root of the weld to be filled up. This leads to smaller distortions of the plates. According to the low total heat input, EB with filler wire will also be studied in filling passes. In this work optimal parameters are studied in order to quality level of the welds needed in different welding positions.

6.10.3 Deliverables

The project started late in 2003 and will be continued to 2005. The project will be performed in different sub-tasks:

1. Set-up of filler wire feeder test facilities inside to the vacuum chamber of EB-welding machine of VTT. Modification of through beam current control system for welding with filler wire developed in previous task TW2-TVV-EB-ROOT.
2. Preliminary welding tests for usability of the system.
3. Experimental investigation on root welding using modified rest current control and filler wire feeder.
4. Experimental investigations on filling weld in narrow gap using filler wire with austenitic stainless steel thickness of 60 mm.
5. Final report on auxiliary systems and welding tests.

6.11 Cross-Checking of the Strand Acceptance Tests

Institute:	**Tampere University of Technology** Laboratory of Electromagnetics
Research Scietists:	Risto Mikkonen and Iiro Hiltunen
EFDA Contract:	TW3-TMSC-ASTEST, EFDA 03-1125

6.11.1 Introduction and background

ITER is based on magnetic confinement fusion. It uses the fact that a plasma consists of charged particles and tries to confine them in a region thermally insulated from the surroundings by using a special configuration of magnetic fields which are created with NbTi and Nb_3Sn superconductors. The objective of the task is to measure the recently developed Nb_3Sn strands procured in the framework of an EFDA technology task. These cross-checking tests have to verify whether the performance of the procured advanced strands is according to the strand specification or not.

During year 2004 Laboratory of Electromagnetics in TUT has modified the cryogenic measuring station in the framework of the strand characterisation. The temperature of the samples can be set with a variable temperature device which enables an operating temperature between 1.6 K – 300 K. The external magnetic field is generated with a new hybrid superconducting solenoid providing the magnetic flux density up to 16 T. For the benchmarking EFDA provided samples of Nb_3Sn strand. The benchmarking tests were made twice in accordance to the specifications made by EFDA.

6.11.2 Research methods and benchmarking measurements

The SEM image of the polished cross section of the superconducting wire is shown in Figure 6.23.

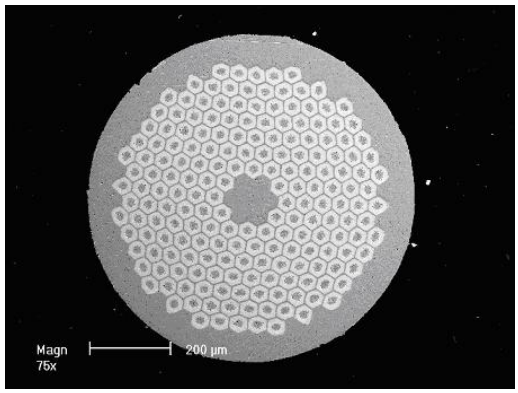

Figure 6.23: SEM image of the polished Nb_3Sn conductor.

The dimensional benchmarking measurements included the following sample characterisations: (1) Twist pitch length is the linear distance over which a filament of twisted multifilamentary conductor makes one complete revolution. The twist pitch sample was prepared by etching a 4 mm section of strand with HNO_3 until the bundle of filaments became visible. The pitch angle was estimated from an optical micrograph resulting a twist pitch of about 11 mm. (2) The conductor cross-section includes copper as a stabilizer. The strand sample was mounted in resin and sample surfaces were polished. Photograph from the strand cross-section was taken with an optical microscope. Cu:non-Cu ratio was measured by the paper mass method from an optical photograph. A magnified photo of the cross-section of the strand was cut to pieces and the masses of the copper and the non-copper areas were measured which concluded to the Cu:non-Cu mass ratio of 55%. (3) Samples were mounted in resin and sample surfaces were polished. Photograph from the strand cross-section was taken with an optical microscope. The strand diameter was measured on one cross-section at three different locations, spaced by 120^o concluding to the conductor diameter of 800 µm.

The electromagnetic characterisation of the test strand was carried out with the new modified cryogenic measuring system. The critical current sample, attached to its current leads, is placed in liquid helium bath, in a magnetic field parallel to the axis of the sample holder. The field homogeneity at the sample volume and the field accuracy is better than 0.2%. The helium bath temperature is measured with an accuracy of 10 mK. The sample current is measured with an accuracy of 0.1% and the voltage of the test section is sensed with an accuracy of 20 nV. The sample holder and the test cryostat is shown in Figure 6.24.

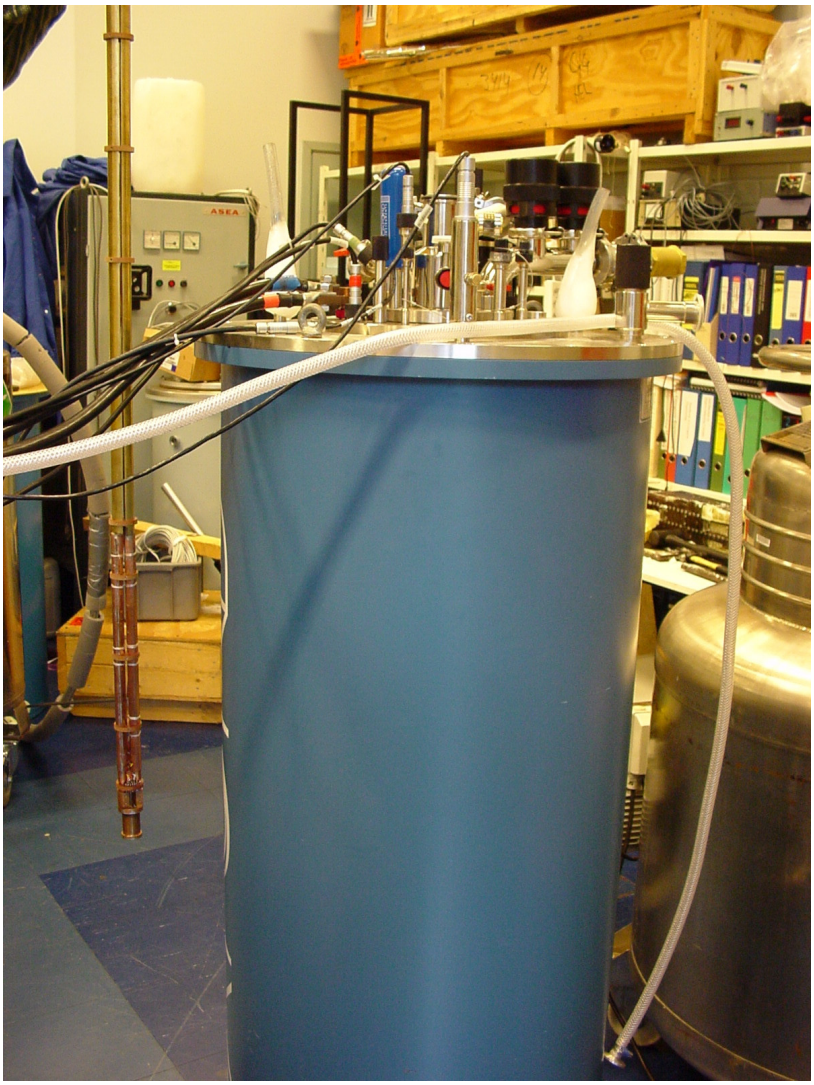

Figure 6.24: The sample holder used in the benchmarking tests of the Nb_3Sn strand.

The electromagnetic characterisation included the following measurements: (1) RRR (Residual Resistivity Ratio) is the ratio of a metal's (copper stabilizer in this case) electrical resistivity at 273 K to that at low temperatures, a parameter to express the metal's purity. The resistance of the sample was measured at self field both at the room temperature and at T = 20 K, which is well above the critical temperature of Nb_3Sn. During the measurement a current value of 1 A was used. (2) The critical current, I_c of the test sample was measured at liquid helium temperature. The I_c value was determined with an external magnetic field of 12 T. The current ramp rate of the sample near the transition was about 0.4 A/s. The voltage signals from the two pairs of voltage taps were recorded; the I_c was derived from the voltage of a 500 mm strand section. The voltage versus current curve was determined with a high precision data acquisition system with a nanovolt meter. The sample critical current was 390 A at 12 T and 4.2 K. (3) The *n*-value determines how sharp is the transition from the superconducting to normal state. It is advisable to reach high *n*-values which means that there is practically no heat generation in the conductor before the transition. The *n*-value of the sample was measured together with the I_c measurements. The measured voltage-current curves were fitted to the well known power law and the *n*-value was determined by using a least squares method. The measured *n*-values varied from 46 to 48 which indicate a fairly sharp transition behaviour.

6.11.3 Conclusions

The worldwide development in the last few years indicates that Nb_3Sn strand performances still have margins of improvements for critical current densities and/or hysteresis loss. Nevertheless electromagnetic characterisation of single Nb_3Sn strands are required for the optimisation and final design of the ITER conductor. The benchmarking activities indicate the required measurements can be done in TUT. The characterisation of five actual samples (according to the contract) are scheduled to the spring 2005. All together six European conductor manufacturers will deliver strand samples to the qualified Associations for the strand characterisation.

7 FUSION TECHNOLOGY – SYSTEM STUDIES

7.1 External Costs of Fusion and Fusion as a Part of Energy Systems – New Evaluation Methodologies

Institute: **VTT Processes**

Research Scientist: R. Korhonen

EFDA Tasks: TW2-TRE-EFCA, TW3-TRE-FESAC

7.1.1 Background

The study (Identification and comparative evaluation of environmental impacts of fusion and other possible future energy production technologies) has been performed in the framework of the Socio-Economic Research of Fusion (SERF). Assessments of monetarised external impacts of the fusion fuel cycle have earlier been performed in the SERF studies. Fusion power plants were assumed to be installed around 2050. Occupational accidents, road accidents and impacts of emissions were studied during the whole fuel cycle. SERF 4 is titled Fusion as a part of energy systems. VTT participated in SERF 4 by evaluating further long term environmental impacts of fusion and also by comparing fusion with (advanced) fission concepts. Long time horizons in the estimation of environmental impacts have been an important focus of the work of VTT in SERF work.

Restriction of global warming is important when future energy alternatives are developed. Especially carbon dioxide emissions have long term impacts. Fusion and fission energy production give rather minimal carbon dioxide (or other greenhouse gas) emissions. Some long term radionuclide impacts are possible, if radionuclides caused by fission of nuclides (fission energy production) or by bombardment of neutrons (fission and fusion energy production) reach the environment either in normal operation or from waste repositories.

The primary aim of SERF-Externalities studies in earlier SERF work was to estimate environmental costs of fusion using ExternE methods as external costs of other main alternatives were earlier evaluated in other EU-projects. Waste disposal was in SERF work considered to be necessary for fusion. The inventories of C-14 in fusion waste were considered to be important from the point of view of external costs in SERF. This was the basic finding in SERF 1. Then also local scale individual doses were evaluated and estimated to give that retention of the order of 20,000 years is necessary, when critical individual is studied. In this project (SERF4, VTT/Tekes) especially the question about necessity of waste disposal is studied.

7.1.2 Research methods

Power Plant Conceptual Studies (PPCS) are considered and used in the re-evaluation. Finnish disposal experience was used in the evaluation of realistic disposal assumptions. Finnish and international regulations have been studied.

Disposal is studied by studying various retention periods, release periods, and local and global scenarios. Individual dose rates and collective doses (local and global) are estimated for chosen indicative radionuclides.

Cycling of carbon is an important part in the evaluation of global warming and C-14 impacts. Simplified models have been built for two kinds of transfer situations. Then also the concept carbon-years in the atmosphere has been evaluated and used in the study. Simplified approach might be useful in various situations including also stationary situations. The difference of the decrease behaviour of carbon dioxide and C-14 is possible to present in a simple model. Collective doses and GWP factors are closely related concepts which are actually based on carbon-years in the atmosphere.

7.1.3 Main results

Clearing and recycling has been considered to be possible after 100 years of cooling in PPCS studies (Forrest 2003). This has been questioned in this study in the light of regulations. Activity concentrations (Bq/g) of studied radionuclides are much higher than limits in the present international regulations. Regulations (IAEA, EU) are based on somewhat conservative assumptions for doses to critical individual. However, it seems that clearing or recycling had to change considerably, before fusion waste might be cleared. Options like recycling within nuclear industry or under continued control might be possible, at least for part of waste materials. These are not actual clearing options. This should be studied further. Collective global doses are not considered in these regulations.

Disposal alternative has been studied. Limits for individual doses cause that retention of radionuclides, especially C-14 should be more than 20,000 years. Radionuclide C-14 is relatively easily released and transferred if in contact with water and barriers should be rather effective. About the same retention is also required by the external cost studies based on long term global doses.

It has been suggested in this study that the Finnish limit for C-14 emission in disposal 0.3 G Bq/a might be very low and has been chosen on the basis of rather pessimistic assumptions about local scale especially in the case of deep repositories. Actually then limits might be lower. Possibly they have been chosen in the situation of much lower C-14 inventories. However, C-14 is somewhat critical also in the case of fission waste.

Local scale doses are very dependent on considered scenario assumptions. Volumes of reservoirs, water exchange rates etc. are assumptions which largely impact estimation of doses. Choice of assumptions might easily have an impact of the order of hundred.

In the SERF studies a local well was assumed. For the shallow land burial case the water exchange rate was assumed to be 10^3 m^3/a and for the deep repository 10^5 m^3/a. The annual use of water as a drinking water was assumed to be 500 l for the critical individual. These assumptions give dose conversion factors 3×10^{-13} Sv/Bq for the shallow land burial case and 3×10^{-15} Sv/Bq and for the deep repository case in the case of C-14. For the radionuclide Nb-94 dose conversion factors 8.5×10^{-13} Sv/Bq for the shallow land burial case and 8.5×10^{-15} Sv/Bq and for the deep repository case have been estimated. If these factors are used, retention of C-14 for rather long time spans is necessary. Also Finnish regulations are rather strict for C-14 releases from repositories.

Limits for clearing and recycling are rather strict in Finnish regulations. Premises for removal of regulatory control give activity concentrations of the order 10 Bq/g or less for nuclear waste materials. Higher limits for smaller amount of materials are also given in international regulations. Recycling in nuclear industry might be possible.

Re-evaluation of C-14 impacts has included consideration of the impact of increased carbon dioxide concentrations on the C-14 transfer and impacts. Increased carbon dioxide concentrations are generally assumed to cause dilution of C-14/C ratio in the atmosphere (Suess effect). It has been indicated in the re-evaluation study using simplified model concepts that increased flows of carbon will also increase the accumulation of C-14 in the atmosphere. The impact of Suess effect is therefore evaluated to decrease and estimated to lose its importance in a few decades. Therefore increasing carbon dioxide concentrations will not decrease the future radiation dose impacts of C-14 emissions e.g. due to nuclear energy. This might have some scientific importance.

Restriction of global warming is one very important constraint which causes that fusion energy might have an important role in the energy production after some decades, when technical development has solved the problems. In future SERF-work fusion will be studied as a part of energy system. Impacts of global warming are very important reasons for development of fusion. Especially dynamics of carbon is an important part in TIMES or other models which estimate energy future.

However, it is also very important to study also the environmental impacts of fusion and especially production and then management of radionuclides. It might then be possible to find optimal solutions for materials in that respect at an early stage and also discuss the possibility to avoid disposal of radioactive fusion waste. In the SERF study somewhat indicative estimation has been performed.

7.2 IFMIF Test Facilities

Institute: **VTT Processes**

Research Scientists: F. Wasastjerna

EFDA Task: TW4-TTMI-003

The aim of the Task was to update the global geometry model for the entire IFMIF (International Fusion Materials Irradiation Facility) test module assembly and to perform a 3D calculation of the entire nuclear response.

The IFMIF test facility will play an essential part in the global fusion research program, providing data about how well materials and components can stand intense neutron irradiation. Since producing an intense flux of high-energy neutrons and exposing the materials and components to be tested is the whole purpose of the project, neutronics calculations are obviously an essential part of the design work. They are needed both to ensure that the test volumes are subject to an adequate flux, with a spectrum simulating that in a fusion reactor sufficently closely, and to verify the adequacy of the shielding. The calculations are performed using the program McDeLicious, a version of MCNP4C modified to simulate the interaction between deuteron beams and the lithium jet and the ensuing interactions of neutrons with energies up to 55 MeV with materials.

The objective of the work described here was not to carry out the actual calculations but to prepare an input file for McDeLicious with a good description of the geometry and materials. A preliminary such file had already been created in 2003, but it needed to be updated. There were essentially 3 things that needed to be done:

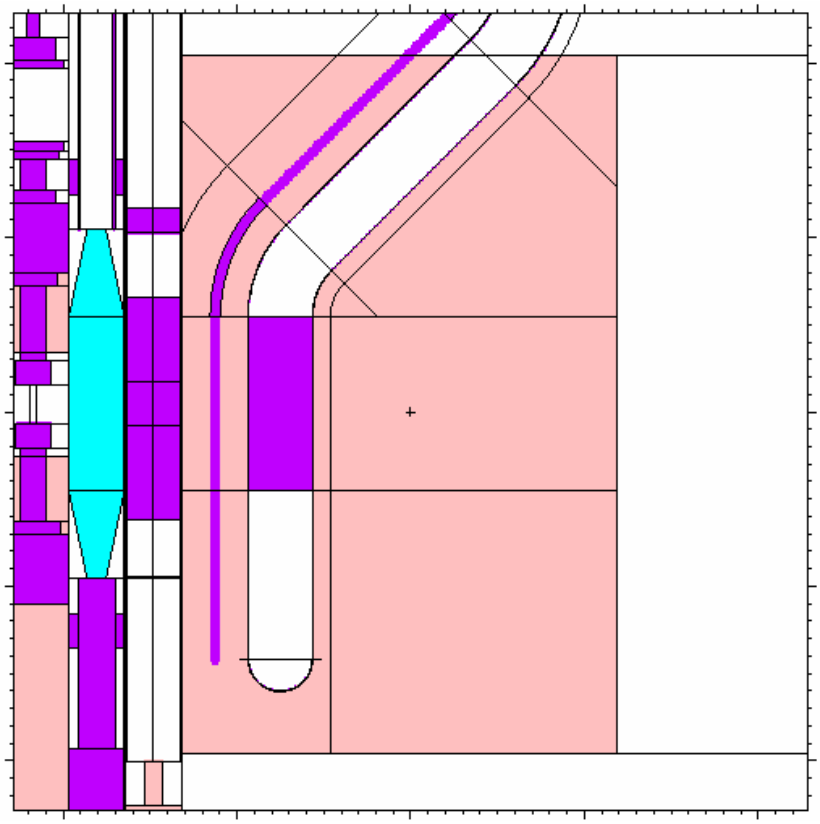

Figure 7.1: In the current model (md33) the low / very low flux irradiation positions are imbedded in a block of graphite. The picture plane is slightly off the symmetry plane, showing one irradiation tube in the far bank (very low flux) and a small part of the tube wall for one tube in the near bank (low flux).

1. Updating the geometry. The information available in 2003 was seriously inadequate where the low and very low flux test modules and the test cell cover were concerned, so the original model had to be based on guesswork in these areas. By the spring of 2004, a reasonably complete preliminary design was available for the cover. For the low/very low flux test modules that was still not the case, but enough information was available for a greatly improved guess. This information was incorporated in the new model, which now treats the cover in sufficient detail and with sufficient realism to calculate the probably quite considerable streaming. Minor design changes elsewhere were also included in the model.

2. Modifying the model at the request of users, to facilitate geometry changes such as removing the Universal Testing Machine and the tungsten spectral shifter and moving the Tritium Release Module closer to the neutron source. These modifications were carried out. Other modifications were made to improve the resolution of importance or weight windows, needed to reduce the variance in shielding calculations.

3. Determining for which nuclides cross section data was available in the energy region from 20 to 55 MeV, above the range covered by normal MCNP libraries. It was found that data was available for all the important nuclides, which are now included in the model. For some nuclides present only in small amounts data was not available. These were simply omitted, except in the case of the lesser potassium isotopes, which were replaced by K-39. These approximations do not have a significant impact on the accuracy of the calculations.

Although the official deadline for this work was 2004-12-31, the users of the model had requested that it should be finished by the beginning of April 2004. This objective was achieved. The test calculations that had originally been envisaged as part of this task could not be performed in this time frame, but they were not needed since the model was immediately used in actual calculations and performed well.

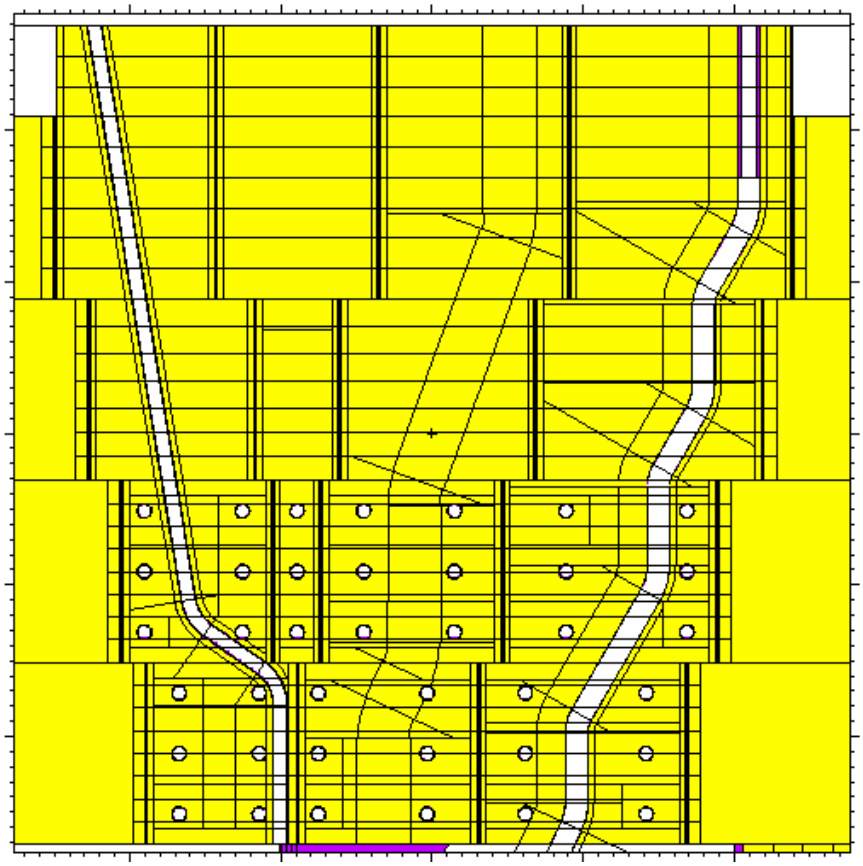

Figure 7.2: Reasonably adequate design information about the test cell cover is now available, and it has been modeled in considerable detail, also paying attention to the need for sufficient spatial resolution for the neutron importances needed for variance reduction in Monte Carlo calculations. Only a few of the many ducts in the cover are visible in this cut.

7.3 Helium-Cooled Pebble Bed Test Blanket Module Shielding Calculations

Institute: **VTT Processes**

Researcher Scientists: P. Kotiluoto, F.Wasastjerna

The blanket of ITER does not provide tritium breeding. However, such breeding is essential in fusion reactors intended for power production, at least if fusion is to be used on a large scale. Therefore test blanket modules (TBMs) will be inserted in some of the equatorial ports.

The designs to be tested include a helium-cooled pebble bed design (HCPB). The neutronics calculations for the actual breeding blanket, such as calculations of the breeding and the heating, have already been performed at Forschungszentrum Karlsruhe. However,

the shielding calculations, in which it is determined whether the shield behind the test blanket module is adequate to limit the shutdown dose rate at the end of the port and the heating in the cryogenic components, will be performed by VTT PRO. This work can be divided into three stages: preparing the geometry model, preparing the rest of the input file (especially the starting importances needed for variance reduction in a Monte Carlo calculation), and the actual calculations.

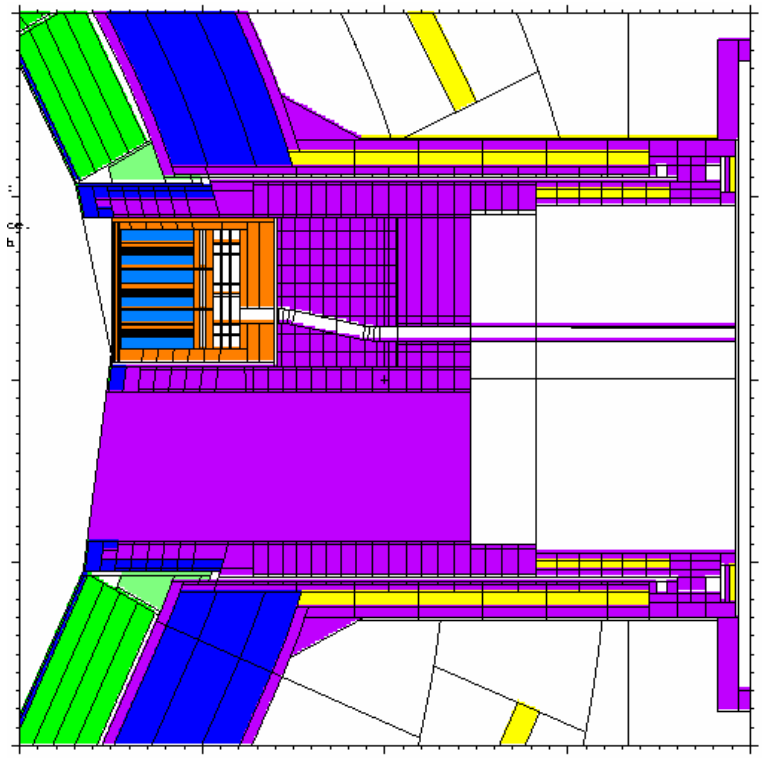

Figure 7.3: This figure shows a vertical cut through the equatorial port containing an HCPB TBM. The calculation concerns only the upper half of the port. Any neutrons entering the undifferentiated steel mass in the lower part are killed. The slight mismatch between the cell boundaries and material colour boundaries in the figure is due to the limited spatial resolution of the geometry plot.

The geometry model is based on the standard 20-degree model of ITER with two half ports included at each level (upper, equatorial and divertor ports). A model of the port plug with the shield was developed at VTT PRO, and the existing model of the TBM was incorporated into this. Most of the model was finished in 2004, but some parts still remained. The model will be finished in 2005, and the calculations will be done using a version of the Monte Carlo code MCNP4C modified to model the neutron source distribution in a tokamak more accurately and to permit a calculation of the neutron flux, activation and subsequent gamma transport in a single step.

7.4 Power Plant Conceptual Studies – Safety Assessment

Institute:	**Helsinki University of Technology**
Company:	**Fortum Nuclear Services**
Research Scientists:	Prof. Rainer Salomaa, MSc Gintaras Zemulis
EFDA Task:	TW1-TRP-PPCS4

The Subtask 4 of the Power Plant Conceptual Studies involved thermohydraulic analysis of various accident scenarios in a tokamak reactor concept with water-cooling and lithium-lead breeding blanket (Model A). Within the APROS simulation environment we have built a thermohydraulic model for such a fusion power plant including the relevant first-wall and breeding blanket structures, vacuum vessel, the primary and secondary cooling circuits together with the pressure suppression systems and the drainage tanks. The results obtained were incorporated into the final report "Power Plant Conceptual Study, Final Report on Safety Assessment of PPCS Plant Models A and B" by L. Di Pace (PPCS/ENEA/TW1-TRP-PPCS4/7 Rev. 0, EFDA Task TW1 TRP PPCS4, Deliverable 9). During 2004 we have improved the APROS-submodel on chemical reactions of liquid lithium-lead with steam and tungsten. A new revision of the simulation code was adopted.

8 UNDERLYING TECHNOLOGY

8.1 In-Vessel Materials

Institute: **VTT Industrial Systems**

Research Scientists: S. Tähtinen, M. Valo, K. Wallin, P. Moilanen, T. Saario, P. Kauppinen

8.1.1 Further development of fracture resistance test methods and verification of specimen size effects

The objectives is to generate fracture mechanical data on candidate fusion materials by using three point bend and to verify effect of the specimen type and size on fracture mechanical properties in order to utilise miniature specimens used in irradiation test programs. An important aspect of the method development is to make it possible to test small activated specimens in simulated coolant water environment.

8.1.2 Development of in-situ mechanical test methods

Pneumatic loading devices were further developed for material testing purposes. The load frames have been designed for the changeable specimen systems, i.e., the system consists of the moveable (by manipulator) cassette system with the thin folio specimens.

New software for the servo controlled pressure adjusting loop were developed for tensile and fatigue testing systems. The Moog controlling software for the pneumatic pressure controlling loop has been updated for the MACS (Motion Axis Control System) controlling language. Furthermore, all electrical components of the Moog programmable servo cards have been updated and changed for the MACS technology.

The pneumatic pressure adjusting loops have been equipped with the additional servo valves to minimize the pressure variations and maximize the safety factors during the tests. Furthermore, two pneumatic servo controlled pressure loops have been built up for the laboratory and hot cell reference tests of the Cu and CuCrZr samples.

New software to collect fatigue data with high frequency was develop for in-situ fatigue tests. The special data acquisition system to collect and analyze the fatigue test data have been developed and tested and sent to Mol. The data collection system is moveable and it has been designed to use at test reactor environment.

8.1.3 The effects of straining on oxide films and passivity of copper in nitrite solution at ambient temperature

Objectives

The effect of strain rate on interactions between copper and the oxide layer growing on it, has been studied. The electrochemical oxidation process of copper in a neutral electrolyte at room temperature is accompanied by the generation of vacancies at the copper-Cu_2O interface, at potentials when the CuO-type oxide layer begins to build up on the Cu_2O barrier oxide layer. Diffusion of vacancies into the metal or annihilation of vacancies by

dislocation reactions is required in order for oxidation to continue with a high current density. Sufficiently slow straining without breaking the passive film on the copper leads to re-arrangement of the dislocation structure at the interface, which in turn helps to consume the oxidation-generated vacancies. Maintaining such an equilibrium between straining and oxidation/dissolution produces an environmentally-enhanced plasticity in the copper substrate, and simultaneously accelerated corrosion, conditions occurring as long as the strain rate is slow, i.e., on the order of $<10^{-8}$/s. However, strain-induced cracking of the passive film and its subsequent re-passivation results in a lower oxidation/dissolution rate than does straining without film rupture, while the oxidation ceases in the absence of continued straining.

The effects of slow straining rates on the corrosion behaviour of copper have been studied at room temperature, using high purity copper specimens strained at various rates, even as low as 10^{-10} s^{-1}. The electrochemical oxidation behaviour of copper has been recorded by polarisation monitoring during specimen straining. The synergistic behaviour between the oxidation/dissolution process and the dislocation structure at the surface layers of metallic copper will be discussed.

Results

Test material used in the experimental part of this study was pure copper (99.998 wt. %) containing a maximum of 75 ppm oxygen. In order to simulate the material near the tip of an advancing stress corrosion crack, the material was cold deformed by rolling and appropriate intermediate heat treatments, to produce a 1.00 mm thick strip. The yield strength of the cold- deformed copper at room temperature was about 400 N/mm^2. Small flat tensile test specimens with 1×5 mm^2 cross section and 15 mm gauge length were manufactured by electric discharge machining and then wet grinding down to a uniform 0.5 mm thickness. The total surface area exposed to a $NaNO_2$ solution was about 1 cm^2. Polarization curves, recorded at a 1 mV/min scan rate, were generated for specimens strained at a rate of 10^{-6} to 10^{-10} s^{-1}, in a room temperature solution of pH 8.3, 0.3 M $NaNO_2$, deoxidized by nitrogen gas purging. Slow straining rates were produced via a pneumatic loading device that is capable of generating linear displacement rates down to $5x10^{-9}$ mm/s. The specimens were preloaded to 0.2% elongation before start of the potential sweep at -700 mV_{SCE}. A platinum plate was used as a counter electrode, while the reference electrode was of the saturated calomel type.

Straining of 0.2% preloaded specimens in a room temperature solution of 0.3 M $NaNO_2$ solution was initiated simultaneously with a potential scan from -700 mV_{SCE}. During the potential sweep from -700 mV_{SCE} up to the transpassive potential of +500 mV_{SCE}, the total strain experienced by the specimen was always < 0.1%. This strain was not enough to initiate cracks in the specimens. In the first phase of the potential scan, reduction of the existing atmospheric oxide film on specimens occurred. While the applied sweep rate caused the measured corrosion potential of copper to deviate to some degree from the thermodynamically calculated Cu_2O formation potential, mechanical straining consistently led to an elevation in the corrosion potential values measured. However, reduction in the rate of the straining led to the corrosion potential values approaching the equilibrium value, Figure 8.1.

Strain rates of 10^{-6} and 10^{-7} s^{-1} produced continuous film rupture on specimen surface, indicated by the absence of real passivation after the cuprous film formation, yet a constantly increasing current density. Current increase continued in these specimens until

cupric film formation passivated the specimen surface. Passivation of the strained specimen surface occurred at the same potential at which the TGSCC in pure copper in $NaNO_2$ solutions ceases.

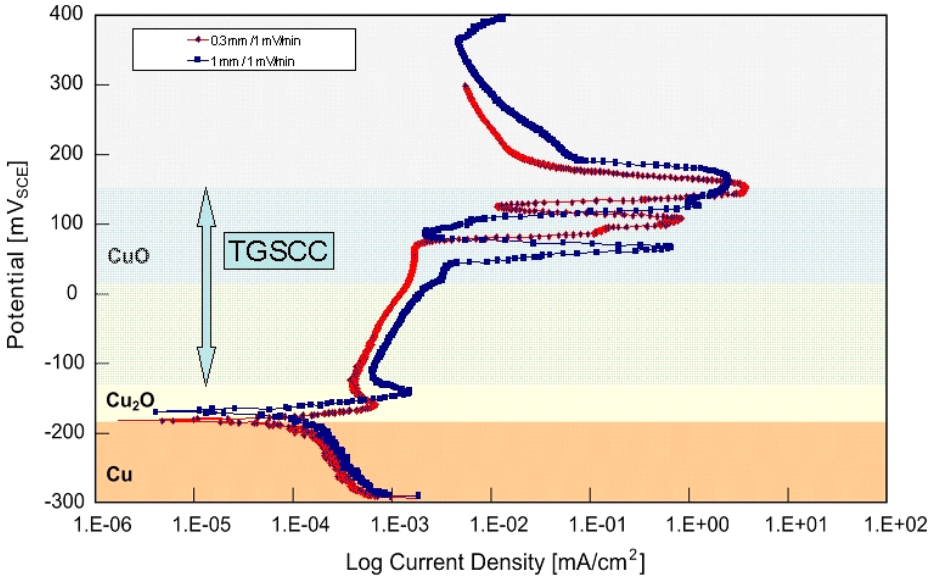

Figure 8.1: Slow scan rate (1 mV/min) polarisation curves for copper in 0.3 M $NaNO_2$ solution at room temperature measured for both thick and thin, non-strained samples. The plot indicates the thermodynamic equilibrium potentials for oxide formation reactions as well as the literature reported potential range for TGSCC in copper in $NaNO_2$ solutions.

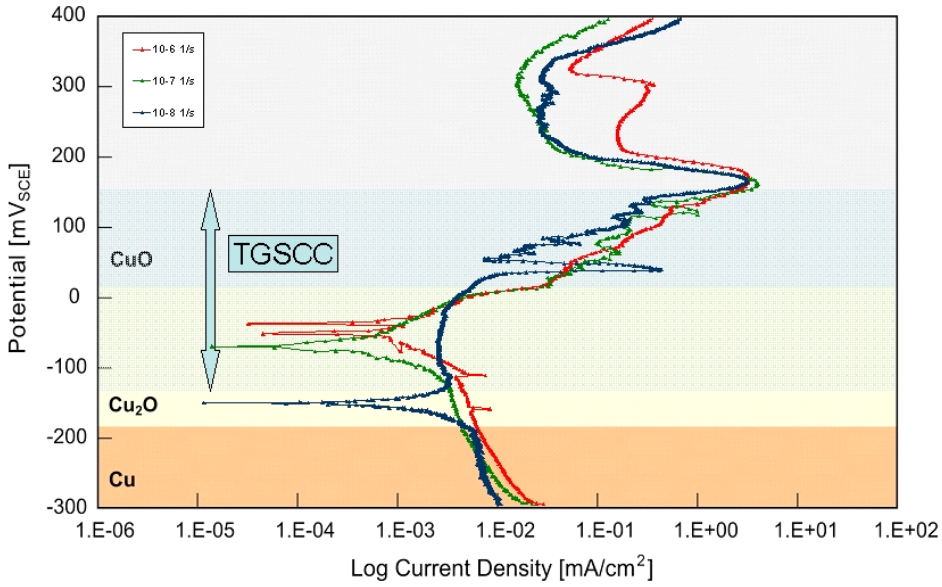

Figure 8.2: Electrochemical polarisation curves measured on strained tensile specimens with slow scan rate (1 mV/min) in 0.3 M $NaNO_2$ at room temperature. The plot indicates the thermodynamic equilibrium potentials for oxide formation reactions, as well as the literature reported potential range for TGSCC in copper in $NaNO_2$ solutions.

A strain rate 10^{-8} s^{-1} did not rupture the passive film of the copper specimen, and provided a clear passive potential range following the cuprous film formation. With this strain rate the second active peak associated with the formation of cupric oxide, divides into two parts if compared to curves obtained with higher strain rates. The first part is closely related with the thermodynamic formation potential, about 40 mV_{SCE}, of the cupric oxide and the other with the potential, 170 mV_{SCE}, where cupric film formation passivates the specimen surface at the same potential at which the TGSCC in pure copper in $NaNO_2$ solutions ceases, Figure 8.2. The potential range between these two peaks correlates with that potential range where 100% TGSCC in pure copper exposed to $NaNO_2$ solutions has been reported. At lover potentials of the TGSCC potential range reported in the literature, between -100 mV_{SCE} and 40 mV_{SCE}, fracture surface always contained in addition to TGSCC also ductile fracture.

One can suppose that the Cu2O epitaxial semi-coherent film a few ten of nanometer in thickness is formed on the copper substrate in the passive state. The film has a minor electric conductivity performed by Cu+ cation diffusion transport from the film/metal to the film/solution interface and it is exposed together with the copper substrate to heavy elastic stresses due to conditions of epitaxy. The epitaxial stresses play a key role in the following consideration because they have a strong effect on the semiconductor film electrical conductivity and the copper substrate creep. In fact, a coherent interaction between the film electrical conductivity and creep in the substrate causes the potential oscillation in the galvanostatic regime of the polarisation. The elastic stresses, which are strongly affected by creep, provide a positive feedback on the film electrical conductivity. As ever the potential approach a certain value, which depends on the elastic stress and crystalline defects in film (the higher stress, the higher potential is), the cation Cu++ start to generate in the film (probably, at the film/solution interface) and cation current increases rapidly with potential. Because the cations Cu++ come into solution and do not take part in the epitaxial film expansion, some cation vacancies start to generate at the f/s surface and drift into film under electric field applied. The vacancies flux is equal to the dissolution current measured. The cation vacancies transform in metal vacancies at f/m interface and accumulate in the subsurface layer of copper. The metal vacancy accumulation lead to increase of cation vacancy concentration at f/m interface in the film as well and an electric charge caused by them will generate a counterpart electric field, which can reduce the vacancy electric drift (current).

Under external load for creep the average value of the potential can keep constant, that means that all of cation vacancies produced in dissolution reaction are consumed by dislocation flow in the bulk metal by the metal vacancy transformation. Finally, a dramatic increase of the average potential after some period of dissolution can be caused by CuO deposition on f/s interface or loses of coherency at f/m interface when cation vacancies can consume without their transformation into metal ones. This is, as you can see, a general view on the potential oscillation origin. Any calculations and estimations of oscillation parameters can be done after development of some constitutive equations for cation vacancy transport including creep flow in the substrate.

8.2 Remote Handling – Water Hydraulics

Institute: **Tampere University of Technology**,
Institute of hydraulics and automation (TUT/IHA)

Research Scientists: M. Siuko, M. Pitkäaho, M. Toivo, J. Mattila, J. Poutanen, M. Vilenius, H. Saarinen, A. Raneda, H. Mäkinen, S. Verho, A. Mäkelä, H. Koivisto, A. Muhammad, T. Nykänen

8.2.1 Water hydraulic cartridge valve development

Introduction

In ITER environment is vide variety of operations where heavy components are handled. Due to its compactness and reliability hydraulics provides good solutions for many of these applications. However, instead of oil, hydraulic systems will use water as a pressure fluid to eliminate the risk of contaminating the reactor elements. TUT/IHA has worked on water hydraulics for ITER several years developing various equipment for divertor maintenance. This project continues the work.

Aim of the project presented here was to continue work on robust control valve development started in 2003.

Water hydraulic cartridge valve development

Aim of the valve development was to design compact and robust water hydraulic valves. Additional target was compactness and simplicity of the complete hydraulic system to be able to replace it remotely when necessary. These requirements lead us towards to cartridge valves, which are typically used to integrate several functions into same valve blocks in mobile machinery.

At the beginning of the project, cartridge valve theory was studied and the theories were adopted to water hydraulics. Along that, also commercial oil hydraulic cartridge valves were studied to find suitable components to be modified for water use.

The cartridge valves are installed into borings of the valve blocks. All the valves of the system can be installed into the same block, which makes system compact and simplifies the overall design.

The cartridge valves provide several advantages:

- reduced piping
- more compact valve arrangement
- flow routes shorten
- flow losses decrease
- system efficiency increases.

Also, because of less piping and simpler design, cartridge valve system is easier to design for remote operated assembly and disassembly.

Testing

Two different types of cartridge valves were developed:

- a pilot controlled 4/3-on/off-valve
- a direct controlled 3/2-on/off valve.

A prototype valve of each valve type was designed for testing purposes. Designs were based on suggestions got from theory and practical experiences from oil components.

At first, numerical simulation models of the valves were developed. With the simulation model the valve design was balanced and optimised.

Pressure surfaces, orifice sizes and springs were optimised in order to achieve a good compromise between the features of the valve, like opening and closing times, pressure drops, sensitivity to different conditions etc. The same design principles will be used also for developing smaller size cartridge valves. The development and test process will be continued and the ideas learned will be adopted also for other type of valves needed in generic hydraulic systems.

Design of the pilot controlled 4/3 valve
The designed pilot controlled valve comprises 4-main cartridge mugs, CVa1,CVa2,CVb1 and CVb2 which are pilot controlled by pilot valves PVa1, PVa2, PVb1 and PV2 (see Figure 8.3). The valve body material is AISI 316L. The cartridge mug material is PEEK Ca30% and the mug seal material is UHWPE. The four pilot valves were commercial Flo Control Q2R-B108, DC24V, Kv = 0.5 l/min/ bar of water, 60 bar.

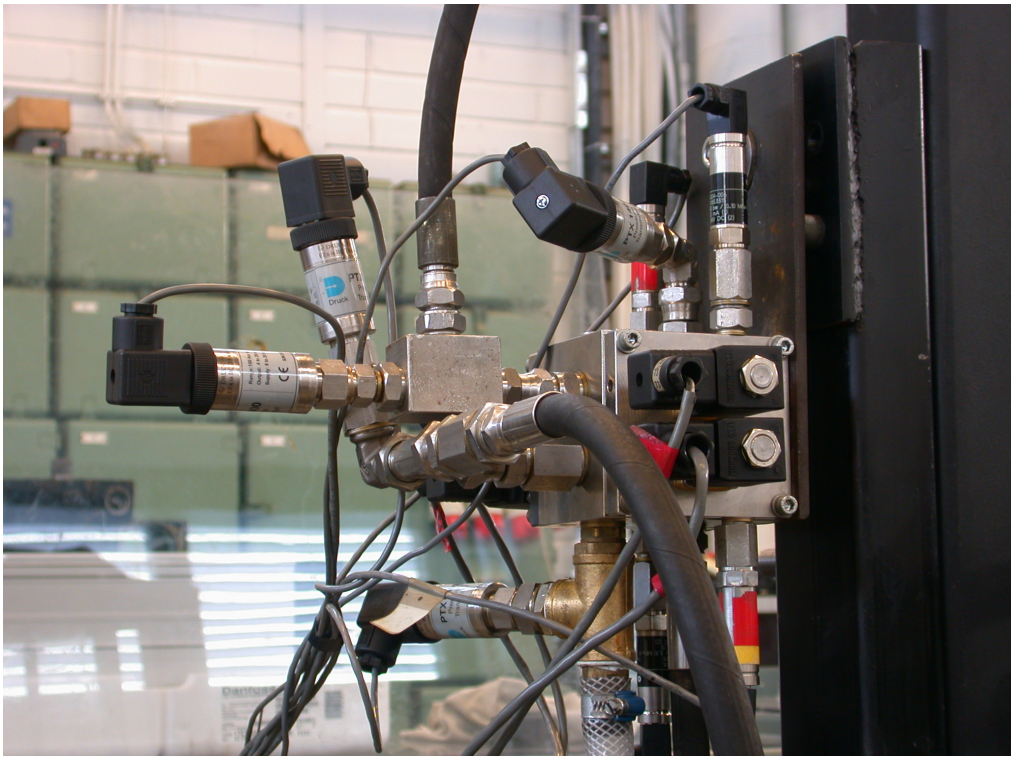

Figure 8.3: The pilot controlled cartridge valve in test installation.

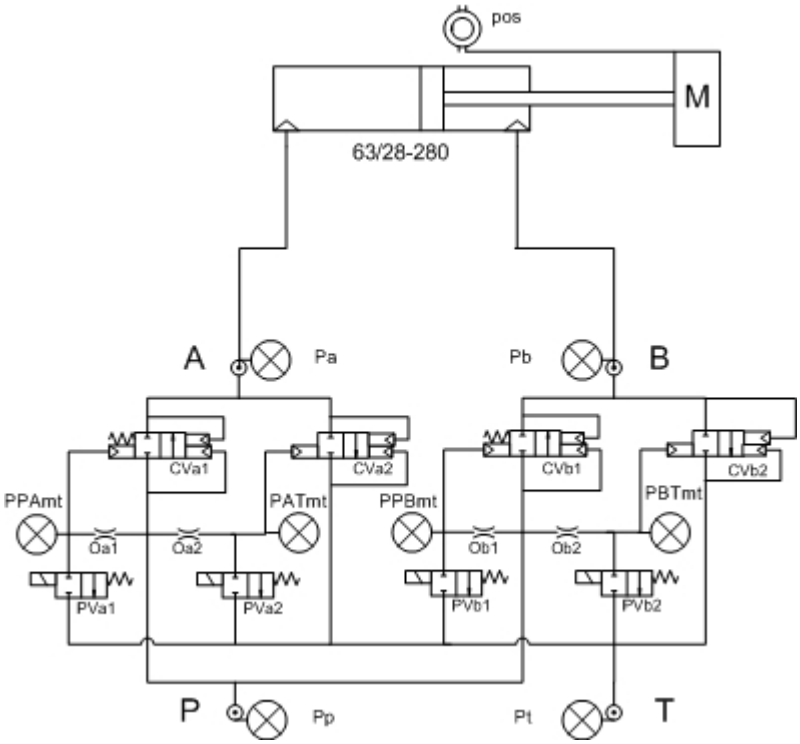

Figure 8.4: Shematic diagram of the valve in test arrangement with a hydraulic cylinder.

Tests

First tests were made with low pressure (60 bar). Later tests were made also with high pressure (210 bar). At first, the basic characteristics of the valve were measured:

- Pressure was measured in eight points: in the P-, A-, B- and T-lines and all the pressures in the chambers behind the mugs.
- Opening- and closing times of the valve, pressure/flow curves, leakages.

After the first tests the valve operation was tested in circuit where hydraulic cylinder was acting as a load (see test arrangement in Figure 8.4). The cylinder actual position was measured and compared to the instruction given to pilot valves. From the data it was calculated:

- The time to start the cylinder motion
- The time to stop the cylinder motion
- Time to change cylinder motion direction.

Delays of control signals to pilot valves were tested in order to prevent short circuit in the valve when changing cylinder motion direction.

Valve characteristics at current design are:

- Flow capacity: 0–35 liter/min
- Operating pressure: 60 bar (limited by operating pressure of the pilot valves)
- No leakage
- Opening time: 60–100 ms depending on operating conditions
- Closing time: 100–400 ms depending on operating conditions.

Conclusions

The designed valve prototype works as expected. The construction of the valve is simple and it is easy to modify for different conditions. The characteristics of the valve and balance between them only by changing mug strokes, springs or orifices. Operation and characteristics of the valve are learned thoroughly via the combination of the many tests and mathematical equations. As a consequence, the future R&D with the water hydraulic cartridge valves for direction-, pressure- and flow applications is possible to carry out with the 2-way-logic-valves.

Next actions are to test the operation with higher pressures, to adjust the opening and closing times and to make modifications in order to make valve more robust to operational conditions. Later the same principles are applied to other control valves. Similar test procedure will later be carried out also for the designed direct controlled 3/2 valve.

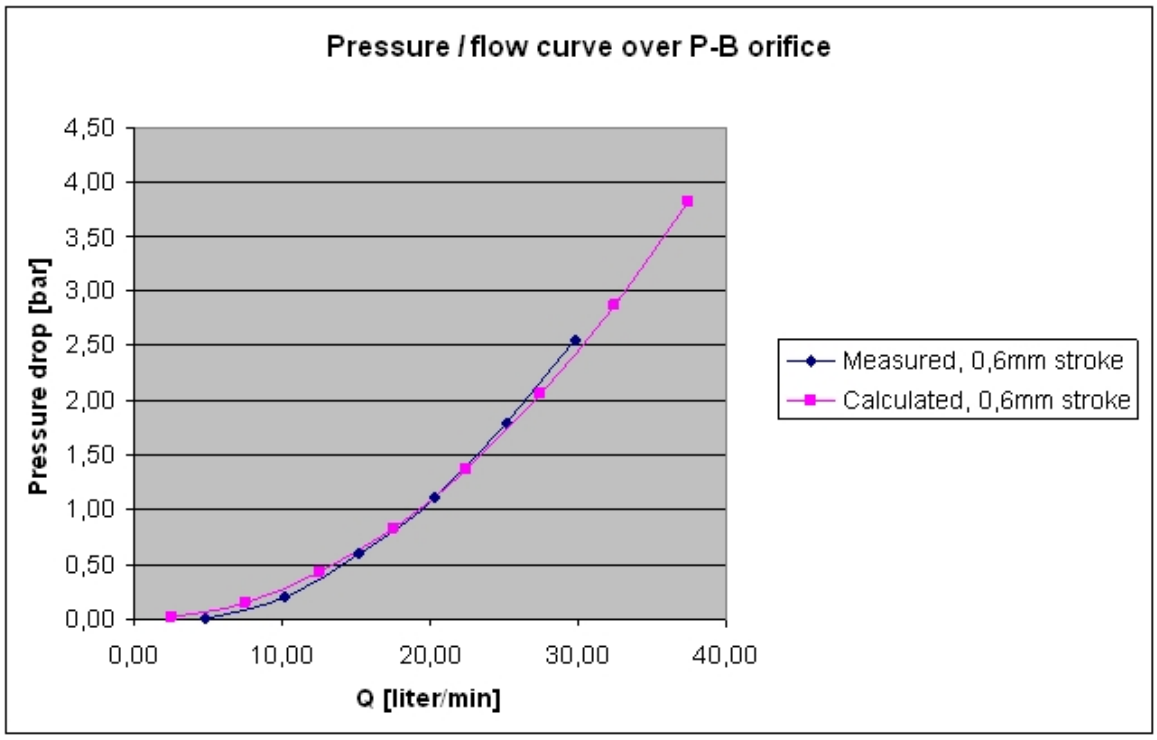

Figure 8.5: Measured and calculated pressure drop over the P-B orifice.

9 SUMMARY OF EFDA TECHNOLOGY AND JET ACTIVITIES

The EFDA Technology Tasks and Contracts (EFDA Art. 5.1a and 5.1b), which were completed or which are underway are summarised in Table 9-1 below. Industry is involved in many of the Association Technology Tasks.

Table 9-1: Tekes Technology Tasks (Art. 5.1a and Art. 5.1b) for the EFDA Technology Workprogramme 2004.

EFDA Reference	Task Title	Institute
TW3-TVM-TICRFA	Effect of low dose neutron irradiation on Ti alloy mechanical properties	VTT
TW3-TVV-EBEAMS	Further development of e-beam welding process with filler wire and through beam control	VTT
TW3-TVV-ROBASS	Upgrade of robot to include water hydraulics and linear track	LUT
TW4-TVR-WHMAN	Development of Water Hydraulic Manipulator	TUT
TW4-TVV-ROBOT	Further Development of Stability, Safety and Accuracy of IWR Robot	LUT
TW4-TTMI-003	IFMIF test facilities	VTT
TW3-TRE-FESA	Identification and comparative evaluation of fusion and other possible future energy production alternatives	VTT
JET-FT-3.15	Material transport and erosion/deposition in the JET torus	VTT
EFDA/03-1037	JET EP: Diagnostics – tritium retention studies, prepare and perform smart tile coating processes (Art. 5.1b Contract)	VTT
TW3-TMSC-ASTEST	Tests of Advanced Nb3Sn Strands (Art 5.1b Contract)	TUT
TW4-TVD-PFCATT/1	Testing of revised PFC multilink attachments (Art. 5.1b Contract)	TUT
EFDA/01-602 (Suppl. 1)	Ultrasonic tests of primary first wall panels and mock-ups (Art. 5.1b Contract)	VTT
UT-INPILE-2004	In-reactor testing and NDE development	VTT
UT-WH-2004	Water hydraulic further development	TUT
TW4-TVM-CUSSPIT	Testing of irradiated CuCrZr/SS joints produced under different blanket manufacturing conditions	VTT
UT-INPILE-2004	In-reactor testing and NDE development	VTT
UT-WH-2004	Water hydraulic further development	VTT

Regarding the EFDA JET activities, Association Euratom-Tekes participated in the data analysis and publishing the results of the experimental campaigns C7-C14 of EFDA JET Workprogrammes 2003 and 2004. S/T Order and Notification work in Task Forces S1 and S2 (Confinement), H (Heating), T (Transport), M (MHD), D (Diagnostics), E (Edge), and FT (Fusion Technology) was performed. These studies were related to ELMy H-mode physics, integrated transport modelling, advanced tokamak scenarios, transport barriers, real time control, ICRF heating and LHCD, trace-tritium experiments and edge/SOL physics including plasma-wall interactions.

Mervi Mantsinen served as Task Force H Deputy Leader, Session Leader and scientific coordinator of several ICRH experiments. Tuomas Tala started as Deputy Task Force Leader in TF T. Jukka Heikkinen and Karin Rantamäki acted as scientific coordinator in TF H experiments related ICRF antenna phasing and LHCD experiments.

The following scientists participated in the EFDA S/T Order work at JET: Jukka Heikkinen, Timo Kiviniemi, Jari Likonen, Johnny Lönnroth, Mervi Mantsinen, Karin Rantamäki, Samuli Saarelma, Antti Salmi, Marko Santala and Tuomas Tala.

The secondment actions to the UKAEA Operators Team and EFDA Close Support Units in 2004 were:

UKAEA JET Operators Team, secondment of Antti Salmi (TKK) from 1 January – 28 February 2004 (code development, rf physics).

UKAEA JET Operators Team, secondment of Johnny Lönnroth (TKK) from 1 January – 31 December 2004 (code development, code integration).

UKAEA JET Operators Team, secondment of Marko Santalah (TKK) from 1 January – 31 December 2004 (diagnostics, NPA).

EFDA Close Support Unit (CSU) – Garching, secondment of Hannu Kaikkonen (Fortum) from 1 February – 31 December 2004 (head of project control).

EFDA Close Support Unit (CSU) – Garching, secondment of Hannu Rajainmäki (Outokumpu Research) from 1 October – 31 December 2004 (magnets).

Remote access to JET and ASDEX UG computers and databases from VTT and TKK is well established. Remote participation tools are being further developed.

10 CONFERENCES, VISITS AND VISITORS

10.1 Conferences, Workshops and Meetings

S. Tähtinen participated in the review Meeting on “design rules and fracture mechanics”, NRG Petten, Nederlands, 14 January 2004.

V. Kujanpää participated in the Photonics West conference in San Jose, CA, U.S.A., 25–29 January 2004.

T. Kiviniemi, J. Lönnroth and T. Tala participated in the Task Force T Workshop at JET, UK, 28–30 January 2004.

J. Likonen participated in the Task Force FT Workshop, JET, UK, 4–5 February 2004.

M. Siuko, M. Pitkäaho and P. Kunttu participated in the EFDA MOVER-meeting, Garching, Germany, 9–10 February 2004.

T.Kiviniemi and J. Lönnroth participated in the JET Edge Modelling Meeting, Culham, UK, 11–13 February 2004.

R. Salomaa participated in the STAC AHG on “The EFDA heating and current drive program”, Garching, Germany, 11–12 February 2004.

S. Karttunen participated in the XXXIV Eesti Füüsikapäevad, Annual Meeting of the Estonian Physical Society, Tartu, Estonia, 13–14 February 2004.

J. Lönnroth participated in the ITPA Pedestal and Edge Group Meeting, Culham, Oxfordshire, UK, 1–3 March 2004.

S. Karttunen participated in the 3rd Public Information Group meeting, Padova, Italy, 4–5 March, 2004.

T. Ahlgren, K. Nordlund and P. Träskelin participated in the XXXXVIII Annual Conference of the Finnish Physical Society, Oulu, Finland, 18–20 March 2004.

H. Handroos and H. Wu visited Robotics EXPO Paris, France, 22–24 March 2004.

S. Tähtinen participated in the EU Copper meeting, EFDA Close Support Unit, Garching, Germany, 2 April 2004.

M. Mantsinen, K. Rantamäki, M. Santala and A. Salmi participated in the Task Force H Reporting and Planning Meeting, Ringberg-Castle, Rottach-Egern, Germany, 19–21 April, 2004.

K. Nordlund participated in the 3rd FeCr Modelling Workshop, Stockholm, Sweden, 6–7 May, 2004.

F. Wasastjerna participated in the ICRS-10 and RPS-2004, Madeira, Portugal, 9–14 May, 2004.

R. Salomaa participated in the STAC AHG on “Progress in lower hybrid activity”, Frascati, Italy, 10 May, 2004.

O. Dumbrajs participated in the 13th Joint Workshop on Electron Cyclotron Emission and Electron Cyclotron Resonance Heating, Nizhny Novgorod, Russia, 17–20 May 2004.

J. Likonen participated in 7th International Workshop on Hydrogen Isotopes in Fusion Reactor Materials, Sebasco Resort, Maine, USA, 20–21 May 2004.

K. Heinola, J. Likonen and P. Träskelin participated in the 16th Plasma-Surface Interactions Conference (PSI), Portland, USA, 20–28 May 2004.

S. Karttunen participated in the Enlargement of the EU Integration of New and Recent Partners in the Euratom Fusion Programme, Garching Germany, 24–25 May 2004.

M. Siuko participated in the IAEA CEG Workshop EC-JRC, Petten, Netherlands, 26–28 May 2004.

Over 50 participants participated in the Annual Seminar of the Association Euratom-Tekes, Tampere, Finland, 1–2 June 2004.

K. Nordlund participate in the EFDA Task TW4-TTMS-007 meeting at the Paul-Scherrer-Institut, Switzerland, 21–23 June 2004.

J. Heikkinen, S. Janhunen, J. Lönnroth, A. Salmi and M. Santala participated in the 31st EPS conference, London, UK, 28 June – 2 July 2004.

The Accelerator Laboratory arranged the 7th international conference on computer simulation of radiation effects in solids (COSIRES) on 28 June – 2 July 2004. The chairman was Kai Nordlund, the co-chairman Juhani Keinonen. About 1/3 of the conference presentations dealt with radiation effects in fusion reactor materials.

A. Raneda participated in the Fluid Power Network International PhD Symposium on Fluid Power, Terrassa, Spain, 30 June – 2 July 2004.

K. Henriksson participated in the 21st International Conference on Atomic Collisions in Solids in Genua, Italy, 4–9 July 2004.

V. Kujanpää participated in the International Institute of Welding Annual Meeting in Osaka, Japan, 11–15 July 2004.

T. Kurki-Suonio participated in the ASDEX Upgrade Programme Committee meeting, in IPP Garching, Germany, 14 July 2004.

V. Hynönen and M. Nora participated in the 41st Culham Plasma Physics Summer School, UK, 19–30 July 2004.

V. Kujanpää participated in the Finnish – German – Japan Welding Seminar, Awaji, Japan, 20–21 July 2004.

S. Karttunen participated in the Tapiola Rotary lunch meeting, 27 August, 2004.

K. Rantamäki participated in the Joint Varenna – Lausanne Workshop on Theory of Fusion Plasmas, Varenna, Italy, 30 August – 3 September 2004.

K. Nordlund and K. Henriksson participated in the 14th International Conference on Ion Beam Modification of Materials, Monterey, California, USA, 3–11 September 2004.

T. Tala participated in the Task Force Leader preparation meeting for JET 2005 Campaigns, JET, UK, 13–17 September 2004.

O. Dumbrajs participated 10th International Conference on Mathematical Methods in Electromagnetic Theory, Dniepropetrovsk, Ukraine, 14–17 September 2004.

T. Kurki-Suonio, K. Rantamäki and E. Vainonen-Ahlgren participated in the "Säteilevät Naiset" Seminar, Helsinki, Finland, 15 September 2004.

R. Korhonen participated in the SERF 2005 program definition meeting in Garching, Germany, 15 September 2004.

S. Karttunen, J. Mattila, R. Rintamaa, S. Saarela, M. Siuko and S. Tähtinen participated in the 23th Symposium on Fusion Technology, Venice, Italy, 20–24 September, 2004.

O. Dumbrajs participated 29th International Conference on Infrared and Millimeter Waves, Karlsruhe, Germany, 27 September – 1 October 2004.

V. Kujanpää and T. Jokinen participated in the International conference on Lasers and Electro-Optics, San Francisco, CA, USA., 3–7 October 2004.

R. Mikkonen participated in the Applied Superconductivity Conference, Jacksonville USA, 3–8 October 2004.

J. Heikkinen, K. Rantamäki, A. Salmi and E. Vainonen-Ahlgren participated in the 12th Finnish-Russian Symposium on Fusion Research and Plasma Physics, St. Petersburg, Russia, 4–5 October 2004.

J. Likonen participated in the Workshop on Options for testing ITER relevant materials in JET, JET, UK, 4–5 October 2004.

R. Salomaa participated in the 3rd Nordic Symposium on Plasma Physics, Oslo, Norway, 4–7 October 2004.

S. Karttunen participated in the Kees Braams Memorial Meting, Nieuwegein, The Netherlands, 7 October 2004.

J. Likonen participated in the EU-PWI TF Task Force meeting, Juelich, Germany, 14–15 October 2004.

T. Kurki-Suonio and J. Likonen participated in the AUG Ringberg seminar, Ringberg, Germany, 18–22 October 2004.

S. Karttunen participated in the René Pellat Memorial Day, Paris, France, 20 October 2004.

S. Karttunen, T. Kiviniemi, R. Salomaa and T. Tala participated in the 20th IAEA Fusion Energy Conference, Vilamoura, Portugal, 1–6 November 2004.

M. Nora, K. Rantamäki and T. Tala participated in the JET code training session, JET, UK on 29 November – 3 December 2004.

S. Tähtinen participated in the Materials Review Meeting on Voluntary R&D and ITER MPH for In-vessel Materials, Garching EFDA, 30 November – 3 December 2004.

Kai Nordlund participated in the meeting of EFDA task TW4-TTMS-007 in Madrid, Spain, 8–9 December 2004.

10.2 Visits

M. Santala was seconded to UKAEA JOC 1st January – 31st December, 2004.

A. Salmi was seconded to UKAEA JOC 1st January – 5 March, 2004.

J. Lönnroth was seconded to UKAEA JOC 1st January – 31st December, 2004.

M. Mantsinen visited EFDA-JET under S/T Order on 1st January – 31st March, 2004.

F. Wasastjerna visited FZK Karlsruhe, Germany on 9 January – 3 April, 2004.

T. Kiviniemi visited EFDA-JET under S/T Order on 11 January – 14 February, 2004.

K. Rantamäki visited EFDA-JET under S/T Order on 12 January – 6 February, 2004.

T. Tala visited EFDA-JET under S/T Order on 26–30 January, 2004.

J. Likonen visited EFDA-JET under S/T Order on 4–5 February and 21 June – 9 July, 2004.

S. Saarelma visited EFDA-JET under S/T Order on 15 February – 28 February, 2004.

P. Träskelin visited the Technical University of Darmstadt, Germany, 12–21 January 2004.

A. Raneda participated in CeBIT Hannover, Germany in March 2004.

M. Airila visited Institut für Plasmaphysik, Forschungszentrum Jülich, Germany, 22–26 March 2004.

O. Dumbrajs visited the National Technical University of Athens, Association Euratom-Hellenic Republic under the Staff Mobility agreement, 28 March – 1 May 2004.

J. Lönnroth visited Naka Fusion Research Establishment, Japan Atomic Energy Research Institute, Naka-machi, Naka-gun, Ibaraki-ken, Japan on 29 March – 9 April 2004 and 30 August – 24 September, 2004.

J. Likonen and E.Vainonen-Ahlgren visited IPP-Garching, Germany on 13–14 April 2004.

V. Kujanpää visited CERN, Geneve, Switzerland, 10–11 May 2004.

S. Karttunen visited IPP Garching, Germany on 24–25 May 2004.

T. Kurki-Suonio visited IPP-MPG, Garching under the Staff Mobility agreement on 8 July – 4 August 2004, and 7–23 October 2004.

S. Karttunen visited FOM Rijnhuizen, The Netherlands, 7–8 October 2004.

V. Kujanpää visited Institute de Soudure, Paris, France, 14–15 June 2004.

N. Juslin visited the Technical University of Darmstadt, Germany, 14–20 June 2004.

E. Vainonen-Ahlgren visited IPP-Garching, Germany, 29–30 July 2004.

P. Moilanen visited SCK-CEN, Mol, Belgium, 21–24 September 2004.

10.3 Visitors

Dr. Bill Lawson (Preco Laser), visited Lappeenranta University of technology and VTT Industrial Systems, 15 January 2004.

Mr. Edgar Bogush and Roland Gottfried from Framatom ANP visited in TUT/IHA on 27–28 January 2004.

S. Mellemans, G. Engelen, and P. Jacquet (SCK-CEN) visited VTT Industrial Systems on 27–29 January 2004.

Mr. David Olivier Yvan Measson (CEA) visited TUT/IHA, 4–5 February 2004.

Klaus Schünemann from Technical University Hamburg visited HUT on 6 February, 2004.

MSc. G. Zemulis from Kaunas University of Technology, Lithuania visited HUT on 1 March – 30 June, 2004.

Dr. Mario Merola from EFDA and Mr. Alan Turner from NNC visited in TUT/IHA on 2 March 2004.

Dr. L. Jones (EFDA CSU Garching), visited Lappeenranta University of Technology and VTT Industrial Systems, Lappeenranta, 14 April 2004.

Paul Coad from UKAEA visited VTT Processes on 15–21 April 2004.

Prof. Bill Steen (University of Liverpool), visited Lappeenranta University of Technology and VTT Industrial Systems, Lappeenranta, 4 May 2004.

M. Tran from EFDA visited IHA/TUT on 1–2 June 2004.

A. Peacock (EFDA), P. Jacquet, (SCK-CEN) and B. N. Singh (RISØ) visited VTT Industrial Systems on 22–23 June 2004.

Dr. Matej Mayer from IPP visited UH/VTT Processes on 27 June – 4 July, 2004.

Prof. Noriako Mori (Osaka University, Japan) visited Lappeenranta University of Technology and VTT Industrial Systems, Lappeenranta, 27 August 2004.

Dr. Pavol Kovác (Slovak Academy of Sciences), visited TUT Laboratory of Electromagnetics in September 2004.

Prof. A.A. Andreev from Vavilov Institute, St. Petersburg visited HUT on 2 Sepember – 30 November, 2004.

Dr. Mario Merola from EFDA visited in TUT/IHA on 3 November 2004.

Dr. Vadym Lutschenko (Institute for Nuclear Research, Kiev, Ukraine) visited HUT on 21 November – 5 December, 2004.

Dr. R. Schneider (IPP), Dr. Manoj Warrior (IPP), Dr. Jon-Erik Dahlin and Dr. Jacob Fredrikssen (Stockholm University) and Dr. Lars Daldorff (University of Oslo) visited HUT on 8–12 November, 2004.

Dr. Sergei Lashkul and Dr. Alexey Popov (A.F. Ioffe Physico-Technical Institute, Sankt-Petersburg, Russia) visited HUT on 1–25 December, 2004.

Dr. Michael Pick and Dr. Jim Palmer from EFDA visited in TUT/IHA on 9 December 2004.

Dr. Alexander Savelyev (A.F. Ioffe Physico-Technical Institute, Sankt-Petersburg, Russia) visited HUT on 9–23 December, 2004.

10.4 Staff Mobility Actions

10.4.1 Updating of the geometry model for the IFMIF test cell

Visiting scientist:	Frej Wasastjerna, VTT Processes
Visited institution:	Forschungszentrum Karlsruhe, Institut für Reaktorsicherheit
Visit Period:	11 January – 3 April 2004, 12 weeks

Objectives: Updating the geometry model of the entire test cell. The model developed in 2003 was based on very inadequate information, particularly with respect to the low/very low flux test modules and test cell cover. Better information was available in early 2004, and the model was updated to incorporate this information. Some other improvements to the geometry model were also made.

Checking the availability of neutron cross sections in the energy range 20–55 MeV. Standard MCNP4C data libraries do not contain data above 20 MeV, but the neutron spectrum in IFMIF will extend to 55 MeV. Data libraries covering the whole energy range up to 55 MeV have been developed and selected for the IFMIF project. In this task the objective was to check for which of the nuclides present in IFMIF cross-sections are available in these libraries.

Results: The geometry model was updated as planned. There are still areas where proper design information is not available, but the model is now adequate for practical

calculations, including calculations of the shielding properties of the cover, which could not be modelled adequately in 2003.

It was found that all important nuclides are included in the cross section libraries. Those which are not available could safely be ignored or replaced with others, at least for the transport calculations themselves, as distinct from activation calculations.

10.4.2 Material Transport in the SOL region of JET

Visiting scientist:	Jari Jikonen
Sending Institution:	VTT Processes
Visited Institution:	UKAEA JET
Visit Periods:	1 March – 5 May 2004 and 21 June – 9 July 2004

1/3/04–5/3/04: Prior to the 2004 shutdown, an experiment was devised to provide specific information on material transport and SOL flows observed at JET. $^{13}CH_4$ and $B(CH_3)_3$ were injected into the plasma boundary from the outer divertor in the last day of discharges using one type of discharge only. The purpose of the experiment was to determine how the ^{13}C and boron are transported around the SOL, and where they are eventually deposited. The amount of puffed ^{13}C was about 3 times bigger than during the previous ^{13}C puffing experiment in 2001. The amount of boron was comparable to the amount of puffed Si in 2001. Boron was detected spectroscopically at the outer divertor. The puffing experiment at JET was very successful. All milestones for this visit were achieved.

Preliminary post-mortem surface analysis has shown that there is ^{13}C deposited on the collector probe. Further post-mortem surface analyses using SIMS and TOF-ERDA will be performed at Tekes after the tiles have been removed from JET.

21/6/04–9/7/04: New marker coatings (C, W) for erosion/deposition studies will be installed at JET during 2004 shutdown. Some test samples and outer poloidal limiter tiles have been analysed with Rutherford backscattering technique (RBS) at the University of Sussex. RBS spectra were simulated using SIMNRA program and the coating thicknesses and compositions were calculated (milestone 1).

All surface analysis results (SIMS, RBS, TOF-ERDA) for JET tiles exposed in 1998–2001 and 1999–2001 were compiled during the visit and an overview paper on the results is preparation (milestone 1 and 2).

New marker coatings have been made at Tekes and the coated tiles have been measured using a surface profiler developed at JET. The purpose of the measurements is to measure the surface profile of the coated area before the tiles are installed at JET. After the tiles will be removed the measurements will be repeated. By comparing the results before and after plasma exposure, erosion/deposition pattern can be determined. The accuracy of the system is about 10 um. During the visit, coated inner wall guard limiter (IWGL) tiles and a graphite test tile were measured. Critical point in the measurements is the positioning of the tile. If the positioning of the tile is not done in a similar way, then the results are not reproducible. Test measurements were done with a test tile by loading and unloading the tile and by repeating the measurements. Agreement between the test measurements was better than 10 um (milestone 3).

All the milestones for this visit were achieved.

10.4.3 Coaxial Gyrotrons for ITER

Name of seconded person:	Olgierd Dumbrajs
Sending Institution:	Helsinki University of Technology
Host Institution:	National Technical University of Athens, Association Euratom-Hellenic Republic
Dates of visit:	28 March – 1 May 2004

A very detailed comparison of the mode competition scenarios obtained in the cold cavity approximation (NTUA code) and in the non-fixed field approximation (HUT code) has been performed. It has been found that the scenarios obtained by the HUT code are significantly shifted to lower voltages with respect to scenarios obtained by the NTUA code. Physical reasons for this shift have been understood and practical consequences evaluated. It has also been agreed that numerical difficulties encountered in solving the gyrotron equations are practically identical in the two codes.

Possibility of improving mode competition scenarios in coaxial cavity gyrotrons operating in second harmonic by using a corrugated insert with variable depth of corrugations has been confirmed.

A new method of analysing the onset of chaos in electron dynamics in gyrotron resonators has been proposed. It is based on the use of the most general Hamiltonian perturbation method.

Cross-checking of predictions for ohmic losses in coaxial gyrotron cavities with corrugated insert has been initiated.

10.4.4 Transport and MHD stability analysis of JET / JT-60U dimensionless pedestal identity experiments

Name of seconded person:	Johnny Lönnroth
Sending Institution:	Helsinki University of Technology
Host Institution:	Japan Atomic Energy Research Institute, Naka Fusion Research Establishment
Dates of visit:	29 March – 9 April and 30 August – 24 September 2004

Background and objectives:
During 2003 and 2004 a series of dimensionless pedestal identitity experiments have been carried out at JET and JT-60U. Despite the enforced match in dimensionless pedestal parameters, identity discharges from the two machines have very different plasma performance. The aim of the work undertaken during the two visits was to explain and understand the observed differences.

First visit:
MHD stability analysis of JET and JT-60U identity plasmas with the codes MISHKA and HELENA revealed that there is no significant difference in MHD stability between discharges from the two machines. Comparable JET and JT-60U discharges often both have access to second stability. It was concluded that a difference in MHD stability is not the reason for why JT-60U plasmas generally have lower pedestal performance than JET identity plasmas.

Given the absence of clear differences between JET and JT-60U discharges in terms of MHD stability, several different parameter scans were performed with the JETTO transport code in order to improve the understanding of the characteristics of JT-60U plasmas. Variation of the pedestal width showed that the generally wide edge transport barrier in JT-60U could result in kink unstable plasma. By varying the bootstrap current, which is to a large extent controlled by the edge density, it was shown that the low edge density in many JT-60U plasmas might also cause a kink instability. These factors could explain the poorer performance than in comparable JET plasmas. A scan in the total current showed that better stability characteristics are obtained with a smaller total current, which is in agreement with experimental observations.

The effect of neutral beam-driven current on the performance of JT-60U plasmas was investigated using JETTO. It was thought that negative ion neutral beam heating (NNB) would lead to a more peaked central current than positive ion neutral beam heating (PNB), which in turn would result in a significantly modified edge current profile. Interpretative modelling of JT-60U discharges, however, showed that the central current is not more peaked with PNB. It was found that the edge current is slightly different in PNB and NNB plasmas anyway, but that this difference is entirely due to bootstrap current, which is related to the edge density profile, and has nothing to do with the neutral beam driven-current. MHD stability analysis revealed that the difference in edge current due to different levels of bootstrap current is often large enough to cause qualitative differences in stability, so that plasmas with NNB generally have good second stability access, whereas pure PNB plasmas do not. These differences seem to explain the experimentally observed better plasma performance with NNB.

Transport analysis of some JT-60U plasmas showed somewhat larger discrepancies between the observed levels of transport and a Bohm / gyro-Bohm model than what is the case for JET identity plasmas. Comparisons with the theory-based Weiland model were also made.

Second visit:
Following the conclusion that differences in MHD stability alone does not account for the results of the dimensionless pedestal identity experiments, plasma rotation and the effects of ripple losses were identified as possible mechanisms that could explain the lower pedestal performance in JT-60U plasmas than in comparable JET plasmas. The rotation profiles are generally quite different in the two devices. (The JT-60U plasmas counter-rotate and the JET identity plasmas co-rotate, among other things.) The toroidal magnetic field ripple is much stronger in JT-60U than in JET because of the lower number of toroidal field coils in JT-60U than in JET (18 coils versus 32 coils). Given these facts, a second visit was undertaken in order to shed further light on the proposed ideas.

Using a version of the MISHKA MHD stability code with first-order effects of plasma rotation taken into account, it was found that rotation does not significantly change overall MHD stability. The growth rates of the unstable modes change only little when toroidal rotation is imposed. Some changes can be seen in the structure of the eigenmodes. However, it was found that overall marginal stability changes very little. This result goes in line with other studies and is supported by transport analysis. Hence, it was concluded that plasma rotation cannot account for the differences in pedestal performance seen between JET and JT-60U identity plasmas.

Predictive transport modelling with the JETTO transport code showed that the most probable cause for the differences in plasma performance between JET and JT-60U is, in fact, the large ripple losses in JT-60U. It was assumed that ripple-induced losses of thermal ions cause an edge-localized perturbation to ion thermal transport. The modelling showed that if the perturbation induced by thermal ion losses is assumed to be concentrated just inside the separatrix to a region significantly narrower than the pedestal width, plasma profiles similar to those observed in JT-60U can be reproduced. In other words, the pedestal height drops and the pressure gradient decreases also in a region inside the top of the pedestal (i.e. overall confinement deteriorates sharply) with this kind of transport modification. This happens because the enhanced transport flattens the pressure profile at the very edge and effectively reduces the pedestal width. It seems likely that this is what occurs in JT-60U plasmas. Interestingly, it was also demonstrated that the opposite effect, i.e. improved overall confinement, can be obtained with a perturbation to ion thermal transport significantly wider than the pedestal width. The explanation for this result is that a wide transport perturbation extending far inside the pedestal increases the build-up time between the ELMs, which raises the average temperature at the top of the pedestal. It should be emphasized that the results are still very preliminary and that the work is still continuing.

Preparations for analysis of ripple-induced fast ion losses were also undertaken during the visit. This analysis would be needed, because in accordance with the above developments, experiments with enhanced toroidal magnetic field ripple are now being planned at JET.

10.4.5 Development of ERO simulation code

Name of seconded person:	Markus Airila
Sending Institution:	Helsinki University of Technology
Host Institution:	FZJ Jülich
Dates of visit:	31 May – 30 June 2004

The purpose of the visit was participation in the development of ERO simulation code, which is used to investigate erosion, local transport, and redeposition of impurities in fusion devices. In particular, a version of the ERO code, which can be used to simulate ^{13}C experiments carried out in the ASDEX Upgrade tokamak, is under development.

FZJ provided a thorough introduction to the structure of the code and the relevant development tools. Access to the computer systems, which are needed for efficient collaboration, was arranged.

Unlike the well-established 3D limiter version of ERO, which was initially developed for the TEXTOR tokamak, the present divertor version of ERO is two-dimensional and requires the background plasma parameters as input. The use of the curvilinear spatial grid of the B2-Eirene plasma code made ERO relatively slow in evaluating the plasma parameters during simulation. A faster solution was implemented and it is now under testing phase. Also the upgrading of the code to three dimensions was initiated.

On the 21st of June, a ^{13}C related workshop of the Special Experts' Working Group on Chemical Erosion in Tokamaks was held in Jülich, with presentations from Jülich, Garching, and Helsinki. It was noted in discussions that new background plasma data of the divertor region of ASDEX are needed for simulations of ^{13}C experiments. These will be provided by the ASDEX physicists.

The code development work will proceed locally in close collaboration between HUT and IPP. Additional short visits to Jülich may become necessary later, but at the moment it seems most relevant to establish relations to Garching as well.

10.4.6 Evaluation of fast particle distributions in AUG

Name of seconded person:	Taina Kurki-Suonio
Sending Institution:	Helsinki University of Technology
Host Institution:	IPP Garching
Dates of visit:	8 July – 4 August 2004

The proposed visit was part of the European experimental programme carried out at ASDEX Upgrade tokamak. The physics issues require reversed toroidal magnetic field, a campaign carried out at ASDEX Upgrade in the spring 2004. Unfortunately, during the campaign a macroscopic item fell to the roof baffle, the vessel had to be opened for its removal, and the campaign had to be truncated.

Until summer 2004 the interpolation algorithms used to obtain magnetic backgrounds for ASCOT calculations were too inaccurate to reliably evaluate NBI slowing down distributions. A sufficiently accurate interpolation algorithm is now in use, and the fast ion distributions are being evaluated for the existing QHM-shots and their H-mode counterparts. To find if the fast ions have a significant role in the edge MHD behaviour, the distributions thus obtained will be used as input to MHD stability codes such as HAGIS or MISHKA. Simon Pinches agreed to assist in this work. To this end, ASCOT now provides the fast ion distributions in four dimensions (2 spatial and 2 velocity coordinates) and in general enough form to be used by the stability codes.

ASCOT is now directly interfaced to the ASDEX Upgrade experimental profiles. It has a new preprosessor that utilises the pedestal profile database structure (under MDSPlus), proposed by the ITPA Pedestal and Edge Group. Including also the simulation results into the same database is currently under work. The work will involve establishing an MDSPlus server also at Helsinki University of Technology, and will serve the purpose of providing research results openly and efficiently within the fusion community.

Measurements of tungsten erosion at one of the outboard limiters of ASDEX Upgrade suggest that fast particles play an important role. The fast particle loads (fluxes and energy distribution) on the limiter were also simulated using ASCOT. The results were in qualitative agreement with the measurements, but it was concluded that the model used for the toroidal ripple in ASCOT is too crude. Thus a work to create a numerical, divergence-free ripple model was initiated. Naturally, this is also important for the fast ion distributions.

The technical problems experienced with the different video-conferencing systems (H323 vs. VNC) were discussed and tested with Karl Behler.

10.4.7 Fast Ions in AUG Edge Region

Name of seconded person: Taina Kurki-Suonio.
Sending Institution: Helsinki University of Technology
Host Institution: IPP Garching
Dates of secondment: 7–23 October 2004

The aim was to continue studies on the role of the NBI ions in the edge MHD behaviour. To fully understand the physics, the fast ion distribution in the pedestal region has to be evaluated by ASCOT, and the results have to be coupled with MHD stability codes. The relevance of the ELM-free QH-mode depends on the role of counter-injection: if counter-injected fast ions are needed for EHO, the scheme is unlikely to be reactor relevant.
Therefore we would like to plan 'identity' discharges with co- and counter-injection and, possibly, with dominant ICRH as well, for the experimental campaign in 2005.

At the suggestion by Dr. S. Günter, the effect of the large E_r measured in the edge plasma was included in the ASCOT simulations. The resulting *ExB* rotation was found not only to reverse the sign of the toroidal precession so that it now coincides with the experimentally measured one, but in some cases it also brought the precession frequency up to the levels of the measured EHO frequencies. Consequently, efforts to see if there is a simple resonance between the fast ion toroidal precession and the MHD mode were revitalized. The new 4-dimensional fast ion distributions provided by ASCOT simulations were used to identify the most important part of the phase space. New counter-injection experiments are planned for the AUG experimental campaign 2005.

10.4.8 Other Mobility Missions

Visiting Scientist: M. Mantsinen, K. Rantamäki, A. Salmi and M. Santala
Organization: VTT and Helsinki University of Technology
Visits: 19–21 April 2004
Title of the Work: **Task Force H Planning Meeting**

Short description of the work: Mrs Mantsinen, Mrs Rantamäki, Mr Salmi and Mr Santala participated in the Task Force H Reporting and Planning meeting in the Ringberg castle, in Germany. They reported on their work.

Visiting Scientist: M. Nora, K. Rantamäki and T. Tala
Organization: VTT and Helsinki University of Technology
Visits: 29 November – 3 December 2004
Title of the Work: **Task Force H Planning Meeting**

Short description of the work: Mr M. Nora, Mrs K. Rantamäki and Mr T. Tala participated in Preparatory exercises for the 2005 JET Experimental Campaigns relating to the JET Integrated Code Project.

11 PUBLICATIONS

11.1 Fusion Physics and Plasma Engineering

11.1.1 Publications in Scientific Journals – Fusion Plasma Physics

1. G. Zemulis, A. Adomavicius and *R. Salomaa*, “Loss of flow accident analysis of a water-cooled fusion reactor”, In Advances in Heat Transfer Engineering (Eds. B. Sunden, J. Vilemas), Begell House Inc. 2003. Pp. 637–644.

2. *M.J. Mantsinen*, M.-L. Mayoral, D. Van Eester, B. Alper, R. Barnsley, P. Beaumont, J. Bucalossi, I. Coffey, S. Conroy, M. de Baar, P. de Vries, K. Erents, A. Figueiredo, A. Gondhalekar, C. Gowers, T. Hellsten, E. Joffrin, V. Kiptily, P.U. Lamalle, K. Lawson, A. Lyssoivan, J. Mailloux, P. Mantica, F. Meo, F. Milani, I. Monakhov, A. Murari, F. Nguyen, J.-M. Noterdaeme, J. Ongena, Yu. Petrov, E. Rachlew, V. Riccardo, E. Righi, F. Rimini, M. Stamp, A.A. Tuccillo, K.-D. Zastrow, M. Zerbini and JET EFDA contributors, “Localized Bulk Electron Heating with ICRF Mode Conversion in the JET Tokamak,” Nuclear Fusion **44** (2004) 33–46.

3. *J.-S. Lönnroth*, V. Parail, C. Figarella, X. Garbet, G. Corrigan and D. Heading, "Predictive modelling of ELMy H-modes with a new theory-motivated model for ELMs", Plasma Physics and Controlled Fusion **46** (2004) A249.

4. *J.-S. Lönnroth*, V. Parail, G. Huysmans, G. Saibene, H. Wilson, S. Sharapov, G. Corrigan, D. Heading, R. Sartori and M. Bécoulet, "Predictive transport modelling and MHD stability analysis of mixed type I-II ELMy H-mode JET plasmas", Plasma Physics and Controlled Fusion **46** (2004) 767.

5. *J.-S. Lönnroth*, V. Parail, A. Dnestrovskij, C. Figarella, X. Garbet and H. Wilson, "Predictive transport modelling of type I ELMy H-mode dynamics using a theory-motivated combined ballooning-peeling model", Plasma Physics and Controlled Fusion **46** (2004) 1197.

6. *S. Saarelma* and S. Günter, “Edge stability analysis of high βp plasmas”, Plasma Physics and Controlled Fusion **46** (2004) 1259–1270.

7. *V. Hynönen*, *O. Dumbrajs*, A.W. Degeling, *T. Kurki-Suonio* and H. Urano, “The search for chaotic edge localized modes in ASDEX Upgrade”, Plasma Physics and Controlled Fusion **46** (2004) 1409–1422.

8. *O. Dumbrajs*, G.S. Nusinovich and B. Piosczyk, “Reflections in gyrotrons with radial output: consequences for the ITER coaxial gyrotron”, Physics of Plasmas **11** (2004) 5423.

9. G. Zvejnieks, V.N. Kuzovkov, *O. Dumbrajs*, A.W. Degeling, W. Suttrop, H. Urano and H. Zohm, “Autoregressive moving average model for analyzing edge localized mode time-series on axially symmetric divertor experiment upgrade tokamak”, Physics of Plasmas **11** (2004) 5658.

10. *J.A. Heikkinen*, *S. Janhunen*, *T.P. Kiviniemi* and *P. Kåll*, “Full-f particle simulation method for solution of transient edge phenomena”, Contributions to Plasma Physics **44** (2004) 13–17.

11. *O. Dumbrajs* and G.I. Zaginaylov, “Ohmic losses in coaxial gyrotron cavities with corrugated insert,” IEEE Transactions on Plasma Science **32** (2004) 861.

12. *O. Dumbrajs*, T. Idehara, S. Watanabe, A. Kimura, H. Sasagawa, L. Agusu, S. Mitsudo and B. Piosczyk, “Reflections in gyrotrons with axial output,” IEEE Transactions on Plasma Science **32** (2004) 899.

13. *O. Dumbrajs* and G.S. Nusinovich, “Coaxial gyrotrons: past, present, and future (***review***),” invited review article, IEEE Transactions on Plasma Science **32** (2004) 934.

14. *M.I. Airila* and *P. Kåll*, "Effect of reflections on nonstationary gyrotron oscillations", IEEE Transactions on Microwave Theory and Techniques **52** (2004) 522–528.

15. *M.I. Airila* and *O. Dumbrajs*, "Correction to: 'Spatio-temporal chaos in the transverse section of gyrotron resonators'", IEEE Transactions on Plasma Science **32** (2004) 2155.

16. *P. Träskelin*, *E. Salonen*, *K. Nordlund*, *J. Keinonen* and C.H. Wu, “Molecular dynamics simulations of CH_3 sticking on carbon surfaces, angular and energy dependence”, Journal of Nuclear Materials **334** (2004 65.

17. *O. Dumbrajs*, H. Kalis and A. Reinfelds, “Numerical solution of single mode gyrotron equation,” Math. Modelling and Analysis **9** (2004) 1.

18. *K. Heinola, T. Ahlgren*, *W. Rydman, J. Likonen*, L. Khriachtchev, *J. Keinonen* and C.H. Wu, “Effect of hydrogen on flaking of carbon films on Mo and W”, Physica Scripta (2003), Physica Scripta. **T108** (2004) 63.

19. *K.O.E. Henriksson, K. Nordlund, J. Keinonen*, D. Sundholm and M. Patzschke, “Simulations of the initial stages of blistering in helium implanted tungsten”, Physica Scripta **T108** (2004) 95.

20. *K. Nordlund*, “Atomistic simulation of radiation effects in carbon-based materials and nitrides”, Nucl. Instr. Meth. Phys. Res. B **218** (2004) 9.

21. L.-G. Eriksson, T. Johnson, T. Hellsten, C. Giroud, V.G. Kiptily, K. Kirov, J. Brzozowski, M. DeBaar, J. DeGrassie, *M.J. Mantsinen*, A. Meigs, J.-M. Noterdaeme, A. Staebler, A. Tuccillo, H. Weisen, K.-D. Zastrow and JET-EFDA contributors, “Plasma Rotation induced by directed waves in the ion cyclotron range of frequencies”, Phys. Rev. Lett. **92**, (2004) 235001.

22. L.-G. Eriksson, A. Mueck, O. Sauter, S. Coda, *M.J. Mantsinen*, M.L. Mayoral, E. Westerhof, R.J. Buttery, D. McDonald, T. Johnson, J.-M. Noterdaeme, P. de Vries and JET-EFDA contributors, “Destabilisation of Fast Ion Induced Long Sawteeth by Localised Current Drive in the JET Tokamak”, Phys. Rev. Lett. **92**, (2004) 235004.

23. W. Fundamenski, *S. Sipilä* and contributors to the EFDA-JET Work Programme, "Boundary plasma energy transport in JET ELMy H-modes." Nuclear Fusion **44** (2004) 20–32.

24. J. Ongena, P. Monier-Garbet, W. Suttrop, Ph. Andrew, M. Bécoulet, R. Budny, Y. Corre, G. Cordey, P. Dumortier, Th. Eich, L. Garzotti, D.L. Hillis, J. Hogan, L.C. Ingesson, S. Jachmich, E. Joffrin, P. Lang, A. Loarte, P. Lomas, G.P. Maddison, D. McDonald, A. Messiaen, M.F.F. Nave, G. Saibene, R. Sartori, O. Sauter, J.D. Strachan, B. Unterberg, M. Valovic, I. Voitsekhovitch, M. von Hellermann, B. Alper, Y. Baranov, M. Beurskens, G. Bonheure, J. Brzozowski, J. Bucalossi, M. Brix, M. Charlet, I. Coffey, M. De Baar, P. De Vries, C. Giroud, C. Gowers, N. Hawkes, G.L. Jackson, C. Jupen, A. Kallenbach, H.R. Koslowski, K.D. Lawson, *M.J. Mantsinen,* G. Matthews, F. Milani, M. Murakami, A. Murari, R. Neu, V. Parail, S. Podda, M.E. Puiatti, J. Rapp, E. Righi, F. Sartori, Y. Sarazin, A. Staebler, M. Stamp, G. Telesca, M. Valisa, B. Weyssow, K.D. Zastrow and EFDA-JET Workprogramme contributors, "Towards the realization on JET of an integrated H-mode scenario for ITER," Nuclear Fusion **44** (2004) 124–133.

25. T. Hellsten, T. Johnson, J. Carlsson, L.-G. Eriksson, J. Hedin, M. Laxåback and *M.J. Mantsinen*, "Effects of finite drift orbit width and RF-induced spatial transport on plasma heated by ICRH," Nuclear Fusion **44** (2004) 892–908.

26. X. Litaudon, E. Barbato, A. Bécoulet, E.J. Doyle, T. Fujita, P. Gohil, F. Imbeaux, O. Sauter, G. Sips, for the International Tokamak Physics Activity (ITPA) Group on Transport and Internal Tokamak Barrier (ITB) Physics: J. Connor, E.J. Doyle, Yu. Esipchuk, T. Fujita, T. Fukuda, P. Gohil, J. Kinsey, N. Kirneva, S. Lebedev, X. Litaudon, V. Mukhovatov, J. Rice, E. Synakowski, K. Toi, B. Unterberg, V. Vershkov, M. Wakatani; and for the International ITB DatabaseWorking Group and the responsible officers for the ITPA collaborative experiments on the 'hybrid' and 'steady-state' regimes: T. Aniel, Yu.F. Baranov, E. Barbato, A. Bécoulet, R. Behn, C. Bourdelle, G. Bracco, R.V. Budny, P. Buratti, E.J. Doyle, Yu. Esipchuk, B. Esposito, S. Ide, A.R. Field, T. Fujita, T. Fukuda, P. Gohil, C. Gormezano, C. Greenfield, M. Greenwald, T.S. Hahm, G.T. Hoang, J. Hobirk, D. Hogeweij, S. Ide, A. Isayama, F. Imbeaux, E. Joffrin, Y. Kamada, J. Kinsey, N. Kirneva, X. Litaudon, T.C. Luce, M. Murakami, V. Parail, Y-K.M. Peng, F. Ryter, Y. Sakamoto, H. Shirai, G. Sips, T. Suzuki, E. Synakowski, H. Takenaga, T. Takizuka, *T. Tala,* M.R. Wade and J. Weiland, "Status of and prospects for Advanced Tokamak regimes from multi-machine comparisons using the 'International Tokamak Physics Activity' database", Plasma Physics and Controlled Fusion **46** (2004) A19–A34.

27. W. Suttrop, G. D. Conway, L. Fattorini, L. D. Horton, *T. Kurki-Suonio,* C. F. Maggi, M. Maraschek, H. Meister, R. Neu, Th. Pütterich, M. Reich, A. C. C. Sips and the ASDEX Upgrade Team: Study of quiescent H-mode plasmas in ASDEX Upgrade, Plasma Phys. Control. Fusion, **46** (2004) A151.

28. G. Saibene, T. Hatae, D. Campbell, G. Cordey, E. de la Luna, C. Giroud, K. Guenther, Y. Kamada, M. Kempenaars, A. Loarte, *J. Lönnroth*, D. Mc Donald, M. Nave, N. Oyama, V. Parail, R. Sartori, J. Stober, T. Suzuki, M. Takechi and K. Toi, "Dimensionless pedestal identity experiments in JT-60U and JET in ELMy H-mode plasmas", Plasma Physics and Controlled Fusion **46** (2004) A195.

29. X. Garbet, P. Mantica, C. Angioni, E. Asp, Y. Baranov, C. Bourdelle, R. Budny, F. Crisanti, G. Cordey, L. Garzotti, N. Kirneva, D. Hogeweij, T. Hoang, F. Imbeaux, E. Joffrin, X. Litaudon, A. Manini, D.C. McDonald, H. Nordman, V.Parail, A. Peeters, F. Ryter, C. Sozzi, M. Valovic, T. Tala, A. Thyagaraja, I. Voitsekhovitch, J. Weiland, H. Weisen, A. Zabolotsky and the JET EFDA Contributors, "Physics of Transport in Tokamaks", Plasma Physics and Controlled Fusion **46** (2004) B557–B574.

30. Yu.F. Baranov, X. Garbet, N.C. Hawkes, B. Alper, R. Barnsley, C.D. Challis, C. Giroud, E. Joffrin, *M.J. Mantsinen*, F. Orsitto, V. Parail, S.E. Sharapov and the JET EFDA Contributors, "On the link between q-profile and Internal Transport Barriers", Plasma Physics and Controlled Fusion **46** (2004) 1181–1196.

31. T. Onjun, A. Kritz, G. Bateman, V. Parail, H. Wilson, *J. Lönnroth*, G. Huysmans and A. Dnestrovskij, "Stability analysis of H-mode pedestal and edge localized modes in a Joint European Torus power scan", Physics of Plasmas **11** (2004) 1469.

32. M.-L. Mayoral, R. Buttery, T.T.C. Jones, V. Kiptily, S. Sharapov, *M.J. Mantsinen*, S. Coda, O. Sauter, L.-G. Eriksson, F. Nguyen, D.N. Borba, A. Mück, S.D. Pinches, J.-M. Noterdaeme and JET-EFDA Contributors, "Studies of burning plasma physics in the Joint European Torus", Physics of Plasmas **11** (2004) 2607.

33. A. Loarte, G. Saibene, R. Sartori, T. Eich, A. Kallenbach W. Suttrop, M. Kempenaars, M. Beurskens, M. de Baar, *J. Lönnroth*, P.J. Lomas, G. Matthews, W. Fundamenski, V. Parail, M. Becoulet, P. Monier-Garbet, E. de la Luna, B. Gonçalves and C. Silva, Y. Corre, "Characterization of pedestal parameters and edge localized mode energy losses in the Joint European Torus and predictions for the International Thermonuclear Experimental Reactor", Physics of Plasmas **11** (2004) 2668.

34. T. Onjun, A. Kritz, G. Bateman, V. Parail, *J. Lönnroth* and G. Huysmans, "Integrated pedestal and core modeling of Joint European Torus (JET) triangularity scan discharges", Physics of Plasmas **11** (2004) 3006.

35. M. Warrier, R. Schneider, *E. Salonen*, and *K. Nordlund*, "Multi scale modeling of hydrogen isotope diffusion in graphite", Contributions to Plasma Physics **44** (2004) 307.

36. M.J. Rubel, J.P.Coad, K. Stenström, P. Wienhold, *J. Likonen*, G.F. Matthews and V. Philipps, "Overview of tracer techniques in studies of material erosion, re-deposition and fuel inventory in tokamaks", Journal of Nuclear Materials **329–333** (2004) 795–799.

37. B. Piosczyk, G. Dammertz, *O. Dumbrajs*, M.V. Kartikeyan, M.K. Thumm and X. Yang, "165-GHz coaxial cavity gyrotron", IEEE Transactions on Plasma Science **32** (2004) 853.

38. La Agusu, T. Idehara and *O. Dumbrajs*, "Mode selection for a terahertz gyrotron based on a pulse magnet system," Int. J. Infrared and Millimeter Waves **25** (2004) 1023.

39. M. Warrier, R. Schneider, *E. Salonen* and *K. Nordlund*, "Modelling of the diffusion of hydrogen in porous graphite", Physica Scripta **T108** (2004) 85.

40. *O. Dumbrajs* and *V. Hynönen*, "Methods of detecting unstable periodic orbits in chaotic ELM experimetal data", accepted for publication in Computer Modelling and New Technologies (2002) (in print).

41. *P. Träskelin, K. Nordlund* and *J. Keinonen*, “He, Ne, Ar-bombardment of carbon first wall structures”, accepted for publication in Nucl. Instr. Meth. Phys. Res. B (2004).

42. L. Laborde, D. Mazon, D. Moreau, A. Murari, R. Felton, L. Zabeo, R. Albanese, M. Ariola, J. Bucalossi, F. Crisanti, M. de Baar, G. de Tommasi, P. de Vries, E. Joffrin, M. Lennholm, X. Litaudon, A. Pironti, T. Tala and A. Tuccillo, “A model-based technique for integrated real-time profile control in the JET tokamak”, accepted for publication in Plasma Physics and Controlled Fusion [Plasma Physics and Controlled Fusion **47** (2005) 155–183].

43. *S. Saarelma*, V. Parail, Y. Andrew, E. de la Luna, A. Kallenbach, M. Kempenaars, A. Korotkov, A. Loarte, *J. Lönnroth*, P. Monier-Garbet, J. Stober, W. Suttrop and Contributors to the EFDA-JET workprogramme, "MHD Stability Analysis of Diagnostic Optimized Configuration (DOC) shots in JET", accepted for publication in Plasma Physics and Controlled Fusion.

44. *T.M.J. Ikonen* and *O. Dumbrajs*, ”Search for deterministic chaos in ELM time series of ASDEX Upgrade tokamak,” accepted for publication in IEEE Transactions on Plasma Science (2004).

45. *T.J.J. Tala*, F. Imbeaux, V.V. Parail, C. Bourdelle, G. Corrigan, X. Garbet, D. Heading, X. Litaudon, P.I. Strand, J. Weiland and JET EFDA contributors, “Fully Predictive Transport Simulations of ITB Plasmas in JET, JT-60U and DIII-D”, submitted for publication in Nuclear Fusion (2004).

46. *T. Tala*, L. Laborde, D. Mazon, D. Moreau, G. Corrigan, F. Crisanti, X. Garbet, D. Heading, E. Joffrin, X. Litaudon, V. Parail, A. Salmi and contributors to the EFDAJET workprogramme, “Fully Predictive Simulations of Current and Temperature Profile Control in JET Advanced Tokamak Plasmas and Comparison with Experiments”, submitted for publication in Nuclear Fusion (2004).

47. *K.M. Rantamäki*, V. Petržílka, P. Andrew, I. Coffey, A. Ekedahl, K. Erents, V. Fuchs, M. Goniche, G. Granucci, E. Joffrin, *S.J. Karttunen*, P. Lomas, J. Mailloux, *M.J. Mantsinen*, M.-L. Mayoral, D.C. McDonald, J.-M. Noterdaeme, V. Parail, A.A. Tuccillo, F. Žáček and contributors to the EFDA – JET work programme, “Bright Spots Generated by Lower Hybrid Waves on JET”, submitted for publication in Plasma Physics and Controlled Fusion (2004).

48. *T.P. Kiviniemi*, *J.A. Heikkinen*, *T. Kurki-Suonio*, *S.K. Sipilä*, W. Fundamenski and A.G. Peeters, “Monte Carlo Guiding-Centre Simulations of Edge Radial Electric Field and Divertor Load”, submitted for publication in Advances in Plasma Physics (2004).

49. *T. Ekholm*, *S. Janhunen*, *J.A. Heikkinen*, *S. Henriksson* and *T.P. Kiviniemi*, “Characteristics of Transport Barrier Generation from Gyrokinetic Simulation in a Tokamak”, submitted for publication in IEEE Transactions on Plasma Science (2004).

50. *M.I. Airila*, *O. Dumbrajs*, J. Geiger, H.-J. Hartfuss, M. Hirsch and U. Neuner, “Sightline optimization of the multichannel laser interferometer for W7-X”, submitted for publication in Review of Scientific Instruments (2003) [Rev. Sci. Instrum. **76** (2005) 023501].

51. F. Nguyen, J.-M. Noterdaeme, I. Monakhov, F. Meo, H.-U. Fahrbach, C.F. Maggi, R. Neu, A. Stäbler, W. Suttrop, *T. Kurki-Suonio*, *S.K. Sipilä*, M. Brambilla, D. Hartmann, F. Wesner, and the ASDEX Upgrade Team, "ICRF heating with mode converted ion Bernstein wave at 3/s D cyclotron harmonic on the tokamak ASDEX Upgrade", submitted for publication in Physical Review Letters (2003).

52. C. Bourdelle, X. Litaudon, C.M. Roach, *T. Tala* for the ITPA Topical Group on Transport and ITB Physics, and the International ITB Databse Working Group, "Impact of α on the microstability of internal transport barriers", submitted for publication in Nuclear Fusion (2004).

53. J.P. Coad, *J. Likonen*, M. Rubel, *E. Vainonen-Ahlgren*, D.E. Hole, *T. Sajavaara*, *T. Renvall* and G.F. Matthews, "Overview of Material Re-deposition and Fuel Retention Studies at JET with the Gas Box Divertor", submitted for publication in Nuclear Fusion (2004).

54. A. Ekedahl, G. Granucci, J. Mailloux, Y. Baranov, K. Erents, E. Joffrin, X. Litaudon, P. Lomas, *M.J. Mantsinen*, D. McDonald, J.-M. Noterdaeme, V. Petrzilka, *K. Rantamäki*, C. Silva, A.A. Tuccillo and EFDA-JET Contributors, "Long Distance Coupling of Lower Hybrid Waves in JET Plasmas with Edge and Core Transport Barriers", submitted for publication in Nuclear Fusion (2004).

55. T. Hellsten, M. Laxåback, T. Bergkvist, T. Johnson, F. Meo, F. Nguyen, C.C. Petty, *M.J. Mantsinen*, G. Matthews, J.-M. Noterdaeme, *T. Tala*, D. van Eester, P. Andrew, P. Beaumont, M. Brix, J. Brzozowski, L.-G. Eriksson, C. Giround, E. Joffrin, V. Kiptily, J. Mailloux, M.-L. Mayoral, I. Monakhov, R. Sartori, A. Staebler, E. Rachlew, E. Tennfors, A. Tuccillo, A. Walden, B. Volodymyr, K.-D. Zastrow and JET-EFDA contributors, "On the Parasitic Absorption in FWCD Experiments in JET ITB Plasmas", submitted for publication in Nuclear Fusion (2004).

56. E. Joffrin, A.C.C. Sips, J.F. Artaud, A. Becoulet, R. Budny, P. Buratti, P. Belo, C.D. Challis, F. Crisanti, M. de Baar, P. de Vries, C. Gormezano, C. Giroud, O. Gruber, G.T.A. Huysmans, F. Imbeaux, A. Isayama, X. Litaudon, P.J. Lomas, D.C. McDonald, Y.S. Na, S.D. Pinches, A. Staebler, T. Tala, A. Tuccillo, K.-D. Zastrow and Contributors to the EFDA-JET Work Programme, "The "hybrid" scenario in JET: towards its validation for ITER", submitted for publication in Nuclear Fusion (2004).

57. J.E. Kinsey, F. Imbeaux, G. Staebler, R. Budny, C. Bourdelle, A. Fukuyama, X. Garbet, T. Tala and V. Parail for the ITPA Topical Group on Transport Physics and the ITB Database Working Group, "Transport Modeling and Gyrokinetic Analysis of Advanced High Performance Discharges", submitted for publication in Nuclear Fusion (2004).

58. P.U. Lamalle, M.J. Mantsinen, J.-M. Noterdaeme, B. Alper, P. Beaumont, L. Bertalot, T. Blackman, V.V. Bobkov, G. Bonheure, J. Brzozowski, C. Castaldo, S. Conroy, M. de Baar, E. de la Luna, P. de Vries, F. Durodié, G. Ericsson, L.-G. Eriksson, C. Gowers, R. Felton, J. Heikkinen, T. Hellsten, V. Kiptily, K. Lawson, M. Laxåback, E. Lerche, P. Lomas, A. Lyssoivan, M.-L. Mayoral, F. Meo, M. Mirnov, I. Monakhov, I. Nunes, S. Popovichev, A. Salmi, M.I.K. Santala, S. Sharapov, T. Tala, M. Tardocchi, D. Van Eester, B. Weyssow and JET EFDA contributors, "Expanding the operating space of ICRF on JET with a view to ITER", submitted for publication in Nuclear Fusion (2004).

59. A. Lyssoivan, D.A. Hartmann, J.-M. Noterdaeme, R. Koch, V. Bobkov, S.D. Pinches, H.L. Berk, D.N. Borba, B.N. Breizman, S. Briguglio, A. Fasoli, G. Fogaccia, M.P. Gryaznevich, V. Kiptily, *M. J. Mantsinen,* S.E. Sharapov, D. Testa, R.G.L. Vann, G. Vlad, F. Zonca and JET-EFDA Contributors, "The Role of Energetic Particles in Fusion Plasmas", submitted for publication in Plasma Physics and Controlled Fusion (2004).

60. F. Nabais, D. Borba, *M.J. Mantsinen*, M.F.F. Nave, S. E. Sharapov and JET-EFDA contributors, "Numerical analysis of sawtooth stabilization by high energy ICRH driven fast ions", submitted for publication in Plasma Physics and Controlled Fusion (2003).

61. G. Saibene, R. Sartori, A. Loarte, P.J. Lomas, V. Parail, K.D. Zastrow, Y. Andrew, S. Sharapov, A. Korotkov, D.C. McDonald, K. Guenther, A.G. Meigs, S.A. Arshad, M. Becoulet, P.R. Thomas, P. Monier-Garbet, F.G. Rimini, H.R. Koslowski, C.P. Perez, J. Stober, G.D. Conway, M.A.H. Kempenaars, L.C. Ingesson and *J.S. Lönnroth*, "Characterisation of small ELM experiments in highly shaped Single Null and Quasi Double Null plasmas in JET", submitted for publication in Plasma Physics Controlled Fusion (2004).

62. J. Weiland, E. Asp, X. Garbet, P. Mantica, V. Parail, P. Thomas, W. Suttrop, T. Tala and the EFDA-JET contributors, "Effects of temperature ratio on JET transport in hot ion and hot electron regimes", submitted for publication in Plasma Physics and Controlled Fusion (2004).

63. Y. Kominis, *O. Dumbrajs*, K.A. Avramides, K. Hizanidis, and J.L. Vomvoridis, "Chaotic electron dynamics in gyrotron resonators," submitted for publication in Physics of Plasmas (2004).

64. T. Blackman, F. Braun, M. Cox, P. de Vries, H.G. Esser, H.-U. Fahrbach, J. Gafert, E. Gauthier, O. Gehre, M. Graham, G. Haas, A. Huber, K. Lawson, P.J. Lomas, *M.J. Mantsinen*, G. Matthews, M.-L. Mayoral, A. Meigs, Ph. Mertens, V. Mertens, I. Monakhov, J. Neuhauser, V. Philipps, V. Rohde, *M. Santala*, W. Suttrop, A. Walden, D. Van Eester and F. Wesner, ASDEX Upgrade Team and JET EFDA Contributors, "Development of ICRF wall conditioning technique on divertor-type tokamaks ASDEX Upgrade and JET", submitted for publication in Journal of Nuclear Materials (2004).

11.1.2 Conference Articles – Fusion Plasma Physics

1. Ekedahl, G. Granucci, J. Mailloux, V. Petrzilka, *K. Rantamäki*, Y. Baranov, K. Erents, M. Goniche, E. Joffrin, P.J. Lomas, *M.J. Mantsinen*, D. McDonald, J.-M. Noterdaeme, V. Pericoli, R. Sartori, C. Silva, M. Stamp, A.A. Tuccillo, F. Zacek and EFDA-JET Contributors, "Long Distance Coupling of Lower Hybrid Waves in ITER Relevant Edge Conditions in JET Reversed Shear Plasmas", Radio-Frequency Power in Plasmas (Proc. 15th Topical Conference on Radio Frequency Power in Plasmas 19–21 May, 2003, Moran, Wyoming, USA), AIP, New York (2003) 227–234.

2. D. Moreau, F.Crisanti, X. Litaudon, D. Mazon, P. De Vries, R. Felton, E. Joffrin, L. Laborde, M. Lennholm, A. Murari, V. Pericoli-Ridolfini, M. Riva, *T. Tala*, G. Tresset, L. Zabeo and K. D. Zastrow, "Real-Time Control of the Current Profile in JET", Radio-Frequency Power in Plasmas (Proc. 15th Topical Conference on Radio Frequency Power in Plasmas 19–21 May, 2003, Moran, Wyoming, USA), AIP, New York (2003) 279–282.

3. D. Moreau, F. Crisanti, L. Laborde, X. Litaudon, D. Mazon, A. Murari, *T. Tala*, P. De Vries, R. Felton, F. Imbeaux, E. Joffrin, M. Lennholm, V. Pericoli-Ridolfini, M. Riva, L. Zabeo, K.D. Zastrow and contributors to the EFDA-JET workprogramme, "Real-time control of internal transport barriers in JET: Experiments and simulations", Joint Meeting of US-Japan JIFT Workshop on Theory-Based Modeling and Integrated Simulation of Burning Plasmas, and 21COE Workshop on Plasma Theory, Kyoto Japan, December 15–17, 2003.

4. N.C Hawkes, Y. Baranov, L. Bertalota, P. Blanchard, M. Brix, C. Challis, S. Conroy, S. Cortes,E. De La Luna, V. Goloborod'ko, T. Hender, G. Huysmans, E. Joffrin, V. Kiptily, J. Mailloux, V. Parail, V. Pericoli, S. Pinches, S. Popovichev, E. Rachlew, K .Schöpf, S. Sharapov, P. Smeulders, E. Solano, B. Stratton, *T. Tala*, D. Testa, V. Yavorski, L. Zakharov and contributors to the EFDA-JET programme, "Current-Hole Studies at JET", Large Tokamak Workshop on the Physics of the Current Hole, Naka, 3–4 February 2004.

5. *S. Karttunen*, "European Fusion Programme and International ITER Project", XXXIV EESTI Füüsikapäevad,Annual meeting of the Estonian Physical Society,Tartu, Estonia 13.–14 February 2004 (2004) 48–49 invited paper.

6. C. Schlatter, D. Testa, M. Cecconello, A. Murari, *M. Santala* and JET-EFDA contributors, "Error Estimation and Parameter Dependence of the Calculation of the Fast Ion Distribution Function, Temperature and Density using Data from the KF1 High Energy NPA on JET", Proceedings of the 15th HTPD Conference (San Diego, California, USA, 18–22 April 2004).

7. *O. Dumbrajs* and G.I. Zaginaylov, "Ohmic losses in coaxial gyrotron cavities with corrugated insert," "Vacuum Electronics and Displays" – 10th Triennial Conference, Garmisch Partenkirchen, Germany, May 3–4, 2004.

8. B. Piosczyk, A. Arnold, H. Budig, G. Dammertz, *O. Dumbrajs*, S. Illy, J. Jin, G. Michel, T. Rzesnicki, M. Thumm and D. Wagner, "2MW, CW, 170 GHz coaxial cavity gyrotron," "Vacuum Electronics and Displays" – 10th Triennial Conference, Garmisch Partenkirchen, Germany, May 3–4, 2004.

9. B. Piosczyk, A. Arnold, E. Borie, G. Dammertz, *O. Dumbrajs*, R. Heidinger, S. Illy, J. Jin, K. Koppenburg, G. Michel, T. Rzesnicki, M. Thumm, D. Wagner and X. Yang, "Development of advanced high power gyrotrons for ECH&CD applications in fusion plasmas," 13th Joint Workshop on Electron Cyclotron Emission and Electron Cyclotron Resonance Heating, Nizhny Novgorod, Russia, May 17–20, 2004.

10. M. Becoulet, G. Huysmans, P. Thomas, E. Joffrin, F. Rimini, P. Monier-Garbet, A. Grosman, P. Ghendrih, V.Parail, P. Lomas, G. Matthews, H. Wilson, M. Gryaznevich, G. Counsell, A.Loarte, G. Saibene, R. Sartori, A.Leonard, P. Snyder, L. Lao, T. Evans, P. Gohil, H. Burell, R. Moyer, Y. Kamada, N. Oyama, T. Hatae, A. Degeling, Y. Martin, J. Lister, J. Rapp, C. Perez, P. Lang, A. Chankin, T. Eich, A. Sips, J. Stober, L. Horton, A. Kallenbach, W. Suttrop, *S. Saarelma*, S. Cowley, *J. Lönnroth*, K. Kamiya, M. Shimada, A. Polevoi and G. Federici, "Edge Localized Modes Control: Experiment and Theory", Proceedings of the 16th PSI – Plasma Surface Interactions conference, (Portland, Maine, USA, 24–28 May 2004).

11. W. Fundamenski, P. Andrew, K. Erents, A. Huber, G. Kirnev, G. Matthews, R. Pitts, V. Riccardo, *S. Sipilä* and EFDA JET contributors, "Effect of B×∇B direction on SOL energy transport in JET", Proceedings of the 16th PSI – Plasma Surface Interactions conference (Portland, Maine, USA, 24–28 May 2004) [Journal of Nuclear Materials 337–339 (2005) 305–309].

12. K. Krieger, *J. Likonen*, M. Mayer, V. Rohde and *E. Vainonen-Ahlgren*, ASDEX Upgrade Team, "Tungsten redistribution patterns in ASDEX Upgrade", Proceedings of the 16th PSI – Plasma Surface Interactions conference (Portland, Maine, USA, 24–28 May 2004).

13. *J. Likonen*, *E. Vainonen-Ahlgren*, J.P. Coad, *R. Zilliacus*, *T. Renvall*, D.E. Hole, M. Rubel, *K. Arstila*, G.F. Matthews, M. Stamp and JET- EFDA Contributors, "Beryllium accumulation at the inner divertor of JET", Proceedings of the 16th PSI – Plasma Surface Interactions conference (Portland, Maine, USA, 24–28 May 2004).

14. A. Lyssoivan, D.A. Hartmann, J.-M. Noterdaeme, R. Koch, V. Bobkov, T. Blackman, F. Braun, M. Cox, P. de Vries, H.G. Esser, H.-U. Fahrbach, J. Gafert, E. Gauthier, O. Gehre, M. Graham, G. Haas, A. Huber, K. Lawson, P.J. Lomas, *M.J. Mantsinen*, G. Matthews, M.-L. Mayoral, A. Meigs, Ph. Mertens, V. Mertens, I. Monakhov, J. Neuhauser, V. Philipps, V. Rohde, *M. Santala*, W. Suttrop, A. Walden, D. Van Eester, F. Wesner and ASDEX Upgrade Teamand JET EFDA contributors, "Development of ICRF Wall Conditioning Technique on Divertor-Type Tokamaks ASDEX Upgrade and JET", Proceedings of the 16th PSI – Plasma Surface Interactions conference (Portland, Maine, USA, 24–28 May 2004).

15. G.F. Matthews, P. Coad, *J. Likonen*, K. Krieger, V. Philipps, M. Rubel, M. Stamp, J.D. Strachan, *E. Vainonen-Ahlgren* and JET EFDA Contributors, "Beryllium and carbon migration in JET", Proceedings of the 16th PSI – Plasma Surface Interactions conference (Portland, Maine, USA, 24–28 May 2004).

16. M. Mayer, V. Rohde, *J. Likonen*, *E. Vainonen-Ahlgren*, K. Krieger, X. Gong, J. Chen and ASDEX Upgrade Team, "Carbon Erosion and Deposition on the ASDEX Upgrade Divertor Tiles", Proceedings of the 16th PSI – Plasma Surface Interactions conference (Portland, Maine, USA, 24–28 May 2004).

17. R. Pugno, A. Kallenbach, *J. Likonen*, *E. Vainonen-Ahlgren*, D. Coster, A. Kirschner, K. Krieger, V. Rohde, U. Frantz and ASDEX Upgrade Team, "Parameter dependence of Carbon erosion in divertor plasmas", Proceedings of the 16th PSI – Plasma Surface Interactions conference (Portland, Maine, USA, 24–28 May 2004).

18. V. Rohde, M. Mayer, *J. Likonen*, R. Neu, T. Puetterich and ASDEX Upgrade Team, "Present Understanding of Carbon erosion and deposition at the divertor of ASDEX Upgrade", Proceedings of the 16th PSI – Plasma Surface Interactions conference (Portland, Maine, USA, 24–28 May 2004).

19. M. Rubel, J.P. Coad, *J. Likonen*, G.F. Matthews, *E. Vainonen-Ahlgren* and JET-EFDA Contributors, "In-vessel Diagnostic for Erosion and Re-deposition Studies in JET:High-Z Metal Coated Divertor and Limiter Marker Tiles", Proceedings of the 16th PSI – Plasma Surface Interactions conference (Portland, Maine, USA, 24–28 May 2004).

20. *E. Vainonen-Ahlgren*, *J. Likonen*, *T. Renvall*, *K. Arstila*, V. Rohde, R. Neu, R. Pugno, K. Krieger, M. Mayer and ASDEX Upgrade Team, "Studies on 13C transport and deposition at ASDEX Upgrade", Proceedings of the 16th PSI – Plasma Surface Interactions conference (Portland, Maine, USA, 24–28 May 2004).

21. P. Mantica, T. Tala, F. Imbeaux, M. Nora, V. Parail, J. Weiland and the JET EFDA contributors, "Predictive modelling of electron temperature modulation experiments in JET L- and H-mode plasmas", 31st EPS Conference on Controlled Fusion and Plasma Physics, London, 28 June – 2 July 2004, European Conference Abstract **28G** (2004) P-1.153.

22. P. Mantica, F. Imbeaux, *M.J. Mantsinen*, D. Van Eester, A. Marinoni, N. Hawkes, E. Joffrin, V. Kiptily, S. Pinches, *A. Salmi*, S. Sharapov, I. Voitsekhovitc, P. de Vries, K.-D. Zastrow and the JET EFDA contributors, "Power modulation experiments in JET ITB plasmas", 31st EPS Conference on Plasma Physics London, 28 June – 2 July 2004, European Conference Abstracts **28G** (2004) P-1.154.

23. J. Weiland, E. Asp, X. Garbet, P. Mantica, V. Parail, P. Thomas, W. Suttrop, T. Tala and the EFDA-JET contributors, "Effects of temperature ratio on JET transport in hot ion and hot electron regimes", 31st EPS Conference on Controlled Fusion and Plasma Physics, London, 28 June – 2 July 2004, European Conference Abstract **28G** (2004) P-1.160.

24. M.F.F. Nave, S. Coda, R. Galvão, J. Graves, R. Koslowski, *M.J. Mantsinen*, F. Nabais, S. Sharapov, P. de Vries, R. Buttery, M. de Baar, C. Challis, J. Ferreira, C. Giroud, M. Mayoral, S. D. Pinches, M. Stamp and JET-EFDA contributors, "Small sawtooth regimes in JET plasmas," 31st EPS Conference on Plasma Physics London, 28 June – 2 July 2004, European Conference Abstracts **28G** (2004) P-1.162.

25. *S.J. Janhunen*, *T.P. Kiviniemi* and *J.A. Heikkinen*, "Validation of gyrokinetic particle code ELMFIRE for tokamak edge transport analysis", 31st EPS Conference on Controlled Fusion and Plasma Physics, London UK, 28 June – 2 July, 2004, Europhysics Conference Abstracts **28G** (2004) P5-147.

26. *J.A. Heikkinen*, *S.J. Janhunen* and *T.P. Kiviniemi*, "Gyrokinetic simulation of neoclassical and turbulent transport", 31st EPS Conference on Controlled Fusion and Plasma Physics, London UK, 28 June – 2 July, 2004, Europhysics Conference Abstracts **28G** (2004) P-5.161.

27. *J.A. Heikkinen*, V.V. Bobkov, D.A. D'Ippolito, D.A. Hartmann, J. Myra, K.M. Rantamäki, *A. Salmi,* T. Hellsten, Ph. U. Lamalle, *M.J. Mantsinen,* J.-M. Noterdaeme and JET EFDA Contributors, "Experiments on ICRF Coupling with Different Phasings", 31st EPS Conference on Plasma Physics London, 28 June – 2 July 2004, European Conference Abstracts **28G** (2004) P-5.162.

28. P. U. Lamalle, *M. J. Mantsinen*, B. Alper, P. Beaumont, L. Bertalot, V.V. Bobkov, G. Bonheure, J. Brzozowski, S. Conroy, M. de Baar, P. de Vries, G. Ericsson, V. Kiptily, M. Laxåback, K. Lawson, E. A. Lerche, M. Mironov, J.-M. Noterdaeme, S. Popovichev, *M. Santala*, M. Tardocchi, D. Van Eester and JET EFDA contributors, "Investigation of low concentration tritium ICRF heating on JET," 31st EPS Conference on Plasma Physics London, 28 June – 2 July 2004, European Conference Abstracts **28G** (2004) P-5.165.

29. *A. Salmi*, P. Beaumont, P. de Vries, L.-G. Eriksson, C. Gowers, P. Helander, M. Laxåback, *M.J. Mantsinen*, J.-M. Noterdaeme, D. Testa and EFDA JET contributors, "JET Experiments to Assess Finite Larmor Radius Effects on Resonant Ion Energy Distribution during ICRF Heating", 31st EPS Conference on Plasma Physics London, 28 June – 2 July 2004, European Conference Abstracts **28G** (2004) P-5.167.

30. D. Mazon, A. Murari, M. Ariola, L. Laborde, X. Litaudon, D. Moreau, *T. Tala*, L. Zabeo, R. Albanese, F. Crisanti, M. De Baar, E. De la Luna, G. De Tommasi, P. De Vries, R. Felton, E. Joffrin, V. Pericoli-Ridolfini, A. Pironti, A. Tuccillo, G. Corrigan and JET-EFDA Contributors, "Current profile and ITB control for the development of advanced steady state plasmas in JET: experiments and modelling", 31st EPS Conference on Controlled Fusion and Plasma Physics, London UK, 28 June – 2 July, 2004, Europhysics Conference Abstracts **28G** (2004) P-5.168.

31. *J.-S. Lönnroth* et al., "Modelling of ELM heat pulse propagation with the integrated core-SOL transport code COCONUT", 31st EPS Conference on Plasma Physics London, 28 June – 2 July 2004, European Conference Abstracts **28G** (2004).

32. G. Saibene, P.J. Lomas, R. Sartori, A. Loarte, P.R. Thomas, V.V. Parail, *J.S. Lönnroth*, H.R. Koslowski, C.P. Perez, F.G. Rimini, M.F.F. Nave, P. Belo, D.C. McDonald, Y. Andrew, A.G. Meigs, P. Monier-Garbet, G.D. Conway, J. Stober and M. Kempenaars, "Small ELM experiments in H-mode plasmas in JET", 31st EPS Conference on Plasma Physics London, 28 June – 2 July 2004, European Conference Abstracts **28G** (2004).

33. M. Mironov, V. Afanasyev, A. Murari, *M. Santala*, P. Beaumont and JET EFDA Contributors, "Tritium Transport Studies with JET ISEP NPA During the Trace Tritium Experimental Campaign", 31st EPS Conference on Plasma Physics London, 28 June – 2 July 2004, European Conference Abstracts **28G** (2004).

34. *M.I.K. Santala*, *M.J. Mantsinen*, Yu. Baranov, P. Beaumont, P. Belo, L. Bertalot, J. Brzozowski, M. Cecconello, S. Conroy, M. deBaar, P. deVries, C. Gowers, V. Kiptily, J.-M. Noterdaeme, S. Popovichev, *A. Salmi,* C. Schlatter, S. Sharapov and JET EFDA Contributors, "pT Fusion by RF-heated Protons in JET Trace Tritium Discharges", 31st EPS Conference on Plasma Physics London, 28 June – 2 July 2004, European Conference Abstracts **28G** (2004).

35. A. Andreev, V.G. Bespalov, E.V. Ermolaeva and *R.R.E. Salomaa*, Compression of high-intensity laser pulse by inhomogeneous plasma, Proc. of "Laser Optics 2003 – Superintense Light Fields and Ultrafast Processes", St. Petersburg, Russia, 30 June – 4 July, 2003 (Eds. V. E. Yashin and A. A. Andreev), Proc. SPIE 5482, (2004) 124–135.

36. *K.M. Rantamäki*, *A.T. Salmi* and *S.J. Karttunen*, "Particle-in-cell simulations of the near-field of a lower hybrid grill", Proceedings of the Joint Varenna-Lausanne International Workshop, Varenna, 30 August – 3 September 2004, International School of Plasma Physics "Piero Caldirola". Theory of Fusion Plasmas, J.W. Connor, O. Sauter and E. Sindoni (eds.), (Societa Italiana di Fisica, Bologna 2004). Pp. 167–176.

37. G. Zvejnieks, V.N. Kuzovkov, *O. Dumbrajs*, A.W. Degeling, W. Suttrop, H. Urano, and H. Zohm, "Distinguishing the deterministic and noise components in the ASDEX Upgrade ELM time series," Proceedings of the Joint Varenna-Lausanne International Workshop, Varenna, 30 August – 3 September 2004, International School of Plasma

Physics "Piero Caldirola". Theory of Fusion Plasmas, J.W. Connor, O. Sauter and E. Sindoni (eds.), (Societa Italiana di Fisica, Bologna 2004).

38. X. Garbet, P. Mantica, E. Asp, F. Imbeaux, F. Ryter, C. Sozzi, *T. Tala* and the JET EFDA Contributors, "Interplay between electron and ion heat channels", 10th EU-US Transport Task Force Workshop, Varenna, Italy, September 6–9,2004.

39. C. Bourdelle, X. Litaudon, C.M. Roach, *T. Tala*, for the ITPA Topical Group on Transport and ITB Physics, and the International ITB Database Working Group, "Impact of α on the microstability of internal transport barriers", 10th EU-US Transport Task Force Workshop, Varenna, Italy, September 6–9,2004.

40. J.P. Coad, M. Rubel, N. Bekris, D. Brennan, D. Hole, *J. Likonen*, *E. Vainonen-Ahlgren* and EFDA-JET Contributors, "Distribution of hydrogen isotopes, carbon and beryllium on in-vessel surfaces in the various JET divertors", TRITIUM 2004 – 7th International Conference on Tritium Science and Technology, Baden-Baden, Germany, 12–17 September, 2004.

41. S. Rosanvallon, N. Bekris, J. Braet, P. Coad, G. Counsell, I. Cristescu, C. Grisolia, F. Le Guern, G. Ionita, *J. Likonen*, A. Perevezenstev, G. Piazza, C. Poletiko, M. Rubel, J.M. Weulersse and J. Williams, "Tritium related studies within JET Fusion Technology workprogramme", TRITIUM 2004 – 7th International Conference on Tritium Science and Technology, Baden-Baden, Germany, 12–17 September, 2004.

42. M. Rubel, J.P. Coad, D. Hole, *J. Likonen*, *E. Vainonen-Ahlgren* and EFDA-JET Contributors, "Fuel Retention in the Gas Box Divertor at JET", TRITIUM 2004 – 7th International Conference on Tritium Science and Technology, Baden-Baden, Germany, 12–17 September, 2004.

43. *O. Dumbrajs*, "Modeling of stochastic processes in gyrotrons," (invited plenary talk) 10th International Conference on Mathematical Methods in Electromagnetic Theory, Dniepropetrovsk, Ukraine, September 14–17, 2004.

44. Ph. Bibet, B. Beaumont, J.H. Belo, L. Delpech, A. Ekedahl, G. Granucci, F. Kazarian, J. Mailloux, F. Mirizzi, V. Pericoli, M. Prou, *K. Rantamäki* and A. Tuccillo, "Toward an LHCD system for ITER", 23rd Symposium on Fusion Technology, Fondazione Cini, Venice, Italy, 20–24 September 2004.

45. J.P. Coad, H-G. Esser, *J. Likonen*, M. Mayer, G. Neill, V. Philipps, M. Rubel, J. Vince and EFDA-JET Contributors, "Diagnostics for studying tritium retention at JET", 23rd Symposium on Fusion Technology, Fondazione Cini, Venice, Italy, 20–24 September 2004.

46. C. Grisolia, N. Bekris, *J. Likonen*, P. Coad, A. Semerok, D. Brennan, G. Piazza, S. Rosanvallon and JET-EFDA Contributors, "JET contribution to ITER fuel cycle issues", 23rd Symposium on Fusion Technology, Fondazione Cini, Venice, Italy, 20–24 September 2004.

47. B. Piosczyk, A. Arnold, H. Budig, G. Dammertz, *O. Dumbrajs*, R. Heidinger, S. Illy, J. Jin, G. Michel, T. Rzesnicki, M. Thumm and X. Yang, "Experiments on a 170 GHz coaxial cavity gyrotron," 23rd Symposium on Fusion Technology, Fondazione Cini, Venice, Italy, 20–24 September 2004.

48. *O. Dumbrajs*, G.S. Nusinovich and B. Piosczyk, "Reflections in gyrotrons with radial output: consequences for the ITER coaxial gyrotron", (invited keynote) 29th Int. Conf. Infrared Millimeter Waves, Karlsruhe, Germany, 27 September – 1st October 2004.

49. B. Piosczyk, T. Rzesnicki, A. Arnold, H. Budig, G. Dammertz, *O. Dumbrajs*, S. Illy, J. Jin, K. Koppenburg, W. Leonhard, G. Michel, M. Schmid, M. Thumm and X. Yang, "Progress in the development of the 170 GHz coaxial cavity gyrotron,"(invited keynote) 29th Int. Conf. Infrared Millimeter Waves, Karlsruhe, Germany, 27 September – 1st October 2004.

50. Y. Kominis, *O. Dumbrajs*, K.A. Avramides, K. Hizanidis and J.L. Vomvoridis, "Chaotic electron dynamics in gyrotron resonators," 29th Int. Conf. Infrared Millimeter Waves, Karlsruhe, Germany, 27 September – 1st October 2004.

51. M.Q. Tran, S. Alberti, A. Arnold, D. Bariou, E. Borie, G. Dammertz, C. Darbos, *O. Dumbrajs*, G. Gantenbein, E. Giguet, R. Heidinger, J.P. Hogge, S. Illy, W. Kasparek, C. Lievin, R. Magne, G. Michel, B. Piosczyk and M. Thumm, "Development of high power gyrotrons for fusion plasma applications in the EU", (invited plenary talk) 29th Int. Conf. Infrared Millimeter Waves, Karlsruhe, Germany, 27 September – 1st October 2004.

52. *T. Tala*, C. Bourdelle, F. Imbeaux, D. Moreau, V. Parail, Y. Baranov, G. Corrigan, F. Crisanti, X. Garbet, D. Heading, E. Joffrin, L. Laborde, X. Litaudon, *J. Lönnroth*, P. Mantica, D. Mazon, *A. Salmi*, P. Strand, J. Weiland and contributors to the EFDA-JET workprogramme, "Progress in Transport Modelling of Internal Transport Barrier and Hybrid Scenario Plasmas in JET", 20th IAEA Fusion Energy Conference, Vilamoura, Portugal, 1–6 November 2004 TH/P2-9.

53. *T.P. Kiviniemi*, *J.A. Heikkinen*, *S. Janhunen*, *T. Kurki-Suonio* and *S.K. Sipilä*, "Particle simulation of plasma turbulence and neoclassical Er at tokamak plasma edge", 20th IAEA Fusion Energy Conference, Vilamoura, Portugal, 1–6 November 2004 TH/P3-7.

54. D.P. Coster, X. Bonnin, A. Chankin, G. Corrigan, S.K. Erents, W. Fundamenski, J. Hogan, A. Huber, A. Kallenbach, G. Kirnev, A. Kirschner, *T. Kiviniem*i, S. Kuhn, A. Loarte, *J. Lönnroth,* G.F. Matthews, R.A. Pitts, *S. Sipilä*, J. Spence, J. Strachan, F. Subba, E. Tsitrone, D. Tskhakaya, S. Wiesen, M. Warrier, M. Wischmeier, R. Zanino and contributors to the EFDA-JET work programme, "Integrated modelling of material migration and target plate power handling at JET", 20th IAEA Fusion Energy Conference, Vilamoura, Portugal, 1–6 November 2004.

55. W. Fundamenski, P. Andrew, T. Eich, G.F Matthews, R.A. Pitts, V. Riccardo, W. Sailer, *S. Sipilä* and JET EFDA contributors, "Power Exhaust on JET: An Overview of Dedicated Experiments", 20th IAEA Fusion Energy Conference, Vilamoura, Portugal, 1–6 November 2004.

56. N.N. Gorelenkov, V.G. Kiptily, *M. J. Mantsinen*, S.E. Sharapov, C.Z. Cheng and the JET-EFDA contributors, "Fast ion effects on fishbones and n=1 kinks in JET simulated by a non-perturbative NOVA-KN code", 20th IAEA Fusion Energy Conference, Vilamoura, Portugal, 1–6 November 2004.

57. E. Joffrin, A.C.C. Sips, A. Becoulet, R. Budny, P. Buratti, P. da Silva Aresta Belo, F. Crisanti, M. de Baar, P. de Vries, C. Gormezano, C. Giroud, O. Gruber, F. Imbeaux,

A. Isayama, X. Litaudon, P. Lomas, Y.S. Na, A. Staebler, *T. Tala*, A. Tuccillo, S.D. Pinches, K.-D. Zastrow and Contributors to the EFDA-JET Work Programme, "The "hybrid" scenario in JET: towards its validation for ITER", 20th IAEA Fusion Energy Conference, Vilamoura, Portugal, 1–6 November 2004 EX/4.2.

58. J. Kinsley, F. Imbeaux, G. Staebler, R. Budny, C. Bourdelle, A. Fukuyama, X. Garbet, *T. Tala* and V. Parail for the ITPA Topical Group on Transport Physics and the ITB Database Working Group, "Transport Modeling and Gyrokinetic Analysis of Advanced High Performance Discharges", 20th IAEA Fusion Energy Conference, Vilamoura, Portugal, 1–6 November 2004 IT/P3-37.

59. V.G. Kiptily, J.M. Adams, Yu.F. Baranov, L. Bertalot, S. Conroy, L.-G. Eriksson, L.C. Ingesson, *M.J. Mantsinen*, A. Murari, S.V. Popovichev, S.E. Sharapov, D. Stork, V. Yavorskij, B. Alper, R. Barnsley, P. de Vries, C. Gowers, N.C. Hawkes, P. Lomas, A. Meigs, F.P. Orsitto, K.-D. Zastrow and JET EFDA contributors, "Overview of the Latest Results in Gamma-Ray Diagnosis at JET", 20th IAEA Fusion Energy Conference, Vilamoura, Portugal, 1–6 November.

60. P.U. Lamalle, *M.J. Mantsinen*, J.-M. Noterdaeme, B. Alper, P. Beaumont, L. Bertalot, T. Blackman, V.V. Bobkov, G. Bonheure, J. Brzozowski, C. Castaldo, S. Conroy, M. de Baar, E. de la Luna, P. de Vries, F. Durodié, G. Ericsson, L.-G. Eriksson, C. Gowers, R. Felton, *J. Heikkinen*, T. Hellsten, V. Kiptily, K. Lawson, M. Laxåback, E. Lerche, P. Lomas, A. Lyssoivan, M.-L. Mayoral, F. Meo, M. Mirnov, I. Monakhov, I. Nunes, S. Popovichev, A. Salmi, M.I.K. Santala, S. Sharapov, *T. Tala*, M. Tardocchi, D. Van Eester, B. Weyssow and JET EFDA contributors, "Expanding the operating space of ICRF on JET with a view to ITER", 20th IAEA Fusion Energy Conference, Vilamoura, Portugal, 1–6 November 2004 EX/P4–26.

61. J. Mailloux, A. Ekedahl, G. Granucci, M. Goniche, V. Petržílka, *K. Rantamäki*, P. Andrew, J.-F. Artaud, Yu. Baranov, V. Basiuk, I. Coffey, K. Erents, E. Joffrin, K. Kirov, X. Litaudon, P. Lomas, G. Matthews, D.C. McDonald, V. Parail, V. Pericoli-Ridolfini, F. Rimini, R. Sartori, C. Silva, M. Stamp, A.A. Tuccillo, F. Žáček and JET-EFDA contributors, "ITER relevant coupling of Lower Hybrid Waves in JET", 20th IAEA Fusion Energy Conference, Vilamoura, Portugal, 1–6 November 2004 EX/P4–28.

62. P. Mantica, X. Garbet, C. Angioni, E. Asp, M. de Baar, Y. Baranov, R. Budny, G. Cordey, F. Crisanti, N. Hawkes, G.M.D. Hogeweij, F. Imbeaux, E. Joffrin, N. Kirneva, E. Lazzaro, X. Litaudon, *M.J. Mantsinen*, A. Marinoni, D. McDonald, *M. Nora*, H. Nordman, V. Parail, A. Peeters, F. Ryter, C. Sozzi, *T. Tala*, A. Thyagaraja, D. Van Eester, I. Voitsekhovitch, P. de Vries, J. Weiland, K.-D. Zastrow and the JET EFDA contributors, "Progress in understanding heat transport at JET", 20th IAEA Fusion Energy Conference, Vilamoura, Portugal, 1–6 November 2004 EX/P6–18.

63. M. Mayer, V. Rohde, *J. Likonen*, *E. Vainonen-Ahlgren*, J. Chen, X. Gong, K. Krieger, ASDEX Upgrade Team, "Carbon Deposition and Deuterium Inventory in the ASDEX Upgrade", 20th IAEA Fusion Energy Conference, Vilamoura, Portugal, 1–6 November 2004 Ex/5–24.

64. D. Moreau, F. Crisanti, L. Laborde, X. Litaudon, D. Mazon, A. Murari, T. Tala, L. Zabeo, R. Albanese, M. Ariola, G. De Tommasi, R. Felton, E. Joffrin, M. Lennholm, V. Pericoli-Ridolfini, A. Pironti, M. Riva, A. Tuccillo, M. De Baar, E. De la Luna,

P. De Vries, K.D. Zastrow and JET-EFDA Contributors., "Development of Integrated Real-Time Control of Internal Transport Barriers in Advanced Operation Scenarios on JET", 20th IAEA Fusion Energy Conference, Vilamoura, Portugal, 1–6 November 2004 EX/P2–5.

65. F. Nabais, D. Borba, *M.J. Mantsinen*, M. F. F. Nave, S. Sharapov and JET-EFDA contributors, "Internal kink mode stability in the presence of ICRH driven fast ions populations", 20th IAEA Fusion Energy Conference, Vilamoura, Portugal, 1–6 November 2004.

66. G. Saibene, N. Oyama, Y. Andrew, J.G. Cordey, E. de la Luna, C. Giroud, K. Guenther, T. Hatae, Y. Kamada, M.A.H. Kempenaars, A. Loarte, *J. Lönnroth*, D. McDonald, A. Meiggs, M.F.F. Nave, V. Parail, R. Sartori, J. Stober, T. Suzuki, M. Takechi and K. Toi, "Dimensionless identity experiments in JT-60U and JET", 20th IAEA Fusion Energy Conference, Vilamoura, Portugal, 1–6 November 2004.

67. D. Stork, K.-D. Zastrow, M. Adams, L. Bertalot, J.H. Brzozowski, C.D. Challis, S. Conroy, M. de Baar, P. de Vries, G. Ericsson, L. Garzotti, G. Gorini, N.C. Hawkes, T.C. Hender, E. Joffrin, V. Kiptily, P. Lamalle, A. Loarte, P.J. Lomas, J. Mailloux, *M. Mantsinen,* D.C. McDonald, A. Murari, R. Neu, J. Ongena, S. Popovichev, G. Saibene, *M. Santala*, R. Sartori, S. Sharapov, M. Stamp, J. Stober, M. Valovic, I. Voitsekhovitch, H. Weisen, A.D Whiteford, V. Yavorskij, A. Zabolotsky and JET EFDA contributors, "Overview of Transport, Fast Particle and Heating and Current Drive Physics using Tritium in JET plasmas", 20th IAEA Fusion Energy Conference, Vilamoura, Portugal, 1–6 November 2004.

68. W. Suttrop, *V. Hynönen*, P.T. Lang, *T. Kurki-Suonio*, M. Maraschek, R. Neu, A. Stäbler, G.D. Conway, S. Hacquin, M. Kempenaars, P.J. Lomas, R.A. Pitts and K.-D. Zastrow, the ASDEX Upgrade team and contributors to the JET-EFDA workprogramme, "Studies of the Quiescent H-mode regime in ASDEX Upgrade and JET", 20th IAEA Fusion Energy Conference, Vilamoura, Portugal, 1–6 November 2004.

69. D. Testa, A.Fasoli, R. Bertizzolo, D. Borba, R. Chavan, S. Huntley, *M. Mantsinen,* V. iccardo, S. Sanders, J.A. Snipes, P. Titus, R. Walton and M. Way, JET-EFDA contributors, "Experimental Studies of Alfvén Mode Stability in the JET Tokamak", 20th IAEA Fusion Energy Conference, Vilamoura, Portugal, 1–6 November 2004.

70. A.A. Tuccillo, F. Crisanti, X. Litaudon, Yu. F. Baranov, A. Becoulet, M. Becoulet, L. Bertalot, C.D. Challis, M.R. De Baar, P.C. de Vries, B. Esposito, D. Frigione, L. Garzotti, E. Giovannozzi, C. Giroud, G. Gorini, C. Gormezano, N.C. Hawkes, J. Hobirk, F. Imbeaux, E. Joffrin, P.J. Lomas, J. Mailloux, P. Mantica, *M.J. Mantsinen*, D. Mazon, D. Moreau, A. Murari, V. Pericoli-Ridolfini, F. Rimini, A.C.C. Sips, O. Tudisco, D. Van Eester, K.-D. Zastrow and JET-EFDA Workprogramme Contributors, "Development on JET of Advanced Tokamak Operations for ITER," 20th IAEA Fusion Energy Conference, Vilamoura, Portugal, 1–6 November 2004.

71. H. Weisen, C. Angioni, A. Bortolon, C. Bourdelle, L. Carraro, I. Coffey, R. Dux, I. Furno, X. Garbet, L. Garzotti, C. Giroud, H. Leggate, P. Mantica, D. Mazon, D. McDonald, M.F.F. Nave, R. Neu, V. Parail, M.E. Puiatti, *K. Rantamäki*, J. Rapp, J. Stober, *T. Tala*, M. Tokar, M. Valisa, M. Valovic, J. Weiland, L. Zabeo, A. Zabolotsky, K.-D. Zastrowand and JET-EFDA contributors, "Anomalous particle and impurity transport in JET and implications for ITER", 20th IAEA Fusion Energy Conference, Vilamoura, Portugal, 1–6 November 2004 EX/P6–31.

11.2 Fusion Technology

11.2.1 Publications in Scientific Journals – Fusion Technology

1. A.T. Peacock, V. Barabash, W. Dänner, M. Rödig, P. Lorenzetto, P. Marmy, M. Merola, B.N. Singh, *S. Tähtinen*, J. van der Laan and C.H. Wu, "Overview of recent European materials R&D activities related to ITER", Journal of Nuclear Materials **329–333** (2004) 173–177.

2. *J. Tuisku*, *M. Ahoranta, A. Korpela, J. Lehtonen, R. Mikkonen* and *R. Perälä*, "Cryogenic design of an isodynamic magnetic separator", IEEE Transactions on Applied Superconductivity **14** (2004) 1580–1583.

3. *T. Hartikainen, A. Korpela, J. Lehtonen* and *R. Mikkonen*, "A comparative life-cycle assessment between NbTi and copper magnets", IEEE Transactions on Applied Superconductivity **14** (2004) 1882–1885.

4. *H. Pantsar, A. Salminen, A. Jansson* and *V. Kujanpää,* "Quality and Costs Analysis of Laser Welded All Steel Sandwich Panels", Journal of Laser Applications **16**, (2004) 66–72.

5. *H. Pantsar* and *V. Kujanpää*, "Diode laser beam absorption in laser transformation hardening of low alloy steel", Journal of Laser Applications **16** (2004) 147–153.

6. R. Karppi and *V. Kujanpää*, "Trendi v tehynologiji in prenos tehnologije na finskem – S posebnim ozirom na varjenje in tehnike spanjanja" (Trends in technology and technology transfer in Finland – with special reference to welding and joining techniques), Varilna Teknika, **53** (2004) 30–38.

7. *V. Kujanpää* and H. Martikka, "Analytical and nonlinear FEM simulation of contact damage of hardened gearsars", IFNA-ANS International Journal "Problems of nonlinear analysis in engineering systems" **10** (2004) 14–25.

8. *A. Laukkanen*, *K. Wallin*, *P. Nevasmaa* and *S. Tähtinen*, "Transferability properties of local approach modeling in the ductile to brittle transition reason", ASTM STP:1429, 2004.

9. *T. Hartikainen, A. Korpela, J. Lehtonen* and *R. Mikkonen*, "A comparative life-cycle assessment between NbTi and copper magnets" IEEE Transactions on Applied Superconductivity **14** (2004) 1882–1885.

11.2.2 Conference Articles – Fusion Technology

1. P. Norajitra, L. Bühler, A. Buenaventura, E. Diegele, U. Fischer, S. Gordeev, E. Hutter, R. Kruessmann, S. Malang, D. Maisonnier, A. Orden, G. Reimann, J. Reimann, G. Vieider, D. Ward and *F. Wasastjerna*, "Conceptual Design of the EU Dual-Coolant Blanket (Model C)", Symposium on Fusion Engineering (SOFE), San Diego CA, USA October 14–17, 2003.

2. *H. Handroos, H. Wu* and *P. Pessi*, "Design of Mechatronic Water Hydraulic Parallel Robot for Machining in Fusion Reactor", Mechatronics Day 2004, DTU, Denmark.

3. *H. Wu, H. Handroos, J. Kilkki, Kovanen, P. Pessi* and L. Jones, "Development of a Parallel Mechanism Machine for a Fusion Reactor", ISR2004, Paris.

4. *H. Wu, H. Handroos* and *P. Pessi*, "Design and Development of a Water Hydraulic Parallel Robot for Machining in Fusion Reactor", ICMA'04, Osaka.

5. *A. Salminen, A. Fellman* and *V. Kujanpää*, "Effect of Joint Configuration on the Efficiency of High Power Diode Laser Welding of Steel", Photonics West 2004, High-Power Diode Laser Technology and Applications II, Proceedings of SPIE, 26–27 January, 2004, San Jose California, USA., Ed. M.S. Ediker, Vol. 5336, pp. 84–94.

6. J. Palmer, P. Agostin, R. Gottfried, M. Irving, E. Martin, M. Siuko, A. Tesini and M. Van Uffelen, "Remote Maintenance of the ITER Divertor", ANS 10th International Conference on Robotics and Remote Systems for Hazardous Environments, Gainesville, Florida, March 28–31, 2004.

7. Y. Chen, *F. Wasastjerna*, U. Fischer and S.P. Simakov, "Three-dimensional shielding calculations of the IFMIF neutron source using a coupled Monte Carlo deterministic computational scheme", 10th International Conference on Radiation Shielding/13th Topical Meeting on Radiation Protection and Shielding, Funchal, Madeira, May 9–14, 2004.

8. U. Fischer, Y. Chen, S.P. Simakov, P. Vladimirov and *F. Wasastjerna*, "Overview of Recent Progress in IFMIF Neutronics", ISFNT-7, Tokio, Japan, May 22–27 2004.

9. *V. Kujanpää* and *A. Salminen*, "Reflections of laser beam and pool phenomena in laser welding with filler wire and arc", IIW Annual Meeting, Osaka, Japan, 12–17 July 2004, IIW IV-870-04.

10. *V. Kujanpää*, "Absorption phenomena in laser welding", Finnish-German Japanese seminar, Awaji, Japan, 20–21 July 2004

11. *A. Laitinen, J. Liimatainen, M. Korhonen, P. Hallila and S. Tähtinen*, "Manufacturing Technology Development for the Vacuum Vessel and Plasma Facing Components", 23rd Symposium on Fusion Technology, Fondazione Cini, Venice, Italy, 20–24 September 2004.

12. *S. Tähtinen*, B. N. Singh*, P. Moilanen*, P. Jacquet and J. Dekeyser, D.J. Edwards, "Deformation Behaviour of Copper Under Under In-reactor Uniaxial Tensile Tests", 23rd Symposium on Fusion Technology, Fondazione Cini, Venice, Italy, 20–24 September 2004.

13. S.P. Simakov, U. Fischer, A. Möslang, P. Vladimirov, *F. Wasastjerna* and P.P.H. Wilson, "Neutronics and Activation Characteristics of the International Fusion Material Irradiation Facility", 23rd Symposium on Fusion Technology, Fondazione Cini, Venice, Italy, 20–24 September 2004.

14. *H. Wu, P. Pessi, H. Handroos* and L. Jones, "Development towards a parallel water hydraulic weld/cut robot for machining processes in ITER vacuum vessel", 23rd Symposium on Fusion Technology, Fondazione Cini, Venice, Italy, 20–24 September 2004.

15. P. Lorenzetto, B. Boireau, C. Boudot, Ph. Bucci, A. Fumarek, K. Ioki, *J. Liimatainen*, A. Peacock, P. Sherlok and *S. Tähtinen*, "Manufacture of Blanket Shield Modules for ITER", 23rd Symposium on Fusion Technology, Fondazione Cini, Venice, Italy, 20–24 September 2004.

16. M. Irving, J. Palmer and *M. Siuko*, "Generic control system design for the cassette multifunction mover and other ITER remote handling equipment", 23rd Symposium on Fusion Technology, Fondazione Cini, Venice, Italy, 20–24 September 2004.

17. J. Palmer, *M. Siuko*, P. Agostini, R. Gottfried, M. Irving, A. Tesini and M. Van Uffelen, "Recent developments towards ITER 2001 divertor maintenance", 23rd Symposium on Fusion Technology, Fondazione Cini, Venice, Italy, 20–24 September 2004.

18. *A. Fellman, A. Salminen* and *V. Kujanpää*, "The effect of welding parameters in CO2 laser-MAG hybrid welding of butt joints", Laser Assisted Net shape Engineering 4, ed. M. Geiger, A. Otto, Proc. Conf. LANE 2004, September 21–24, 2004, Erlangen, Germany, 145–157.

19. *A. Fellman, A. Salminen* and *V. Kujanpää*, "The comparison of the effects of welding parameters and weld properties of T-butt Joints between CO2-laser, Nd:YAG-laser and CO2-GMA hybrid welding", 23rd Int. Congress on ICALEO 2004 Applications of Lasers & Electro-Optics, October 4–7, 2004, San Francisco, CA, U.S.A, 9 p.

20. *A. Salminen, A. Fellman* and *V. Kujanpää*, "Effect of Material Thickness and Joint Configuration on the Efficiency of High Power Diode Laser Welding of Steel", 23rd Int. Congress on ICALEO 2004 Applications of Lasers & Electro-Optics, October 4–7, 2004, San Francisco, CA, U.S.A, 8 p.

21. *H. Pantsar* and *V. Kujanpää*, "The effect of Processing parameters on the microstructure and hardness of laser transformation hardened tool steel", 23rd Int. Congress on ICALEO 2004 Applications of Lasers & Electro-Optics, October 4–7, 2004, San Francisco, CA, U.S.A.

11.2.3 Research Reports – Fusion Technology

1. *P. Moilanen, S. Tähtinen*, B.N. Singh and P. Jacquet "TW2-TVV-SITU, In-situ investigation of the mechanical performance and life time of copper", VTT Technical Research Centre of Finland, Research Report BTUO76-031127, Espoo, 2004.

2. *H. Handroos, H. Wu, J. Kovanen, P. Pessi, K. Dufva* and Y. Liu, "TW2-TVV-ROBOT; Dynamic Test Rig for Intersector Welding Robot (IWR) for VV Sector Field Joining", Final Report.

3. *M. Karhu, T. Jokinen* and *V. Kujanpää*, "TW2-TVV/EBROOT, Controlling Root Welding Made by Electron Beam with Adaptive System", Research Report BTUO25-041257, VTT Industrial systems, Espoo, 2004, 27 p.

4. *T. Jokinen, M. Karhu* and *V. Kujanpää*, "Hybrid welding in the manufacturing of vacuum vessel for fusion reactor", accepted for publication in Industrial Systems Review, 2004.

5. *R. Korhonen,* Long term impacts of fusion. Progress report of SERF4 subtasks: Re-evaluation of the impacts of C-14 in SERF-studies and Comparison of fusion and fission, 2003. 9 p.

6. *R. Korhonen*, Long term impacts of fusion. Re-evaluation of the impacts of C-14 in SERF-studies, 2004. 52 p.

7. *F. Wasastjerna*, "User's manual for neutronics model md33 of ther IFMIF test cell, Final report on the EFDA task TW4-TTMI-003-D5a", Internal Report, Forschungszentrum Karlsruhe, IRS-Nr. 03/04-FUSION NR 226.

8. B.N. Singh, D.J. Edwards, *S. Tähtinen*, *P. Moilanen*, P. Jacquet and J. Dekeyser, "Final Report on In-Reactor Tensile Tests on OFHC -Copper and CuCrZr Alloy", Riso National Laboratory, Materials Research Department, Roskilde, Denmark, Riso-R-1481(EN), 2004. 47 p.

9. B.N. Singh, D.J. Edwards and *S. Tähtinen*, "Effect of Heat Treatments on Precipitate Microstructure and Mechanical Properties of CuCrZrAlloy", Riso National Laboratory, Materials Research Department, Roskilde, Denmark, Riso-R-1234(DA), 2004. 24 p.

11.3 General Articles and Annual Reports

1. *S. Karttunen* and *K. Rantamäki*, (eds.), "FUSION Yearbook. Association Euratom-Tekes. Annual Report 2003", VTT Publications 530, VTT Processes, Espoo 2004 127 p. + app. 10 p. ISBN 951-38-6379-4; 951-38-6380-8. http://www.vtt.fi/inf/pdf/publications/2004/P530.pdf

2. *M. Airila* and *V. Hynönen*, "Fuusio harppaa eteenpäin", Tietoyhteys 2/2004, pp. 13–15 (in Finnish).

3. *M. Airila* (ed.), Advanced Energy Systems – Annual Report 2003, Helsinki University of Technology Publications in Engineering Physics TKK-F-C196, Espoo 2004.

11.4 Doctoral and Graduate Theses

1. M. Airila, "Chaos in high-power high-frequency gyrotrons", Helsinki University of Technology Publications in Engineering Physics TKK-F-A825, Espoo 2004 (Doctorate Thesis at Helsinki University of Technology).

2. T. Jokinen, "Novel ways of using Nd:YAG laser for welding thick section austenitic stainless steel", VTT Publications 522, Espoo 2004, 120 p. + app. 12 p. (Doctorate Thesis at Lappeenranta University of Technology).

3. P. Moilanen, "Pneumatic servo-controlled material testing device capable of operating at high temperature water and irradiation conditions", VTT Publications 532, VTT Industrial Systems, Espoo 2004, 154 p. (Doctorate Thesis at Helsinki University of Technology). ISBN 951-38-6384-0; 951-38-6385-9. http://www.vtt.fi/inf/pdf/publications/2004/P532.pdf

4. A. Raneda, “Impedance control of a water hydraulic manipulator for teleoperation applicatios”, PhD Thesis, Tampere, TUT, 2004, 144 p. (Doctorate Thesis at Tampere University of Technology).

5. S. Janhunen, “Gyrokinetic field-particle code for plasma turbulence studies”, Diploma thesis, Master of Science Helsinki University of Technology, 2004 (Master's Thesis at Helsinki University of Technology).

6. K. Kallio, “Fuusioreaktorin huoltolaitteen lujuusopillinen tarkastelu”, Diploma thesis, Master of Science Tampere University of Technology, 2004. (Master's Thesis at Tampere University of Technology).

7. S. Henriksson, “Plasmaturbulenssin karakterisointi tilastollisten suureiden avulla FT-2 -tokamakin gyrokineettisissä simulaatioissa”, Master's thesis, University of Turku, to be published in 2005, (in Finnish).

APPENDIX A INTRODUCTION TO FUSION

A.1 Energy Demand Is Increasing

Most projections show world energy demand doubling or trebling in the next 50 years. This derives from fast population growth and rapid economic development. Energy sources that are not yet fully tapped include biomass, hydropower, geo-thermal, wind, solar, nuclear fission and fusion. All of them must be developed to meet future needs. Each alternative has its advantages and disadvantages regarding the availability of the resource, its distribution globally, environmental impact, and public acceptability. Fusion is a good candidate for supplying base load electricity on a large scale. Fusion has practically unlimited fuel resources, and it is safe and environmentally sound.

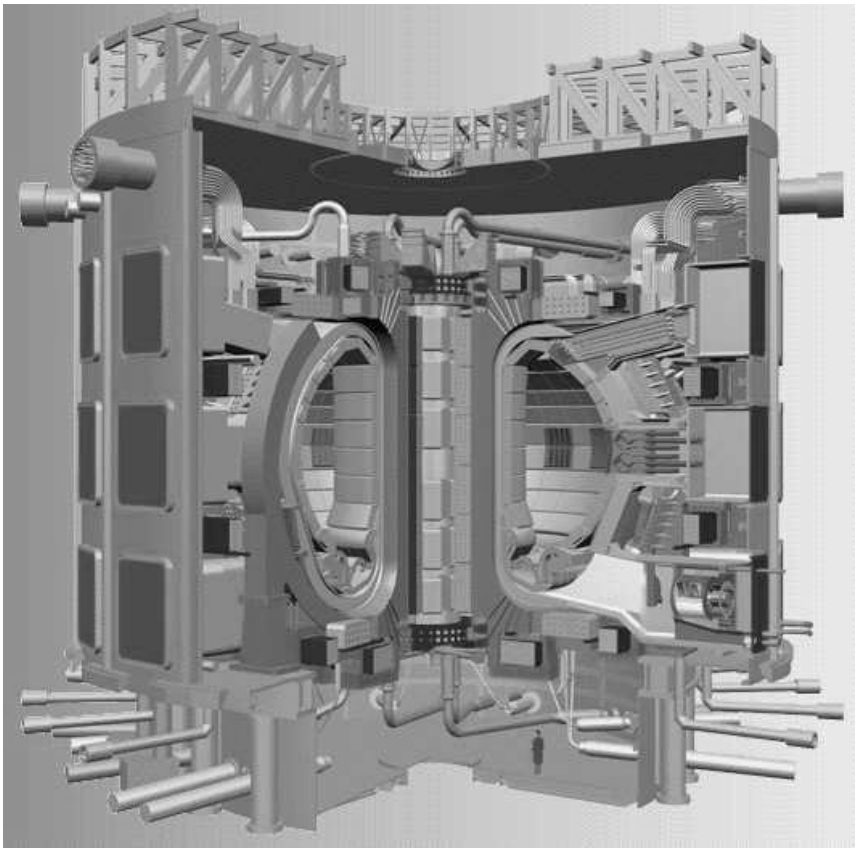

Figure 1: A design model for the experimental fusion reactor ITER.

A.2 What Is Fusion Energy?

Fusion is the energy source of the sun and other stars, and all life on Earth is based on fusion energy. The fuels burned in a fusion reactor are hydrogen isotopes, deuterium and tritium. Deuterium resources are practically unlimited, and tritium can be produced from lithium, which is abundant. The fusion reactions occur only at very high temperatures. For the deuterium-tritium reaction, temperatures over 100 million °C are required for sufficient fusion burn. At these temperatures, the fuel gas is fully ionised plasma. High temperatures can be achieved by injecting energetic particle beams or radio-frequency (RF) waves into the plasma. The hot plasma can be thermally isolated from the material walls by strong magnetic fields, which form a “magnetic bottle” to confine the fuel. With a sufficiently

large plasma volume, much more energy is released from fusion reactions than is required to heat and confine the fuel plasma, i.e, a large amount of net energy is produced.

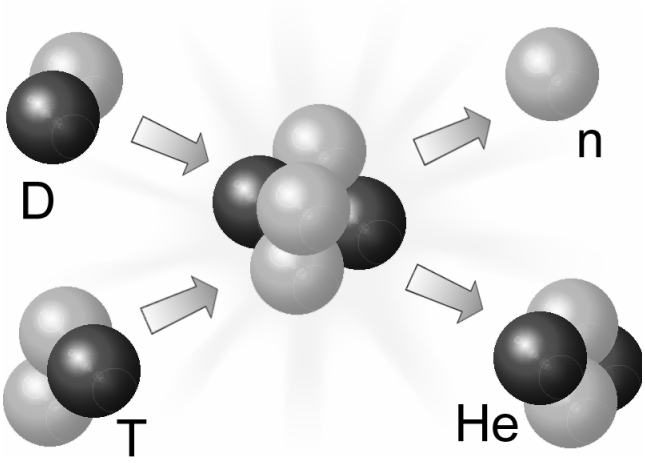

Figure 2: In a fusion reaction, deuterium (D) and tritium (T) fuse together forming a helium nucleus (^{4}He) and releasing a large amount of energy which is mostly carried by the neutron (n).

A.3 The European Fusion Programme

Harnessing fusion energy is the primary goal of the Euratom Fusion Progremme in the 6th Framework Programme. The reactor orientation of the programme has provided the drive and the cohesion that makes Europe the world leader in fusion research. The world record of 16 megawatts of fusion power is held by JET device, the Joint European Torus.

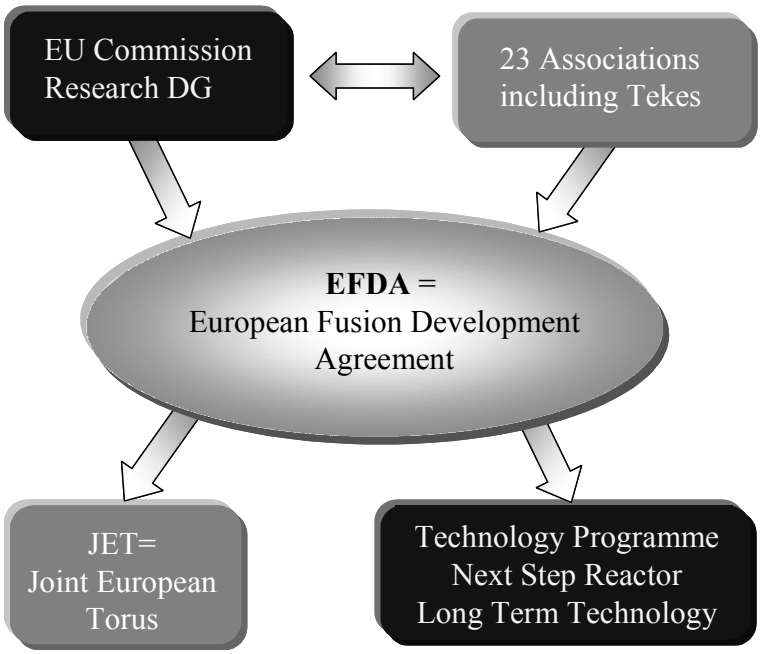

Figure 3: Multilateral EFDA covers JET research activities, fusion technology work for ITER and long term technology development. Tekes is one of the twenty one Euratom Associations.

The multilateral European Fusion Development Agreement (EFDA) between all the Associations and Euratom facilitates the joint exploitation of the JET facilities and the fusion technology programme, which covers ITER related R&D and long-term technology.

A.4 ITER International Fusion Energy Organisation

To advance significantly beyond the present generation of fusion devices, a next step device, enabling the investigation of burning plasma in near-reactor conditions, is needed. The detailed design and the extensive technical preparations have been completed and permitting to start the construction in 2005–2006. ITER parties have agreed in most issues and the final decision to start the construction is expected to take place soon. ITER tokamak would be the smallest tokamak enabling an investigation of burning plasmas at fusion power levels of 400–500 megawatts with energy amplification exceeding 10. Latest results from various tokamaks indicate that even larger amplification factors could be attained in this device.

APPENDIX B INDUSTRIAL PARTICIPATION

Group:	**The Finnish Blanket Group** consisting of Technip Offshore Finland, Diarc Technology Oy, Fortum Power and Heat Oy, Hollming Works Oy, High Speed Tech Oy, Kankaanpää Works Oy, Metso Powdermet Oy, Outokumpu Poricopper Oy and PI-Rauma Oy
Technology:	Metal structures and plasma facing components.
Contact:	Jari Liimatainen jari.liimatainen@metso.com

Group:	**The Finnish Remote Handling Group** consisting of Adwatec Oy, Fortum Power and Heat Oy, Hytar Oy, PI-Rauma Oy, Platom Oy, Creanex Oy, Rocla Oy and Delfoi Oy
Technology:	Remote handling, virtual reality, water hydraulics.
Contact:	Timo Mustonen timo.mustonen@creanex.com

Company:	**ABB – Finland**
Technology:	Power and automation
Contact:	P.O.Box 661, FI-65101 Vaasa, Finland Tel. +358 50 332 3515 Ralf Granholm ralf.granholm@fi.abb.com

Company:	**Adwatec Oy**
Technology:	Remote handling, water hydraulics, actuators and drives.
Contact:	Adwatec Oy, Polunmäenkatu 39 H 9, FI-33720 Tampere, Tel. +358 3 389 0860, Fax +358 3 389 0861 www.adwatec.com Arto Verronen rto.verronen@adwatec.com

Company:	**Aspocomp Oy**
Technology:	Electronics manufacturing, thick film technology, component mounting (SMT), and mounting of chips (COB) in mechanical and electrical micro systems (MEMS) and multi-chip modules (MCM), PWB (or also called PCB), sheet metal manufacturing and assembly.
Contact:	Aspocomp Oy, Yrittäjäntie 13, FI-01800 Klaukkala, Tel. +358 9 878 01244, Fax +358 9 878 01200 www.aspocomp.com Markku Palmu markku.palmu@aspocomp.com

Company:	**Corrotech Oy**
Technology:	Clean rooms, sheet metal production, mechanical engineering and surface treatment.
Contact:	Corrotech Oy, Teollisuuskatu 8, FI-95420 Tornio, Mobile: +358-40 777 9441, Fax +358 16 446 462 www.corrotech.fi Esko Hilden esko.hilden@corrotech.fi

Company **Creanex Oy**
Technology: Remote handling, teleoperation and walking platforms.
Contact: Creanex Oy, Nuolialantie 62, FI-33900 Tampere, Finland
Fax +358 33683 244, GSM +358 50 311 0300
www.creanex.com
Timo Mustonen timo.mustonen@creanex.com

Company: **Delfoi Oy**
Technology: Telerobotics, task level programming.
Contact: Delfoi Oy, Vänrikinkuja 2, FI-02600 Espoo, Finland
Tel. +358 9 4300 70, Fax +358 9 4300 7277
www.delfoi.com
Heikki Aalto heikki.aalto@delfoi.com

Company: **DIARC Technology Oy**
Technology: Diamond like DLC and DLC (Si, D) doped carbon coatings plus other coatings with potential plasma facing material in thermonuclear fusion machines.
Contact: Diarc Technology, Olarinluoma 15, FI-02200 Espoo,
Tel. +358 9 2517 6130, Fax +358 9 2517 6140
www.diarc.fi
Jukka Kolehmainen jukka.kolehmainen@diarc.fi

Company: **Ekono-Electrowatt/Jaakko Pöyry Group**
Technology: International consulting and engineering expert within the Jaakko Pöyry Group serving the energy sector. Core areas of expertise: management consulting, hydropower, renewable energy, power & heat, oil & gas, project services for nuclear safety and industrial processes.
Contact: P.O.Box 93, Tekniikantie 4 A, FI-02151 Espoo, Finland
Tel. +358 46911, Fax +358 9 469 1981
www.poyry.com
Vilho Salovaara vilho.salovaara@poyry.fi

Company: **Ellego Powertec Oy**
Technology: Power electronics, transformers, power sources, rectifiers based on modern chopper and thyristor technology.
Contact: Ellego Powertec Oy, P.O.Box 93, FI-24101 Salo,
Tel. +358 2 737 250, Fax +358 2 737 2530
www.trafotek.fi
Pasi Lauri pasi.lauri@ellego.fi

Company: **Elektrobit Microwave Oy**
Technology: Product development, test solutions and manufacturing for microwave and RF-technologies, high-tech solutions ranging from space equipment to commercial telecommunication systems.
Contact: Teollisuustie 9A, FI-02700 Kauniainen, Finland
Tel. +358 40 344 2000, Fax +358 9 5055 547
www.elektrobit.com
Marko.Koski marko.koski@elektrobit.com

Company: **Enprima Oy**
Technology: Design, engineering, consulting and project management services in the field of power generation and district heating. EPCM services.
Contact: P.O.Box 61, FI-01601 Vantaa, Finland
Tel. +358 40 348 5511, Fax +358 9 3487 0810
www.enprima.com
Jarmo Raussi jarmo.raussi@enprima.com

Company: **Exel Oyj**
Technology: Composite profiless, glass-, carbon- or aramid-fibres combined with polyester, vinylester or epoxy resins, superconducting current leads isolation profiles.
Contact: Exel Oyj, Muovilaaksontie 2, FI-82110 Heinävaara,
Tel. +358 13 73711, Fax +358 13 7371500
www.exel.fi
Matti Suominen matti.suominen@exel.fi

Company: **Fortum Power and Heat Oy**
Technology: Nuclear Engineering.
Contact: Fortum Nuclear Services Oy, Keilaniementie 1, Espoo,
FI-00048 Fortum, Finland
Tel. +358 10 4511, Fax +358 10 453 3403
www.fortum.com
Harri Tuomisto harri.tuomisto@fortum.com

Company **High Speed Tech Oy**
Technology: Copper to stainless steel bonding by explosive welding.
Contact: High Speed Tech Oy, Tekniikantie 4 D, FI-02150 Espoo,
Fax +358 9 455 5267
www.highspeedtech.fi
Jaakko Säiläkivi jaakko.sailakivi@highspeed.sci.fi

Company: **Hollming Works Oy**
Technology: Mechanical engineering, fabrication of heavy stainless steel structures.
Contact: Hollming Works Oy, Puunaulakatu 3, P.O.Box 96, FI-28101 Pori,
Tel. +358 20 486 5040, Fax +358 20 486 5041
www.hollmingworks.com
Jari Mattila jari.mattila@hollmingworks.com

Company: **Hytar Oy**
Technology: Remote handling, water hydraulics.
Contact: Hytar Oy, Ilmailukatu 13, P.O.Box 534, FI-33101 Tampere,
Tel. +358 3 389 9340, Fax +358 3 389 9341
Olli Pohls olli.pohls@avs-yhtiot.fi

Company: **Instrumentti-Mattila Oy**
Technology: Designs and manufacturing of vacuum technology devices.
Contact: Valpperintie 263, FI-21270 Nousiainen, Finland
Tel. +358 2 435 3611, Fax +358 2 431 8744
www.instrumentti-mattila.fi
Veikko Mattila veikko.mattila@instrumentti-mattila.fi

Company: **Kankaanpää Works Oy**
Technology: Mechanical engineering, fabrication of heavy stainless steel structures including 3D cold forming of stainless steel.
Contact: Kankaanpää Works Oy, P.O.Box 56, FI-38701 Kankaanpää,
Tel. +358 20 486 5034, Fax +358 20 486 5035
www.hollmingworks.com
Jarmo Huttunen jarmo.huttunen@hollmingworks.com

Company: **Mansner Oy Hienomekaniikka**
Technology: Precision mechanics: milling, turning, welding, and assembling. From stainless steels to copper.
Contact: Mansner Oy Hienomekaniikka, Yrittäjäntie 73, FI-03620 Karkkila,
Tel. +358 9 2248 7323, Fax +358 9 2248 7341
www.mansner.com
Sami Mansner sami.mansner@mansner.fi

Company: **Marioff Corporation Oy**
Technology: Mist fire protection systems.
Contact: Marioff Corporation Oy, P.O.Box 25, FI-01511 Vantaa,
Tel. +358 9 8708 5342, Fax +358 9 8708 5399
www.hi-fog.com
Pekka Saari pekka.saari@marioff.fi

Company: **Metso Powdermet Oy**
Technology: Special stainless steels, powder metallurgy, component technology/ engineering, design, production and installation.
Contact: Metso Powdermet Oy, P.O.Box 1100, FI-33541 Tampere,
Tel. +358 20 484 120, Fax +358 20 484 121
www.metsopowdermet.com
Jari Liimatainen jari.liimatainen@metso.com

Company: **Outokumpu Poricopper Oy**
Technology: Superconducting strands and copper products.
Contact: Outokumpu Poricopper Oy, Kuparitie, P.O Box 60, FI-28101 Pori,
Tel. +358 2 626 6111, Fax +358 2 626 5314
Antti Kilpinen antti.kilpinen@outokumpu.com
Rauno Liikamaa rauno.liikamaa@outokumpu.com
Ben Karlemo ben.karlemo@outokumpu.com

Company: **Oxford Instruments Analytical**
Technology: Plasma diagnostics.
Contact: Nihtisillankuja, P.O.Box 85, FI-02631 Espoo, Finland
Tel. +358 9 329411, Fax: +358 9 23941300
Heikki Sipilä heikki.sipila@oxinst.fi

Company: **PI-Rauma Oy**
Technology: Computer aided engineering with CATIA.
Contact: PI-Rauma Oy, Mäntyluoto, FI-28880 Pori,
Tel. +358 2 528 2521, fax +358 2 528 2500
www.pi-rauma.fi
Matti Mattila matti.mattila@pi-rauma.com

Company: **Platom Oy**
Technology: Remote handling, thermal cutting tools and radioactive waste handling.
Contact: Platom Oy, Graanintie 5, P.O.Box 300, FI-50101 Mikkeli,
Tel. +358 44 5504 300, Fax +358 15 369 270
www.platom.fi
Miika Puukko miika.puukko@platom.fi

Company: **Polartest Oy**
Technology: 3-party inspection, NDT, documentation and receiving inspection.
Contact: Polartest Oy, Laajaniityntie 3, P.O.Box 41, FI-01620 Vantaa,
Tel. +358 9 878 020, Fax +358 9 878 6653
www.polartest.fi
Matti Andersson matti.andersson@polartest.fi

Company: **PPF Products Oy**
Service: Industry activation and support.
Contact. Portaantie 548, FI-31340 Porras
Tel. +358 3 434 1970, +358 50 40 79 799
Pertti Pale pertti.pale@surffi.net

Company: **Prizztech Oy**
Role: Co-ordination of the industry participation in the Fusion Programme.
Contact: Prizztech Oy, Teknologiakeskus Pripoli, Tiedepuisto 4,
FI-28600 Pori, Finland
Tel. +358 2 620 5330, Fax +358 2 620 5399
www.prizz.fi
Leena Annila leena.annila@prizz.fi

Company: **Rados Technology Oy**
Technology: Dosimetry, waste & contamination monitoring and environmental monitoring.
Contact: Rados Technology Oy, P.O.Box 506, FI-20101 Turku,
Tel. +358 2 4684 600, Fax +358 2 4684 601
www.rados.fi
Erik Lehtonen erik.lehtonen@rados.fi

Company: **Rejlers Oy**
Technology: System and subsystem level design, FE modelling and analysis with ANSYS, studies and technical documentation, installation and maintenance instructions, 3D modelling and visualisation of machines and components.
Contact: Rejlers Oy, Myllykatu 3, FI-05840 Hyvinkää,
Tel. +358 19 2660 600, Fax +358 19 2660 601
www.rejlers.fi
Jouni Vidqvist jouni.vidqvist@rejlers.fi

Company: **Rocla Oyj**
Technology: Heavy Automated guided vehicles.
Contact: Rocla Oyj, P.O.Box 88, FI-04401 Järvenpää,
Tel. +358 9 271 471, Fax +358 9 271 47 430
www.rocla.fi
Pekka Joensuu pekka.joensuu@rocla.com

Company: **Selmic Oy**
Technology: Microelectronics design and manufacturing, packaging technologies and contract manufacturing services.
Contact: Selmic Oy, Vanha Porvoontie 229, FI-01380 Vantaa,
Tel. +358 9 2706 3911, Fax +358 9 2705 2602
www.selmic.com
Patrick Sederholm patrick.sederholm@selmic.com

Company: **Solving Oy**
Technology: Heavy automated guided vehicles. Equipment for heavy assembly and material handling based on air film technology for weights up to hundreds of tons.
Contact: Solving Oy, P.O.Box 98, FI-68601 Pietarsaari,
Tel. +358 6 781 7500, Fax +358 6 781 7510
www.solving.fi
Bo-Goran Eriksson bo-goran.eriksson@solving.fi

Company: **Sweco PIC Oy**
Technology: Consulting and engineering company operating world-wide, providing consulting, design, engineering and project management services for industrial customers in plant investments, product development and production.
Contact: Liesikuja 5, P.O.Box 31, FI-01601 Vantaa, Finland
Tel. +358 9 53091
Kari Harsunen kari.harsunen@sweco.fi

Company: **Tankki Oy**
Technology: Production and engineering of stainless steel tanks and vessels for use in different types of industrial installations.
Contact: Oikotie 2, FI-63700 Ähtäri, Finland
Tel. +358 6 510 1111, Fax +358 6 510 1200
Jukka Lehto jukka.lehto@tankki.fi

Company: **Technip Offshore Finland** (earlier Mäntyluoto Works Oy)
Technology: Fabrication of Heavy Steel constructions by using an effective modulus technology, pressure vessels and piping.
Contact: Mäntyluoto Works Oy, FI-28880 Pori,
Tel. +358 2 528 2411, Fax +358 2 528 2419
www.coflexipstenaoffshore.com

Company: **TVO Nuclear Services Oy**
Technology: Nuclear power technologies; service, maintenance, radiation protection and safety.
Contact: TVO Nuclear Services Oy, FI-27160 Olkiluoto,
Tel. +358 2 83 811, Fax +358 2 8381 2109
www.tvo.fi
Antti Piirto antti.piirto@tvo.fi

Company: **Veslatec Oy**
Technology: Micro cutting-laser welding-laser drilling-laser marking.
Contact: Veslatec Oy, Strömbergin puistotie 4D, FI-65320 Vaasa,
Tel. +358 6 315 89 00, Fax +358 6 315 28 77
www.veslatec.com
Olli Saarniaho olli.saarniaho@veslatec.com

Company: **Woikoski Oy**
Technology: Production, development, applications and distribution of gases and liquid helium.
Contact: Voikoski, P.O.Box 1, FI-47901 Vuohijärvi, Finland
Tel. +358 15 7700700, Fax +358 15 7700720
www.woikoski.fi
Kalevi Korjala kalevi.korjala@woikoski.fi

APPENDIX C CONTACT INFORMATION

National Technology Agency of Finland (Tekes)

Kyllikinportti 2, Länsi-Pasila
P.O.Box 69, FI-00101 Helsinki, Finland
Tel. +358 105 2151, Fax +358 105 215903
www.tekes.fi

Reijo Munther	reijo.munther@tekes.fi
Juha Linden	juha.linden@tekes.fi

Research Unit

Technical Research Centre of Finland (VTT)

VTT Processes
Otakaari 3A, Espoo
P.O.Box 1608, FI-02044 VTT, Finland
Tel. +358 20 722 111, Fax +358 20 722 6390
www.vtt.fi

Seppo Karttunen	seppo.karttunen@vtt.fi
Jukka Heikkinen	jukka.heikkinen@vtt.fi
Riitta Korhonen	riitta.korhonen@vtt.fi
Petri Kotiluoto	petri.kotiluoto@vtt.fi
Antti Lehtilä	antti.lehtilä@vtt.fi
Jari Likonen	jari.likonen@vtt.fi
Karin Rantamäki	karin.rantamaki@vtt.fi
Tommi Renvall	tommi.renvall@vtt.fi
Vesa Suolanen	vesa.suolanen@vtt.fi
Tuomas Tala	tuomas.tala@vtt.fi
Frej Wasastjerna	frej.wasastjerna@vtt.fi
Elizaveta Vainonen-Ahlgren	elizaveta.vainonen-ahlgren@vtt.fi

VTT Industrial Systems
Kemistintie 3, Espoo
P.O.Box 1704, FI-02044 VTT, Finland
Tel. +358 20 722 111, Fax +358 20 722 7002
www.vtt.fi

Rauno Rintamaa	rauno.rintamaa@vtt.fi
Seppo Tähtinen	seppo.tahtinen@vtt.fi
Pekka Moilanen	pekka.moilanen@vtt.fi

VTT Industrial Systems
P.O.Box 17021, FI-53851 Lappeenranta, Finland
Tel. +358 20 722 111, Fax +358 20 722 2893
www.vtt.fi

Veli Kujanpää	veli.kujanpaa@vtt.fi
Tommi Jokinen	tommi.jokinen@vtt.fi

VTT Industrial Systems
P.O.Box 1307, FI-33101 Tampere, Finland
Tel. +358 20 722 111, Fax +358 20 722 3495
www.vtt.fi
Arto Timperi arto.timperi@vtt.fi
Jorma Järvenpää jorma.jarvenpaa@vtt.fi

VTT Electronics
Kaitoväylä 1
P.O.Box 1100, FI-90571 Oulu, Finland
Tel. +358 20 722 111, Fax +358 20 722 2320
www.vtt.fi
Heikki Ailisto heikki.ailisto@vtt.fi
Veli Heikkinen veli.heikkinen@vtt.fi

Helsinki University of Technology (TKK)

Helsinki University of Technology
Advanced Energy Systems
P.O.Box 2200, FI-02015 TKK, Finland
Tel. +358 9 4511, Fax +358 9 451 3195
www.hut.fi
Rainer Salomaa rainer.salomaa@hut.fi
Markus Airila markus.airila@hut.fi
Olgierd Dumbrajs olgierd.dumbrajs@hut.fi
Ville Hynönen ville.hynonen@hut.fi
Salomon Janhunen salomon.janhunen@hut.fi
Timo Kiviniemi timo.kiviniemi@hut.fi
Taina Kurki-Suonio taina.kurki-suonio@hut.fi
Seppo Sipilä seppo.sipila@hut.fi

Helsinki University of Technology
Automation Technology
P.O.Box 3000, FI-02015 TKK, Finland
Tel. +358 9 4511, Fax +358 9 451 3308
www.hut.fi
Aarne Halme aarne.halme@hut.fi
Peter Jakubik peter.jakubik@hut.fi
Jussi Suomela jussi.suomela@hut.fi

Tampere University of Technology (TUT)

Tampere University of Technology
Institute of Hydraulics and Automation
Korkeakoulunkatu 2
P.O.Box 589, FI-33101 Tampere, Finland
Tel. +358 3115 2111, Fax +358 3115 2240
www.iha.tut.fi
Matti Vilenius matti.vilenius@tut.fi
Kari Koskinen kari.t.koskinen@tut.fi
Mikko Siuko mikko.siuko@tut.fi

Tampere University of Technology
Laboratory of Electromagnetics
Korkeakoulunkatu 2
P.O.Box 589, FI-33101 Tampere, Finland
Tel. +358 3115 3602, Fax +358 3115 2160
www.tut.fi
Risto Mikkonen risto.mikkonen@tut.fi
Iiro Hiltunen iiro.hiltunen@tut.fi

Lappeenranta University of Technology
Laboratory of Machine Automation
Skinnarilankatu 34
P.O.Box 20, FI-53851 Lappeenranta, Finland
Tel. +358 5 621 11, Fax +358 5 621 2350
www.lut.fi
Heikki Handroos heikki.handroos@lut.fi
Huapeng Wu huapeng.wu@lut.fi

University of Helsinki
Accelerator Laboratory
P.O.Box 43, FI-00014 University of Helsinki, Finland
Tel. +358 9 191 40005, Fax +358 9 191 40042
www.beam.helsinki.fi
Juhani Keinonen juhani.keinonen@helsinki.fi
Tommi Ahlgren tommy.ahlgren@helsinki.fi
Kai Nordlund kai.nordlund@helsinki.fi

Published by

Series title, number and report code of publication

VTT Publications 567
VTT–PUBS–567

Author(s)
Karttunen, Seppo & Rantamäki, Karin (eds.)

Title

FUSION Yearbook

Association Euratom-Tekes. Annual Report 2004

Abstract

This report summarises the results of the Tekes FUSION technology programme and the fusion research activities by the Association Euratom-Tekes in 2004. The research areas are fusion physics, plasma engineering, fusion technology and a smaller effort to socio-economic studies. Fusion technology research is carried out in close collaboration with Finnish industry.

The emphasis in fusion physics and plasma engineering is in theoretical and computational studies on turbulent transport and modelling of radio-frequency heating experiments and the real time control of transport barriers in JET plasmas, predictive integrated modelling of tokamak plasmas, and studies on material transport in the edge plasmas supported by surface analysis of the JET divertor and limiter tiles.

The work in fusion technology for the EFDA Technology Programme and ITER is strongly focused into vessel/in-vessel materials covering research and characterisation of first wall materials, mechanical testing of reactor materials under neutron irradiation, characterisation of irradiated Ti-alloys, simulations of carbon and tungsten sputtering, joining and welding methods and surface physics studies on plasma facing materials. A second domain of fusion technology consists of remote handling systems including water hydraulic manipulators for the ITER divertor maintenance as well as prototyping of intersector welding and cutting robot. Virtual modelling is an essential element in the remote handling engineering. Preparations to host the ITER divertor test platform (DTP2) were completed in 2004 and the DTP2 facility will be hosted by VTT. Some effort was also devoted to neutronics, socio-economic and power plant studies. Several EFDA technology tasks were successfully completed in 2004.

Keywords
fusion, fusion reactors, reactor materials, fusion physics, remote handling, testing, Joint European Torus, modelling, control

Activity unit
VTT Processes, Otakaari 3 A, P.O.Box 1608, FI–02044 VTT, Finland

ISBN			Project number
951–38–6642–4 (soft back ed.) 951–38–6643–2 (URL: http://www.vtt.fi/inf/pdf/)			C4SU00345
Date May 2005	Language English	Pages 129 p. + app. 13 p.	Price C
Name of project FUSION, European Fusion Research Area, 6th Frame Work Programme		Commissioned by Tekes	
Series title and ISSN VTT Publications 1235–0621 (soft back edition) 1455–0849 (URL: http://www.vtt.fi/inf/pdf/)		Sold by VTT Information Service P.O.Box 2000, FI–02044 VTT, Finland Phone internat. +358 20 722 4404 Fax +358 20 722 4374	

This report summarises the results of the Tekes FUSION technology programme and the fusion research activities by the Association Euratom-Tekes in 2004. The research areas are fusion physics, plasma engineering, fusion technology and a smaller effort to socio-economic studies. Fusion technology research is carried out in close collaboration with Finnish industry.

The emphasis in fusion physics and plasma engineering is in theoretical and computational studies on turbulent transport and modelling of radio-frequency heating experiments and the real time control of transport barriers in JET plasmas, predictive integrated modelling of tokamak plasmas, and studies on material transport in the edge plasmas supported by surface analysis of the JET divertor and limiter tiles.

The work in fusion technology for the EFDA Technology Programme and ITER is strongly focused into vessel/in-vessel materials covering research and characterisation of first wall materials, mechanical testing of reactor materials under neutron irradiation, characterisation of irradiated Ti-alloys, simulations of carbon and tungsten sputtering, joining and welding methods and surface physics studies on plasma facing materials. A second domain of fusion technology consists of remote handling systems including water hydraulic manipulators for the ITER divertor maintenance as well as prototyping of intersector welding and cutting robot. Virtual modelling is an essential element in the remote handling engineering. Preparations to host the ITER divertor test platform (DTP2) were completed in 2004 and the DTP2 facility will be hosted by VTT. Some effort was also devoted to neutronics, socio-economic and power plant studies. Several EFDA technology tasks were successfully completed in 2004.

VTT PUBLICATIONS 567

FUSION Yearbook. Association Euratom-Tekes. Annual Report 2004

NATIONAL TECHNOLOGY AGENCY
P.O. Box 69, FI-00101 Helsinki, Finland
Tel. +358 105 2151, Fax +358 105 215905
www.tekes.fi

VTT TECHNICAL RESEARCH CENTRE OF FINLAND
VTT PROCESSES
P.O. Box 1608, FI–02044 VTT, Finland
Tel. +358 20 722 111, Fax +358 20 722 6390
www.vtt.fi

Tätä julkaisua myy

VTT TIETOPALVELU
PL 2000
02044 VTT
Puh. 020 722 4404
Faksi 020 722 4374

Denna publikation säljs av

VTT INFORMATIONSTJÄNST
PB 2000
02044 VTT
Tel. 020 722 4404
Fax 020 722 4374

This publication is available from

VTT INFORMATION SERVICE
P.O.Box 2000
FI–02044 VTT, Finland
Phone internat. +358 20 722 4404
Fax +358 20 722 4374

ISBN 951–38–6642–4 (soft back ed.)
ISSN 1235–0621 (soft back ed.)

ISBN 951–38–6643–2 (URL: http://www.vtt.fi/inf/pdf/)
ISSN 1455–0849 (URL: http://www.vtt.fi/inf/pdf/)